ANALYSIS OF HEMOLYMPH PROTEINASE 16 AND SERPIN-3 FROM THE HEMOLYMPH OF *MANDUCA SEXTA*

by

JAYNE M. CHRISTEN

B.S., Kansas State University, 2003
M.S., Kansas State University, 2005

AN ABSTRACT OF A DISSERTATION

submitted in partial fulfillment of the requirements for the degree

DOCTOR OF PHILOSOPHY

Biochemistry Graduate Group

KANSAS STATE UNIVERSITY
Manhattan, Kansas

2011

Abstract

Insect innate immune responses include prophenoloxidase activation and antimicrobial peptide production. These responses involve extracellular serine proteinase cascades that are regulated by serpins. This work involved the study of serine proteinase 16 (HP16) and serpin-3 from hemolymph of the tobacco hornworm, *Manduca sexta*.

HP16 has an amino-terminal domain with no similarity to any characterized protein and a carboxyl-terminal S1 family serine proteinase domain. HP16 levels in plasma were highest during the wandering, prepupal, and pupal stages. HP16 mRNA levels in fat body were highest at the wandering stage. Injection of bacteria into fifth instar larvae stimulated HP16 expression. To further characterize and investigate the biological function of HP16, recombinant proteins for proHP16, two HP16 mutants, the amino-terminal domain (NT16), and three NT16 mutants were purified. Recombinant HP16 was cleaved at the predicted activation site during expression, and its amino-terminal and catalytic domains remained connected by a disulfide bond. ProHP16 in plasma was apparently activated in the presence of the microbial elicitor, zymosan. Recombinant HP16 formed a complex with serpin-1Z, indicating that it was catalytically active, but no other natural or artificial substrates were identified. Analysis of NT16 and NT16 mutants led to the discovery that multiple disulfide bond arrangements were formed in the recombinant amino-terminal domain of HP16. This work furthered the understanding of HP16 and laid a foundation for subsequent experiments involving the proteolytic activity, regulation, and biological function of HP16.

Active serine proteinases in insect hemolymph are often regulated by serpins. Immunoaffinity chromatography was used to identify plasma proteinases that are inhibited by serpin-3. Four serpin-3-proteinase complexes purified from plasma were identified by immunoblot analysis as serpin-3 complexes with HP8, PAP-1, PAP-2, and PAP-3. MALDI-TOF/TOF or ESI-MS/MS analysis after separation by 1D- or 2D-PAGE confirmed serpin-3 complex formation with HP8, PAP-1, and PAP-3. ProHP8 in plasma was activated by exposure to the β-1,3-glucan curdlan and inhibited by serpin-3. Purified recombinant serpin-3 and active HP8-Xa formed an SDS-stable complex *in vitro*. Identification of serpin-3-proteinase complexes

in plasma provides insight into proteinase targets of serpin-3 and extends the understanding of serpin/proteinase function in the immune response of *M. sexta*.

ANALYSIS OF HEMOLYMPH PROTEINASE 16 AND SERPIN-3 FROM THE HEMOLYMPH OF *MANDUCA SEXTA*

by

JAYNE M. CHRISTEN

B.S., Kansas State University, 2003
M.S. Kansas State University, 2005

A DISSERTATION

submitted in partial fulfillment of the requirements for the degree

DOCTOR OF PHILOSOPHY

Biochemistry Graduate Group

KANSAS STATE UNIVERSITY
Manhattan, Kansas

2011

Approved by:

Major Professor
Michael R. Kanost
Department of Biochemistry

Copyright

Abstract

Insect innate immune responses include prophenoloxidase activation and antimicrobial peptide production. These responses involve extracellular serine proteinase cascades that are regulated by serpins. This work involved the study of serine proteinase 16 (HP16) and serpin-3 from hemolymph of the tobacco hornworm, *Manduca sexta*.

HP16 has an amino-terminal domain with no similarity to any characterized protein and a carboxyl-terminal S1 family serine proteinase domain. HP16 levels in plasma were highest during the wandering, prepupal, and pupal stages. HP16 mRNA levels in fat body were highest at the wandering stage. Injection of bacteria into fifth instar larvae stimulated HP16 expression. To further characterize and investigate the biological function of HP16, recombinant proteins for proHP16, two HP16 mutants, the amino-terminal domain (NT16), and three NT16 mutants were purified. Recombinant HP16 was cleaved at the predicted activation site during expression, and its amino-terminal and catalytic domains remained connected by a disulfide bond. ProHP16 in plasma was apparently activated in the presence of the microbial elicitor, zymosan. Recombinant HP16 formed a complex with serpin-1Z, indicating that it was catalytically active, but no other natural or artificial substrates were identified. Analysis of NT16 and NT16 mutants led to the discovery that multiple disulfide bond arrangements were formed in the recombinant amino-terminal domain of HP16. This work furthered the understanding of HP16 and laid a foundation for subsequent experiments involving the proteolytic activity, regulation, and biological function of HP16.

Active serine proteinases in insect hemolymph are often regulated by serpins. Immunoaffinity chromatography was used to identify plasma proteinases that are inhibited by serpin-3. Four serpin-3-proteinase complexes purified from plasma were identified by immunoblot analysis as serpin-3 complexes with HP8, PAP-1, PAP-2, and PAP-3. MALDI-TOF/TOF or ESI-MS/MS analysis after separation by 1D- or 2D-PAGE confirmed serpin-3 complex formation with HP8, PAP-1, and PAP-3. ProHP8 in plasma was activated by exposure to the β-1,3-glucan curdlan and inhibited by serpin-3. Purified recombinant serpin-3 and active HP8-Xa formed an SDS-stable complex *in vitro*. Identification of serpin-3-proteinase complexes

in plasma provides insight into proteinase targets of serpin-3 and extends the understanding of serpin/proteinase function in the immune response of *M. sexta*.

Table of Contents

List of Figures

List of Tables

List of Abbreviations

1D	one dimensional
2D	two dimensional
Ala	alanine
AMP	antimicrobial peptide
Arg	arginine
βGRP	β-1,3-glucan recognition proteins
CI	confidence interval
CPC	cetylpyridinium chloride
Cys	cysteine
DAP	diaminopimelic acid
ESI	electrospray ionization
EST	expressed sequence tag
Gly	glycine
GNBP	gram-negative binding protein
h	hours
HIC	hydrophobic interaction chromatography
HP	hemolymph proteinase
Ile	isoleucine
IML	immulectin
kDa	kilodalton
Lys	lysine
MALDI	matrix assisted laser desorption ionization
MBP	microbe binding protein
min	minutes
MIP	melanization-inhibiting protein
MS	mass spectrometry
PAGE	polyacrylamide gel electrophoresis
PAP	prophenoloxidase-activating proteinase
PCR	polymerase chain reaction
pfu/mL	plaque forming units/milliliter
PGRP	peptidoglycan recognition protein
Phe	phenylalanine
PO	phenoloxidase
POI	phenoloxidase inhibitor
proPO	prophenoloxidase
PVDF	polyvinylidene difluoride
RCL	reactive center loop
RNAi	RNA interference

RT	room temperature
RT-PCR	reverse transcriptase-polymerase chain reaction
s	seconds
SDS	sodium dodecyl sulfate
Ser	serine
SPE	spätzle-processing enzyme
SPH	serine proteinase homolog
Trp	tryptophan
Tyr	tyrosine
Val	valine

Acknowledgements

I would like to express my appreciation for my major professor, Dr. Michael Kanost, for the opportunity to study and conduct research in his laboratory. I also thank my committee members Drs. Michal Zolkiewski, S. Muthukrishnan, and Yoonseong Park for their support, suggestions, and interest in my research. A special thanks to Dr. Lorena Passarelli for her willingness to serve as my outside chairperson for my doctoral defense.

Thanks is expressed to Dr. Chunju An for her guidance during the development of my project and for her willingness to take time out of her busy research schedule to discuss my results with me and to show me new techniques. I would like to give special thanks to Drs. Emily Ragan and Maureen Gorman for always making time for me when I had questions, for helping me through the frustrating times when experiments continually produced unusable results, and for making me laugh. I thank Stewart Gardner for helping with the expression and purification of numerous serpin-1 isoforms and serpin-3. Appreciation is expressed to Dr. Neal Dittmer and other members of the Kanost lab for their help and camaraderie. I thank Rebekah Woolsey from the Nevada Proteomics Center and Dr. Yasuaki Hiromasa from the Biotechnology Core/Proteomics Facility at Kansas State University for performing mass spectrometry.

I wish to extend my thanks to all of my friends, both inside and outside, of the Department of Biochemistry. A special thanks to Adam Sparks for his ongoing support, friendship, and willingness to listen to me talk about the same thing time and time again. I also thank him for teaching me that no matter what life throws at you, you can persevere and reach your goals. I would like to thank Christine Aikens and the members of my city league volleyball teams for providing me with an outlet to relieve stress and a way to have fun. Appreciation is also expressed to Ginny Hagin, Jen Skelsey, Kendra Siebert, Scott Schlender, and Tara Dean for helping me through a difficult time in my personal life.

Finally, I would like to thank my family for their support, encouragement, and love. Whether I needed support in terms of pursuing my dreams, finishing my degree, or making it through life's ups and downs, I always know that they are there for me and will do anything that they can do to help.

Dedication

I dedicate this dissertation to my parents, Joe and Joan Christen. Your never ending belief in me has always helped me see the light at the end of the tunnel no matter how dark the days may be along the way. You have taught me that time, effort, and patience will help me go far and that hard work is always the best way to go. Most of all, you have taught me to believe in myself, to fight for what I want, and not to let anything stand in the way of my dreams.

CHAPTER 1 - LITERATURE REVIEW

Introduction

Manduca sexta, commonly known as the tobacco hornworm, belongs to the insect order Lepidoptera and the family Sphingidae. As a holometabolous insect, *M. sexta* undergoes complete metamorphosis, which means that each life stage is dramatically different from the other. After 3-5 days, blue-green eggs hatch into larvae (= feeding stage). Larvae undergo larval to larval molts in which the old cuticle is shed to allow for an increase in size with each molt. After the 5^{th} instar, feeding larvae enter the non-feeding wandering stage. During this stage, larvae wander around, looking for a place in the soil to pupate. Under non-diapause conditions, adults will emerge from the pupal case in nineteen to twenty-three days. Adults disperse by flight, feed on nectar, and reproduce (Dunn, 1990). After successful mating, the female lays her eggs on the underside of foliage to start the life cycle again.

This insect is often used as a model organism in biochemical studies involving innate immunity due to its large size, hemolymph volume, relatively short life cycle, and ability to be reared year-round on artificial diet (Dunn, 1990; Kanost et al., 2004). Individual 5^{th} instar caterpillars can contain 1-2 mL of hemolymph and 10^6 hemocytes, which make *M. sexta* an ideal candidate for studies involving hemocytes and hemolymph proteins (Kanost et al., 2004). Using *M. sexta* to advance the understanding of mechanisms behind innate immunity can enhance our understanding of immune systems in other insects. This, in turn, may lead to the development of new pest control measures as well as improvement in the health of beneficial insects. Furthermore, since there are some similarities in the innate immune systems of insects and mammals, discoveries in insect immunity could help us better understand the human immune response and evolution of innate immunity.

Immunity in Insects

Invertebrates, like all organisms, can experience invasion by bacteria, fungi, or other pathogens. The first line of defense for an insect is a physical barrier in the form of a hard exoskeleton, the peritrophic matrix of the midgut, and tracheae lined with cuticle (Dunn, 1990;

Lavine and Strand, 2002; Iwanaga and Lee, 2005; Jiravanichpaisal et al., 2006). If the invaders survive and pass through these barriers into the hemocoel, the insects must rely on their innate immune systems as they lack adaptive immunity. Innate immunity can be divided into two categories: cellular and humoral responses. Cellular responses are mediated by hemocytes and include phagocytosis, encapsulation, and nodulation (Lavine and Strand, 2002; Jiravanichpaisal et al., 2006; Marmaras and Lampropoulou, 2009). Humoral responses include the production of antimicrobial peptides, prophenoloxidase activation that leads to melanization, and production of reactive intermediate oxygen or nitrogen species (Lavine and Strand, 2002; Jiravanichpaisal et al., 2006; Marmaras and Lampropoulou, 2009; Cerenius et al., 2010).

Hemolymph

Many immune responses begin when foreign invaders enter the insect's hemocoel, or body cavity. Insects have an open circulatory system in which hemolymph, or insect blood, fills the hemocoel, is pumped around the hemocoel by the dorsal vessel, and surrounds organs and tissues (Wyatt and Pan, 1978; Chapman, 1998; Uvell and Engström, 2007). Hemolymph is comprised of a fluid, called plasma, and blood cells, called hemocytes. Within the plasma are inorganic ions, such as sodium, potassium, calcium, and magnesium (Wyatt, 1961; Wyatt and Pan, 1978; Chapman, 1998; Klowden, 2002), high levels of free amino acids (Wyatt, 1961; Wyatt and Pan, 1978; Chapman, 1998; Klowden, 2002), products of nitrogen metabolism, such as uric acid, ammonia, urea, and allantoin (Wyatt, 1961; Chapman, 1998), organic acids like citrate, malate, and succinate (Wyatt, 1961), lipids (Wyatt, 1961), and carbohydrates, especially trehalose (Wyatt, 1961; Chapman, 1998). Plasma also contains hexamerins (Willott et al., 1989; Kanost et al., 1990; Burmester, 1999; Burmester, 2002), lipid transport proteins (Wyatt and Pan, 1978; Kanost et al., 1990; Ryan and Van der Horst, 2000; Smolenaars et al., 2007; Van der Horst et al., 2009), pattern recognition proteins, enzymes, proteinases, proteinase inhibitors, antimicrobial peptides, hormones, and chromoproteins (Kanost et al., 1990).

Hemocytes and cellular immune responses in lepidopterans with an emphasis on Manduca sexta

Hemocytes, or insect blood cells, are important mediators of immune responses. Common types of insect hemocytes include prohemocytes, plasmatocytes, granular cells, oenocytoids, and spherule cells (Lavine and Strand, 2002; Jiravanichpaisal et al., 2006; Strand,

2008). Prohemocytes account for a small portion (<1%) of all hemocytes and are thought to be equivalent to stem cells (Lavine and Strand, 2002; Jiravanichpaisal et al., 2006; Strand, 2008). However, these cells have not been found in *M. sexta* (Beetz et al., 2004). Non-adherent oenocytoids synthesize and release prophenoloxidase. The role of spherule cells is poorly defined (Jiang et al., 2010). In lepidopterans, plasmatocytes and granular cells have the ability to adhere to foreign invaders and are key players in phagocytosis, nodulation, and encapsulation. (Lavine and Strand, 2002; Kanost and Nardi, 2008; Strand, 2008; Jiang et al., 2010). In 2004 (Dean et al.), hyper-spreading plasmatocyte-like hemocytes were found in *M. sexta*. These hemocytes were very thin, could spread up to 120 μm on glass, and appeared as "fried egg" or speckled type. The hyper-spreading cells attached to bacteria and initiated hemocyte aggregation followed by nodule formation. Wounding did not stimulate the presence of these cells, but infection by *Beauveria bassiana* or *Photorhabdus luminescens* did. Interestingly, these hemocytes are present only before pathogen proliferation. Once pathogen growth begins, the number of these hyper-spreading cells plummets to zero (Dean et al., 2004). Two years later, Nardi et al. (2006) identified a subpopulation of plasmatocytes that exhibited characteristics similar to the hyper-spreading plasmatocyte-like hemocytes described by Dean et al. (2004). Monoclonal antibodies specific to β1-intergin (MS13), neuroglian (3B11), or an unknown antigen on granular cells (MS2) were used to distinguish hemocyte types. All plasmatocytes were detected by MS13 and a small proportion was also detected by 3B11, which indicated that there were two distinct populations of circulating plasmatocytes (neuroglian-negative and neuroglian-positive). Neuroglian-positive, but not neuroglian-negative plasmatocytes serve as initiators of hemocyte aggregation and effective adhesion of neuroglian-positive plasmatocytes to foreign materials depends on the presence of granular cells or some unidentified factor produced by the granular cells (Nardi et al., 2006).

Phagocytosis is a process that removes small particles, such as bacteria, yeast, or apoptotic cells, from an insect (Jiravanichpaisal et al., 2006; Stuart and Ezekowitz, 2008; Marmaras and Lampropoulou, 2009). The phagocytic process involves recognition of non-self, binding of particle to phagocytic cell, signal transduction, activation of pseudopodium formation, ingestion of particle, formation of phagosome, fusion of phagosome and lysosome to form phagolysosome, and destruction of particle (Gillespie et al., 1997; Stuart and Ezekowitz, 2005; Jiravanichpaisal et al., 2006). Plasmatocytes appear to be the main phagocytic cells in

Drosophila while both plasmatocytes and granular cells play a role in lepidopterans (Lavine and Strand, 2002; Jiravanichpaisal et al., 2006).

Large numbers of foreign invaders can be removed from an insect by another cellular response called nodulation. Nodulation is the entrapment of foreign invaders by hemocyte aggregates (Gillespie et al., 1997; Jiravanichpaisal et al., 2006). Encapsulation is similar to nodulation, but is the process by which large invaders such as nematodes and parasitoids are removed. Encapsulation of latex beads by *M. sexta* revealed that plasmatocytes adhere directly to the beads followed by layers containing both plasmatocytes and granular cells until capsule formation is complete (Wiegand et al., 2000). In contrast, encapsulation by *Pseudoplusia includens* starts with granular cells, is followed by plasmatocytes, and ends with a layer of granular cells (Pech and Strand, 1996), which suggests that the process of capsule formation is not the same for all insects. Nodulation and encapsulation are usually accompanied by melanization and once the capsule is formed, the invader is destined to die. Factors involved in death are thought to include asphyxiation, production of toxic compounds from the prophenoloxidase pathway, production of reactive oxygen or nitrogen species, and the production of antimicrobial peptides (Jiravanichpaisal et al., 2006; Marmaras and Lampropoulou, 2009).

Work completed in the early 1980s characterized the fate of pathogenic and non-pathogenic bacteria injected into *M. sexta* (Dunn and Drake, 1983; Horohov and Dunn, 1983). *Escherichia coli*, a non-pathogenic bacterium, injected into *M. sexta* larvae did not cause insect mortality and a reduction in viable bacteria was observed in the insect after approximately 30 min (Dunn and Drake, 1983). Mortality caused by *Pseudomonas aeruginosa* ranged from 25-100% depending on the strain and dose used. The fate of viable *E. coli* or *P. aeruginosa* injected into immunized larvae revealed an initial reduction in the number of viable bacteria that was followed by a period of no change in bacterial concentration and elimination of the bacteria from the insect or host death. From these observations, it was hypothesized that the immune response began with nodulation at the injection site, was followed by phagocytosis, and ended with bacterial clearance due to bactericidal factors (Dunn and Drake, 1983). Horohov and Dunn (1983) examined this hypothesis in more detail and defined three stages (nodulation, phagocytosis, and antibacterial reactions) of immune response. Nodulation was characterized by a reduction in circulating bacteria and the presence of melanized nodules in dissected larvae. In

stage two, or phagocytosis, there was no evidence of nodule formation, many granular cells were present, and signs of intracellular digestion were observed (Horohov and Dunn, 1983).

Hemocyte numbers vary between insects, but in some lepidopterans the hemocyte number per larva can be on the order of 10^4 to10^6 hemocytes; however, this number is not constant (Jiang et al., 2010). In *M. sexta*, the number and type of circulating hemocytes changed throughout development (Beetz et al., 2004, Beetz et al., 2008; Eleftherianos et al., 2008). Total hemocyte numbers increased during the 4th larval instar, peaked before molting to 5th instar larvae, and decreased during the 5th instar and pupal stages (Beetz et al., 2008). At the same time, changes in hemocyte type were observed. Granular cells dominated the hemocyte population early in the 5th larval instar while plasmatocytes were the dominant cell type in pupae. Oenocytoids and spherule cells disappeared during the wandering stage. Gender differences, although not statistically significant, were also observed. In general, females had higher hemocyte numbers than males, and plasmatocytes represented the majority of hemocytes from the beginning of the 5th larval instar until the onset of the wandering stage in females (Beetz et al., 2008). Differences in gender suggest that females are more immunocompetent than males with overall fitness being defined by the investment of energy in different activities. In 2008, Eleftherianos et al., found that hemocyte number decreases throughout the development of the 5th instar and was accompanied by a decrease in phenoloxidase activity, lower levels of phagocytosis, and less melanotic nodule formation, which indicate that the immune function in older larvae is reduced compared to young larvae. As a result, injection of *P. luminescens* resulted in higher levels of bacterial growth, increased bacterial colonization of the gut, and increased mortality (Eleftherianos et al., 2008). Such results suggest that developmental stage can have a dramatic impact on the stimulation of immune responses.

Mediators of hemocyte immune responses

An important step in nodulation and encapsulation is the adhesion of hemocytes to the foreign invader. Hemocyte adhesion molecules, such as integrins, tetraspanins, and neuroglian, mediate the attachment of hemocytes (Jiang, 2008; Kanost and Nardi, 2008; Jiang et al, 2010). Integrins are heterodimeric proteins that are found on the surface of hemocytes, and are composed of α and β subunits (Burke, 1999; Takada et al., 2007; Zhuang et al., 2008). In *M. sexta*, one integrin heterodimer has been identified (α1β1) and is referred to as hemocyte-specific

integrin (Levin et al., 2005; Zhuang et al., 2007b). Two additional α subunits have been found, and RNAi knockdown of each subunit abolished encapsulation, which supports the role of integrins in this cellular response (Levin et al., 2005; Zhuang et al., 2008). Another type of protein found on the surface of hemocytes is tetraspanin, an integral membrane protein that plays a role in cell adhesion. Tetraspanin D76 interacts with hemocyte-specific integrin during encapsulation of foreign invaders by *M. sexta* (Zhuang et al., 2007b). The monoclonal antibody, MS13 (specific to β1-integrin), or dsRNA for β1-integrin disrupted the binding of the large extracellular loop from D76 to the integrin, and subsequently, cell adhesion. Injection of mAb 1G2, an antibody specific for D76, into larvae decreased the encapsulation of latex beads (Zhuang et al., 2007b). These results were similar to those obtained by injecting an antibody specific to β1-integrin or dsRNA for β1-integrin (Levin et al., 2005). Neuroglian can be found on the surface of granular cells and a subpopulation of plasmatocytes, and is characterized by having six immunoglobulin domains. Binding of neuroglian to integrins is accomplished through the immunoglobulin domains and can be disrupted by the addition of an antibody specific to these domains (Zhuang et al., 2007a). Furthermore, encapsulation is disrupted when *M. sexta* larvae are treated with dsRNA for neuroglian (Zhuang et al., 2007a).

In addition to hemocyte adhesion molecules, a number of proteins have been identified as mediators of cellular responses. Hemolin and hemocyte aggregation inhibitor protein (HAIP) have been found to negatively regulate hemocyte adhesiveness in *M. sexta* (Ladendorff and Kanost, 1991; Kanost et al., 1994). Cytokines from the ENF family, such as plasmatocyte spreading peptide (PSP), stimulate the spreading and adhesion of plasmatocytes and reduce bleeding (Clark et al., 1997; Wang et al., 1999; Kanost et al., 2004). Knockdown of PSP decreases hemocyte aggregation in *M. sexta* larvae injected with *E. coli* and nodulation in larvae injected with *E. coli* or *P. luminescens* (Eleftherianos et al., 2009). Lacunin, a ligand for peanut agglutinin lectin, and hemocytin are all molecules produced and released by granular cells. Lacunin and a glycoprotein detected by peanut agglutinin bind to granular cells and plasmatocytes, possibly through interactions with integrins and neuroglian (Nardi et al., 2005).

Eicosanoids are regulators of some insect hemocyte responses (Shrestha and Kim, 2008; Shrestha and Kim, 2009; Stanley et al., 2009). Seven eicosanoids including six prostaglandins and one leukotriene were able to induce phagocytosis and nodulation after *Spodoptera exigua* larvae were treated with an eicosanoid biosynthesis inhibitor and subjected to immune challenge

(Shrestha and Kim, 2009). Prostaglandins, but not leukotriene stimulate the rupture of oenocytoids and release of prophenoloxidase (Shrestha and Kim, 2008; Shrestha and Kim, 2009). Release of prophenoloxidase increased phenoloxidase activity and was negatively correlated to intact oenocytoid density (Shrestha and Kim, 2008).

Pattern Recognition Proteins

Response to infection starts with the recognition of fungi, microbial cells, or cell surface components, such as peptidoglycan, lipopolysaccharide, β-1,3-glucan, or lipoteichoic acid by pattern recognition proteins in hemolymph. In the past, pattern recognition proteins have been cloned and/or purified from a number of insects, including several lepidopterans. Peptidoglycan recognition protein (PGRP) was purified and cDNA cloned from *Bombyx mori* (Yoshida et al., 1996), cloned from *Trichoplusia ni* (Kang et al., 1998), and isolated and cDNA cloned from *Manduca sexta* (Yu et al., 2002; Sumathipala and Jiang, 2010). *B. mori* (Ochiai and Ashida, 1988), *M. sexta* (Ma and Kanost, 2001; Jiang et al., 2004), and *Plodia interpunctella* (Fabrick et al., 2003; Fabrick et al., 2004) contain at least one β-1,3-glucan recognition protein (βGRP) that recognizes β-1,3-glucan and lipopolysaccharide. Gram-negative binding protein (GNBP) is similar to βGRP and has been purified from *B. mori* (Lee et al., 1996) and *Drosophila melanogaster* (Lemaitre and Hoffman, 2007). Four C-type lectins, referred to as immulectins, have been purified and characterized from *M. sexta* (Yu et al., 1999; Yu and Kanost, 2000; Yu et al., 2005; Yu et al., 2006). Hemolin was isolated from *Hyalophora cecropia* (Sun et al., 1990) and *M. sexta* (Ladendorff and Kanost, 1990; Ladendorff and Kanost, 1991). Subsequent discussion will focus on pattern recognition proteins found in *M. sexta*.

Hemolin

Hemolin is a 48 kDa glycoprotein belonging to the immunoglobulin supefamily found in *M. sexta* (Ladendorff and Kanost, 1990; Ladendorff and Kanost, 1991). Four immunoglobulin-like domains are found within hemolin and arrange in such a way that the three-dimensional structure resembles a horseshoe (Su et al., 1998). Hemolin concentration in hemolymph and hemolin mRNA levels in fat body increased upon bacterial challenge, which indicated a possible role in immune reactions (Ladendorff and Kanost, 1990; Ladendorff and Kanost, 1991). Experiments have shown that hemolin associated with hemocytes and blocked hemocyte

aggregation (Ladendorff and Kanost, 1991). Hemolin is present at low levels in hemolymph of naïve larvae until larvae enter the wandering stage. At this time, hemolymph concentration increased and continued to increase to higher levels in pupae and adults. In addition, expression of hemolin mRNA increased in the fat body and midgut of wandering stage larvae (Yu and Kanost, 1999). Hemolin bound to bacteria (Ladendorff and Kanost, 1991) and more specifically, to lipopolysaccharide from gram-negative bacteria and lipoteichoic acid from gram-positive bacteria (Yu and Kanost, 2002). RNAi knockdown of hemolin resulted in decreased numbers of hemocytes and increased numbers of bacteria in larvae challenged with *E. coli*. Decreased phagocytosis, nodulation, and hemocyte aggregation were also observed in RNAi treated insects (Eleftherianos et al., 2007). Similar to RNAi knockdown of hemolin, the presence of recombinant CcV1 (endosymbiont bracovirus of *Cotesia congregata*) decreased hemocyte aggregation by hemolin. Binding of hemolin to lipopolysaccharide was also reduced in the presence of CcV1 (Labropoulou et al., 2008). These results indicate that hemolin may function as a pattern recognition protein or as a modulator of cell-cell interactions during infection.

Peptidoglycan recognition proteins

Peptidoglycan is a component of gram-positive and gram-negative bacterial cell walls. Polymers of peptidoglycan consist of linear glycan strands containing alternating *N*-acetylglucosamine and *N*-acetylmuramic acid residues linked in a β-1,4 manner and are cross-linked by short peptide chains (Vollmer et al., 2008). For gram-negative bacteria and *Bacillus* species a meso-diaminopimelic acid (DAP) group is in the third position of the peptide chain while a lysine is present in gram-positive bacteria. Peptidoglycan is recognized by proteins referred to as peptidoglycan recognition proteins (PGRPs).

PGRP is a 19 kDa protein that is constitutively expressed in fat body; however, upon bacterial challenge, the levels of PGRP mRNA increase (Yu et al., 2002). Two cDNA clones for PGRP were identified by substractive hydridization, but only differed in the amino acid sequence of the predicted signal peptide (Zhu et al., 2003a). Sumathipala and Jiang (2010) showed that recombinant PGRP-1 binds to soluble peptidoglycan from *E. coli*, but not peptidoglycan from *Staphylococcus aureus*. PGRP-1 bound to insoluble peptidoglycan from *Micrococcus luteus*, *Bacillus megaterium*, and *Bacillus subtilis*, but no binding was observed with insoluble peptidoglycan from *S. aureus* (Sumathipala and Jiang, 2010). Phenoloxidase activity increased in

a dose dependent manner when recombinant PGRP-1 was added to naïve plasma. Futhermore, samples containing PGRP-1, naïve plasma, and elicitor produced higher levels of PO activity when compared to samples with only naïve plasma and elicitor. These results indicate that PGRP-1 is involved in the proPO activation pathway of *M. sexta* (Sumathipala and Jiang, 2010).

β-1,3-glucan recognition proteins

An important component of fungal cell walls is β-1,3-glucan. Pattern recognition proteins that bind to β-1,3-glucan are called β-1,3-glucan recognition proteins. Two βGRPs from *M. sexta* have been isolated and characterized (Ma and Kanost, 2000; Jiang et al., 2004). Like other βGRPs, they bind β-1,3-glucan and contain a C-terminal glucanase-like domain. βGRP-1 is constitutively expressed in fat body, but not integument or hemocytes (Ma and Kanost, 2000). βGRP-1 bound and agglutinated cells from *Saccharomyces cerevisiae, Micrococcus lysodeikticus* (=*luteus*), and *E. coli*. The presence of βGRP-1, laminarin, and naïve plasma stimulated proPO activation. Unlike βGRP-1, βGRP-2 is present only in wandering, non-feeding larvae (Jiang et al., 2004). Transcripts of βGRP-2 are not present in fat body from naïve larvae, but levels increase in larvae challenged by yeast or bacteria. Yeast and bacterial cells are agglutinated by βGRP-2. βGRP-2 binds to laminarin and lipoteichoic acid, but not lipopolysaccharide. Addition of βGRP-2 to induced hemolymph incubated with laminarin dramatically increases PO activity, whereas incubation with lipoteichoic acid or lipopolysaccharide did not stimulate proPO activation (Jiang et al., 2004).

Microbe binding protein: A new member of the β-1,3-glucanase-related protein superfamily

Pyrosequencing analysis of expressed sequences tags (ESTs) for hemolymph proteins in *M. sexta* revealed 218 previously unknown sequences coding for defense molecules (Zou et al., 2008). Of these new cDNA sequences, six encoded polypeptides similar to the gram-negative binding protein (GNBP) from *Bombyx mori* (Lee et al., 1996). The complete sequence, minus the first nucleotide, of microbe binding protein (MBP) was obtained by screening plaques of an induced fat body cDNA library and searching EST databases (Wang et al., 2011). MBP is an inducible 51 kDa protein with five potential glycosylation sites and six cysteine residues. The sequence of MBP is 61% identical to *B. mori* GNBP and 34-36% identical to *M. sexta* βGRP-1 and -2. To study the binding properties and potential function of MBP, recombinant protein was

produced using a baculovirus system. Purified MBP bound to intact bacteria and fungi as well as to specific insoluble and soluble cell surface components (insoluble: β-1,3-glucan, DAP-type peptidoglycan from *Bacillus subtilis* and *Escherichia coli*, and Lys-type peptidoglycan from *Staphylococcus aureus*; soluble: lipopolysaccharide, lipoteichoic acid, *E. coli* DAP-type peptidoglycan, *S. aureus* Lys-type peptidoglycan, and laminarin) (Wang et al., 2011). When MBP was mixed with naïve or induced plasma in the absence of elicitor, a concentration-dependent increase in activation of proPO was observed. Following this experiment, recombinant MBP was mixed with various elicitors to investigate if the addition of MBP could enhance proPO activation. Plasma alone or plasma plus MBP produced low levels of PO activity. PO activity was detected in mixtures containing plasma plus elicitor, but higher levels of PO activity were observed if plasma was incubated with MBP and elicitor. Statistically significant increases in PO activity were observed when the elicitor was DAP-type peptidoglycan from *E. coli*, *B. subtilis*, or *Bacillus megaterium*, Lys-type peptidoglycan from *Micrococcus luteus*, and lipoteichoic acid (Wang et al., 2011). Binding to a variety of microbial cells and cell surface components suggest that MBP serves as a pattern recognition protein during infection, and the ability of MBP to enhance proPO activation indicates that this protein works in concert with other defense molecules to stimulate the activation of proPO.

Immulectins

M. sexta contains at least four C-type lectins, named immulectins 1-4 (IML 1-4) (Yu et al., 1999; Yu and Kanost, 2000; Yu et al., 2005; Yu et al., 2006). Immulectins contain two carbohydrate recognition domains that may or may not bind the same type of carbohydrate (Yu and Kanost, 2008). IMLs 1-4 can agglutinate gram-negative bacteria (*E. coli*), gram-positive bacteria (*S. aureus*), and yeast (*S. cerevisiae*) (Yu et al., 1999; Yu et al., 2005; Yu et al., 2006). IML-2 can also agglutinate erythrocytes from horse, human, and sheep (Yu and Kanost, 2000). In all cases, agglutination is calcium and IML concentration dependent. mRNA levels in fat body of all four IMLs are upregulated after injection of bacteria (Yu et al., 1999; Yu and Kanost, 2000; Yu et al., 2005; Yu et al., 2006). IML-1 binds lipopolysaccharide from *E. coli* and sugars, including mannose, glucose, and galactose; however, IML-1 does not bind laminarin (Yu et al., 1999). Immobilized lipopolysaccharide from *E. coli*, bacterial lipid A, lipoteichoic acid, peptidoglycan, fungal mannan, β-1,3-glucan are bound by IML-2 (Yu and Kanost, 2000; Yu and

Ma, 2006). IML-3 and IML-4 bind lipopolysaccharide, lipoteichoic acid, and laminarin (Yu et al., 2005; Yu et al., 2006). IML-1 and IML-2 bind lipopolysaccharide to stimulate proPO activation in plasma (Yu et al., 1999; Yu and Kanost, 2000). Encapsulation by hemocytes is enhanced by IML-1, IML-2, IML-3, or IML-4, but only IML-2 and IML-4 enhance melanization of immulectin coated beads (Yu and Kanost, 2004; Ling and Yu, 2006; Yu et al., 2005). The ability of immulectins to bind bacteria and cell surface components, stimulate proPO activation, and enhance encapsulation by hemocytes indicates that immulectins play an important role as pattern recognition proteins in response to infection.

Prophenoloxidase Pathway

One important component of innate immunity is the prophenoloxidase (proPO or PPO) activation pathway. Prophenoloxidase activation can be triggered by foreign invaders or by mechanical injury (Cerenius and Söderhäll, 2004). Activation of proPO in response to infection starts with the recognition of microbial cells or cell surface components by pattern recognition proteins in hemolymph followed by stimulation of a serine proteinase cascade that terminates in the activation of proPO (proPO) to phenoloxidase (PO). Phenoloxidase is a copper-containing enzyme found in insect hemolymph that is important for melanization and wound healing. PO is synthesized as an inactive zymogen in oenocytoids, and is released into the hemolymph upon oenocytoid rupture (Kanost and Gorman, 2008; Shrestha and Kim, 2008). Active PO is involved in the production of cytotoxic compounds, production of melanin, and encapsulation of foreign invaders (Cerenius et al., 2008; Kanost and Gorman, 2008). Chemically speaking, PO is an essential component in the conversion of monophenols to o-diphenols by hydroxylation and o-diphenols to quinones by oxidation.

Activation of prophenoloxidase

Active PO is generated by specific proteolysis of proPO or by the presence of certain alcohols, organic compounds, detergents, or phospholipids. Prophenoloxidase purified from *Drosophila melanogaster* pupae was found to be activated by various alcohols and organic compounds (Asada et al., 1993). Highest proPO activation was observed with the addition of 2-propanol (Asada et al., 1993; Asada, 1998). Purified *M. sexta* proPO can be activated in the presence of the cationic detergent, cetylpyridinium chloride (CPC), but anionic or non-ionic

detergents did not activate proPO (Hall et al., 1995). Kinetic constants to characterize the binding and activation of proPO by CPC were determined using purified proPO from the blowfly, *Sarcophaga bullata* (Xie et al., 2007). Phospholipids have also been shown to activate proPO (Sugumaran and Nellaiappan, 1991; Bidla et al., 2009). In 1991, Sugumaran and Nellaiappan found that proPO from the lobster, *Homarus americanas*, could be activated by some anionic (sodium dodecyl sulfate) and cationic (CPC) detergents, fatty acids (linoleate, oleate, and palmitate), and phospholipids. Of all potential activators tested, the addition of lysolecithin resulted in the highest levels of proPO activation. More recently, Bidla et al. (2009) found that the addition of inner membrane phospholipids (phosphatidylserine and phosphatidylinositol), but not outer membrane phospholipids (phosphatidylcholine and phosphatidylethanolamine) to hemolymph from *D. melanogaster* stimulated PO activity. Results of the prior two studies suggest that the release of phospholipids from damaged cells could stimulate the activation of proPO after an insect has been injured.

proPO activation in Manduca sexta

M. sexta contains two proPO polypeptides, proPO-p1 (Jiang et al., 1997) and proPO-p2 (Hall et al., 1995). Each polypeptide is ~80 kDa. Crystal structure analysis of proPO confirmed that the protein is composed of two polypeptides, which form a heterodimer. ProPO-p1 and proPO-p2 consist of four domains; pro-region, domain 1, domain 2, and domain 3 (Li et al., 2009). In terms of secondary structure, domains 1 and 2 are dominated by α-helices, while domain 3 contains a seven-stranded, antiparallel β-sheet. The proteolytic cleavage site, Arg 51 is located within the α-helical pro-region, but is bordered by a two-stranded, parallel β-sheet. Each subunit contains a type 3 di-nuclear copper center in the active site found in domain 2, and each copper atom coordinates three His residues (Li et al., 2009). The amino acid sequence of *M. sexta* proPO-p1 is 78% identical to *Bombyx mori* proPO-p1 and 50% identical to *M. sexta* proPO-p2 while *M. sexta* proPO-p2 is 77% identical to *B. mori* proPO-p2 and 49% identical to *B. mori* proPO-p1 (Jiang et al., 1997). In addition, the proPO sequence is homologous to arthropod hemocyanins, which are oxygen-transport proteins, and insect hexamerin storage proteins. Synthesis of proPO occurs only in oenocytoids (Jiang et al., 1997), does not contain a signal peptide, and is released into the hemolymph when the oenocytoids rupture.

Prophenoloxidase freely circulates in the hemolymph as an inactive protein, but can become active in response to immune challenge.

Three prophenoloxidase-activating proteinases (PAPs 1-3) were discovered, and are involved in the activation of *M. sexta* proPO (Jiang et al., 1998; Jiang et al., 2003a, Jiang et al., 2003b). All PAPs are synthesized as zymogens and must be activated by proteolytic cleavage. PAP-1 is a 44 kDa protein that was isolated from a cuticular extract. This protein contains a signal peptide and one amino-terminal clip domain. Proteolytic activation of proPAP-1 occurs between Arg-127 and Ile-128 (Jiang et al., 1998). PAP-2 and PAP-3 were isolated from *M. sexta* hemolymph and contain two amino-terminal clip domains (Jiang et al., 2003a; Jiang et al., 2003b). PAP-2 undergoes proteolytic cleavage at Lys-153 (Jiang et al., 2003a) while PAP-3 is cleaved at Lys-146 (Jiang et al., 2003b). Active PAPs cleave proPO at Arg-51 to form PO, but little PO activity is generated. To increase levels of PO activity, serine proteinase homologs (SPHs) must be present, along with PAPs and proPO (Jiang et al., 1998; Jiang et al., 2003a; Jiang et al., 2003b; Gupta et al., 2005). SPHs contain an amino-terminal clip domain like several known serine proteinases, but the active site Ser has been replaced with Gly. SPH-1 and SPH-2 levels are stimulated by immune challenge, interact with immulectin-2, and enhance proPO activation (Yu et al., 2003).

Inhibition of the phenoloxidase pathway

Compounds produced by active PO can be detrimental to the health of an insect as some of them are cytotoxic. Therefore, it is of the utmost importance for proPO activation and PO activity to be regulated. One way that PO is regulated is by the synthesis of a protein zymogen that must be activated by proteolytic cleavage (Cerenius and Söderhäll, 2004) in response to a foreign invader. Proteinase inhibitors also play an important role in preventing unnecessary activation of proPO.

In the early 1990s, a competitive inhibitor of PO activity was discovered in the hemolymph of *Musca domestica* and named phenoloxidase inhibitor, or POI (Tsukamoto et al., 1992; Daquinag et al., 1995). POI is a peptide with a mass of 4.2 kDa. Sequence analysis revealed that POI is rich in cysteine and lysine residues, and contains a tyrosine residue (residue 32) that has been hydroxylated to 3,4-dihydroxyphenylalanine (DOPA). Such a modification

may play a role in binding to PO (Daquinag et al., 1995), but experimental evidence of this interaction is lacking.

Based on homology to *M. domestica* POI, a PO inhibitor from *Anopheles gambiae* was cloned and characterized (Shi et al., 2006). The protein had a molecular weight of 33.8 kDa and contained five cysteine knot motifs. POI was expressed in all developmental stages tested and further analysis revealed that the highest mRNA levels were in the adult fat body. Wounding or injection with Sephadex beads resulted in an increase of POI mRNA, but mRNA levels decreased after a blood meal. RNA interference (RNAi) was successfully used to knockdown POI transcript levels. RNAi treated mosquitoes had more melanization around the wound site than non-RNAi treated mosquitoes; however, melanization of Sephadex beads was not affected by RNAi treatment. These results suggest that POI plays a role in regulating the activity of PO. Sequence analysis identified similarity to two ESTs for a *M. sexta* POI. Recombinant POI production for one of the EST sequences was successful, but the POI could only inhibit PO at high concentrations (Lu and Jiang, 2007). Thus, the relevance of this *M. sexta* POI as a PO inhibitor is still in question. In the same study, a low molecular weight compound was isolated and exhibited strong inhibition of PO and mushroom tyrosinase.

Epidermal growth factor-like 1.0 (Egf1.0) is a protein that is similar to small serine proteinase inhibitors (smapin family), and is encoded by the *Microplitis demolitor* bracovirus (MdBV) (Beck and Strand, 2007). Recombinant Egf1.0 added to hemolymph from *M. sexta* decreased PO activity in a dose-dependent manner. Amino acid sequence alignment of Egf1.0 with several small serine proteinase inhibitors predicted P1-P1' residues to be Arg-Phe, which happens to be the P1-P1' site of most insect proPOs. The authors hypothesized that Egf1.0 may interact with prophenoloxidase-activating proteinases to inhibit melanization (Beck and Strand, 2007). Addition of Egf1.0 to PAP-3 impaired the ability of PAP-3 to cleave an artificial substrate, indicating that Egf1.0 is an effective inhibitor of PAP-3. To further verify the results, the authors used an Egf1.0 mutant in which the P1 Arg was changed to an Ala. This mutant was not able to block PAP-3 amidase activity. Finally, if PO was already activated, the addition of Egf1.0 could not inhibit PO activity. This further suggests that Egf1.0 inhibits proPO activation. Egf1.0 also inhibits the activity of *M. sexta* PAP-1, the processing of proPAP-1 and proPAP-3, and the processing of proPO and serine proteinase homologs 1 and 2 (SPH1-2) (Lu et al., 2008).

Blocking of proPO activation by *M. demolitor* allows for successful host parasitization and prevents the death of the wasp's offspring by the host immune system.

Venom from the endoparasitoid, *Leptopilina boulardi*, inhibits the PO pathway in *Drosophila yakuba* larvae (Colinet et al., 2009). The venom contains a 46 kDa serine proteinase inhibitor (serpin family), LbSPNy, which blocks PO activation. Hemolymph injected with venom or recombinant LbSPNy exhibited little or no melanization when compared to hemolymph injected with bovine serum albumin. Analysis of LbSPNy predicted that the P1 residue was Arg, which suggests that LbSPNy targets proteinases with trypsin-like specificity. Sequence alignment of the reactive center loop from LbSPNy and several known serpins revealed that the P3-P1' residues of LbSPNy matched those of *M. sexta* serpin-6, a known inhibitor of PAP-3 (Wang and Jiang, 2004). Therefore, LbSPNy may inhibit proteinases required for proPO activation. Results from this study led authors to hypothesize that LbSPNy inhibits steps prior to proPO activation and not PO activity directly (Colinet et al., 2009).

In the late 1990s, a melanization preventing factor (MPF) was discovered on Sephadex carboxymethyl (CM) beads injected into and recovered from *Anopheles gambiae* strain 4a rr (non-melanizing strain). When these beads were transferred into strain L3-5 (melanizing strain), no melanization was observed, and treatment of beads with protease K abolished MPF activity indicating the MPF was a protein (Paskewitz and Riehle, 1998). Proteins bound to CM beads recovered from 4a rr mosquitoes were subjected to electrophoresis followed by silver staining. Amino-terminal sequencing revealed the presence of lysozyme c-1 (Lys c-1) and cytochrome C (Li and Paskewitz, 2006). Knockdown of Lys c-1 in 4a rr mosquitoes resulted in decreased MPF activity and increased melanization of CM beads transferred to the melanizing strain G3 while purified Lys c-1 from *An. gambiae* cell line 4a3B inhibited dopachrome formation by phenoloxidase. How these results translate to the melanization of malarial parasites or pathogens is not clear, but the authors hypothesized that lysozyme may prevent melanization under certain conditions (Li and Paskewitz, 2006). Injection of dsLYSC-1 into one day old *An. gambiae* G3 females followed by injection of *M. luteus* did not impact mosquito survival as the bacteria were rapidly melanized. However, the opposite impact was observed with injection of *E. coli* indicating that the role of lysozyme in an immune response may depend on the invading pathogen (Kajla et al., 2010). *In vitro* experiments suggest that lysozyme (0.25 µg/µL) inhibits proPO activation in naïve plasma (2 µL) from *M. sexta*, but not in plasma pre-activated by

laminarin (Rao et al., 2010). Purified *M. sexta* lysozyme in combination with naïve plasma contained proPO, but not PO. Conversely, when bovine serum albumin was added to naïve plasma, both proPO and PO were detected. Moreover, the addition of lysozyme appeared to stimulate the degradation of proSPH-2 and proPAP-1, two key components in the PO cascade. Pattern recognition proteins, such as immulectin-2 and -3 were not degraded by the addition of lysozyme. These results suggest that lysozyme inhibits the PO pathway by preventing the conversion of proPO to PO (Rao et al., 2010). The biological relevance of lysozyme as an inhibitor of proPO activation in *M. sexta* remains unknown, and *in vivo* experiments must be completed.

Inhibition of phenoloxidase-induced melanin synthesis

Active PO catalyzes several reactions that lead to the formation of melanin. Excessive melanin production can be detrimental to an organism and must be regulated. A novel melanization-inhibiting protein (MIP) was isolated from hemolymph of the beetle, *Tenebrio molitor* (Zhao et al., 2005). Recombinant MIP (rMIP) added to crude hemolymph in the presence of dopamine, calcium, and β-1,3-glucan inhibited melanin synthesis in a dose-dependent manner. However, PO and amidase activity were not impacted by the presence of rMIP, which indicates that MIP does not inhibit proPO activation. Knockdown of *mip* using dsRNA for MIP resulted in increased melanin synthesis when compared to larvae injected with dsRNA for green fluorescent protein, further confirming that MIP is a regulator of melanin synthesis (Zhao et al., 2005). A functionally similar protein to *Tenebrio* MIP was isolated from the crayfish, *Pacifastacus leniusculus* (Söderhäll et al., 2009). Unlike *Tenebrio* MIP, *Pl*-MIP contains a fibrinogen-like domain and an Asp-rich region that may be important calcium binding. Recombinant *Pl*-MIP inhibited PO activity in a dose-dependent manner when added to a mixture containing hemocyte lysate supernatant, lipopolysaccharide-peptidoglycan or β-1,3-glucan, and L-DOPA as substrate. However, if hemolymph was pre-activated, the addition of recombinant *Pl*-MIP did not inhibit PO activity. Deletion of the Asp residues decreased the ability of *Pl*-MIP to inhibit PO activity, indicating that this region is important for protein function. Plasma was depleted of MIP protein by the addition of *Pl*-MIP antibodies and added to a culture of granular cells. After incubation, the cells were melanized and melanized particles were found throughout the dish. Control plasma

containing *Pl*-MIP exhibited little or no melanization. These results indicate that *Pl*-MIP regulates proPO activation and subsequent melanin synthesis (Söderhäll et al., 2009).

Toll Pathway

In the 1980s, the Toll pathway was first identified in the dorsal-ventral patterning of *Drosophila melanogaster* embryos (Anderson et al., 1985; Imler and Hoffmann, 2001). Since then, research has been conducted to identify the serine proteinases that are involved in a proteolytic cascade that ends with the activation of the cytokine, spätzle, which binds to a receptor called Toll. The initiation of this pathway has not been well characterized, but it has been suggested that a product produced by pipe serves as the necessary signal to determine dorsal-ventral polarity (Anderson, 1998; Sen et al., 1998; LeMosy et al., 2001). Within the oocyte, pipe is located in ventral follicle cells and encodes an enzyme that is similar to heparin sulfate 2-O-sulfotransferase (Sen et al., 1998). Once initiated, the cascade takes place in the perivitelline space (Morisato and Anderson, 1995) and involves four serine proteinases; nudel, gastrulation defective, snake, and easter (LeMosy and Hashimoto, 2000; Dissing et al., 2001; LeMosy et al., 2001; Rose et al., 2003). Nudel activation is poorly understood, but appears to be independent of gastrulation defective, snake, and easter (LeMosy et al., 1998). After activation, nudel has been speculated to play a role in the cleavage of gastrulation defective (Rose et al., 2003; Kanost and Clarke, 2005). However, it has also been suggested that gastrulation defective undergoes autoactivation when in contact with the zymogen of snake (Dissing et al., 2001). In the same study, it was shown that snake can cleave gastrulation defective in different locations to function as a feedback mechanism. Gastrulation defective cleaves snake, a clip domain serine proteinase. In turn, snake cleaves another clip domain serine proteinase, easter (LeMosy et al., 2001; Rose et al., 2003). Finally, easter, whose activity is regulated by serpin-27A (Ligoxygakis et al., 2003), activates spätzle. Spätzle binds and activates Toll at the plasma membrane. Activation of Toll leads to a signal transduction pathway that involves Myd88, Tube, Pelle, Cactus, and a member of the Rel family of transcription factors, Dorsal (Belvin and Anderson, 1996; Imler and Hoffmann, 2001).

Insects have multiple strategies to combat the presence of foreign pathogens including bacteria and fungi. One of these strategies is the rapid synthesis of antimicrobial peptides in the fat body with subsequent secretion into the hemolymph. Production of antimicrobial peptides in

response to gram-positive bacteria or fungi occurs after the activation of the Toll pathway. The first documented case of the involvement of the Toll pathway in immune responses came in 1996, when Lemaitre et al., showed that *spätzle*, *Toll*, *tube*, *pelle*, and *cactus* controlled the antifungal response in *D. melanogaster* adults. Interestingly, mutations in *snake* or *easter*, had no impact on antifungal response, indicating that different genes/proteinases may be involved in the Toll pathway for immune response (Lemaitre et al., 1996). In *Drosophila*, antimicrobial peptides include drosomycin and metchnikowin in response to fungi (Fehlbaum et al., 1994; Lemaitre and Hoffmann, 2007), attacin, diptericin, drosocin, defensin, and cecropin A1. Diptericin, attacin, drosocin, and cecropin A1 are mostly in response to gram-negative bacteria while defensin acts in response to infection by gram-positive bacteria (Hoffmann, 2003; Lemaitre and Hoffman, 2007). However, attacin and cecropin A1 were found to be active against some fungi as well (Lemaitre and Hoffman, 2007).

In *Drosophila*, induction of the Toll pathway in response to fungi starts with the recognition of fungal cell wall components (*i.e.* β-1,3-glucan) by gram-negative binding proteins, which are similar to βGRPs. Members of this family contain an amino-terminal domain that binds to β-1,3-glucan and a carboxyl-terminal domain that is similar to a β-glucanase. However, the C-terminal domain is not active due to the lack of a key residue that confers glucanase-like activity. Specifically, GNBP3 is involved in the recognition of fungal cell wall components and activation of the Toll pathway (Gottar et al., 2006). Furthermore, the amino-terminal domain of GNBP3 binds to long chains, but not short chains of β-1,3-glucans (Mishima et al., 2009). After recognition, a serine proteinase cascade is set in motion. Persephone was the first proteinase found to be involved in the response to fungi (Ligoxygakis et al., 2002). Activity of persephone is thought to be regulated by the serine proteinase inhibitor, necrotic (Levashina et al., 1999; Robertson et al., 2003). Another proteinase found in this cascade is spätzle-processing enzyme (SPE) (Jang et al., 2006). SPE activates spätzle, which in turn binds to Toll. After binding to Toll, an intracellular signal transduction cascade is initiated that results in the nuclear uptake of Dorsal-related immunity factor (DIF) and production of drosomycin. Additionally, the activation of the Toll pathway via persephone can occur in response to the secreted fungal virulence factor, PR1, a protease (Gottar et al., 2006).

Initiation of the Toll pathway in *Drosophila* in the presence of gram-positive bacteria requires peptidoglycan recognition proteins (PGRPs). Lys-type peptidoglycan found in gram-

positive bacteria can be recognized by PGRP-SA or PGRP-SD (Michel et al., 2001; Bischoff et al., 2004). Moreover, PGRP-SA forms a complex with GNBP1 to activate a serine proteinase cascade that leads to the activation of Toll (Gobert et al., 2003; Pili-Floury et al., 2004). Characterization of complex formation between PGRP-SA and GNBP1 is still unclear, but it is thought that GNBP1 hydrolyzes Lys-type peptidoglycan into smaller fragments (muropeptides) to provide a processed form of peptidoglycan to PGRP-SA. PGRP-SA binds to these smaller peptidoglycan fragments while physically interacting with GNBP1 to stimulate downstream signaling (Wang et al., 2006). In addition, the presence of PGRP-SD appears to enhance the ability of GNBP1 to bind to peptidoglycan which in turn enhances the interaction between PGRP-SA and GNBP1 (Wang et al., 2008). After recognition, it has been suggested that a modular serine protease, lacking a clip domain, links the PGRP-SA/GNBP1 complex to the remainder of the serine proteinase cascade that leads to the production of antimicrobial peptides (Buchon et al., 2009). Downstream of modular serine protease are the clip domain containing proteinases Grass, Spirit (Kambris et al., 2006; El Chamy et al., 2008) and SPE (Jang et al., 2006). Once activated, SPE cleaves and activates pro-spätzle (Jang et al., 2006). As with the response to fungal infection, activated spätzle will bind Toll, which initiates an intracellular signal transduction pathway that leads to the production of antimicrobial peptides.

In addition to *Drosophila*, Toll-like receptors have been found in other insect species in five different orders which include Orthoptera, Hymenoptera, Coleoptera, Lepidoptera, and Diptera (Ao et al., 2008). Within the past several years, the extracellular activation of the Toll pathway of *Tenebrio molitor* and the proteinases involved have been well-characterized (Kim et al., 2008; Roh et al., 2009; Jiang et al., 2009). Similar to *Drosophila*, *T. molitor* recognizes Lys-type peptidoglycan from gram-positive bacteria via a PGRP-SA and GNBP1 complex (Park et al., 2007). Following recognition is a serine proteinase cascade that involves modular serine protease, SPE-activating enzyme (SAE), and spätzle-activating enzyme (SPE). The proteinases SAE and SPE both contain a clip domain. Activation of SPE is followed by the cleavage of pro-spätzle to spätzle and binding of spätzle to Toll (Kim et al., 2008). Binding to Toll stimulates an intracellular signal transduction pathway that results in the production of two antimicrobial peptides, tenecin 1 and tenecin 2 (Roh et al., 2009). Interestingly, activation of the Toll pathway in response to fungal infection utilizes the same three proteinases as determined for the response to gram-positive bacteria. The difference occurs at the step of recognition. Here, GNBP3

recognizes β-1,3-glucan located on the fungal cell wall (Roh et al., 2009). The serine proteinases involved in this pathway, and therefore, the production of antimicrobial peptides in response to infection are regulated by serine proteinase inhibitors. Modular serine protease activity is inhibited by SPN40 while SAE was inhibited by SPN55 and SPE by SPN48 (Jiang et al., 2009).

Understanding the role of the Toll pathway in the immune response of lepidopteran insects has been slow. In 2008, a Toll receptor cDNA was cloned from *Manduca sexta* (Ao et al.). Expression analysis revealed that MsToll was found in the hemocytes, fat body, epidermis, midgut, and Malpighian tubules. Furthermore, upon immune challenge with *E. coli*, mRNA levels were up-regulated in hemocytes, but not fat body (Ao et al., 2008). Injection of *B. mori* spätzle-1 stimulates the transcription of antimicrobial peptides in both *Bombyx* and *M. sexta*. Additionally, when pro-BmSpz1 and *Micrococcus luteus* were incubated with plasma from *M. sexta* larvae, processing of pro-BmSpz1 was observed (Wang et al., 2007). Recently, pro-spätzle-1 was isolated from *M. sexta* and characterized (An et al., 2010). Pro-spätzle-1 mRNA levels in hemocytes increased by 20-fold when larvae had been injected by *E. coli* or *M. luteus*. As discussed below, recombinant pro-spätzle-1 is cleaved and activated by hemolymph proteinase 8. When active spätzle was injected in larvae, mRNA levels of several antimicrobial peptides increased (An et al., 2010). The results from these three studies clearly indicate that a Toll pathway in response to immune challenge functions in lepidopteran insects.

Antimicrobial Peptides and Proteins

Antimicrobial peptides and proteins (AMPs) are synthesized in response to bacterial challenge, and are secreted into the hemolymph. AMPs are highly expressed by the fat body, but can also be produced in hemocytes, pericardial cells, Malpighian tubules, and midgut (Gillespie et al., 1997). AMPs are expressed in extra-embryonic tissues in eggs of *M. sexta* in response to bacterial challenge (Gorman et al., 2004) and in epidermal cells of *B. mori* in response to wounding or infection of the cuticle (Brey et al., 1993; Lee and Brey, 1995). AMPs have been isolated, cloned, and biochemically characterized in various insects; however, the following discussion will be focused on those found in lepidopteran insects, with emphasis on *M. sexta*. AMPs found in *M. sexta* include lysozyme (Mulnix and Dunn, 1994; López-Zavala et al., 2004), cecropins (Dickinson et al., 1988; Zhu et al., 2003a), attacins (Kanost et al., 1990; Zhu et al.,

2003a), lebocins (Zhu et al., 2003a; Rayaprolu et al., 2010), moricin (Zhu et al., 2003a; Dai et al., 2008), and gloverin (Zhu et al., 2003a).

Lysozyme is a ubiquitous protein that degrades peptidoglycan in bacterial cell walls by hydrolyzing β-1,4-glycosidic linkages between N-acetylmuramic acid and N-acetylglucosamine. This ~ 14 kDa protein has been identified in a number of lepidopteran species, including *Galleria mellonella* (Powning and Davidson, 1973; Mak et al., 2010), *Hyalophora cecropia* (Hultmark et al., 1980), *M. sexta* (Mulnix and Dunn, 1994), *B. mori* (Croizier and Croizier, 1978; Lee and Brey, 1995), *Samia cynthia ricini* (Fujimoto et al., 2001), *Antheraea mylitta* (Jain et al., 2001), *Spodoptera exigua* (Bae and Kim, 2003), *Pseudoplusia includens* (Lavine et al., 2005), *Trichoplusia ni* (Freitak et al., 2007), *Helicoverpa armigera* (Zhang et al., 2009), and *Spodoptera frugiperda* (Chapelle et al., 2009). Complete amino acid and nucleotide sequences from an invertebrate were obtained from analysis of *H. cecropia* lysozyme (Engström et al., 1985). Comparison of cecropia lysozyme to other lysozymes revealed that the protein contains eight conserved Cys residues for the stabilization of the protein by disulfide bonds and two amino acids that contain carboxylic acid side chains required for catalytic activity (Engström et al., 1985). Lysozyme from *M. sexta* shares 78.3% and 80% identity to the amino acid sequences of *H. cecropia* and *B. mori*, respectively (Mulnix and Dunn, 1994; López-Zavala et al., 2004). Circular dichroism revealed the secondary structure of *M. sexta* lysozyme to be 57% α-helix, 2.5% β-sheet, 20% loops and turns, and 20.5% random coil (López-Zavala et al., 2004). Lysozyme mRNA levels increase in the presence of injected gram-positive bacteria (Lee and Brey, 1995), lipopolysaccharide and a phorbol ester, phorbol 12-myristate 13-acetate (Sun et al., 1991), and injected peptidoglycan fragments (Mulnix and Dunn, 1994). Highest mRNA levels were in fat body. Lysozyme activity in *M. sexta* was increased by the injection of gram-negative and gram-positive bacteria with different cell surface components and pathogenicity to *M. sexta*, with highest activity in hemolymph from larvae injected with *Escherichia coli* 0111:B4 (Kanost et al., 1988). Induction of lysozyme activity was also observed with injected particles (India ink and latex particles), polysaccharides (zymosan, glucan, and mannan), bacterial components (lipopolysaccharide and Lipid A), and purified *M. luteus* cell walls. The most significant increase in lysozyme activity was observed with injected *M. luteus* cell walls (Kanost et al., 1988). Peptidoglycan is a major component of *M. luteus* cell walls. Injection of soluble peptidoglycan or peptidoglycan fragments generated by digestion with hen egg white lysozyme were good

inducers of lysozyme activity, indicating that peptidoglycan plays a role in stimulating the production of antimicrobial peptides in the immune response of *M. sexta*. In addition to killing bacteria, lysozyme appears to regulate proPO activation in *M. sexta* (Rao et al., 2010).

Cecropins were first isolated and purified from immunized pupae of *H. cecropia* (Hultmark et al., 1980). They are ~4 kDa basic proteins (Jiang et al., 2010) that have lytic activity against gram-negative and gram-positive bacteria (Steiner et al., 1981; Hultmark et al., 1982). Three cecropin D-like peptides were isolated and characterized from *M. sexta* larvae (Dickinson et al., 1988). Cecropin mRNA was expressed in several tissues, including midgut, malpighian tubules, salivary gland, muscle, pericardial cell complex, epidermis with cuticle, hemocytes, and fat body. Highest mRNA levels were detected in fat body (Dickinson et al., 1988). Subtractive suppression hybridization identified one EST from the fat body of *M. sexta* that showed similarity to preprocecropin D from *H. cecropia* (Zhu et al., 2003a; Gorman et al., 2004), which was different from the cecropins discovered by Dickinson et al. (1988).

Another group of inducible, antibacterial peptides, called attacins, was isolated from *H. cecropia* (Hultmark et al., 1983). Attacins are ~20 kDa, glycine-rich, and can be categorized as basic or acidic depending on their amino acid composition. These proteins are effective killers of gram-negative bacteria such as *E. coli*, *Acinetobacter calcoaceticus*, and *Pseudomonas maltophilia*, but not gram-positive bacteria (Hultmark et al., 1983). Attacin acts by increasing the permeability of the outer membrane (Engström et al., 1984) and disrupting outer membrane protein synthesis in *E. coli* (Carlsson et al., 1991). Ten ESTs found in the fat body of *M. sexta* were similar to attacin (Zhu et al., 2003a). Of the ten ESTs, five showed identity to the amino-terminus of acidic attacin. Further comparison revealed that *M. sexta* contains at least four genes that encode sequences for attacin (Zhu et al., 2003a). Injection of *M. sexta* larvae with lipopolysaccharide or peptidoglycan from *E. coli*, lipoteichoic acid or peptidoglycan from *B. subtilis*, and lipoteichoic acid or peptidoglycan from *S. aureus* significantly increased the expression of attacin in fat body and hemocytes compared to saline-injected larvae (Rao and Yu, 2010). Expression also increased in a dose-dependent manner, and the degree of increase depended on the bacterial component being tested and the bacterial source of the component.

Gloverin, like attacin, is a glycine-rich protein. This inducible, antibacterial protein is ~13.8 kDa and was first isolated from *Hyalophora gloveri* pupae (Axén et al., 1997). Gloverin effectively inhibits the growth of *E. coli*, a gram-negative bacterium, by using a similar

mechanism as attacin. After interacting with lipopolysaccharide, gloverin inhibits the synthesis of outer membrane components, which increases the permeability of the outer membrane. Gloverin is heat-stable at 100°C for at least 10 min; however, antibacterial activity is lost when magnesium or free lipopolysaccharide is present (Axén et al., 1997). Studies involving gloverin have also been conducted in *Trichoplusia ni* (Lundström et al., 2002) and *B. mori* (Kawaoka et al., 2008). Six ESTs corresponding to the gloverin precursor in *T. ni* were identified in *M. sexta* (Zhu et al., 2003a).

A proline-rich inducible, antimicrobial peptide, called lebocin, was originally isolated from *B. mori* (Hara and Yamakawa, 1995b; Chowdhury et al., 1995; Furukawa et al., 1997) and later from *T. ni* (Liu et al., 2000) and *Pseudoplusia includens* (Lavine et al., 2005). Mature lebocin is ~3.5 kDa and O-glycosylated on threonine residues (Hara and Yamakawa, 1995b; Liu et al., 2000). Synthetic peptides, which lack O-glycosylation, exhibited little or no antibacterial activity when compared to wild-type lebocin, suggesting that this modification is essential for peptide function (Hara and Yamakawa, 1995b). Lebocin appears to target bacterial membranes and increases the permeability of liposomes at low ionic strength (Hara and Yamakawa, 1995b). Seven *M. sexta* ESTs corresponding to lebocin were identified. Five were similar to lebocin 4 precursor of *B. mori* and two were similar to lebocin-like protein from *T. ni*, indicating that at least two genes encoding for lebocin are present (Zhu et al., 2003a). Recently, 17 lebocin-like cDNA clones were isolated and sequenced from *M. sexta* (Rayaprolu et al., 2010). Three RXXR motifs, which can be recognized by an intracellular processing enzyme to generate five peptides, were found during sequence analysis of the pro-segment. Four of the possible peptides were chemically synthesized, purified, and tested for antibacterial activity. Peptide 1 (Q^{1}-R^{22}) inhibited growth of both gram-positive and gram-negative bacteria whereas peptide 3 (S^{67}-R^{101}) showed low activity against *E. coli*, and peptides 2 (E^{23}-R^{66}) and 4 (S^{102}-R^{128}) were inactive (Rayaprolu et al., 2010). Peptides 1, 2, and 3 were found in larval hemolymph, which supports the hypothesis that post-translational processing of pro-lebocin to active lebocin is important for function (Rayaprolu et al., 2010).

Originally isolated from *B. mori*, moricin is a 42-amino acid residue protein that is highly basic and predicted to have an amino-terminal α-helix (Hara and Yamakawa, 1995a). Moricin has also been found in *M. sexta* (Zhu et al., 2003a), *Spodoptera litura* (Oizumi et al., 2005), *Galleria mellonella* (Brown et al., 2008; Brown et al., 2009), and *Helicoverpa armigera* (Wang

et al., 2010). Injection with bacteria increases moricin mRNA levels in fat body and hemocytes (Furukawa et al., 1999; Dai et al., 2008), and expression can be stimulated by lipopolysaccharide and lipid A from *E. coli* (Furukawa et al., 1999; Rao and Yu, 2010). Increases in expression have also been observed in *M. sexta* larvae injected with lipoteichoic acid and peptidoglycan (Rao and Yu, 2010). Moricin has a broad spectrum of activity as it can prevent the growth of gram-positive and gram-negative bacteria (Hara and Yamakawa, 1995a; Oizumi et al., 2005; Brown et al., 2008), fungi (Brown et al., 2008), and yeast (Brown et al., 2008). The solution structure of *B. mori* (Hemmi et al., 2002), *S. litura* (Oizumi et al., 2005), and *M. sexta* (Dai et al., 2008) moricin revealed an eight-turn α-helix that almost spans the full length of the protein, and is speculated to play a role in protein function (Hara and Yamakawa, 1995a; Hemmi et al., 2002). To kill invading bacteria, moricin is hypothesized to target the bacterial membrane and increase membrane permeability (Hara and Yamakawa, 1995a).

Hemolymph Proteinases Found in *Manduca sexta*

Hemolymph of the caterpillar, *M. sexta*, contains at least twenty-seven serine proteinases (Jiang et al., 1999; Jiang et al., 2005; Wang et al., 2006). Hemolymph proteinases (HPs) are synthesized as zymogens and are activated by specific proteolytic cleavage. Once activated, some of these proteinases may function in aspects of innate immune responses, including the activation of cytokine precursors and prophenoloxidase (Kanost et al., 2001).

Expression analysis of these hemolymph proteinases revealed that transcripts are present in hemocytes (HPs 13, 15, and 18), fat body (HPs 12, 20-22), or both tissues (HPs 1-7, 9-11, 14, 16, 19) (Jiang et al., 2005; Wang et al., 2006). HP12 mRNA was also found in the tracheae and integument of day 3, fifth instar larvae and in the midgut of day 3 wandering larvae, suggesting that it may function in the protection against pathogen invasion (Wang et al., 2006). HP17 was not present in hemocytes or fat body from naïve larvae, but was detected after immune challenge (Jiang et al., 2005), whereas HP24 transcripts were not found in hemocytes or fat body of naïve or immune-challenged larvae (Wang et al., 2006). Additionally, the expression of many HPs (2, 5, 7, 9, 10, 13-17, 19-21) can be stimulated when an insect has been immune challenged, indicating a possible role in the innate immune response of the insect. mRNA levels for HPs 3, 4, 11 decreased after immune challenge in both hemocytes and fat body (Jiang et al., 2005). Transcripts for HP6 and HP8 were constitutively expressed in hemocytes and fat body, and

transcript levels did not increase after larvae were injected with *E. coli*, *M. luteus*, or curdlan from *Alcaligenes faecalis* (An et al., 2009).

Of the known hemolymph proteinases, sixteen contain at least one amino-terminal clip domain (Jiang et al., 1999; Jiang et al., 2005; Wang et al., 2006). A clip domain is composed of 37-55 amino acid residues with three disulfide bonds. Although the function of the clip domain(s) is unknown, it is thought that they may play a role in proteinase regulation. The amino-terminal clip domain is attached to the carboxyl-terminal serine proteinase domain by a linker region that ranges in length from 23 to 101 amino acid residues (Jiang and Kanost, 2000). Activation of these proteinases occurs via proteolytic cleavage between the clip and serine proteinase domains. After cleavage, the two domains remain connected through a disulfide bond (Jiang and Kanost, 2000; Kanost et al., 2001).

Since the discovery of these proteinases, the task has been to investigate their function within the insect. Through the production of recombinant proteinases, the role of seven proteinases has been elucidated (Ji et al., 2004; Gorman et al., 2007; Wang and Jiang, 2007; An et al., 2009; An et al., 2010). In response to peptidoglycan from gram-positive bacteria or fungi plus β-1,3-glucan recognition protein (βGRP-2), HP14 autoactivates (Ji et al., 2004) to start the prophenoloxidase activation pathway. HP14, which exhibits chymotrypsin-like specificity, cleaves proHP21. Activation of proHP21 has been observed by proteolysis between Leu and Ile, the predicted activation site (Wang and Jiang, 2007), and at a site different from the expected activation site (Gorman et al., 2007). Active HP21 proteolytically cleaves prophenoloxidase-activating proteinase-2 (PAP-2; Wang and Jiang, 2007) or PAP-3 (Gorman et al., 2007). Finally, PAP-2 or PAP-3, in the presence of cleaved serine proteinase homologs (SPHs), activates prophenoloxidase (Gorman et al., 2007; Wang and Jiang, 2007). Active phenoloxidase catalyzes oxidation of catechols to quinones. Further reactions involving the quinones result in the formation of melanin.

In another study, An et al. (2009), found a role for HP6 in the activation of prophenoloxidase and activation of cytokine-like proteins. HP6 contains one amino-terminal clip domain and is most similar to *Drosophila* Persephone (Jiang et al., 2005; An et al., 2009). When bacteria or fungi are present, HP6 is cleaved and activated by an unknown proteinase (An et al., 2009). Next, HP6 activates proPAP-1 (An et al., 2009). Finally, in the presence of SPHs, PAP-1 activates proPO and leads to melanin synthesis. In addition, HP6 can cleave and activate another

serine proteinase, HP8 (An et al., 2009). HP8 also contains one amino-terminal clip domain and is the most similar to *Drosophila* Easter, *Drosophila* spätzle-processing enzyme (SPE), and *Tenebrio* SPE (An et al., 2009). The latter group of enzymes has been implicated in the activation of the cytokine precursor, prospätzle, in the Toll pathway. Injection of larvae with active HP6 or HP8 induced the expression of several antimicrobial peptides and proteins, including attacin, cecropin, gloverin, moricin, and lysozyme (An et al., 2009). These results suggest that HP8, when activated by HP6 plays a role in the activation of a Toll-like pathway. In a subsequent study, recombinant HP8 was shown to cleave recombinant *M. sexta* prospätzle and release active spätzle C108 (An et al., 2010). Spätzle C108 corresponds to the C-terminal 108 residue domain of prospätzle and is a disulfide-linked homodimer. When spätzle C108 was injected into larvae, expression levels of moricin, attacin-1, cecropin-6, and hemolin increased when compared to injection of buffer or prospätzle (An et al., 2010). Results from these two studies (An et al., 2009; An et al., 2010) provide evidence supporting the hypothesis that HP6 and HP8 are involved in the activation of a Toll-like pathway in *M. sexta* that leads to the production of antimicrobial peptides.

Serpins and Serpin Mode of Action

Serpins belong to a superfamily of proteins that inhibit serine proteinases through a suicide inhibition mechanism. However, not all serpins inhibit serine proteinases and not all serpins are inhibitory. Noninhibitory serpins have been shown to function as chaperones in rats (Clarke et al., 1991) and hormone transporters in humans (Hammond et al., 1987). Inhibitory serpins have been found in higher animals, plants, insects and other arthropods, nematodes, viruses, green algae, unicellular eukaryotes, prokaryotes, and fungi (Potempa et al., 1994; Irving et al., 2000; Irving et al., 2002; Riahi et al., 2004; Roberts et al., 2004; Steenbakkers et al., 2008). In humans, such inhibitors play a crucial role in the maintenance of homeostasis, and when present in plasma, target proteinases that are involved in phagocytosis, coagulation, complement activation, and fibrinolysis (Potempa et al., 1994).

In 2004, Riahi et al., identified the first serpin from a unicellular eukaryote, *Entamoeba histolytica*. The serpin (*Ehserp*) from this gastrointestinal protozoan parasite is located in the cytoplasm of resting cells, lacks a signal peptide, and is released when the trophozoites come into contact with mammalian cells. When tested for inhibitory activity against serine proteinases,

recombinant *Ehserp* showed no activity. However, when the secretion product of activated trophozoites was tested, human cathepsin G was inhibited. Further analysis of the interaction between the secretion product and cathepsin G identified a stable complex between *Ehserp* and cathepsin G. These results suggest that the presence of *Ehserp* may help the parasite survive by evading the host defense system (Riahi et al., 2004; Roberts et al., 2004).

The function of serpins in plants remains unclear, but it is hypothesized that they may play a role in the regulation of proteolysis that is important for plant growth, development, response to stress, defense against insects and pathogens, and protection of seed storage proteins from exogenous proteinases (Roberts et al., 2003; Roberts and Hejgaard, 2008). Studies involving wheat, barley, rye, oats, pumpkin, apple, and *Arabidopisis* have shown that plant serpins can inhibit chymotrypsin serine proteinases from mammals *in vitro* (Rosenkrands et al., 1994; Roberts and Hejgaard, 2008); however, plants do not contain chymotrypsin proteinases. Recombinant *Arabidopisis* serpin1 can inhibit trypsin and the cysteine proteinase, metacaspase 9 (Vercammen et al., 2006). Inhibition of metacaspase 9 suggests that this serpin may be involved in the regulation of programmed cell death.

Serpins consist of a single chain of 350-400 amino acid residues and share a highly conserved structure composed of β-sheets and α-helices (Silverman et al., 2001). Between β-sheets A and C, is a flexible region termed the reactive center loop (RCL) that contains the P1 residue. It is the sequence of the RCL that determines serpin specificity. Inhibition of the target proteinase begins with the formation of a noncovalent complex between the serpin and the serine proteinase. However, once the proteinase cleaves the serpin at the P1 residue of the RCL, a covalent ester linkage is formed and the serpin is cleaved. Once cleaved, the serpin undergoes a dramatic conformational change. The RCL is inserted into β-sheet A, causing a 70Å translocation and active site distortion of the proteinase (Schulze et al., 1994; Wright, 1996; Silverman et al., 2001).

Serine Proteinase Inhibitors in Arthropods

Serine proteinase inhibitors found in arthropods can be classified into several different families which include Kazal, Kunitz, α-macroglobulins, and serpins (Kanost, 1999). Inhibitors in hemolymph may function to inhibit proteinases from bacteria and fungi as well as regulating endogenous proteinases involved in coagulation, prophenoloxidase activation, and cytokine

activation. In crayfish, a member of the Kazal family has been shown to inhibit chymotrypsin and subtilisin (Johansson et al., 1994). Members of the Kunitz family inhibit proteinases present in the horseshoe crab, *B. mori* (Sasaki, 1984), *M. sexta* (Ramesh et al., 1988), and *Sarcophaga bullata* (Papayannopoulos and Biemann, 1992). Serpins have been found in crayfish (Liang and Söderhäll, 1995; Liang et al., 1997), insects (Sasaki, 1984; Kanost et al., 1989; Stark et al., 1998; Cherqui et al., 2001; de Gregorio et al., 2002; Zou et al., 2006; Zou et al., 2007; Zou et al., 2009), horseshoe crabs (Miura et al., 1994; Miura et al., 1995; Agarwala et al., 1996), shrimp (Liu et al., 2009; Homvises et al., 2010), and ticks (Mulenga et al., 2003; Mulenga et al., 2007; Mulenga et al., 2009).

Serpins in *Manduca sexta*

At present, seven serpins have been found in *M. sexta* (Kanost, 2007). Of the known serpins, serpin-1 is unique because the gene that encodes for its production undergoes alternative splicing of exon 9 to produce 12 isoforms that exhibit different reactive center loops and, therefore, different proteinase specificity (Kanost et al., 1989; Jiang et al., 1994; Jiang et al., 1996; Jiang and Kanost, 1997). For example, serpin-1A has an Arg at the P1 site and was able to inhibit trypsin and plasmin while serpin-1B (Ala at P1) inhibited porcine pancreatic elastase. Serpin-1H, 1K, and 1Z all have a Tyr at the P1 site which allowed them to inhibit bovine pancreatic α-chymotrypsin and human cathepsin G. Serpin-1I (Leu at P1 site) inhibited elastase and chymotrypsin (Jiang and Kanost, 1997). In addition, serpin-1I has been shown to inhibit the activity of HP14 (Wang and Jiang, 2006) while serpin-1J inhibits PAP-2&3 (Jiang et al., 2003b). With a variety of techniques, stable complexes have been identified between HP8 and serpin-1A, 1E, and 1J (Ragan et al., 2010; An et al., 2011). Serpin-1J was the most efficient of these isoforms as an inhibitor of HP8 (An et al., 2011). SDS-PAGE and MALDI-TOF/TOF analysis of serpin-1 immunoaffinity purified from lipopolysaccharide-treated plasma revealed a complex between serpin-1K and midgut chymotrypsin and between HP1 and an unidentified serpin-1 isoform (Ragan et al., 2010). Expression of the serpin-1 gene is constitutive in both the fat body and hemocytes. Serpin-1 mRNA is abundant in feeding 4^{th} and 5^{th} instar larvae, but decreased quickly at the time of molting. Expression was negatively regulated by 20-hydroxyecdysone, a steroid hormone that triggers molting. No mRNA was detected by northern blot in pupae and adults (Kanost et al., 1995).

Serpin-2 is expressed in granular hemocytes, lacks a signal peptide, and expression is up-regulated upon bacterial challenge (Gan et al., 2001). Recombinant serpin-2 inhibited human cathepsin G (chymotrypsin/elastase-like specificity), but not bovine trypsin or chymotrypsin, porcine pancreatic elastase, porcine plasmin, human neutrophil elastase, or the cysteine proteinase papain. However, the biological function of this serpin in the insect is unknown (Gan et al., 2001).

Serpin-3 is a 435 amino acid residue protein that includes a 45-50 residue amino-terminal extension that is not observed in the other serpins and a secretion signal peptide. It is expressed in fat body, and its expression is up-regulated in the presence of bacteria (Zhu et al., 2003b). Functionally, serpin-3 abolishes the activation of proPO by inhibiting all three PAPs (Zhu et al., 2003b).

Serpins-4 and 5 are constitutively expressed in the fat body and hemocytes of larvae. Upon immune challenge, the expression levels of these serpins dramatically increase. Recombinant serpins-4 and -5 are poor inhibitors of PAPs. However, they inhibit the activation of the proPO pathway (Tong and Kanost, 2005). Since the PAPs are the final proteinases in the proPO activation pathway, this suggests that these serpins inhibit proteinases that occur upstream in the serine proteinase cascade. This is the case, as serpin-4 inhibits HP-1, HP-6, and HP-21 while serpin-5 inhibits, HP-1 and HP-6 (Tong et al., 2005; An and Kanost, 2010).

Serpin-6, like serpins-1, 4, and 5, is constitutively expressed in the fat body and hemocytes. Similarly, expression levels increase upon immune challenge (Zou and Jiang, 2005). Serpin-6 plays a role in the inhibition of the proPO pathway by inhibiting PAP-3, but not PAP-1 or PAP-2 (Wang and Jiang, 2004; Zou and Jiang, 2005). In addition, serpin-6 was shown to form a complex with HP8 (Zou and Jiang, 2005).

Goals of Current Research

My first project focused on hemolymph proteinase 16. HP16 is one of at least twenty-seven proteinaseses found in the hemolymph of *M. sexta* (Jiang et al., 1999; Jiang et al., 2005; Wang et al., 2006). These proteinases are synthesized as zymogens and are activated by specific proteolytic cleavage. Once activated, some of these proteinases may function in aspects of innate immune responses (Kanost et al., 2001). Since the discovery of these proteinases, the task has been to investigate their function within the insect. Thus, the goal of this project was to further

characterize HP16 and investigate its function in the innate immune response. To address this goal, I completed experiments to answer the following questions:

(1) Do HP16 protein levels in plasma and HP16 mRNA levels in fat body fluctuate during larval to pupal development?
(2) Are HP16 protein and HP16 mRNA expression levels stimulated by the injection of bacteria?
(3) Expression and purification of recombinant HP16 are necessary to elucidate the function of HP16; how can this be accomplished?
(4) Is HP16 activated upon exposure of plasma to microbial elicitors?
(5) What, if any, serpin-1 isoforms form a covalent complex with active HP16?

In my second project, work focused on the identification of serine proteinases in plasma that are inhibited by serpin-3. Original studies to identify endogenous proteinase targets of serpin-3 (Zhu et al., 2003b) were completed prior to obtaining sequences of many hemolymph proteinases (Jiang et al., 2005; Wang et al., 2006). I hypothesized that additional proteinases are also proteinase targets of serpin-3. To test this hypothesis, I performed experiments to investigate the following questions:

(1) Does exposure of plasma to bacteria stimulate the activation of plasma proteinases and the formation of serpin-proteinase complexes?
(2) What plasma proteins does serpin-3 inhibit?
(3) Can active hemolymph proteinase 8 (HP8) in plasma form a complex with serpin-3?
(4) Is a complex formed between purified, active HP8 and recombinant serpin-3?

My expection is that results from these two projects will provide a better understanding of hemolymph proteinase pathways involved in the innate immune response of *M. sexta* and their regulation. I also expect that findings from this work will lay a foundation for subsequent experiments involving the proteolytic activity, regulation, and biological function of HP16 as well as for experiments investigating the inhibitory activity of serpins against candidate proteinases.

References

Agarwala KL, Kawabata S, Miura Y, Kuroki Y, & Iwanaga S (1996) Limulus intracellular coagulation inhibitor type 3. Purification, characterization cDNA cloning, and tissue localization. *J Biol Chem* **271**: 23768-23774

An C, Ishibashi J, Ragan EJ, Jiang H, & Kanost MR (2009) Functions of *Manduca sexta* hemolymph proteinases HP6 and HP8 in two innate immune pathways. *J Biol Chem* **284**: 19716-19726

An C, Jiang H, & Kanost MR (2010) Proteolytic activation and function of the cytokine Spätzle in the innate immune response of a lepidopteran insect, *Manduca sexta*. *FEBS J* **277**: 148-162

An C & Kanost MR (2010) *Manduca sexta* serpin-5 regulates prophenoloxidase activation and the Toll signaling pathway by inhibiting hemolymph proteinase HP6. *Insect Biochem Mol Biol* **40**: 683-689

An C, Ragan EJ, & Kanost MR (2011) Serpin-1 splicing isoform J inhibits the proSpätzle-activating proteinase HP8 to regulate expression of antimicrobial hemolymph proteins in *Manduca sexta*. *Dev Comp Immunol* **35**: 135-141

Anderson KV (1998) Pinning down positional information: dorsal-ventral polarity in the *Drosophila* embryo. *Cell* **95**: 439-442

Anderson KV, Jurgens G, & Nusslein-Volhard C (1985) Establishment of dorsal-ventral polarity in the *Drosophila* embryo: genetic studies on the role of the Toll gene product. *Cell* **42**: 779-789

Ao JQ, Ling E, & Yu XQ (2008) A Toll receptor from *Manduca sexta* is in response to *Escherichia coli* infection. *Mol Immunol* **45**: 543-552

Asada N (1998) Reversible activation of prophenoloxidase with 2-propanol in *Drosophila melanogaster*. *J Exp Zool* **282**: 28-31

Asada N, Fukumitsu T, Fujimoto K, & Masuda K (1993) Activation of prophenoloxidase with 2-propanol and other organic compounds in *Drosophila melanogaster*. *Insect Biochem Mol Biol* **23**: 515-520

Axén A, Carlsson A, Engström A, & Bennich H (1997) Gloverin, an antibacterial protein from the immune hemolymph of *Hyalophora* pupae. *Eur J Biochem* **247**: 614-619

Bae S & Kim Y (2003) Lysozyme of the beet armyworm, *Spodoptera exigua*: activity induction and cDNA structure. *Comp Biochem Physiol B Biochem Mol Biol* **135**: 511-519

Beck MH & Strand MR (2007) A novel polydnavirus protein inhibits the insect prophenoloxidase activation pathway. *Proc Natl Acad Sci USA* **104**: 19267-19272

Beetz S, Brinkmann M, & Trenczek T (2004) Differences between larval and pupal hemocytes of the tobacco hornworm, *Manduca sexta*, determined by monoclonal antibodies and density centrifugation. *J Insect Physiol* **50**: 805-819

Beetz S, Holthusen TK, Koolman J, & Trenczek T (2008) Correlation of hemocyte counts with different developmental parameters during the last larval instar of the tobacco hornworm, *Manduca sexta*. *Arch Insect Biochem Physiol* **67**: 63-75

Belvin MP & Anderson KV (1996) A conserved signaling pathway: the *Drosophila* toll-dorsal pathway. *Annu Rev Cell Dev Biol* **12**: 393-416

Bidla G, Hauling T, Dushay MS, & Theopold U (2009) Activation of insect phenoloxidase after injury: endogenous versus foreign elicitors. *J Innate Immun* **1**: 301-308

Bischoff V, Vignal C, Boneca IG, Michel T, Hoffmann JA, & Royet J (2004) Function of the *Drosophila* pattern-recognition receptor PGRP-SD in the detection of Gram-positive bacteria. *Nat Immunol* **5**: 1175-1180

Brey PT, Lee WJ, Yamakawa M, Koizumi Y, Perrot S, Francois M, & Ashida M (1993) Role of the integument in insect immunity: epicuticular abrasion and induction of cecropin synthesis in cuticular epithelial cells. *Proc Natl Acad Sci USA* **90**: 6275-6279

Brown SE, Howard A, Kasprzak AB, Gordon KH, & East PD (2009) A peptidomics study reveals the impressive antimicrobial peptide arsenal of the wax moth *Galleria mellonella*. *Insect Biochem Mol Biol* **39**: 792-800

Brown SE, Howard A, Kasprzak AB, Gordon KH, & East PD (2008) The discovery and analysis of a diverged family of novel antifungal moricin-like peptides in the wax moth *Galleria mellonella*. *Insect Biochem Mol Biol* **38**: 201-212

Buchon N, Poidevin M, Kwon HM, Guillou A, Sottas V, Lee BL, & Lemaitre B (2009) A single modular serine protease integrates signals from pattern-recognition receptors upstream of the *Drosophila* Toll pathway. *Proc Natl Acad Sci USA* **106**: 12442-12447

Burke RD (1999) Invertebrate integrins: structure, function, and evolution. *Int Rev Cytol* **191**: 257-284

Burmester T (2002) Origin and evolution of arthropod hemocyanins and related proteins. *J Comp Physiol B* **172**: 95-107

Burmester T (1999) Evolution and function of the insect hexamerins. *Eur J Entomol* **96**: 213-225

Carlsson A, Engström P, Palva ET, & Bennich H (1991) Attacin, an antibacterial protein from *Hyalophora cecropia*, inhibits synthesis of outer membrane proteins in *Escherichia coli* by interfering with *omp* gene transcription. *Infect Immun* **59**: 3040-3045

Cerenius L, Kawabata S, Lee BL, Nonaka M, & Söderhäll K (2010) Proteolytic cascades and their involvement in invertebrate immunity. *Trends Biochem Sci* **35**: 575-583

Cerenius L, Lee BL, & Söderhäll K (2008) The proPO-system: pros and cons for its role in invertebrate immunity. *Trends Immunol* **29**: 263-271

Cerenius L & Söderhäll K (2004) The prophenoloxidase-activating system in invertebrates. *Immunol Rev* **198**: 116-126

Chapelle M, Girard PA, Cousserans F, Volkoff NA, & Duvic B (2009) Lysozymes and lysozyme-like proteins from the fall armyworm, *Spodoptera frugiperda*. *Mol Immunol* **47**: 261-269

Chapman RF (1998) *Insects: Structure and function.* Cambridge University Press: Cambridge UK

Cherqui A, Cruz N, & Simoes N (2001) Purification and characterization of two serine protease inhibitors from the hemolymph of *Mythimna unipuncta*. *Insect Biochem Mol Biol* **31**: 761-769

Chowdhury S, Taniai K, Hara S, Kadono-Okuda K, Kato Y, Yamamoto M, Xu J, Choi SK, Debnath NC, & Choi HK (1995) cDNA cloning and gene expression of lebocin, a novel member of antibacterial peptides from the silkworm, *Bombyx mori*. *Biochem Biophys Res Commun* **214**: 271-278

Clark KD, Pech LL, & Strand MR (1997) Isolation and identification of a plasmatocyte-spreading peptide from the hemolymph of the lepidopteran insect *Pseudoplusia includens*. *J Biol Chem* **272**: 23440-23447

Clarke EP, Cates GA, Ball EH, & Sanwal BD (1991) A collagen-binding protein in the endoplasmic reticulum of myoblasts exhibits relationship with serine protease inhibitors. *J Biol Chem* **266**: 17230-17235

Colinet D, Dubuffet A, Cazes D, Moreau S, Drezen JM, & Poirie M (2009) A serpin from the parasitoid wasp *Leptopilina boulardi* targets the *Drosophila* phenoloxidase cascade. *Dev Comp Immunol* **33**: 681-689

Croizier G & Croizier L (1978) Purification et comparaison immunologique de 2 lysozymes d'insects. *C R Acad Sci Paris* **286D**: 469-472

Dai H, Rayaprolu S, Gong Y, Huang R, Prakash O, & Jiang H (2008) Solution structure, antibacterial activity, and expression profile of *Manduca sexta* moricin. *J Pept Sci* **14**: 855-863

Daquinag AC, Nakamura S, Takao T, Shimonishi Y, & Tsukamoto T (1995) Primary structure of a potent endogenous dopa-containing inhibitor of phenol oxidase from *Musca domestica*. *Proc Natl Acad Sci USA* **92**: 2964-2968

De Gregorio E, Han SJ, Lee WJ, Baek MJ, Osaki T, Kawabata S, Lee BL, Iwanaga S, Lemaitre B, & Brey PT (2002) An immune-responsive Serpin regulates the melanization cascade in *Drosophila*. *Dev Cell* **3**: 581-592

Dean P, Richards EH, Edwards JP, Reynolds SE, & Charnley K (2004) Microbial infection causes the appearance of hemocytes with extreme spreading ability in monolayers of the tobacco hornworm *Manduca sexta*. *Dev Comp Immunol* **28**: 689-700

Dickinson L, Russell V, & Dunn PE (1988) A family of bacteria-regulated, cecropin D-like peptides from *Manduca sexta*. *J Biol Chem* **263**: 19424-19429

Dissing M, Giordano H, & DeLotto R (2001) Autoproteolysis and feedback in a protease cascade directing *Drosophila* dorsal-ventral cell fate. *EMBO J* **20**: 2387-2393

Dunn PE (1990) Humoral immunity in insects. *Bioscience* **40**: 738-744

Dunn PE & Drake D (1983) Fate of bacteria injected into naive and immunized larvae of the tobacco hornworm, *Manduca sexta*. *J Invertebr Pathol* **41**: 77-85

El Chamy L, Leclerc V, Caldelari I, & Reichhart JM (2008) Sensing of 'danger signals' and pathogen-associated molecular patterns defines binary signaling pathways 'upstream' of Toll. *Nat Immunol* **9**: 1165-1170

Eleftherianos I, Baldwin H, ffrench-Constant RH, & Reynolds SE (2008) Developmental modulation of immunity: changes within the feeding period of the fifth larval stage in the defence reactions of *Manduca sexta* to infection by *Photorhabdus*. *J Insect Physiol* **54**: 309-318

Eleftherianos I, Gökcen F, Felföldi G, Millichap PJ, Trenczek TE, ffrench-Constant RH, & Reynolds SE (2007) The immunoglobulin family protein Hemolin mediates cellular immune responses to bacteria in the insect *Manduca sexta*. *Cell Microbiol* **9**: 1137-1147

Eleftherianos I, Xu M, Yadi H, Ffrench-Constant RH, & Reynolds SE (2009) Plasmatocyte-spreading peptide (PSP) plays a central role in insect cellular immune defenses against bacterial infection. *J Exp Biol* **212**: 1840-1848

Engström A, Xanthopoulos KG, Boman HG, & Bennich H (1985) Amino acid and cDNA sequences of lysozyme from *Hyalophora cecropia*. *EMBO J* **4**: 2119-2122

Engström P, Carlsson A, Engström A, Tao ZJ, & Bennich H (1984) The antibacterial effect of attacins from the silk moth *Hyalophora cecropia* is directed against the outer membrane of *Escherichia coli*. *EMBO J* **3**: 3347-3351

Fabrick JA, Baker JE, & Kanost MR (2004) Innate immunity in a pyralid moth: functional evaluation of domains from a beta-1,3-glucan recognition protein. *J Biol Chem* **279**: 26605-26611

Fabrick JA, Baker JE, & Kanost MR (2003) cDNA cloning, purification, properties, and function of a beta-1,3-glucan recognition protein from a pyralid moth, *Plodia interpunctella*. *Insect Biochem Mol Biol* **33**: 579-594

Fehlbaum P, Bulet P, Michaut L, Lagueux M, Broekaert WF, Hetru C, & Hoffmann JA (1994) Insect immunity. Septic injury of *Drosophila* induces the synthesis of a potent antifungal peptide with sequence homology to plant antifungal peptides. *J Biol Chem* **269**: 33159-33163

Freitak D, Wheat CW, Heckel DG, & Vogel H (2007) Immune system responses and fitness costs associated with consumption of bacteria in larvae of *Trichoplusia ni*. *BMC Biol* **5**: 56

Fujimoto S, Toshimori-Tsuda I, Kishimoto K, Yamano Y, & Morishima I (2001) Protein purification, cDNA cloning and gene expression of lysozyme from eri-silkworm, *Samia cynthia ricini*. *Comp Biochem Physiol B Biochem Mol Biol* **128**: 709-718

Furukawa S, Tanaka H, Nakazawa H, Ishibashi J, Shono T, & Yamakawa M (1999) Inducible gene expression of moricin, a unique antibacterial peptide from the silkworm (*Bombyx mori*). *Biochem J* **340 (Pt 1)**: 265-271

Furukawa S, Taniai K, Ishibashi J, Hara S, Shono T, & Yamakawa M (1997) A novel member of lebocin gene family from the silkworm, *Bombyx mori*. *Biochem Biophys Res Commun* **238**: 769-774

Gan H, Wang Y, Jiang H, Mita K, & Kanost MR (2001) A bacteria-induced, intracellular serpin in granular hemocytes of *Manduca sexta*. *Insect Biochem Mol Biol* **31**: 887-898

Gillespie JP, Kanost MR, & Trenczek T (1997) Biological mediators of insect immunity. *Annu Rev Entomol* **42**: 611-643

Gobert V, Gottar M, Matskevich AA, Rutschmann S, Royet J, Belvin M, Hoffmann JA, & Ferrandon D (2003) Dual activation of the *Drosophila* toll pathway by two pattern recognition receptors. *Science* **302**: 2126-2130

Gorman MJ, Kankanala P, & Kanost MR (2004) Bacterial challenge stimulates innate immune responses in extra-embryonic tissues of tobacco hornworm eggs. *Insect Mol Biol* **13**: 19-24

Gorman MJ, Wang Y, Jiang H, & Kanost MR (2007) *Manduca sexta* hemolymph proteinase 21 activates prophenoloxidase-activating proteinase 3 in an insect innate immune response proteinase cascade. *J Biol Chem* **282**: 11742-11749

Gottar M, Gobert V, Matskevich AA, Reichhart JM, Wang C, Butt TM, Belvin M, Hoffmann JA, & Ferrandon D (2006) Dual detection of fungal infections in *Drosophila* via recognition of glucans and sensing of virulence factors. *Cell* **127**: 1425-1437

Gupta S, Wang Y, & Jiang H (2005) *Manduca sexta* prophenoloxidase (proPO) activation requires proPO-activating proteinase (PAP) and serine proteinase homologs (SPHs) simultaneously. *Insect Biochem Mol Biol* **35**: 241-248

Hall M, Scott T, Sugumaran M, Söderhäll K, & Law JH (1995) Proenzyme of *Manduca sexta* phenol oxidase: purification, activation, substrate specificity of the active enzyme, and molecular cloning. *Proc Natl Acad Sci USA* **92**: 7764-7768

Hammond GL, Smith CL, Goping IS, Underhill DA, Harley MJ, Reventos J, Musto NA, Gunsalus GL, & Bardin CW (1987) Primary structure of human corticosteroid binding globulin, deduced from hepatic and pulmonary cDNAs, exhibits homology with serine protease inhibitors. *Proc Natl Acad Sci USA* **84**: 5153-5157

Hara S & Yamakawa M (1995a) Moricin, a novel type of antibacterial peptide isolated from the silkworm, *Bombyx mori*. *J Biol Chem* **270**: 29923-29927

Hara S & Yamakawa M (1995b) A novel antibacterial peptide family isolated from the silkworm, *Bombyx mori*. *Biochem J* **310 (Pt 2)**: 651-656

Hemmi H, Ishibashi J, Hara S, & Yamakawa M (2002) Solution structure of moricin, an antibacterial peptide, isolated from the silkworm *Bombyx mori*. *FEBS Lett* **518**: 33-38

Hoffmann JA (2003) The immune response of *Drosophila*. *Nature* **426**: 33-38

Homvises T, Tassanakajon A, & Somboonwiwat K (2010) *Penaeus monodon* SERPIN, PmSERPIN6, is implicated in the shrimp innate immunity. *Fish Shellfish Immunol* **29**: 890-898

Horohov DW & Dunn PE (1983) Phagocytosis and nodule formation by hemocytes of *Manduca sexta* larvae following injection of *Pseudomonas aeruginosa*. *J Invertebr Pathol* **41**: 203-213

Hultmark D, Steiner H, Rasmuson T, & Boman HG (1980) Insect immunity. Purification and properties of three inducible bactericidal proteins from hemolymph of immunized pupae of *Hyalophora cecropia*. *Eur J Biochem* **106**: 7-16

Hultmark D, Engström A, Andersson K, Steiner H, Bennich H, & Boman HG (1983) Insect immunity. Attacins, a family of antibacterial proteins from *Hyalophora cecropia*. *EMBO J* **2**: 571-576

Hultmark D, Engström A, Bennich H, Kapur R, & Boman HG (1982) Insect immunity: isolation and structure of cecropin D and four minor antibacterial components from cecropia pupae. *Eur J Biochem* **127**: 207-217

Imler JL & Hoffmann JA (2001) Toll receptors in innate immunity. *Trends Cell Biol* **11**: 304-311

Irving JA, Pike RN, Lesk AM, & Whisstock JC (2000) Phylogeny of the serpin superfamily: implications of patterns of amino acid conservation for structure and function. *Genome Res* **10**: 1845-1864

Irving JA, Steenbakkers PJ, Lesk AM, Op den Camp HJ, Pike RN, & Whisstock JC (2002) Serpins in prokaryotes. *Mol Biol Evol* **19**: 1881-1890

Iwanaga S & Lee BL (2005) Recent advances in the innate immunity of invertebrate animals. *J Biochem Mol Biol* **38**: 128-150

Jain D, Nair DT, Swaminathan GJ, Abraham EG, Nagaraju J, & Salunke DM (2001) Structure of the induced antibacterial protein from tasar silkworm, *Antheraea mylitta*. Implications to molecular evolution. *J Biol Chem* **276**: 41377-41382

Jang IH, Chosa N, Kim SH, Nam HJ, Lemaitre B, Ochiai M, Kambris Z, Brun S, Hashimoto C, Ashida M, Brey PT, & Lee WJ (2006) A Spätzle-processing enzyme required for toll signaling activation in *Drosophila* innate immunity. *Dev Cell* **10**: 45-55

Ji C, Wang Y, Guo X, Hartson S, & Jiang H (2004) A pattern recognition serine proteinase triggers the prophenoloxidase activation cascade in the tobacco hornworm, *Manduca sexta*. *J Biol Chem* **279**: 34101-34106

Jiang H (2008) The biochemical basis of antimicrobial responses in *Manduca sexta*. *Insect Science* **15**: 53-66

Jiang H & Kanost MR (2000) The clip-domain family of serine proteinases in arthropods. *Insect Biochem Mol Biol* **30**: 95-105

Jiang H & Kanost MR (1997) Characterization and functional analysis of 12 naturally occurring reactive site variants of serpin-1 from *Manduca sexta*. *J Biol Chem* **272**: 1082-1087

Jiang H, Ma C, Lu ZQ, & Kanost MR (2004) Beta-1,3-glucan recognition protein-2 (betaGRP-2) from *Manduca sexta*; an acute-phase protein that binds beta-1,3-glucan and lipoteichoic acid to aggregate fungi and bacteria and stimulate prophenoloxidase activation. *Insect Biochem Mol Biol* **34**: 89-100

Jiang H, Vilcinskas A, Kanost MR (2010) Immunity in lepidopteran insects. In *Invertebrate Immunity*, Söderhäll K (ed) Landes Bioscience, http://www.landesbioscience.com/curie/chapter/4692/

Jiang H, Wang Y, Gu Y, Guo X, Zou Z, Scholz F, Trenczek TE, & Kanost MR (2005) Molecular identification of a bevy of serine proteinases in *Manduca sexta* hemolymph. *Insect Biochem Mol Biol* **35**: 931-943

Jiang H, Wang Y, Huang Y, Mulnix AB, Kadel J, Cole K, & Kanost MR (1996) Organization of serpin gene-1 from *Manduca sexta*. Evolution of a family of alternate exons encoding the reactive site loop. *J Biol Chem* **271**: 28017-28023

Jiang H, Wang Y, & Kanost MR (1999) Four serine proteinases expressed in *Manduca sexta* haemocytes. *Insect Mol Biol* **8**: 39-53

Jiang H, Wang Y, & Kanost MR (1998) Pro-phenol oxidase activating proteinase from an insect, *Manduca sexta*: a bacteria-inducible protein similar to *Drosophila* easter. *Proc Natl Acad Sci USA* **95**: 12220-12225

Jiang H, Wang Y, & Kanost MR (1994) Mutually exclusive exon use and reactive center diversity in insect serpins. *J Biol Chem* **269**: 55-58

Jiang H, Wang Y, Ma C, & Kanost MR (1997) Subunit composition of pro-phenol oxidase from *Manduca sexta*: molecular cloning of subunit ProPO-P1. *Insect Biochem Mol Biol* **27**: 835-850

Jiang H, Wang Y, Yu XQ, & Kanost MR (2003a) Prophenoloxidase-activating proteinase-2 from hemolymph of *Manduca sexta*. A bacteria-inducible serine proteinase containing two clip domains. *J Biol Chem* **278**: 3552-3561

Jiang H, Wang Y, Yu XQ, Zhu Y, & Kanost M (2003b) Prophenoloxidase-activating proteinase-3 (PAP-3) from *Manduca sexta* hemolymph: a clip-domain serine proteinase regulated by serpin-1J and serine proteinase homologs. *Insect Biochem Mol Biol* **33**: 1049-1060

Jiang R, Kim EH, Gong JH, Kwon HM, Kim CH, Ryu KH, Park JW, Kurokawa K, Zhang J, Gubb D, & Lee BL (2009) Three pairs of protease-serpin complexes cooperatively regulate the insect innate immune responses. *J Biol Chem* **284**: 35652-35658

Jiravanichpaisal P, Lee BL, & Söderhäll K (2006) Cell-mediated immunity in arthropods: hematopoiesis, coagulation, melanization and opsonization. *Immunobiology* **211**: 213-236

Johansson MW, Keyser P, & Söderhäll K (1994) Purification and cDNA cloning of a four-domain Kazal proteinase inhibitor from crayfish blood cells. *Eur J Biochem* **223**: 389-394

Kajla MK, Andreeva O, Gilbreath TM,3rd, & Paskewitz SM (2010) Characterization of expression, activity and role in antibacterial immunity of *Anopheles gambiae* lysozyme c-1. *Comp Biochem Physiol B Biochem Mol Biol* **155**: 201-209

Kambris Z, Brun S, Jang IH, Nam HJ, Romeo Y, Takahashi K, Lee WJ, Ueda R, & Lemaitre B (2006*) Drosophila* immunity: a large-scale in vivo RNAi screen identifies five serine proteases required for Toll activation. *Curr Biol* **16**: 808-813

Kang D, Liu G, Lundstrom A, Gelius E, & Steiner H (1998) A peptidoglycan recognition protein in innate immunity conserved from insects to humans. *Proc Natl Acad Sci USA* **95**: 10078-10082

Kanost MR (2007) Serpins in a lepidopteran insect, *Manduca sexta*. In *The Serpinopathies: Molecular and Cellular Aspects of Serpins and their Disorders,* Silverman GA & Lomas DA (eds) pp 229-242. World Scientific Publishing Co.: Hackensack, NJ

Kanost MR (1999) Serine proteinase inhibitors in arthropod immunity. *Dev Comp Immunol* **23**: 291-301

Kanost MR & Clarke T (2005) Proteases. In *Comprehensive Molecular Insect Science,* Gilbert LI, Iatrou K, Gill SS (eds) pp 247-265. Elsevier

Kanost MR, Dai W, & Dunn PE (1988) Peptidoglycan fragments elicit antibacterial protein synthesis in larvae of *Manduca sexta*. *Arch Insect Biochem Physiol* **8**: 147-164

Kanost MR & Gorman MJ (2008) Phenoloxidases in insect immunity. In *Insect Immunity,* Beckage NE (ed) pp 69-96. Elsevier

Kanost MR, Jiang H, Wang Y, Yu XQ, Ma C, & Zhu Y (2001) Hemolymph proteinases in immune responses of *Manduca sexta*. *Adv Exp Med Biol* **484**: 319-328

Kanost MR, Jiang H, & Yu XQ (2004) Innate immune responses of a lepidopteran insect, *Manduca sexta*. *Immunol Rev* **198**: 97-105

Kanost MR, Kawooya JK, Law JH, Ryan RO, Van Heusden MC, Ziegler R (1990) Insect haemolymph proteins. In *Advances in Insect Physiology,* Evans PD & Wigglesworth VB (eds) pp 299-396. Academic Press: San Diego

Kanost MR & Nardi JB (2008) Innate immune responses of *Manduca sexta*. In *Molecular Biology and Genetics of Lepidoptera,* Goldsmith MR & Marec F (eds) pp 271-291. CRC: Boca Raton, FL

Kanost MR, Prasad SV, Huang Y, & Willott E (1995) Regulation of serpin gene-1 in *Manduca sexta*. *Insect Biochem Mol Biol* **25**: 285-291

Kanost MR, Prasad SV, & Wells MA (1989) Primary structure of a member of the serpin superfamily of proteinase inhibitors from an insect, *Manduca sexta*. *J Biol Chem* **264**: 965-972

Kanost MR, Zepp MK, Ladendorff NE, & Andersson LA (1994) Isolation and characterization of a hemocyte aggregation inhibitor from hemolymph of *Manduca sexta* larvae. *Arch Insect Biochem Physiol* **27**: 123-136

Kawaoka S, Katsuma S, Daimon T, Isono R, Omuro N, Mita K, & Shimada T (2008) Functional analysis of four *Gloverin*-like genes in the silkworm, *Bombyx mori*. *Arch Insect Biochem Physiol* **67**: 87-96

Kim CH, Kim SJ, Kan H, Kwon HM, Roh KB, Jiang R, Yang Y, Park JW, Lee HH, Ha NC, Kang HJ, Nonaka M, Söderhäll K, & Lee BL (2008) A three-step proteolytic cascade mediates the activation of the peptidoglycan-induced toll pathway in an insect. *J Biol Chem* **283**: 7599-7607

Klowden MJ (2002) *Physiological systems in insects.* Academic Press: San Diego, CA

Labropoulou V, Douris V, Stefanou D, Magrioti C, Swevers L, & Iatrou K (2008) Endoparasitoid wasp bracovirus-mediated inhibition of hemolin function and lepidopteran host immunosuppression. *Cell Microbiol* **10**: 2118-2128

Ladendorff NE & Kanost MR (1991) Bacteria-induced protein P4 (hemolin) from *Manduca sexta*: a member of the immunoglobulin superfamily which can inhibit hemocyte aggregation. *Arch Insect Biochem Physiol* **18**: 285-300

Ladendorff NE & Kanost MR (1990) Isolation and characterization of bacteria-induced protein P4 from hemolymph of *Manduca sexta*. *Arch Insect Biochem Physiol* **15**: 33-41

Lavine MD, Chen G, & Strand MR (2005) Immune challenge differentially affects transcript abundance of three antimicrobial peptides in hemocytes from the moth *Pseudoplusia includens*. *Insect Biochem Mol Biol* **35**: 1335-1346

Lavine MD & Strand MR (2002) Insect hemocytes and their role in immunity. *Insect Biochem Mol Biol* **32**: 1295-1309

Lee WJ & Brey PT (1995) Isolation and characterization of the lysozyme-encoding gene from the silkworm *Bombyx mori*. *Gene* **161**: 199-203

Lee WJ, Lee JD, Kravchenko VV, Ulevitch RJ, & Brey PT (1996) Purification and molecular cloning of an inducible gram-negative bacteria-binding protein from the silkworm, *Bombyx mori*. *Proc Natl Acad Sci USA* **93**: 7888-7893

Lemaitre B & Hoffmann J (2007) The host defense of *Drosophila melanogaster*. *Annu Rev Immunol* **25**: 697-743

Lemaitre B, Nicolas E, Michaut L, Reichhart JM, & Hoffmann JA (1996) The dorsoventral regulatory gene cassette *spätzle/Toll/cactus* controls the potent antifungal response in *Drosophila* adults. *Cell* **86**: 973-983

LeMosy EK & Hashimoto C (2000) The nudel protease of *Drosophila* is required for eggshell biogenesis in addition to embryonic patterning. *Dev Biol* **217**: 352-361

LeMosy EK, Kemler D, & Hashimoto C (1998) Role of Nudel protease activation in triggering dorsoventral polarization of the *Drosophila* embryo. *Development* **125**: 4045-4053

LeMosy EK, Tan YQ, & Hashimoto C (2001) Activation of a protease cascade involved in patterning the *Drosophila* embryo. *Proc Natl Acad Sci USA* **98**: 5055-5060

Levashina EA, Langley E, Green C, Gubb D, Ashburner M, Hoffmann JA, & Reichhart JM (1999) Constitutive activation of toll-mediated antifungal defense in serpin-deficient *Drosophila*. *Science* **285**: 1917-1919

Levin DM, Breuer LN, Zhuang S, Anderson SA, Nardi JB, & Kanost MR (2005) A hemocyte-specific integrin required for hemocytic encapsulation in the tobacco hornworm, *Manduca sexta*. *Insect Biochem Mol Biol* **35**: 369-380

Li B & Paskewitz SM (2006) A role for lysozyme in melanization of Sephadex beads in *Anopheles gambiae*. *J Insect Physiol* **52**: 936-942

Li Y, Wang Y, Jiang H, & Deng J (2009) Crystal structure of *Manduca sexta* prophenoloxidase provides insights into the mechanism of type 3 copper enzymes. *Proc Natl Acad Sci USA* **106**: 17002-17006

Liang Z & Soderhall K (1995) Isolation of cDNA encoding a novel serpin of crayfish hemocytes. *Comp Biochem Physiol B Biochem Mol Biol* **112**: 385-391

Liang Z, Sottrup-Jensen L, Aspan A, Hall M, & Soderhall K (1997) Pacifastin, a novel 155-kDa heterodimeric proteinase inhibitor containing a unique transferrin chain. *Proc Natl Acad Sci USA* **94**: 6682-6687

Ligoxygakis P, Pelte N, Hoffmann JA, & Reichhart JM (2002) Activation of *Drosophila* Toll during fungal infection by a blood serine protease. *Science* **297**: 114-116

Ligoxygakis P, Roth S, & Reichhart JM (2003) A serpin regulates dorsal-ventral axis formation in the *Drosophila* embryo. *Curr Biol* **13**: 2097-2102

Ling E & Yu XQ (2006) Cellular encapsulation and melanization are enhanced by immulectins, pattern recognition receptors from the tobacco hornworm *Manduca sexta*. *Dev Comp Immunol* **30**: 289-299

Liu G, Kang D, & Steiner H (2000) *Trichoplusia ni* lebocin, an inducible immune gene with a downstream insertion element. *Biochem Biophys Res Commun* **269**: 803-807

Liu Y, Li F, Wang B, Dong B, Zhang X, & Xiang J (2009) A serpin from Chinese shrimp *Fenneropenaeus chinensis* is responsive to bacteria and WSSV challenge. *Fish Shellfish Immunol* **26**: 345-351

Lopez-Zavala AA, de-la-Re-Vega E, Calderon-Arredondo SA, Garcia-Orozco KD, Velazquez EF, Islas-Osuna MA, Valdez MA, & Sotelo-Mundo RR (2004) Biophysical characterization of an insect lysozyme from *Manduca sexta*. *Protein Pept Lett* **11**: 85-92

Lu Z, Beck MH, Wang Y, Jiang H, & Strand MR (2008) The viral protein Egf1.0 is a dual activity inhibitor of prophenoloxidase-activating proteinases 1 and 3 from *Manduca sexta*. *J Biol Chem* **283**: 21325-21333

Lu Z & Jiang H (2007) Regulation of phenoloxidase activity by high- and low-molecular-weight inhibitors from the larval hemolymph of *Manduca sexta*. *Insect Biochem Mol Biol* **37**: 478-485

Lundström A, Liu G, Kang D, Berzins K, & Steiner H (2002) *Trichoplusia ni* gloverin, an inducible immune gene encoding an antibacterial insect protein. *Insect Biochem Mol Biol* **32**: 795-801

Ma C & Kanost MR (2001) A beta-1,3-glucan-binding protein from *Manduca sexta*. *Adv Exp Med Biol* **484**: 309-312

Ma C & Kanost MR (2000) A beta-1,3-glucan recognition protein from an insect, *Manduca sexta*, agglutinates microorganisms and activates the phenoloxidase cascade. *J Biol Chem* **275**: 7505-7514

Mak P, Zdybicka-Barabas A, & Cytrynska M (2010) A different repertoire of *Galleria mellonella* antimicrobial peptides in larvae challenged with bacteria and fungi. *Dev Comp Immunol* **34**: 1129-1136

Marmaras VJ & Lampropoulou M (2009) Regulators and signalling in insect haemocyte immunity. *Cell Signal* **21**: 186-195

Michel T, Reichhart JM, Hoffmann JA, & Royet J (2001) *Drosophila* Toll is activated by Gram-positive bacteria through a circulating peptidoglycan recognition protein. *Nature* **414**: 756-759

Mishima Y, Quintin J, Aimanianda V, Kellenberger C, Coste F, Clavaud C, Hetru C, Hoffmann JA, Latge JP, Ferrandon D, & Roussel A (2009) The N-terminal domain of *Drosophila* gram-negative binding protein 3 (GNBP3) defines a novel family of fungal pattern recognition receptors. *J Biol Chem* **284**: 28687-28697

Miura Y, Kawabata S, & Iwanaga S (1994) A Limulus intracellular coagulation inhibitor with characteristics of the serpin superfamily. Purification, characterization, and cDNA cloning. *J Biol Chem* **269**: 542-547

Miura Y, Kawabata S, Wakamiya Y, Nakamura T, & Iwanaga S (1995) A limulus intracellular coagulation inhibitor type 2. Purification, characterization, cDNA cloning, and tissue localization. *J Biol Chem* **270**: 558-565

Morisato D & Anderson KV (1995) Signaling pathways that establish the dorsal-ventral pattern of the *Drosophila* embryo. *Annu Rev Genet* **29**: 371-399

Mulenga A, Khumthong R, & Blandon MA (2007) Molecular and expression analysis of a family of the *Amblyomma americanum* tick Lospins. *J Exp Biol* **210**: 3188-3198

Mulenga A, Khumthong R, & Chalaire KC (2009) *Ixodes scapularis* tick serine proteinase inhibitor (serpin) gene family; annotation and transcriptional analysis. *BMC Genomics* **10**: 217

Mulenga A, Tsuda A, Onuma M, & Sugimoto C (2003) Four serine proteinase inhibitors (serpin) from the brown ear tick, *Rhiphicephalus appendiculatus*; cDNA cloning and preliminary characterization. *Insect Biochem Mol Biol* **33**: 267-276

Mulnix AB & Dunn PE (1994) Structure and induction of a lysozyme gene from the tobacco hornworm, *Manduca sexta*. *Insect Biochem Mol Biol* **24**: 271-281

Nardi JB, Pilas B, Bee CM, Zhuang S, Garsha K, & Kanost MR (2006) Neuroglian-positive plasmatocytes of *Manduca sexta* and the initiation of hemocyte attachment to foreign surfaces. *Dev Comp Immunol* **30**: 447-462

Nardi JB, Zhuang S, Pilas B, Bee CM, & Kanost MR (2005) Clustering of adhesion receptors following exposure of insect blood cells to foreign surfaces. *J Insect Physiol* **51**: 555-564

Ochiai M & Ashida M (1988) Purification of a beta-1,3-glucan recognition protein in the prophenoloxidase activating system from hemolymph of the silkworm, *Bombyx mori*. *J Biol Chem* **263**: 12056-12062

Oizumi Y, Hemmi H, Minami M, Asaoka A, & Yamakawa M (2005) Isolation, gene expression and solution structure of a novel moricin analogue, antibacterial peptide from a lepidopteran insect, *Spodoptera litura*. *Biochim Biophys Acta* **1752**: 83-92

Papayannopoulos IA & Biemann K (1992) Amino acid sequence of a protease inhibitor isolated from *Sarcophaga bullata* determined by mass spectrometry. *Protein Sci* **1**: 278-288

Park JW, Kim CH, Kim JH, Je BR, Roh KB, Kim SJ, Lee HH, Ryu JH, Lim JH, Oh BH, Lee WJ, Ha NC, & Lee BL (2007) Clustering of peptidoglycan recognition protein-SA is required for sensing lysine-type peptidoglycan in insects. *Proc Natl Acad Sci USA* **104**: 6602-6607

Paskewitz SM & Riehle M (1998) A factor preventing melanization of sephadex CM C-25 beads in *Plasmodium*-susceptible and refractory *Anopheles gambiae*. *Exp Parasitol* **90**: 34-41

Pech LL & Strand MR (1996) Granular cells are required for encapsulation of foreign targets by insect haemocytes. *J Cell Sci* **109 (Pt 8)**: 2053-2060

Pili-Floury S, Leulier F, Takahashi K, Saigo K, Samain E, Ueda R, & Lemaitre B (2004) *In vivo* RNA interference analysis reveals an unexpected role for GNBP1 in the defense against Gram-positive bacterial infection in *Drosophila* adults. *J Biol Chem* **279**: 12848-12853

Potempa J, Korzus E, & Travis J (1994) The serpin superfamily of proteinase inhibitors: structure, function, and regulation. *J Biol Chem* **269**: 15957-15960

Powning RF & Davidson WJ (1973) Studies on insect bacteriolytic enzymes. I. Lysozyme in haemolymph of *Galleria mellonella* and *Bombyx mori*. *Comp Biochem Physiol B* **45**: 669-681

Ragan EJ, An C, Yang CT, & Kanost MR (2010) Analysis of mutually exclusive alternatively spliced serpin-1 isoforms and identification of serpin-1 proteinase complexes in *Manduca sexta* hemolymph. *J Biol Chem* **285**: 29642-29650

Ramesh N, Sugumaran M, & Mole JE (1988) Purification and characterization of two trypsin inhibitors from the hemolymph of *Manduca sexta* larvae. *J Biol Chem* **263**: 11523-11527

Rao XJ, Ling E, & Yu XQ (2010) The role of lysozyme in the prophenoloxidase activation system of *Manduca sexta*: an *in vitro* approach. *Dev Comp Immunol* **34**: 264-271

Rao XJ & Yu XQ (2010) Lipoteichoic acid and lipopolysaccharide can activate antimicrobial peptide expression in the tobacco hornworm *Manduca sexta*. *Dev Comp Immunol* **34**: 1119-1128

Rayaprolu S, Wang Y, Kanost MR, Hartson S, & Jiang H (2010) Functional analysis of four processing products from multiple precursors encoded by a lebocin-related gene from *Manduca sexta*. *Dev Comp Immunol* **34**: 638-647

Riahi Y, Siman-Tov R, & Ankri S (2004) Molecular cloning, expression and characterization of a serine proteinase inhibitor gene from *Entamoeba histolytica*. *Mol Biochem Parasitol* **133**: 153-162

Roberts TH & Hejgaard J (2008) Serpins in plants and green algae. *Funct Integr Genomics* **8**: 1-27

Roberts TH, Hejgaard J, Saunders NF, Cavicchioli R, & Curmi PM (2004) Serpins in unicellular *Eukarya*, *Archaea*, and *Bacteria*: sequence analysis and evolution. *J Mol Evol* **59**: 437-447

Roberts TH, Marttila S, Rasmussen SK, & Hejgaard J (2003) Differential gene expression for suicide-substrate serine proteinase inhibitors (serpins) in vegetative and grain tissues of barley. *J Exp Bot* **54**: 2251-2263

Robertson AS, Belorgey D, Lilley KS, Lomas DA, Gubb D, & Dafforn TR (2003) Characterization of the Necrotic Protein That Regulates the Toll-mediated Immune Response in *Drosophila*. *J Biol Chem* **278**: 6175-6180

Roh KB, Kim CH, Lee H, Kwon HM, Park JW, Ryu JH, Kurokawa K, Ha NC, Lee WJ, Lemaitre B, Söderhäll K, & Lee BL (2009) Proteolytic cascade for the activation of the insect toll pathway induced by the fungal cell wall component. *J Biol Chem* **284**: 19474-19481

Rose T, LeMosy EK, Cantwell AM, Banerjee-Roy D, Skeath JB, & Di Cera E (2003) Three-dimensional models of proteases involved in patterning of the *Drosophila* embryo. Crucial role of predicted cation binding sites. *J Biol Chem* **278**: 11320-11330

Rosenkrands I, Hejgaard J, Rasmussen SK, & Bjorn SE (1994) Serpins from wheat grain. *FEBS Lett* **343**: 75-80

Ryan RO & van der Horst DJ (2000) Lipid transport biochemistry and its role in energy production. *Annu Rev Entomol* **45**: 233-260

Sasaki T (1984) Amino acid sequence of a novel Kunitz-type chymotrypsin inhibitor from hemolymph of silkworm larvae *Bombyx mori*. *FEBS Lett* **168**: 227-230

Schulze AJ, Huber R, Bode W, & Engh RA (1994) Structural aspects of serpin inhibition. *FEBS Lett* **344**: 117-124

Sen J, Goltz JS, Stevens L, & Stein D (1998) Spatially restricted expression of *pipe* in the *Drosophila* egg chamber defines embryonic dorsal-ventral polarity. *Cell* **95**: 471-481

Shi L, Li B, & Paskewitz SM (2006) Cloning and characterization of a putative inhibitor of melanization from *Anopheles gambiae*. *Insect Mol Biol* **15**: 313-320

Shrestha S & Kim Y (2009) Various eicosanoids modulate the cellular and humoral immune responses of the beet armyworm, *Spodoptera exigua*. *Biosci Biotechnol Biochem* **73**: 2077-2084

Shrestha S & Kim Y (2008) Eicosanoids mediate prophenoloxidase release from oenocytoids in the beet armyworm Spodoptera exigua. *Insect Biochem Mol Biol* **38**: 99-112

Silverman GA, Bird PI, Carrell RW, Church FC, Coughlin PB, Gettins PG, Irving JA, Lomas DA, Luke CJ, Moyer RW, Pemberton PA, Remold-O'Donnell E, Salvesen GS, Travis J, & Whisstock JC (2001) The serpins are an expanding superfamily of structurally similar but functionally diverse proteins. Evolution, mechanism of inhibition, novel functions, and a revised nomenclature. *J Biol Chem* **276**: 33293-33296

Smolenaars MM, de Morree A, Kerver J, Van der Horst DJ, & Rodenburg KW (2007) Insect lipoprotein biogenesis depends on an amphipathic β cluster in apolipophorin II/I and is stimulated by microsomal triglyceride transfer protein. *J Lipid Res* **48**: 1955-1965

Söderhäll I, Wu C, Novotny M, Lee BL, & Söderhäll K (2009) A novel protein acts as a negative regulator of prophenoloxidase activation and melanization in the freshwater crayfish *Pacifastacus leniusculus*. *J Biol Chem* **284**: 6301-6310

Stanley D, Miller J, & Tunaz H (2009) Eicosanoid actions in insect immunity. *J Innate Immun* **1**: 282-290

Stark KR & James AA (1998) Isolation and characterization of the gene encoding a novel factor Xa-directed anticoagulant from the yellow fever mosquito, *Aedes aegypti*. *J Biol Chem* **273**: 20802-20809

Steenbakkers PJ, Irving JA, Harhangi HR, Swinkels WJ, Akhmanova A, Dijkerman R, Jetten MS, van der Drift C, Whisstock JC, & Op den Camp HJ (2008) A serpin in the cellulosome of the anaerobic fungus *Piromyces* sp. strain E2. *Mycol Res* **112**: 999-1006

Steiner H, Hultmark D, Engström A, Bennich H, & Boman HG (1981) Sequence and specificity of two antibacterial proteins involved in insect immunity. *Nature* **292**: 246-248

Strand MR (2008) Insect hemocytes and their role in immunity. In Beckage NE (ed) pp 25-47. Elsevier

Stuart LM & Ezekowitz RA (2008) Phagocytosis and comparative innate immunity: learning on the fly. *Nat Rev Immunol* **8**: 131-141

Stuart LM & Ezekowitz RA (2005) Phagocytosis: elegant complexity. *Immunity* **22**: 539-550

Su XD, Gastinel LN, Vaughn DE, Faye I, Poon P, & Bjorkman PJ (1998) Crystal structure of hemolin: a horseshoe shape with implications for homophilic adhesion. *Science* **281**: 991-995

Sugumaran M & Nellaiappan K (1991) Lysolecithin--a potent activator of prophenoloxidase from the hemolymph of the lobster, *Homarus americanas*. *Biochem Biophys Res Commun* **176**: 1371-1376

Sumathipala N & Jiang H (2010) Involvement of *Manduca sexta* peptidoglycan recognition protein-1 in the recognition of bacteria and activation of prophenoloxidase system. *Insect Biochem Mol Biol* **40**: 487-495

Sun SC, Asling B, & Faye I (1991) Organization and expression of the immunoresponsive lysozyme gene in the giant silk moth, *Hyalophora cecropia*. *J Biol Chem* **266**: 6644-6649

Sun SC, Lindstrom I, Boman HG, Faye I, & Schmidt O (1990) Hemolin: an insect-immune protein belonging to the immunoglobulin superfamily. *Science* **250**: 1729-1732

Takada Y, Ye X, & Simon S (2007) The integrins. *Genome Biol* **8**: 215

Tong Y, Jiang H, & Kanost MR (2005) Identification of plasma proteases inhibited by *Manduca sexta* serpin-4 and serpin-5 and their association with components of the prophenol oxidase activation pathway. *J Biol Chem* **280**: 14932-14942

Tong Y & Kanost MR (2005) *Manduca sexta* serpin-4 and serpin-5 inhibit the prophenol oxidase activation pathway: cDNA cloning, protein expression, and characterization. *J Biol Chem* **280**: 14923-14931

Tsukamoto T, Ichimaru Y, Kanegae N, Watanabe K, Yamaura I, Katsura Y, & Funatsu M (1992) Identification and isolation of endogenous insect phenoloxidase inhibitors. *Biochem Biophys Res Commun* **184**: 86-92

Uvell H & Engström Y (2007) A multilayered defense against infection: combinatorial control of insect immune genes. *Trends Genet* **23**: 342-349

Van der Horst DJ, Roosendaal SD, & Rodenburg KW (2009) Circulatory lipid transport: lipoprotein assembly and function from an evolutionary perspective. *Mol Cell Biochem* **326**: 105-119

Vercammen D, Belenghi B, van de Cotte B, Beunens T, Gavigan JA, De Rycke R, Brackenier A, Inze D, Harris JL, & Van Breusegem F (2006) Serpin1 of *Arabidopsis thaliana* is a suicide inhibitor for metacaspase 9. *J Mol Biol* **364**: 625-636

Vollmer W, Blanot D, & de Pedro MA (2008) Peptidoglycan structure and architecture. *FEMS Microbiol Rev* **32**: 149-167

Wang L, Gilbert RJ, Atilano ML, Filipe SR, Gay NJ, & Ligoxygakis P (2008) Peptidoglycan recognition protein-SD provides versatility of receptor formation in *Drosophila* immunity. *Proc Natl Acad Sci USA* **105**: 11881-11886

Wang L, Weber AN, Atilano ML, Filipe SR, Gay NJ, & Ligoxygakis P (2006) Sensing of gram-positive bacteria in *Drosophila*: GNBP1 is needed to process and present peptidoglycan to PGRP-SA. *EMBO J* **25**: 5005-5014

Wang Q, Liu Y, He HJ, Zhao XF, & Wang JX (2010) Immune responses of *Helicoverpa armigera* to different kinds of pathogens. *BMC Immunol* **11**: 9

Wang Y, Cheng T, Rayaprolu S, Zou Z, Xia Q, Xiang Z, & Jiang H (2007) Proteolytic activation of pro-spätzle is required for the induced transcription of antimicrobial peptide genes in lepidopteran insects. *Dev Comp Immunol* **31**: 1002-1012

Wang Y & Jiang H (2007) Reconstitution of a branch of the *Manduca sexta* prophenoloxidase activation cascade in vitro: snake-like hemolymph proteinase 21 (HP21) cleaved by HP14 activates prophenoloxidase-activating proteinase-2 precursor. *Insect Biochem Mol Biol* **37**: 1015-1025

Wang Y & Jiang H (2006) Interaction of beta-1,3-glucan with its recognition protein activates hemolymph proteinase 14, an initiation enzyme of the prophenoloxidase activation system in *Manduca sexta*. *J Biol Chem* **281**: 9271-9278

Wang Y & Jiang H (2004) Purification and characterization of *Manduca sexta* serpin-6: a serine proteinase inhibitor that selectively inhibits prophenoloxidase-activating proteinase-3. *Insect Biochem Mol Biol* **34**: 387-395

Wang Y, Jiang H, & Kanost MR (1999) Biological activity of *Manduca sexta* paralytic and plasmatocyte spreading peptide and primary structure of its hemolymph precursor. *Insect Biochem Mol Biol* **29**: 1075-1086

Wang Y, Sumathipala N, Rayaprolu S, & Jiang H (2011) Recognition of microbial molecular patterns and stimulation of prophenoloxidase activation by a beta-1,3-glucanase-related protein in *Manduca sexta* larval plasma. *Insect Biochem Mol Biol* **41**: 322-331

Wang Y, Zou Z, & Jiang H (2006) An expansion of the dual clip-domain serine proteinase family in *Manduca sexta*: gene organization, expression, and evolution of prophenoloxidase-activating proteinase-2, hemolymph proteinase 12, and other related proteinases. *Genomics* **87**: 399-409

Wiegand C, Levin D, Gillespie J, Willott E, Kanost M, & Trenczek T (2000) Monoclonal antibody MS13 identifies a plasmatocyte membrane protein and inhibits encapsulation and spreading reactions of *Manduca sexta* hemocytes. *Arch Insect Biochem Physiol* **45**: 95-108

Willott E, Wang XY, & Wells MA (1989) cDNA and gene sequence of *Manduca sexta* arylphorin, an aromatic amino acid-rich larval serum protein. Homology to arthropod hemocyanins. *J Biol Chem* **264**: 19052-19059

Wright HT (1996) The structural puzzle of how serpin serine proteinase inhibitors work. *Bioessays* **18**: 453-464

Wyatt GR (1961) The biochemistry of insect hemolymph. *Annu Rev Entomol* **6**: 75-102

Wyatt GR & Pan ML (1978) Insect plasma proteins. *Annu Rev Biochem* **47**: 779-817

Xie J, Chen Q, Wang Q, Song K, & Qiu L (2007) Activation kinetics of cetylpyridinium chloride on the phenol oxidase from pupae of blowfly (*Sarcophaga bullata*). *Pestic Biochem Physiol* **87**: 9-13

Yoshida H, Kinoshita K, & Ashida M (1996) Purification of a peptidoglycan recognition protein from hemolymph of the silkworm, *Bombyx mori*. *J Biol Chem* **271**: 13854-13860

Yu X & Kanost MR (2008) Activation of lepidopteran insect innate immune responses by C-type immulectins. In *Animal lectins: A functional view,* Ahmed HA & Vasta GR (eds) pp 383-395. CRC Press: Boca Raton

Yu XQ, Gan H, & Kanost MR (1999) Immulectin, an inducible C-type lectin from an insect, *Manduca sexta*, stimulates activation of plasma prophenol oxidase. *Insect Biochem Mol Biol* **29**: 585-597

Yu XQ, Jiang H, Wang Y, & Kanost MR (2003) Nonproteolytic serine proteinase homologs are involved in prophenoloxidase activation in the tobacco hornworm, *Manduca sexta*. *Insect Biochem Mol Biol* **33**: 197-208

Yu XQ & Kanost MR (2004) Immulectin-2, a pattern recognition receptor that stimulates hemocyte encapsulation and melanization in the tobacco hornworm, *Manduca sexta*. *Dev Comp Immunol* **28**: 891-900

Yu XQ & Kanost MR (2002) Binding of hemolin to bacterial lipopolysaccharide and lipoteichoic acid. An immunoglobulin superfamily member from insects as a pattern-recognition receptor. *Eur J Biochem* **269**: 1827-1834

Yu XQ & Kanost MR (2000) Immulectin-2, a lipopolysaccharide-specific lectin from an insect, *Manduca sexta*, is induced in response to gram-negative bacteria. *J Biol Chem* **275**: 37373-37381

Yu XQ & Kanost MR (1999) Developmental expression of *Manduca sexta* hemolin. *Arch Insect Biochem Physiol* **42**: 198-212

Yu XQ, Ling E, Tracy ME, & Zhu Y (2006) Immulectin-4 from the tobacco hornworm *Manduca sexta* binds to lipopolysaccharide and lipoteichoic acid. *Insect Mol Biol* **15**: 119-128

Yu XQ & Ma Y (2006) Calcium is not required for immulectin-2 binding, but protects the protein from proteinase digestion. *Insect Biochem Mol Biol* **36**: 505-516

Yu XQ, Tracy ME, Ling E, Scholz FR, & Trenczek T (2005) A novel C-type immulectin-3 from *Manduca sexta* is translocated from hemolymph into the cytoplasm of hemocytes. *Insect Biochem Mol Biol* **35**: 285-295

Yu XQ, Zhu YF, Ma C, Fabrick JA, & Kanost MR (2002) Pattern recognition proteins in *Manduca sexta* plasma. *Insect Biochem Mol Biol* **32**: 1287-1293

Zhang Y, Huang J, Zhou B, Zhang C, Liu W, Miao X, & Huang Y (2009) Up-regulation of lysozyme gene expression during metamorphosis and immune challenge of the cotton bollworm, *Helicoverpa armigera*. *Arch Insect Biochem Physiol* **70**: 18-29

Zhao M, Söderhäll I, Park JW, Ma YG, Osaki T, Ha NC, Wu CF, Söderhäll K, & Lee BL (2005) A novel 43-kDa protein as a negative regulatory component of phenoloxidase-induced melanin synthesis. *J Biol Chem* **280**: 24744-24751

Zhu Y, Johnson TJ, Myers AA, & Kanost MR (2003a) Identification by subtractive suppression hybridization of bacteria-induced genes expressed in *Manduca sexta* fat body. *Insect Biochem Mol Biol* **33**: 541-559

Zhu Y, Wang Y, Gorman MJ, Jiang H, & Kanost MR (2003b) *Manduca sexta* serpin-3 regulates prophenoloxidase activation in response to infection by inhibiting prophenoloxidase-activating proteinases. *J Biol Chem* **278**: 46556-46564

Zhuang S, Kelo L, Nardi JB, & Kanost MR (2008) Multiple alpha subunits of integrin are involved in cell-mediated responses of the *Manduca* immune system. *Dev Comp Immunol* **32**: 365-379

Zhuang S, Kelo L, Nardi JB, & Kanost MR (2007a) An integrin-tetraspanin interaction required for cellular innate immune responses of an insect, *Manduca sexta*. *J Biol Chem* **282**: 22563-22572

Zhuang S, Kelo L, Nardi JB, & Kanost MR (2007b) Neuroglian on hemocyte surfaces is involved in homophilic and heterophilic interactions of the innate immune system of *Manduca sexta*. *Dev Comp Immunol* **31**: 1159-1167

Zou Z, Evans JD, Lu Z, Zhao P, Williams M, Sumathipala N, Hetru C, Hultmark D, & Jiang H (2007) Comparative genomic analysis of the *Tribolium* immune system. *Genome Biol* **8**: R177

Zou Z & Jiang H (2005) *Manduca sexta* serpin-6 regulates immune serine proteinases PAP-3 and HP8. cDNA cloning, protein expression, inhibition kinetics, and function elucidation. *J Biol Chem* **280**: 14341-14348

Zou Z, Lopez DL, Kanost MR, Evans JD, & Jiang H (2006) Comparative analysis of serine protease-related genes in the honey bee genome: possible involvement in embryonic development and innate immunity. *Insect Mol Biol* **15**: 603-614

Zou Z, Najar F, Wang Y, Roe B, & Jiang H (2008) Pyrosequence analysis of expressed sequence tags for *Manduca sexta* hemolymph proteins involved in immune responses. *Insect Biochem Mol Biol* **38**: 677-682

Zou Z, Picheng Z, Weng H, Mita K, & Jiang H (2009) A comparative analysis of serpin genes in the silkworm genome. *Genomics* **93**: 367-375

CHAPTER 2 - INVOLVEMENT OF HEMOLYMPH PROTEINASE 16 IN THE INNATE IMMUNE RESPONSE OF *MANDUCA SEXTA*

Introduction

Extracellular serine proteinase cascade pathways are involved in innate immune responses of vertebrates and invertebrates, and promote rapid, non-specific responses to infection and wounding (Krem and Di Cera, 2002; Kanost and Clarke, 2005; Cerenius et al., 2010). Vertebrates utilize proteinase-driven pathways in blood coagulation, fibrinolysis, and complement activation (Salvesen, 2004; Sim and Tsiftsoglou, 2004; Dunkelberger and Song, 2010). After active proteinases perform their functions, they are inactivated by members of the serpin superfamily of serine proteinase inhibitors or by α2-macroglobulin to prevent damage to the organism (Silverman et al., 2001; Gettins, 2002). Serine proteinase cascades are also activated in arthropod hemolymph and have a role in coagulation, melanization, and production of antimicrobial peptides (Kanost and Clarke, 2005; Iwanaga and Lee, 2005; Cerenius et al., 2010).

Hemolymph of the caterpillar, *M. sexta*, contains at least twenty-seven serine proteinases, including sixteen that possess at least one amino-terminal clip domain (Jiang et al., 1999; Jiang et al., 2005; Wang et al., 2006). A clip domain is composed of 37-55 amino acid residues with three disulfide bonds. Although the function of the clip domain(s) is unknown, it is thought that they may play a role in proteinase regulation. The amino-terminal clip domain is attached to the carboxyl-terminal serine proteinase domain by a linker region that ranges in length from 23 to 101 amino acid residues (Jiang and Kanost, 2000). Hemolymph proteinases (HPs) are synthesized as zymogens and are activated by specific proteolytic cleavage. Once activated, some of these proteinases may function in aspects of innate immune responses, including the activation of cytokine precursors and prophenoloxidase (Kanost et al., 2001). Since the discovery of these proteinases, the task has been to investigate their function within the insect.

The function of seven hemolymph proteinases from *M. sexta* has been elucidated through the use of recombinant proteinases (Ji et al., 2004; Gorman et al., 2007; Wang and Jiang, 2007; An et al., 2009; An et al., 2010). In response to bacterial peptidoglycan or fungal β-1,3-glucan

and β-1,3-glucan recognition protein (βGRP-2), HP14 autoactivates (Ji et al., 2004) to start the prophenoloxidase activation pathway. HP14 then activates proHP21 (Gorman et al., 2007; Wang and Jiang, 2007). Finally, HP21 proteolytically cleaves prophenoloxidase-activating proteinase-2 (PAP-2; Wang and Jiang, 2007) or PAP-3 (Gorman et al., 2007), which activates prophenoloxidase in the presence of cleaved serine proteinase homologs (SPHs) (Gorman et al., 2007; Wang and Jiang, 2007). Active phenoloxidase catalyzes oxidation of catechols to quinones that are involved melanin production, encapsulation of foreign invaders, and wound healing (Cerenius et al., 2008; Kanost and Gorman, 2008).

HP6 plays a role in the activation of prophenoloxidase and activation of cytokine-like proteins. When bacteria or fungi are present, HP6 is cleaved and activated by an unknown proteinase (An et al., 2009). Next, HP6 activates proPAP-1 (An et al., 2009). Finally, in the presence of SPHs, PAP-1 activates proPO and leads to melanin synthesis. In addition, HP6 can cleave and activate another serine proteinase, HP8 (An et al., 2009). Injection of larvae with active HP6 or HP8 induced the expression of several antimicrobial peptides and proteins (An et al., 2009), which suggested a role in the activation of a Toll-like pathway. Recently, recombinant HP8 was shown to cleave recombinant *M. sexta* prospätzle and release active spätzle C108, the putative Toll ligand (An et al., 2010). Injection of spätzle C108, a disulfide-linked homodimer of the C-terminal 108 residue domain of prospätzle, into larvae increased expression levels of moricin, attacin-1, cecropin-6, and hemolin when compared to injection of buffer or prospätzle (An et al., 2010). These results further support the hypothesis that HP6 and HP8 are involved in the activation of a Toll-like pathway in *M. sexta* that leads to the production of antimicrobial peptides (An et al., 2009; An et al., 2010).

Hemolymph proteinase 16 (HP16), the focus of this chapter, was identified in *M. sexta* by screening induced hemocyte and fat body cDNA libraries (Jiang et al., 2005). HP16 is a 47 kDa protein that has a carboxyl-terminal S1 family serine proteinase domain with predicted chymotrypsin/elastase-like specificity. HP16 lacks a clip domain, but contains an amino-terminal 170 residue region that has no significant match to any characterized protein in the current databases, whereas the catalytic domain is most similar to *Drosophila* gastrulation defective, a proteinase that functions in embryonic development. Northern blot analysis revealed that HP16 mRNA is present at basal levels in naïve hemocytes and fat body. Both HP16 protein levels in

plasma and mRNA levels in hemocytes and fat body increased dramatically after injection of bacteria, which indicated a possible role in innate immune responses (Jiang et al., 2005).

In this chapter, I investigated the expression of HP16 at the protein and mRNA levels during development and in response to bacterial injection. I developed methods to express and purify recombinant HP16, HP16 mutants, NT16 (amino-terminal residues 1-165), and NT16 mutants to further characterize HP16 and to investigate its potential function in innate immune responses. Experiments were also conducted to deterimine if proHP16 in plasma could be activated in the presence of microbial elicitors and if any serpin-1 isoforms formed a complex with activated HP16-Xa (a mutant activated by bovine factor Xa) *in vitro*. Findings from this work further the understanding of HP16 and lay a foundation for future experiments involving the proteolytic activity, regulation, and biological function of HP16.

Materials and Methods

Insects

Manduca sexta eggs were originally obtained from Carolina Biological Supply and used to establish a laboratory colony. The colony has been maintained by feeding larvae on an artificial diet as previously described by Dunn and Drake (1983).

Collection of hemolymph

Hemolymph was collected from naïve larvae, prepupae, and pupae (day 0-day 5 fifth instar, day 1-day 3 wandering larvae, prepupa, and day 0 pupa). In addition, hemolymph was collected 24 h after injection of day 2 fifth instar larvae injected with 0.85% NaCl (saline), 10^8 cells *E. coli*, or 500 µg *M. luteus*. Larvae were chilled on ice for at least 20 min. The larval posterior horn or the pupal proboscis was clipped to release the hemolymph into individual microcentrifuge tubes. An equal volume of anti-coagulant saline (4 mM sodium chloride, 40 mM potassium chloride, 8 mM EDTA, 9.5 mM citric acid, 27 mM sodium citrate, 5% sucrose, 0.1 % polyvinylpyrollidone, and 1.7 mM PIPES, pH 6.5) containing diethyldithiocarbamic acid (final concentration of 2.25 mg/mL) was added to the hemolymph to prevent coagulation and to inhibit prophenoloxidase. Hemocytes were removed from the hemolymph by centrifugation at 8000-13000 × g for 6-12 min at 4°C depending on developmental stage. The supernatant, or plasma, was removed from the hemocytes, placed into a new microcentrifuge tube, and stored at -80°C.

Isolation of total RNA

Fat body (50-100 mg) of naïve day 2 and day 4 fifth instar larvae, day 1 and day 2 wandering larvae, prepupae, and day 3 fifth instar larvae that were injected (24 h prior to collection) with 0.85% saline, 10^8 cells *E. coli*, or 500 µg *M. luteus* was collected for total RNA extraction (n =3 for each developmental stage or treatment). Hemolymph from each larva was collected prior to fat body collection. Total RNA was extracted using the Tri Reagent (Sigma). Fat body samples were homogenized using a Pellet Pestle Motor containing a plastic pestle (Kontes) in 1 mL of Tri Reagent. Homogenates were centrifuged at 12,000 × g for 10 min at 4°C. The resulting supernatants were transferred to an RNase-free 1.5 mL microfuge tube (Ambion) and allowed to stand for 5 min at room temperature (RT). Chloroform (200 µL) was added to each tube, vigorously shook and vortexed (~15 s), and allowed to stand for 3 min at RT. Following centrifugation at 12,000 × g for 15 min at 4°C, the aqueous layer containing RNA was transferred to an RNase-free 1.5 mL microfuge tube. After addition of 500 µL of isopropanol to each tube, the mixture stood at RT for 10 min and was centrifuged at 12,000 × g for 10 min at 4°C to pellet the RNA. Supernatants were discarded, and 1 mL of 75% ethanol was used to wash the pellet by vortexing. Pellets were centrifuged at 12,000 × g for 5 min at 4°C. Ethanol was carefully removed from the pellet. After the pellet was air dried, 40 µL of Nuclease-free water was added to each tube to dissolve the pellet. Samples were centrifuged at 12,000 × g for 30 min at 4°C to remove glycogen. Supernatants were removed, placed in a new RNase-free tube, and kept at -80°C until use for making cDNA.

Reverse transcriptase-polymerase chain reaction (RT-PCR)

Before cDNA synthesis, total RNA samples were treated with Deoxyribonuclease I Amplification Grade (DNase I; Invitrogen: 18068-015). RNA (1 µg) was added to 1 µL of 10X DNase I reaction buffer, 1 µL DNase I, and Nuclease-free water (Ambion) to bring the total reaction volume to 10 µL. Tubes were incubated at RT for 15 min. Inactivation of DNase I was accomplished by adding 1 µL of 25 mM EDTA and heating for 10 min at 65°C.

First-strand cDNA synthesis for each RNA sample was completed using SuperScript III First-Strand Synthesis System for RT-PCR (Invitrogen). Reaction mixtures were prepared on ice in autoclaved 0.2 mL PCR tubes. Each tube contained 8 µL RNA, 1 µL 50 µM oligo$(DT)_{20}$ primer, and 1 µL 10 mM dNTP mix. Samples were mixed, incubated at 65°C for 5 min, and

chilled on ice for at least 1 min. Components added, in order, to each tube included 2 µL 10X RT buffer, 4 µL of 25 mM $MgCl_2$, 2 µL of 0.1 M DTT, 1 µL RNaseOUT (40 U/µL), and 1 µL SuperScript III RT (200 U/µL). Using a PTC-100 Peltier Thermal Cycler (Bio-Rad), mixtures were incubated for 50 min at 50°C, followed by 5 min at 85°C (termination). Reactions were chilled on ice for 2 min and briefly centrifuged. RNase H (1 µl) was added to each tube, gently mixed, and incubated for 20 min at 37°C. Samples were stored at -20°C.

HP16 was amplified from fat body cDNA using a forward primer (HP16 F: 5'-CCC GCT GAA GAA AAC CAA TA-3') and a reverse primer (HP16 R: 5'-ACG AAT TTG GCT CAT CAA GG-3'). The thermal cycling conditions were 29 cycles of 94°C for 30 s, 53°C for 30 s, 72°C for 30 s followed by incubation at 72°C for 5 min. *M. sexta* ribosomal protein S3 (rpS3) was used as an internal control and amplified using the same set of fat body cDNA. Primers used for rpS3 were 501 (5'-GCC GTT CTT GCC CTC TT-3') and 504 (5'-CGC GAG TTG ACT TCG GT-3'). Thermal cycling conditions were the same as those used for amplification of HP16 with the exception of the number of cycles and annealing temperature. Twenty (Figure 2-2B: larval development) or twenty-three (Figure 2-3B: bacterial injection) cycles were completed for rpS3 amplification with an annealing temperature of 55°C. The PCR products were separated by electrophoresis on a 1.0% agarose gel containing ethidium bromide.

Quantitative real-time PCR

Quantitative real-time PCR was used to determine HP16 and rpS3 mRNA levels using cDNA synthesized from total RNA. Primers used for rpS3 were rpS3-F (5'-CTG GCT GAG GAT GGC TAC TC-3') and rpS3-R (5'-TTT CTC AGC GTA CAG CTC CA-3') and primers for HP16 were HP16RT-F (5'-TGA GGA CAT AGC GTT AGT AAG AC-3') and HP16RT-R (5'-GCC GAC GAC AGT TCC ATA C-3'). Each 25 µL reaction contained 12.5 µL of 2X SYBR buffer mix (Bio-Rad), 1 µL of forward primer (5 pmol/µL), 1 µL of reverse primer (5 pmol/µL), and 10.5 µL of diluted cDNA (1/10 dilution). Thermal cycling conditions were 95°C for 5 min and 40 cycles of 95°C for 30 s, 53°C for 30 s, and 72°C for 40 s. Amplification was monitored on an iCycler (Bio-Rad) by means of SYBR-Green (Bio-Rad). Threshold values were individually calculated for each target gene (Ct). Using the formula $\Delta Ct = Ct_{treated}-Ct_{control}$, transcript abundance values were calculated. For samples analyzed from naïve larvae, an average Ct value for day 2 5^{th} instar larvae was used as the control while an average Ct value for saline

injected larvae was used as the control for injected larvae. Expression levels of HP16 relative to the transcript levels for rpS3 were calculated with the formula $\Delta\Delta Ct = \Delta Ct_{HP16} - \Delta Ct_{rpS3}$. Fold change is equal to $2^{-\Delta\Delta Ct}$.

SDS-PAGE and immunoblotting

SDS-polyacrylamide gel electrophoresis (SDS-PAGE) was performed using a 10% SDS-PAGE gel or NuPAGE 4-12% Bis-Tris gels (Invitrogen). Proteins were treated with sample loading buffer containing SDS and β-mercaptoethanol; however, in some cases, sample loading buffer without β-mercaptoethanol was used. Samples were heated at 95°C for 5 min and briefly centrifuged. Electrophoretic separations were carried out in an XCell SureLock™ Electrophoresis Cell (Invitrogen; Novex Mini-Cell) at a constant voltage of 200 V. Gels were stained for 30-60 min in 0.2% (w/v) Coomassie Blue R-250 in 50% (v/v) methanol and 12% (v/v) acetic acid, followed by destaining with 30% (v/v) methanol and 10% (v/v) acetic acid. Alternatively, when expected protein concentrations were low, gels were silver stained using the SilverXpress® Silver Staining Kit (Invitrogen). Gels were placed in a gel drying solution (20% (v/v) ethanol, 5% (v/v) glycerol) for 30 min and dried between two cellophane membranes (14 × 14 cm; Fisher).

For immunoblotting, proteins were transferred from SDS-PAGE gels to 0.22 or 0.45 µm nitrocellulose membranes using a Trans-Blot SD Semi-Dry Transfer Cell (Bio-Rad). Membranes were blocked for 1 h with 3% dry milk dissolved in TTBS (0.05% Tween 20 in Tris-buffered saline, 25 mM Tris-HCl, pH 7.4, 137 mM NaCl, 2.7 mM KCl), washed for 5 min with TTBS, and incubated for 2 h with an appropriate primary antiserum diluted 1:2000 (unless otherwise specified) in 3% dry milk in TTBS (5 µL antiserum: 10 mL 3% dry milk in TTBS). After three, 5 min washes with TTBS, membranes were incubated for 1 h with a secondary antibody (Goat Anti-Rabbit IgG (H+L)-alkaline phosphatase conjugate; Bio-Rad) diluted 1:3000 in 3% dry milk in TTBS (4 µL antibody: 12 mL 3% dry milk in TTBS). Membranes were washed twice with TTBS and once with TBS (25 mM Tris-HCl, 137 mM NaCl, 2.7 mM KCl, pH 7.4), followed by development using an Alkaline Phosphatase Conjugate Substrate Kit (Bio-Rad).

DNA sequencing

Sequences for plasmid verification were obtained on an Applied Biosystems 3730 DNA Analyzer at the DNA Sequencing and Genotyping Facility located in the Department of Plant

Pathology at Kansas State University in Manhattan, KS. Nucleotide sequences were manually aligned using CAP3 (http://pbil.univ-lyon1.fr/cap3.php) and consensus nucleotide sequences were translated using the ExPASy Translate Tool (http://expasy.org/tools/dna.html). Both nucleotide and amino acid sequences were aligned with the template sequence to ensure that undesired changes were not introduced during PCR using ClustalW2 (http://www.ebi.ac.uk/Tools/msa/clustalw2/).

Mutagenesis and recombinant protein expression

Expression of HP16 and HP16 mutants

The entire coding region for HP16, including signal peptide, was amplified from a cDNA clone (obtained from Haobo Jiang, Oklahoma State University) by PCR using a forward primer (5'-AAG CGG CCG CAT GAA GTT TCT AAT TC-3') in which a NotI site (underlined) was introduced and a reverse primer (5'-GCA AGC TTT TAC AAA TGC CTA GAG ACC-3') in which a HindIII site (underlined) was introduced. A HP16 fragment generated by digestion of the PCR product by NotI and HindIII was gel purified using the QIAquick Gel Extraction Kit (Qiagen) and ligated into the same restriction sites in pFastBac1 (Invitrogen). The resulting HP16-pFastBac1 plasmid, after sequence verification, was used as template to generate two HP16 mutants according to the instructions of QuikChange multisite-directed mutagenesis kit (Stratagene). Using a mutagenic oligonucleotide primer (5'-AAA CGT CAA GTA TTG ATT GAG GGC CGG ATC GTG AAC GGA CAG CCT-3'), residues of the predicted activation site of proHP16 were changed from HTGL to IEGR. This mutant was named HP16-Xa. Another mutant of HP16 (HP16 S-A) was produced by changing the codon for the active site Ser^{382} (AGT) to Ala (GCT) by using a mutagenic oligonucleotide primer (5'- GCC TGT AAT GGT GAC GCT GGT GGT GGC TTC ATG ATC TTC G-3'). After DNA sequence verification, each recombinant plasmid (HP16-pFastBac1, HP16-Xa-pFastBac1, HP16 S-A-pFastBac1) was used to transform Max Efficiency DH10Bac *E. coli* cells (Invitrogen), which contain a bacmid and a helper plasmid. Each recombinant bacmid obtained by transposition of the donor plasmid into the bacmid was isolated with a High Purity Plasmid Purification System (Marligen Biosciences, Inc.). Insertion of HP16 cDNA in the recombinant bacmid was confirmed by PCR using the M13 forward (-20) primer (5'-GTA AAA CGA CGG CCA G-3') and the M13 reverse primer (5'-CAG GAA ACA GCT ATG AC-3') from Invitrogen.

Spodoptera frugiperda Sf-9 cells at a density of 9×10^5 cells/mL were seeded in 2 mL of Sf-900 II serum-free medium (SFM) containing 50 units/mL penicillin and 50 µg/mL streptomycin in a 6-well plate. The transfection of cells with recombinant bacmid DNA was mediated by cationic liposomes using the CellFECTIN reagent and followed the Bac-to-Bac Baculovirus Expression System manual (Invitrogen). After incubation at 27°C for 5 h, the transfection mixture was removed from the cells and replaced by Sf-900 II SFM plus antibiotics. Recombinant baculovirus was collected after the cells were incubated at 27°C for 96 h. The initial recombinant baculovirus (P1 virus) for each construct was amplified twice to obtain the P3 virus. Titer of each P3 virus was determined by performing a plaque assay in 35 mm 6-well plates as described by the manufacturer's manual (Invitrogen). The titers were as follows: 1.8×10^8 plaque forming units/mL (pfu/mL) for wild-type HP16, 3.1×10^8 pfu/mL for HP16-Xa, and 1.1×10^8 pfu/mL for HP16 S-A. Long-term storage of the virus was at -80°C in the presence of 2% fetal bovine serum (Atlanta Biological). Virus to be used immediately for expression was protected from light and stored at 4°C. Expression of wild-type HP16, HP16-Xa, and HP16 S-A was performed by infecting 2×10^6 cells/mL of Sf-9 cells in 2 liters (400 mL medium/1 L flask) of Sf-900 II SFM with the recombinant baculovirus at a multiplicity of infection of 3, 4, or 2, respectively. Cells were incubated at 28°C with shaking at 150 rpm. The culture was harvested 48 h post-infection, and cells were removed by centrifugation at 500 × g for 10 min at 4°C. Media removed from the cells was centrifuged again using the same conditions.

Purification of recombinant wild-type HP16, HP16-Xa, and HP16 S-A

Cell-free media, achieved by centrifugation, was split into four 1 L flasks (~500 mL/flask) and mixed with concanavalin A-Sepharose 4B (GE Healthcare) that had been equilibrated in ConA binding buffer (20 mM Tris-HCl, 0.5 M NaCl, pH 7.5) and proteinase inhibitors (10 mM E-64 to a final concentration of 10 µM and 0.5 M p-aminobenzamidine to a final concentration of 0.5 mM). After shaking at 150 rpm for 8 h at 4°C, the slurry was applied to a 2.5 × 10 cm column and allowed to drain. The column was washed four times with 35 mL of ConA binding buffer at 4°C. Once the A_{280} reading was below 0.06, 35 mL ConA elution buffer (ConA binding buffer with 0.5 M methyl-α-D-mannopyranoside) was added to elute bound proteins. The column was rotated overnight at 4°C. After collection of the first elution fraction, a fresh 35 mL of ConA elution buffer was added to the column and rotated for an additional 4 h at 4°C. The second elution fraction (35 mL) was collected and followed by four, 10 mL elutions

with ConA elution buffer. The eluted fractions were analyzed by SDS-PAGE and immunoblotting.

Fractions containing HP16 were pooled and dialyzed against Q-Sepharose start buffer (20 mM Tris, 5 mM NaCl, pH 8.4 and 0.5 M p-aminobenzamidine to a final concentration of 0.5 mM) (3.5 liters for at least 8 h at 4°C, two times). The dialyzed sample was applied to a Q-Sepharose^{TM} Fast Flow column (GE Healthcare; 1 × 10 cm) equilibrated with Q-Sepharose start buffer (no p-aminobenzamidine) at 1 mL/min. The column was washed with Q-Sepharose start buffer at 1 mL/min until the A_{280} reading was less than 0.025. Proteins bound to the column were eluted with a 60 mL linear gradient of 5-1000 mM NaCl in 20 mM Tris-HCl, pH 8.4 at 1 mL/min. Fractions of 1 mL each were collected and analyzed by SDS-PAGE and immunoblotting.

Q-Sepharose fractions containing HP16 were pooled and prepared for hydrophobic interaction chromatography (HIC). An Econo-Pac Methyl HIC Cartridge (Bio-Rad 732-0053) was prepared for use as described in the manufacturer's manual using a low salt buffer (20 mM Tris-HCl, pH 8.4) and a high salt buffer (20 mM Tris-HCl, 1.5 M ammonium sulfate, pH 8.4). Ammonium sulfate (final concentration = 1.5 M) was dissolved in 3 mL of pooled HP16 Q-Sepharose fractions, and the resulting solution was centrifuged at 12,000 × g for 30 min at 4°C to remove any precipitate. The precipitate was resuspended in 1 mL of 20 mM Tris-HCl, pH 8.4 and stored at 4°C while the supernatant was loaded onto the HIC column at 0.7 mL/min. The column was washed with the high salt buffer for 7 min at 0.7 mL/min. Proteins bound to the column were eluted with a 30 mL linear gradient of 1.5 M to 0 M ammonium sulfate in 20 mM Tris-HCl, pH 8.4 at 0.7 mL/min. Fractions of 0.7 mL each were collected and analyzed by SDS-PAGE, followed by silver staining and immunoblotting.

HIC fractions containing HP16 were pooled and used for further purification by gel permeation chromatography. Partially purified HP16 (4 mL) was loaded at 1 mL/min onto a Sephacryl-S100 High Resolution (GE Healthcare) 1.5 × 100 cm column equilibrated with gel filtration buffer (20 mM Tris-HCl, 150 mM NaCl, pH 8.4). Proteins were eluted from the column with the gel filtration buffer at 1 mL/min. The first eleven fractions were collected at 4 mL/tube as this was determined to be the void volume by running blue dextran (Sigma) through the column. After the void volume, 2 mL fractions were collected. Selected fractions were analyzed

by SDS-PAGE and immunoblotting. Fractions containing the most HP16 and the least contaminating proteins were pooled and stored at -80°C.

Purification of the two HP16 mutant proteins, HP16-Xa and HP16 S-A, utilized the same purification scheme as wild-type HP16 with some modification. First, for both HP16-Xa and HP16 S-A, the proteinase inhibitors, E-64 and p-aminobenzamidine, were not added at any step of purification. Second, changes in procedure occurred during the use of HIC. The change for HP16 S-A was minor as 3.5 mL of pooled Q-Sepharose fractions were applied to the column instead of 3 mL. In addition, Coomassie Blue staining was used to detect proteins eluted from the HIC column instead of silver staining. For HP16-Xa, the high salt buffer contained 2.4 M ammonium sulfate instead of 1.5 M ammonium sulfate. Moreover, proteins bound to the column were eluted with a 24 mL (instead of 30 mL) linear gradient of 2.4 M to 0 M ammonium sulfate in 20 mM Tris-HCl, pH 8.4 (instead of 1.5 M to 0 M ammonium sulfate in 20 mM Tris-HCl). Since the highest levels of HP16-Xa were found in the resuspended precipitate, this solution (3 mL) was used for further purification by gel permeation chromatography. Fractions containing the most HP16-Xa or HP16 S-A were pooled and stored at -80°C.

Expression and purification of recombinant serpin-1Z

Manduca sexta serpin-1Z was expressed in *Escherichia coli* strain XL1-Blue using the H6pQE-60 expression vector, which encodes an amino-terminal 6 x histidine tag (Jiang and Kanost, 1997). A single colony harboring the recombinant plasmid was inoculated into 50 mL of sterile LB containing 50 µL of 50 mg/mL ampicillin in a 250 mL flask and incubated overnight at 37°C with shaking at 300 rpm. Fifteen milliliters of the overnight culture was transferred to two, 2 L flasks containing 500 mL LB and ampicillin (0.5 mL of 50 mg/mL). Flasks were incubated at 37°C with shaking at 300 rpm until OD_{600} was 0.5 to 0.6. Cultures were kept at 37°C, and expression of serpin-1Z was induced by adding 1 M isopropyl-β-D-thiogalactoside (IPTG) to a final concentration of 1 mM. After 4 h, the bacteria were harvested by centrifugation at 4000 × g for 20 min at 4°C. Pellets were frozen at -80°C overnight and resuspended in cold lysis buffer (300 mM NaCl, 10 mM imidazole in 0.5 M sodium phosphate buffer, pH 8.0) at 4 mL lysis buffer/g cells. Proteinase inhibitor cocktail for His-tagged proteins (Sigma P8849) was also added at 50 µL inhibitor/g cells. Samples were transferred to 50 mL polypropylene centrifuge tubes (Fisher Scientific) and placed in an ice-water bath. Cells were sonicated for 8 × 10 seconds with a 10 second rest between bursts using a Sonic Dismembrator Model 100 (Fisher

Scientific) that was set on level 8. After sonication, the lysate was centrifuged at 10,000 × g for 30 min at 4°C.

The soluble serpin-1Z was first purified by nickel-affinity chromatography (Ni^{2+}-NTA). Clear lysate was incubated with Ni^{2+}-NTA agarose (Qiagen) at 1 mL agarose for every 4 mL clear lysate in a 50 mL polypropylene centrifuge tube with rotation for 1 h at 4°C. This mixture was poured into a 1.5 cm diameter column. The column was washed twice with wash buffer (300 mM NaCl, 20 mM imidazole in 0.5 M sodium phosphate buffer, pH 8.0) at a volume equal to that of the clear lysate. Recombinant serpin-1Z was eluted 4 times with 5 mL of elution buffer (300 mM NaCl, 250 mM imidazole in 0.5 M sodium phosphate buffer, pH 8.0). Fractions were analyzed by SDS-PAGE under reducing conditions and immunoblotting. To further purify serpin-1Z, fractions containing serpin-1Z were pooled and dialyzed against dialysis buffer (20 mM Tris-HCl, pH 8.0). Serpin-1Z (1.7 mL) was added to a Slide-A-Lyzer 3.5 K Dialysis Cassette (Thermo Scientific) and dialyzed in 600 mL dialysis buffer (twice, for at least 8 h) at 4°C. The dialyzed sample (2 mL) was applied to an equilibrated Q-Sepharose™ Fast Flow column (1 × 10 cm) at 1 mL/min. Dialysis buffer (25 mL total) was used to wash the column until A_{280} readings were near zero. Proteins bound to the column were eluted with a 60 mL linear gradient of 0-500 mM NaCl in 20 mM Tris-HCl, pH 8.0 at 1 mL/min. Fractions of 1 mL each were collected and analyzed by SDS-PAGE under reducing conditions and immunoblotting. Fractions containing serpin-1Z were pooled and stored at 4°C.

Expression and purification of the amino-terminal region of HP16 (NT16) and NT16 mutants in E. coli

The HP16 DNA sequence encoding amino-terminal residues (1-165) was amplified by PCR using a forward primer (5'-<u>CCA TGG</u> CCC AAA AGT TAT CTG ATG GT-3') in which an NcoI site was introduced (underlined) and a reverse primer (5'-<u>GCG GCC GC</u>*C TA*T TGA CGT TTG CCA CA-3'; reverse complement) in which a NotI site (underlined) and stop codon (italicized) were introduced. The PCR product was recovered after purification by agarose electrophoresis using the QIAquick Gel Extraction Kit (Qiagen). Recovered DNA was cloned into pCR4-TOPO vector following manufacturer's instructions (Invitrogen), and resulting NT16-pCR4 plasmid DNA was digested by NcoI and NotI to verify that NT16 was inserted. After sequence verification, NT16-pCR4 and the expression vector, pProExHTb (Life Technologies), were digested by NcoI and NotI. Digestion products of the expected size for NT16 (~500 bp) and

pProExHTb (~4.7 kb) were excised from a 1% agarose gel and gel purified using the QIAquick Gel Extraction Kit (Qiagen). NT16 and pProExHTb were ligated with T4 DNA ligase (New England BioLabs) at 16°C. After ~17 h, the T4 DNA ligase was heat-inactivated at 65°C for 20 min. The ligation product was used to transform Max Efficiency DH5α competent *E. coli* cells (Invitrogen). Plasmid DNA was isolated from an overnight culture of a single colony in 3 mL of LB with 100 µg/mL ampicillin. The presence of the NT16 DNA insert was checked by restriction digestion using NcoI and NotI.

The NT16-pProExHTb plasmid was used as template to generate three NT16 mutants according to the instructions of QuikChange multisite-directed mutagenesis kit (Stratagene). Using a mutagenic oligonucleotide primer (5'-GCT GCA TGT GAG GCC CTC CGA GGG AGA TAT TAC C-3'), one Cys^{20} residue (TGC) was changed to Ser (TCC) (Figure 2-9A, labeled 20). This mutant was named NT16 C20S. Another mutant of NT16 (NT16 C124S) was produced by introducing a mutation to change the second Cys^{124} residue (TGT) to Ser (TCT) (Figure 2-9A, labeled 124) by using a mutagenic oligonucleotide primer (5'-GCC ATA CCT GAA GAG TTT GGT TAT AAA TAC TAT AGA ATA TTC TAA AAA TGC AAC AAC TGG ATA CTT AGA CAG ATT AAT TCA AGG G-3'). The final mutant, NT16 C161S was generated by mutating the third Cys^{161} residue (TGT) to Ser (TCT) (Figure 2-9A, labeled 161) using a mutagenic oligonucleotide primer (5'-GCA GCG AAA GTA GTC GAT ACG ACT TCT GGC AAA CGT C-3'). After DNA sequence verification, each recombinant plasmid (NT16 C20S, NT16 C124S, or NT16 C161S) was used to transform Max Efficiency DH5α competent *E. coli* cells (Invitrogen). Plasmid DNA was isolated from an overnight culture of a single colony in 10 mL of LB with 100 µg/mL ampicillin and sent for sequencing. Sequences of the wild-type and mutant NT16 constructs were verified using two primers: M13puCR (5'-AGC GGA TAA CAA TTT CAC ACA GG-3') and pProExRev (5'-TCA CTT CTG AGT TCG GCA TC-3').

For expression of recombinant NT16 and NT16 mutants, a single colony harboring the recombinant plasmid (NT16-pProExHTb, NT16 C20S, NT16 C124S, or NT16 C161S), was inoculated into 40 mL of LB containing 40 µL of 50 mg/mL ampicillin in a 250 mL flask and incubated overnight at 37°C with shaking at 275 rpm. Two and a half milliliters of the overnight culture were transferred to individual 500 mL flasks containing 100 mL LB and ampicillin (100 µL of 50 mg/mL). Flasks were incubated at 37°C with shaking at 300 rpm until OD_{600} was 0.5 to 0.6. Cultures were cooled to 16°C with shaking at 150 rpm for 10 min before the addition of

IPTG to a final concentration of 1 mM. Expression was induced by IPTG for 18 h. The bacteria were harvested by centrifugation at 4000 × g for 20 min at 4°C. Pellets were frozen at -80°C overnight and resuspended in 10 mL of cold lysis buffer (300 mM NaCl, 10 mM imidazole in 0.5 M sodium phosphate buffer, pH 8.0). Pellets were then treated as described under the section titled "Expression and purification of recombinant serpin-1Z" with some modification. Cells were sonicated for 10 × 10 seconds with a 10 second rest between bursts using a sonicator connected to a Sonic Dismembrator Model 100 (Fisher Scientific) that was set on level 8.

The soluble fraction of recombinant NT16 and NT16 mutants was purified by nickel-affinity chromatography (Ni^{2+}-NTA) as described for the purification of recombinant serpin-1Z with modification. After the clear lysate (9.4-9.6 mL) was incubated with Ni^{2+}-NTA agarose (Qiagen), the mixture was poured into a 1 cm diameter column, followed by washing. Recombinant NT16 was eluted 4 times with 2.5 mL of elution buffer (300 mM NaCl, 250 mM imidazole in 0.5 M sodium phosphate buffer, pH 8.0). Fractions were analyzed by SDS-PAGE under reducing and non-reducing conditions and immunoblotting. The first elution fraction for purified NT16 and each NT16 mutant was dialyzed against dialysis buffer (20 mM Tris-HCl, 5 mM NaCl, pH 8.0). Each protein (~1.5 mL) was added to a 0.5-3 mL Slide-A-Lyzer 3.5 K Dialysis Cassette (Thermo Scientific) and dialyzed in 1000 mL dialysis buffer (twice, for at least 6 h) at 4°C.

Protein concentration assay

Protein concentrations were determined with the Coomassie Plus™ Protein Assay Reagent (Pierce) using bovine serum albumin (Pierce) as the standard. Alternatively, some samples of purified protein were analyzed by SDS-PAGE together with several bovine serum albumin samples of known amounts to account for the presence of contaminating proteins. This was followed by Coomassie Blue staining and determination of protein concentration by matching to standard bands of similar intensity.

Determination of amino-terminal sequences

To determine amino-terminal sequences, proteins were transferred to a 0.2 µm polyvinylidene difluoride membrane (PVDF; Millipore). The PVDF membrane was washed in 100% methanol for 30 s followed by deionized water for 1 min. Filter paper, fiber pads, PVDF membranes, and gel were soaked in transfer buffer (10 mM CAPS in 10% methanol, pH 11.0)

for 5 min. The transfer cassette was prepared and placed in the blot module (Bio-Rad). A frozen cooling unit was then added to the module and the module was filled with transfer buffer. With stirring, proteins were transferred at 75 V for 1 h, then 60 V for 40 min, and finally, 50 V for 20 min. Membranes were washed three times in deionized water for 5 min each and stained with 0.025% Coomassie Brilliant Blue R-250 in 40% methanol for 5 min. After destaining with 50% methanol for 10 min, the membranes were washed three times in deionized water for 7 min each. Desired bands were excised from the PVDF membrane and subjected to Edman degradation sequencing at the W.M. Keck Foundation Biotechnology Resource Laboratory at Yale University.

Activation of HP16-Xa by bovine factor Xa

Purified recombinant HP16-Xa (100 ng) was incubated with different amounts (50, 100, 200, 300, 400, or 500 ng) of bovine factor Xa (New England Biolabs) in buffer (20 mM Tris-HCl, 150 mM NaCl, pH 8.4) plus $CaCl_2$ (final concentration = 2 mM) and bovine serum albumin (1000 ng). Reaction mixtures were incubated at 37°C for 1 h. Cleavage of HP16-Xa was detected by SDS-PAGE followed by immunoblot analysis using antiserum against HP16 as the primary antibody.

Activity of HP16 using synthetic peptide colorimetric substrates

Amidase activity assays were carried out using the following chromogenic peptides: N-succinyl-Gly-Gly-Phe-*p*-nitroanilide (GGF*p*Na; Sigma S1899), N-succinyl-L-Phe-*p*-nitroanilide (F*p*Na; Sigma S2628), N-succinyl-Ala-Ala-Ala-*p*-nitroanilide (AAA*p*Na; Sigma S4760), N-methoxysuccinyl-Ala-Ala-Pro-Val-*p*-nitroanilide (AAPV*p*Na; Sigma M4765), L-Leu-*p*-nitroanilide (L*p*NA; Sigma L9125), Ala-Ala-Val-Ala-*p*-nitroanilide (AAVA*p*Na; Sigma A9273), N-succinyl-Ala-Ala-Pro-Phe-*p*-nitroanilide (AAPF*p*Na; Sigma S7388), and acetyl-Ile-Glu-Ala-Arg-*p*-nitroanilide (IEAR*p*NA; Kansas State University Microchemical Core Laboratory). ProHP16-Xa (100 ng or 1000 ng) was activated by treatment with bovine factor Xa (500 ng) in buffer (20 mM Tris-HCl, 150 mM NaCl, pH 8.4) plus $CaCl_2$ (final concentration = 2 mM) for 1h at 37°C. Equal volumes of activated HP16-Xa or factor Xa in buffer were applied to wells of a 96-well plate and mixed with 200 µL of 50 µM or 100 µM chromogenic substrate in 0.1 M Tris-HCl, 0.1 M NaCl, 5 mM $CaCl_2$, pH 8.0. Absorbance at 405 nm was measured continuously for 30 min in a PowerWave XS plate reader (BioTek). One unit of activity was defined as a change

in A_{405} of 0.001/min. Amidase activity of HP16-Xa was defined as the activity of HP16-Xa in the presence of factor Xa minus the activity of factor Xa alone.

Estimation of HP16 concentration in plasma

Hemolymph was collected from naïve day 3 fifth instar (n = 3) or from day 3 fifth instar (n = 3) larvae 24 h after injection of *M. luteus* as described in the section titled "Collection of hemolymph" with some modification. Only diethyldithiocarbamic acid was added to prevent melanization, and hemocytes were removed by centrifugation at 8000 × g for 9 min at 4°C. Plasma samples (2 µL) were mixed with water (1 µL), 2X SDS sample buffer (3 µL), and 1X SDS sample buffer (1 µL) followed by heating at 95°C for 5 min. The prepared plasma samples were analyzed by SDS-PAGE together with several HP16-Xa samples of known quantity followed by immunoblot analysis using an HP16 specific antibody. Net pixel intensities determined for each HP16-Xa band using Kodak Digital Science 1D software were used to construct a standard curve (net pixel intensity vs. quantity of HP16-Xa). A line of best fit was determined and used to calculate the concentration of HP16 in naïve and induced plasma.

Activation of proHP16 in naïve plasma incubated with zymosan

Hemolymph from naïve day 3, fifth instar larvae was collected into individual microcentrifuge tubes and centrifuged at 13,100 × g for 12 min at 4°C to remove hemocytes. Cell-free plasma (30 µL) was incubated with 0.4 mg (400 µg) of zymosan A from *Saccharomyces cerevisiae* (Sigma). Day 3, fifth instar plasma only and zymosan A + 30 µL 20 mM Tris-HCl, 150 mM NaCl, pH 8.0 were included as controls. All samples were incubated at room temperature for 1 hr. Incubation was followed by centrifugation at 13,000 × g for 1 min. Supernatant was removed from the pellet and kept for analysis (= unbound). Pellets were washed two times using 300 µL of 20 mM Tris-HCl, 150 mM NaCl, pH 8.0. Each wash was followed by centrifugation at 13,000 × g for 1 min and removal of the buffer. Bound proteins were eluted with 30 µL of 2X SDS sample buffer containing β-mercaptoethanol at 95°C for 5 min. Supernatants, bound protein samples, and control samples were subjected to SDS-PAGE and immunoblot analysis using HP16 antiserum as the primary antibody.

Results

HP16 protein and mRNA levels during development

Immunoblot analysis of larval plasma using an antibody to recombinant HP16 detected a specific band of expected size for proHP16 (~51 kDa). ProHP16 protein levels increased during the larval to pupal transition (Figure 2-2A). Highest expression was observed at the wandering (W1-W3), prepupal (PP), and pupal stages. To investigate if the observed fluctuations in proHP16 protein level correlated with changes in HP16 mRNA level, total RNA samples were collected from fat body of selected developmental stages and analyzed by quantitative RT-PCR (Figure 2-2B). HP16 mRNA levels in W2 larvae were significantly greater than D2, D4, and PP.

HP16 protein and gene expression in immune challenged larvae

To learn more about HP16 protein expression in plasma and regulation of the HP16 gene upon bacterial infection, larvae were injected with 0.85% NaCl (saline), 10^8 cells *E. coli*, or 500 µg *M. luteus*. Plasma samples from injected larvae were separated by SDS-PAGE followed by immunoblot analysis (Figure 2-3A). A specific band corresponding to proHP16 (~51 kDa) was more intense in larvae that had been injected with *E. coli* or *M. luteus*. HP16 concentration in plasma from control (= naïve) larvae was 1.4 µg/mL ± 0.1 µg/mL and increased to 4.9 µg/mL ± 2.3 µg/mL when larvae were injected with *M. luteus* 24 h prior to hemolymph collection (Figure 2-3C). HP16 concentrations between control and injected larvae were not significantly different ($p = 0.0651$). HP16 mRNA levels in fat body samples from larvae injected with *M. luteus* and *E. coli* were significantly greater (8-10 fold) than those from saline-injected insects (Figure 2-3B).

Purification of recombinant HP16 and HP16 mutants

HP16 and two site-directed mutants of HP16 were expressed as recombinant proteins to investigate functions of HP16. Figure 2-4 is a schematic representation of wild-type HP16 and HP16 mutants that were expressed and purified. To obtain a form of HP16 that could be artificially activated, I mutated the predicted activation site of HP16 from HTGL to IEGR, a sequence preferred for cleavage by bovine factor Xa. This mutant was named HP16-Xa. I also prepared a mutation that changed the catalytic Ser residue of wild-type HP16 to Ala to produce an inactive form of HP16 (named HP16 S-A). All of the recombinant proteins were secreted into the Sf9 cell culture medium utilizing their own secretion signal peptides. Wild-type HP16,

HP16-Xa, and HP16 S-A in the cell culture supernatant bound to concanavalin A-Sepharose 4B, indicating that they are glycoproteins. Proteins eluted from the concanavalin A column were further purified by anion exchange chromatography using a Q-Sepharose^{TM} Fast Flow column followed by hydrophobic interaction chromatography (HIC) with an Econo-Pac Methyl HIC Cartridge (wild-type HP16 and HP16 S-A) or ammonium sulfate precipitation (HP16-Xa) and gel permeation chromatography on a Sephacryl-S100 High Resolution column. Analysis by SDS-PAGE and immunoblot detection indicated that wild-type HP16, HP16-Xa, and HP16 S-A were of reasonable purity (Figure 2-5, panels A-C). Wild-type HP16 appeared to be partially cleaved during expression and purification, as two bands corresponding to the predicted size of the catalytic domain (~28.5 kDa) and the amino-terminal domain (~20.4 kDa) were detected. When these two bands were subjected to Edman degradation, the five amino acid residues at the amino-terminus of the 28.5 kDa band were determined to be IVNGQ (Figure 2-1), confirming that wild-type HP16 was cleaved at its putative activation site during expression. However, residues of the 20.4 kDa band, predicted to be the amino-terminal fragment, could not be determined. The sequence of the amino-terminus may be blocked by the formation of pyroglutamate (expected sequence of QKLSD). HP16-Xa and HP16 S-A had an apparent mass of 51 kDa. This mass is slightly larger than the mass of 47 kDa calculated from the amino acid sequence of proHP16 deduced from the cloned cDNA sequence, which is consistent with a conclusion that the proteins are glycosylated. From a starting culture volume of 2 liters, 0.008 mg of wild-type HP16, 0.67 mg of HP16-Xa, and 0.16 mg of HP16 S-A were purified.

HP16 contains an interdomain disulfide bond

An alignment between HP16 and bovine chymotrysinogen (NP_001098924) showed the presence of three conserved pairs of predicted disulfide bonds in the catalytic domain and the potential for a disulfide bond between the amino-terminal and catalytic domains of HP16 (Figure 2-1). To test if the amino-terminal and catalytic domains of HP16 remain connected by a disulfide bond after proteolytic activation, purified wild-type HP16 was mixed in sample buffer with or without β-mercaptoethanol and analyzed by SDS-PAGE and immunoblotting (Figure 2-6). In the absence of reducing agent, a single band co-migrated with the zymogen (~51 kDa), but under reducing conditions, three bands corresponding to HP16 zymogen (~51 kDa), HP16

catalytic domain (~28.5 kDa), and HP16 amino-terminal domain (~20.4 kDa) were detected. This result suggests that the two domains of HP16 are connected by a disulfide bond.

Cleavage of HP16-Xa by bovine factor Xa

In order to use HP16-Xa to investigate the function of HP16 in immune responses, the ability of bovine factor Xa to cleave the recombinant protein was determined. Immunoblot analysis revealed that increased cleavage of HP16-Xa correlated with bovine factor Xa amount (Figure 2-7). Bovine serum albumin added to the reaction mixture slightly improved cleavage efficiency. To determine if HP16-Xa was activated after cleavage by bovine factor Xa and to identify a suitable colorimetric substrate for detecting activity of HP16-Xa, several chromogenic peptides were tested. Chromogenic peptides with aromatic (Phe, Tyr, Trp) or hydrophobic (Ala, Val, Gly, Leu) residues were used, because HP16 is predicted to have chymotrypsin/elastase like specificity. Activated HP16-Xa had no detectable activity for any substrate tried, including the substrate (acetyl-Ile-Glu-Ala-Arg-*p*-nitroanilide) for trypsin-like proteinases. Positive controls using trypsin, chymotrypsin, and elastase confirmed that the assay was working correctly. These results suggest one of two things: (1) substrates tested were not suitable for activated HP16-Xa or (2) proHP16-Xa cleaved by bovine factor Xa is not an active proteinase.

Complex formation between HP16 and serpin-1Z

Inhibition of a proteinase by a serpin is characterized by cleavage of the serpin, resulting in the formation of an SDS-stable serpin-proteinase complex. To detect proteolytic activity of HP16, we investigated whether it could form a complex with *M. sexta* serpin-1Z. The P1 residue at the predicted scissile bond in the RCL of serpin-1Z is Tyr and makes it a potential inhibitor of HP16, as HP16 is predicted to have chymotrypsin/elastase-like specificity. When serpin-1Z was mixed with active HP16-Xa, the 28.5 kDa catalytic domain decreased in intensity, and a new immunoreactive band at ~70 kDa was observed with antibodies to HP16 or serpin-1, consistent with the expected size of a serpin-proteinase complex (Figure 2-8A). This serpin/proteinase complex band was absent in lanes lacking activated HP16-Xa (Figure 2-8A). As a control to confirm that HP16 must be in a catalytically active form to react with serpin-1Z to form an SDS-stable complex and that the ~70 kDa band was not a complex of serpin-1Z with bovine factor Xa, the same experiment was carried out with the catalytically inactive recombinant HP16 S-A protein and serpin-1Z (Figure 2-8B). Recombinant HP16 S-A incubated with bovine factor Xa

and mixed with serpin-1Z did not result in the detection of a serpin-proteinase complex. These results indicate that HP16-Xa was activated by bovine factor Xa and could cleave serpin-1Z to form a serpin-proteinase complex.

Purification of wild-type NT16 and NT16 mutants

HP16 contains an amino-terminal 170 residue region that has no significant match to any characterized protein in the current databases. To characterize this region and investigate its potential function, a recombinant protein containing the amino-terminal 165 residues of HP16, named NT16 (Figure 2-4D), and three NT16 mutants, each lacking one Cys residue (C20S, C124S, and C161S), were expressed in *E. coli*. In SDS-PAGE under reducing conditions, a single band of expected size (21.4 kDa) was observed for wild-type NT16 and each NT16 mutant (Figure 2-9B). However, when analyzed using non-reducing conditions, a band at 42 kDa was also present, indicating that wild-type NT16 and NT16 mutants can exist as both a monomer and disulfide-linked dimer (Figure 2-9B). Moreover, there were multiple bands around 20 kDa for each form, which may represent different disulfide bond arrangements between the three Cys residues. In wild-type NT16 (monomer form), three possible disulfide bonds (Cys20-Cys124; Cys20-Cys161; Cys124-Cys161) could be formed (Figure 2-9A). Upon mutation of a Cys residue, that number goes down to one. Wild-type NT16 had four bands (a, b, c, d) around the expected size for a monomer (21.4 kDa). When Cys^{20} was mutated, bands a, b, and c, but not d were present. Bands a, b, and d (not c) were detected after the mutation of Cys^{124}, whereas bands b and d (not a/c) were observed after the mutation of Cys^{161}. These results suggest that the Cys residues of recombinant NT16 are able to form multiple disulfide pairs. Band c disappeared in both C124S and C161S samples, indicating that these Cys residues may form a disulfide bond. Cys20 may form a disulfide bond with either Cys124 or Cys161 as band d was detected in samples 3 and 4, but not sample 2.

Lack of evidence for autoactivation of HP16

To test the hypothesis that HP16 possesses the ability to undergo autoactivation, active HP16-Xa was incubated with the catalytically inactive mutant, proHP16 S-A. If active HP16-Xa can cleave HP16 at the predicted activation site, the amount of proHP16 S-A should decrease, and the amount of the catalytic and amino-terminal domains of HP16 should increase. However, no difference in the amount of proHP16 S-A (~51 kDa) or the catalytic (~28.5 kDa) and amino-

terminal (~20.4 kDa) domains of HP16 was observed after incubation with active HP16-Xa for 4, 6, or 8 h (Figure 2-10A-C). These results suggest that active HP16 does not cleave proHP16 under the conditions tested.

Activation of HP16 in plasma by treatment with zymosan

To determine if proHP16 activation in plasma could be stimulated by a microbial elicitor, plasma was incubated with zymosan. After removal of zymosan by centrifugation, the supernatant and plasma proteins in the zymosan pellet were subjected to SDS-PAGE followed by immunoblot analysis using an antibody specific to HP16 (Figure 2-11). For plasma alone or supernatant, the HP16 antibody only recognized a band corresponding to the size of proHP16 zymogen (~51 kDa). However, in the pellet fraction, several immunoreactive bands were detected, including bands at 75-86 kDa, a size consistent with that predicted for serpin-proteinase complexes. Bands at ~21 kDa may be the amino-terminal domain of HP16 (expected size = 20.4 kDa). The catalytic domain of HP16 (~28.5 kDa) was not detected in the bound fraction. This may indicate that HP16 was activated in plasma treated with zymosan and rapidly formed a serpin-HP16 complex, which remained associated with zymosan. No HP16 signal was detected in the control supernatant or bound fraction, indicating that observed bands for HP16 in the pellet fraction after incubation of plasma with zymosan were due HP16 in plasma, not components of zymosan.

Discussion

Since the identification of numerous serine proteinases in the hemolymph of *Manduca sexta*, one goal has been to elucidate their function in response to infection by bacteria, fungi, or other pathogens. At present, only a handful of these proteinases have been studied functionally. HP14, HP21, and PAPs 2&3 form a cascade for prophenoloxidase activation (Jiang et al., 2003a; Jiang et al., 2003b; Ji et al., 2004; Wang and Jiang, 2004; Gorman et al., 2007; Wang and Jiang, 2007). HP6 and PAP-1 are involved in activation of prophenoloxidase, whereas HP6 and HP8 are in a pathway resulting in the production of antimicrobial peptides (Jiang et al., 1998; An et al., 2009; An et al., 2010).

Before I could begin to investigate the role of HP16 in innate immune responses, I produced recombinant wild-type HP16 and two HP16 mutants (HP16-Xa and HP16 S-A) in

insect cells and NT16 and three NT16 mutants in *E. coli*. I used a baculovirus expression system and *Spodoptera frugiperda* Sf-9 cells to produce wild-type HP16 and two HP16 mutants under the control of the polyhedrin promoter. Wild-type HP16, HP16-Xa, and HP16 S-A were all successfully expressed using this system.

Expression and purification of wild-type HP16

Wild-type HP16 appeared to be activated during expression, as two bands corresponding to the expected sizes of the catalytic and amino-terminal domains of HP16 were detected by HP16 antibody (Figure 2-5A). Amino-terminal sequencing by Edman degradation confirmed that HP16 had been cleaved at the predicted activation site and that the band at ~28.5 kDa was the catalytic domain of HP16. Phylogenetic analysis showed that the catalytic domain of HP16 is the most similar to *Drosophila* gastrulation defective, but also clusters with HP14, HP19, and HP20 from *M. sexta* and factor C from horseshoe crab (Jiang et al., 2005). HP19 and HP20 have not been studied, but the remaining proteinases have all been shown to autoactivate. Therefore, I hypothesized that HP16 might undergo autoactivation to function in a proteolytic cascade involved in the innate immune response of *M. sexta*.

Several proteinases, including HP14, Factor C, Factor G, and gastrulation defective, found in arthropods serve as the initiating proteinase in an extracellular proteinase cascade in response to infection and possess the ability to autoactivate. HP14 stimulates a pathway leading to the activation of prophenoloxidase. This protein consists of five low-density lipoprotein receptor class A domains, a Sushi domain, a cysteine-rich region (Wonton), and C-terminal serine proteinase domain (Ji et al., 2004). HP14 autoactivates in the presence of peptidoglycan (Ji et al., 2004) or β-1,3-glucan and βGRP2 (Wang and Jiang, 2006). Like HP14, factor C from the horseshoe crab, which is involved in blood coagulation, is composed of a complex domain structure. Factor C contains five Sushi domains, an epidermal growth factor-like domain, a lectin-like domain, a cysteine-rich domain, a proline-rich domain, and a C-terminal serine proteinase domain (Muta et al., 1991). Autoactivation of factor C occurs upon interaction with lipopolysaccharide (Nakamura et al., 1986; Nakamura et al., 1988a), lipid A analogs (Nakamura et al., 1988b), and acidic phospholipids (Nakamura et al., 1988b). Active factor C activates factor B followed by the activation of clotting enzyme. Clotting enzyme stimulates the conversion of coagulogen to coagulin. Factor G is another proteinase from the horseshoe crab that undergoes

autoactivation in response to β-1,3-glucan to stimulate blood coagulation (Muta et al., 1995). Unlike factor C, factor G is a heterodimer consisting of two noncovalently linked subunits. Subunit α is composed of an amino-terminal bacterial β-1,3-glucanase-like sequence followed by three tandom repeat structures found in xylanase A and two tandom repeats found in xylanase Z. The serine proteinase domain is found on subunit β (Muta et al., 1995; Iwanaga et al., 1998). Gastrulation defective is crucial to dorsal-ventral patterning in *Drosophila*. Gastrulation defective contains a ~23 kDa amino-terminal region without any known specialized domains (e.g. Sushi, lectin-like, Cys/Pro-rich) and a C-terminal serine proteinase domain (~34 kDa). Autoactivation of gastrulation defective takes place in the presence of snake zymogen, which is the next proteinase in the cascade (Dissing et al., 2001).

Autoactivating proteinases are also found in the mammalian complement system (classical and lectin pathways). Such proteinases include C1r, mannose-binding lectin (MBL)-associated serine proteinase (MASP)-1, and MASP-2. Each proteinase is composed of five noncatalytic domains followed by one serine proteinase domain. Noncatalytic domains include two C1r/C1s/sea urchin Uegf/bone morphogenic protein (CUB) domains, one epidermal growth factor-like (EGF) domain, and two complement control protein (CCP) modules (Sim and Laich, 2000). The two CUB domains and the EGF-like domain function to facilitate the interaction between the proteinases and the recognition molecules, whereas the CCP modules function to stabilize the serine proteinase domain structure and are involved in the autoactivation of C1r, MASP-1, and MASP-2. In the classical pathway, C1r undergoes autoactivation in the presence of a recognition molecule, C1q (Kardos et al., 2001; Kardos et al., 2008). Active C1r activates C1s, which in turn, cleaves C2 and C4 (Gál et al., 2007). For the lectin pathway, mannose-binding lectin is the recognition molecule that binds to carbohydrates on the pathogen surface. MASP-1 and MASP-2 are proteinases that interact with mannose-binding lectin and undergo autoactivation (Vorup-Jensen et al., 2000; Ambrus et al., 2003; Gál et al., 2005). Active MASP-2 cleaves C2 and C4 to generate the C3 convertase, C4bC2b, and prothrombin to generate thrombin (Ambrus et al., 2003; Gál et al., 2005; Gál et al., 2009) while active MASP-1 cleaves C2, C3, fibrinogen, and protease activated receptor 4 (Hajela et al., 2002; Ambrus et al., 2003; Gál et al., 2009).

To determine if HP16 could undergo autoactivation like the proteinases mentioned above, I conducted an experiment in which I incubated active HP16-Xa with the noncatalytically active

mutant, HP16 S-A. If autoactivation was taking place, I expected an increase in the amount of HP16 catalytic and amino-terminal domains and a decrease in HP16 zymogen in samples containing active HP16-Xa and HP16 S-A when compared to active HP16-Xa alone. However, active HP16-Xa did not cleave proHP16 S-A, indicating that HP16 does not autoactivate (Figure 2-10). When plasma was incubated with zymosan A (yeast cell walls), proHP16 was apparently converted to active HP16. Two observations support this idea: (1) HP16 zymogen disappeared and (2) potential serpin-HP16 complexes formed (Figure 2-11). This result can be interpreted in two ways. First, it is possible that zymosan stimulates activation of an unidentified proteinase that cleaves proHP16. Second, an interaction between zymosan and proHP16 may occur that allows HP16 to autoactivate. The latter would be consistent with the autoactivation of HP14, factors C and G, C1r, MASP-1, and MASP-2. At this point, it is unclear how proHP16 is activated and more experiments are necessary to develop a better understanding of this process.

Fluctuations in HP16 protein and HP16 mRNA levels during larval to pupal development

I found that both HP16 protein level in hemolymph and HP16 mRNA level in fat body increased thoughout the feeding stage (5^{th} instar), peaked on day 2 of the wandering stage (non-feeding), and decreased as larvae entered the prepupal and pupal stages (Figure 2-2). This pattern of protein and mRNA expression matches well with changes in the ecdysteroid titer that controls metamorphosis (Figure 2-12). The first ecdysteroid peak triggers a behavioral change from feeding larvae to non-feeding, wandering larvae, whereas the second ecdysteroid peak triggers molting. This led to the hypothesis that HP16 may have a role in metamorphosis and that the expression of HP16 may be regulated by ecdysteroids. However, this hypothesis was not investigated in the current work. During the larval to pupal transition, the insect undergoes tissue rearrangement, and HP16 may play a role in this process by hydrolyzing components of the extracellular matrix. Futhermore, since HP16 is similar to gastrulation defective from *Drosophila*, it is feasible to speculate that HP16 may be involved in a serine proteinase cascade that leads to the activation of a cytokine, such as spätzle, to aid the insect in development. Alternatively, HP16 may be involved in the immune response of the insect to protect developing larvae or pupae from infection by foreign invaders throughout metamorphosis.

It is well established that molting and metamorphosis are controlled by juvenile hormone and ecdysteroids. Juvenile hormone controls the nature of the molt while ecdysteroids, such as ecdysone and 20-hydroxyecdysone, direct the molting process (Riddiford, 1993; Riddiford et al., 2003; Riddiford, 2008). During molting and metamorphorsis, it is common to observe increases or decreases in protein synthesis and mRNA expression that are likely to be regulated by changes in ecdysteroid and juvenile hormone titers. When such changes are observed, experiments may be completed to test the effect of juvenile hormone and 20-hydroxyecdysone on gene expression.

Kanost et al. (1995) determined the effect of 20-hydroxyecdysone on *M. sexta* serpin-1 protein synthesis and gene expression to explain the decrease in serpin-1 mRNA levels at the larval-larval molt and the onset of the wandering stage. Addition of 20-hydroxyecdysone to cultured fat body led to decreased serpin-1 protein synthesis and mRNA expression. Ligation of larvae eliminated the decrease in mRNA expression, and injection of 20-hydroxyecdysone into ligated larvae exhibited a decrease in serpin-1 mRNA expression that was reminiscent of unligated larvae at the wandering stage, indicating that 20-hydroxyecdysone negatively regulates serpin-1 gene expression (Kanost et al., 1995). Decreases in *M. sexta* prophenoloxidase activating proteinase-1 mRNA expression during development were detected by RT-PCR and correlated with peaks in ecdysteroid levels in late fifth instar larvae and late wandering stage larvae (Zou et al., 2005). The addition of 20-hydroxyecdysone to cultured fat body led to decreased prophenoloxidase-activating proteinase-1 mRNA expression, suggesting negative regulation of expression by this ecdysteroid (Zou et al., 2005). Prophenoloxidase from *Anopheles gambiae* is another immune related gene that is regulated by 20-hydroxyecdysone (Ahmed et al., 1999; Müller et al., 1999). Transcript levels for five out of the six prophenoloxidase genes (1-4, 6) increased in an *A. gambiae* cell line exposed to 20-hydroxyecdysone, while transcript level of prophenoloxidase gene-5 was down-regulated (Ahmed et al., 1999; Müller et al., 1999).

Activation of HP16-Xa by bovine factor Xa produces an active proteinase

One strategy to obtain an active proteinase that can be used to study biological function is to introduce a mutation at the activation site of the proteinase that can be artificially activated by bovine factor Xa. For HP16, I mutated the residues HTGL to IEGR. Purified recombinant HP16-Xa was incubated with different amounts of bovine factor Xa followed by immunoblot analysis using HP16 antibody. I found that all amounts of bovine factor Xa cleaved HP16-Xa, but 500 ng

of bovine factor Xa led to the most complete cleavage, as HP16 zymogen (~51 kDa) disappeared and two bands corresponding to the catalytic and amino-terminal domains increased in intensity (Figure 2-7). The need for such a large amount of bovine factor Xa indicates that cleavage of HP16-Xa was not very efficient. Other factor Xa mutant proteinases were efficiently cleaved with 40 ng or 50 ng of factor Xa (An et al., 2009; An et al., 2010). When using 500 ng of bovine factor Xa in a reaction mixture, it is important to include a factor Xa only control since bovine factor Xa has the ability to non-specifically cleave proteinases. Including this control assures that observed proteinase activity is due to the proteinase and not bovine factor Xa.

To confirm that HP16-Xa incubated with bovine factor Xa was an active proteinase, I mixed active HP16-Xa with several serpin-1 isoforms. Based on the prediction that HP16 has chymotrypsin/elastase-like specificity, I selected serpin-1 isoforms with aromatic or small hydrophobic residues at the predicted P1 residue for analysis (serpin-1B, -1C, -1F, -1G, -1H, -1I, -1K, and -1Z). Only serpin-1Z (P1 residue = Tyr) showed a potential interaction with active HP16-Xa and was selected for further purification and analysis. In samples containing active HP16-Xa and serpin-1Z, serpin-1 and HP16 antibodies recognized a higher molecular weight band (~70 kDa) consistent with the expected size of a serpin-1-HP16 complex. No band was detected in samples containing bovine factor Xa and serpin-1Z indicating that the complex did not include factor Xa. Moreover, when HP16 S-A (a catalytically inactive HP16 protein) was mixed with serpin-1Z, no complex formation was observed with either antibody. These results confirm that HP16-Xa was an active proteinase and cleaved serpin-1Z in the RCL. The biological relevance of serpin-1Z as an inhibitor of HP16 was not examined in the current study, but warrents further investigation.

Bacteria induce increased HP16 protein levels in plasma and mRNA levels in fat body

Consistent with Northern blot results (Jiang et al., 2005), the injection of bacteria (*M. luteus* or *E. coli*) into larvae increased HP16 protein and mRNA levels when compared to larvae injected with saline (Figure 2-3A/B). HP16 concentration in plasma from control (= naïve) larvae was determined to be 1.4 µg/mL ± 0.1 µg/mL and increased to 4.9 µg/mL ± 2.3 µg/mL when larvae were injected with *M. luteus* 24 h prior to plasma collection (Figure 2-3C).

Analysis of NT16 and NT16 mutants

The amino-terminal 170 residue region of HP16 is unique and has no significant match to any characterized protein in the current databases although a homologous sequence is present in ESTs from some other lepidopteran species. With the goal of further characterizing this region, I purified recombinant NT16 (residues 1-165) and three NT16 mutants. This region contains three Cys residues, one of which may form an interdomain disulfide bond. I attempted to determine the Cys-Cys linkage pattern by disulfide mapping, but was not successful. Success was limited by the matrix conditions available for use with MALDI mass spectrometry.

I produced recombinant NT16 and three NT16 mutants by performing site-directed mutagenesis to change each Cys residue to Ser. Under reducing conditions, all four NT16 proteins ran as a single band at the expected size (~21.4 kDa). When the same samples were subjected to non-reducing conditions, each protein showed multiple monomer and dimer forms, indicating that different disulfide bond arrangements were possible and that the different arrangements observed depended on which Cys residue was mutated. Disulfide bonds are stabilizers of protein structure, and it is reasonable to hypothesize that one of more of the introduced mutations could result in the loss of proper protein folding, providing that this portion of HP16 is structured.

Challenges in working with serine proteinases

Proteinases can be difficult to study because of inherent instability during purification, sensitivity to assay conditions (e.g. temperature, pH, ionic strength, and presence of detergents), stability during storage, susceptibility to degradation by other proteinases, and the inability to identify a proper substrate to investigate proteinase activity (Beynon and Bond, 1989). One of the first challenges that can be faced is finding the best expression system and purification scheme for the serine proteinase of interest. This process can take from a few months to over a year. There are many choices, and the process usually begins by using a system that has been used by others in the lab. Based on success with other hemolymph proteinases, I first tried wild-type HP16 expression using the *Drosophila* S2 cell system. Recombinant wild-type HP16 was produced by this system; however, the molecular weight was much higher than the expected size (51 kDa; data not shown). This suggests that wild-type HP16 may have been activated during expression and reacted with a serpin made by the *Drosophila* S2 cells. Since recombinant HP16

was not of expected size, a baculovirus expression system was the next system tried. Trying multiple expression systems is not uncommon, which suggests that not all proteinases behave in the same way and what worked for one proteinase may not work for another (Beynon and Bond, 1989). Optimization of the expression system is followed by determination of the purification scheme to be used. Deciding what purification steps to use entails a considerable amount of trial and error. Each step exploits a different characteristic of the proteinase (e.g. glycosylation, charge, hydrophobicity, size, and N- or C-terminal tags) to be purified. The inherent instability of proteinases is a challenge during purification. Additionally, the amount of proteinase zymogen secreted from an expression in an insect cell line is often low.

After successful purification of a proteinase, the next challenge that may be encountered is proteinase stability during storage. Wild-type HP16 was not stable during storage at -80°C. In addition, HP16-Xa tended to form insoluble aggregates during storage.

Working with proteinases is hard and they do not always behave the way you expect them to. To alleviate some of the challenges that I mentioned above, it is important to have a plan of what experiments are to be conducted before expressing and purifying a proteinase. Once the proteinase is purified, experiments should be rapidly done while the preparation is active.

Future Directions

I believe that the work presented in this chapter furthered the understanding of HP16 and helped lay a foundation for future experiments involving the proteolytic activity, regulation, and biological function. The following questions should be investigated in the future.

(1) Is HP16 involved in prophenoloxidase activation or production of antimicrobial peptides?
(2) Is HP16 activated by another hemolymph proteinase?
(3) What is the substrate(s) of HP16?
(4) What serpin(s) regulates HP16 activity?
(5) What is the function of the amino-terminal domain of HP16?
(6) Is HP16 expression regulated by ecdysteroids?
(7) Does HP16 have a role in metamorphosis?

References

Ahmed A, Martin D, Manetti AG, Han SJ, Lee WJ, Mathiopoulos KD, Müller HM, Kafatos FC, Raikhel A, & Brey PT (1999) Genomic structure and ecdysone regulation of the prophenoloxidase 1 gene in the malaria vector *Anopheles gambiae*. *Proc Natl Acad Sci USA* **96**: 14795-14800

Ambrus G, Gál P, Kojima M, Szilágyi K, Balczer J, Antal J, Gráf L, Laich A, Moffatt BE, Schwaeble W, Sim RB, & Závodszky P (2003) Natural substrates and inhibitors of mannan-binding lectin-associated serine protease-1 and -2: a study on recombinant catalytic fragments. *J Immunol* **170**: 1374-1382

An C, Ishibashi J, Ragan EJ, Jiang H, & Kanost MR (2009) Functions of *Manduca sexta* hemolymph proteinases HP6 and HP8 in two innate immune pathways. *J Biol Chem* **284**: 19716-19726

An C, Jiang H, & Kanost MR (2010) Proteolytic activation and function of the cytokine Spätzle in the innate immune response of a lepidopteran insect, *Manduca sexta*. *FEBS J* **277**: 148-162

Beynon RJ & Bond JS (eds) (1989) *Proteolytic enzymes: a practical approach.* IRL Press at Oxford University Press: Oxford, England

Bollenbacher WE, Smith SL, Goodman W, & Gilbert LI (1981) Ecdysteroid titer during larval-pupal-adult development of the tobacco hornworm, *Manduca sexta*. *Gen Comp Endocrinol* **44**: 302-306

Cerenius L, Kawabata S, Lee BL, Nonaka M, & Söderhäll K (2010) Proteolytic cascades and their involvement in invertebrate immunity. *Trends Biochem Sci* **35**: 575-583

Cerenius L, Lee BL, & Söderhäll K (2008) The proPO-system: pros and cons for its role in invertebrate immunity. *Trends Immunol* **29**: 263-271

Dissing M, Giordano H, & DeLotto R (2001) Autoproteolysis and feedback in a protease cascade directing *Drosophila* dorsal-ventral cell fate. *EMBO J* **20**: 2387-2393

Dunkelberger JR & Song WC (2010) Complement and its role in innate and adaptive immune responses. *Cell Res* **20**: 34-50

Dunn PE & Drake D (1983) Fate of bacteria injected into naive and immunized larvae of the tobacco hornworm, *Manduca sexta*. *J Invertebr Pathol* **41**: 77-85

Gál P, Barna L, Kocsis A, & Závodszky P (2007) Serine proteases of the classical and lectin pathways: similarities and differences. *Immunobiology* **212**: 267-277

Gál P, Dobó J, Závodszky P, & Sim RB (2009) Early complement proteases: C1r, C1s and MASPs. A structural insight into activation and functions. *Mol Immunol* **46**: 2745-2752

Gál P, Harmat V, Kocsis A, Bián T, Barna L, Ambrus G, Végh B, Balczer J, Sim RB, Naray-Szabó G, & Závodszky P (2005) A true autoactivating enzyme. Structural insight into mannose-binding lectin-associated serine protease-2 activations. *J Biol Chem* **280**: 33435-33444

Gettins PG (2002) Serpin structure, mechanism, and function. *Chem Rev* **102**: 4751-4804

Gorman MJ, Wang Y, Jiang H, & Kanost MR (2007) *Manduca sexta* hemolymph proteinase 21 activates prophenoloxidase-activating proteinase 3 in an insect innate immune response proteinase cascade. *J Biol Chem* **282**: 11742-11749

Hajela K, Kojima M, Ambrus G, Wong KH, Moffatt BE, Ferluga J, Hajela S, Gál P, & Sim RB (2002) The biological functions of MBL-associated serine proteases (MASPs). *Immunobiology* **205**: 467-475

Iwanaga S, Kawabata S, & Muta T (1998) New types of clotting factors and defense molecules found in horseshoe crab hemolymph: their structures and functions. *J Biochem* **123**: 1-15

Iwanaga S & Lee BL (2005) Recent advances in the innate immunity of invertebrate animals. *J Biochem Mol Biol* **38**: 128-150

Ji C, Wang Y, Guo X, Hartson S, & Jiang H (2004) A pattern recognition serine proteinase triggers the prophenoloxidase activation cascade in the tobacco hornworm, *Manduca sexta*. *J Biol Chem* **279**: 34101-34106

Jiang H & Kanost MR (2000) The clip-domain family of serine proteinases in arthropods. *Insect Biochem Mol Biol* **30**: 95-105

Jiang H & Kanost MR (1997) Characterization and functional analysis of 12 naturally occurring reactive site variants of serpin-1 from *Manduca sexta*. *J Biol Chem* **272**: 1082-1087

Jiang H, Wang Y, Gu Y, Guo X, Zou Z, Scholz F, Trenczek TE, & Kanost MR (2005) Molecular identification of a bevy of serine proteinases in *Manduca sexta* hemolymph. *Insect Biochem Mol Biol* **35**: 931-943

Jiang H, Wang Y, & Kanost MR (1999) Four serine proteinases expressed in *Manduca sexta* haemocytes. *Insect Mol Biol* **8**: 39-53

Jiang H, Wang Y, & Kanost MR (1998) Pro-phenol oxidase activating proteinase from an insect, *Manduca sexta*: a bacteria-inducible protein similar to *Drosophila* easter. *Proc Natl Acad Sci USA* **95**: 12220-12225

Jiang H, Wang Y, Yu XQ, & Kanost MR (2003a) Prophenoloxidase-activating proteinase-2 from hemolymph of *Manduca sexta*. A bacteria-inducible serine proteinase containing two clip domains. *J Biol Chem* **278**: 3552-3561

Jiang H, Wang Y, Yu XQ, Zhu Y, & Kanost M (2003b) Prophenoloxidase-activating proteinase-3 (PAP-3) from *Manduca sexta* hemolymph: a clip-domain serine proteinase regulated by serpin-1J and serine proteinase homologs. *Insect Biochem Mol Biol* **33**: 1049-1060

Kanost MR & Clarke T (2005) Proteases. In *Comprehensive Molecular Insect Science,* Gilbert LI, Iatrou K, Gill SS (eds) pp 247-265. Elsevier

Kanost MR & Gorman MJ (2008) Phenoloxidases in insect immunity. In *Insect Immunity,* Beckage NE (ed) pp 69-96. Elsevier

Kanost MR, Jiang H, Wang Y, Yu XQ, Ma C, & Zhu Y (2001) Hemolymph proteinases in immune responses of *Manduca sexta*. *Adv Exp Med Biol* **484**: 319-328

Kanost MR, Prasad SV, Huang Y, & Willott E (1995) Regulation of serpin gene-1 in *Manduca sexta*. *Insect Biochem Mol Biol* **25**: 285-291

Kardos J, Gál P, Szilágyi L, Thielens NM, Szilágyi K, Lõrincz Z, Kulcsár P, Gráf L, Arlaud GJ, & Závodszky P (2001) The role of the individual domains in the structure and function of the catalytic region of a modular serine protease, C1r. *J Immunol* **167**: 5202-5208

Kardos J, Harmat V, Palló A, Barabás O, Szilágyi K, Gráf L, Naray-Szabó G, Goto Y, Závodszky P, & Gál P (2008) Revisiting the mechanism of the autoactivation of the complement protease C1r in the C1 complex: structure of the active catalytic region of C1r. *Mol Immunol* **45**: 1752-1760

Krem MM & Di Cera E (2002) Evolution of enzyme cascades from embryonic development to blood coagulation. *Trends Biochem Sci* **27**: 67-74

Müller HM, Dimopoulos G, Blass C, & Kafatos FC (1999) A hemocyte-like cell line established from the malaria vector *Anopheles gambiae* expresses six prophenoloxidase genes. *J Biol Chem* **274**: 11727-11735

Muta T, Miyata T, Misumi Y, Tokunaga F, Nakamura T, Toh Y, Ikehara Y, & Iwanaga S (1991) Limulus factor C. An endotoxin-sensitive serine protease zymogen with a mosaic structure of complement-like, epidermal growth factor-like, and lectin-like domains. *J Biol Chem* **266**: 6554-6561

Muta T, Seki N, Takaki Y, Hashimoto R, Oda T, Iwanaga A, Tokunaga F, & Iwanaga S (1995) Purified horseshoe crab factor G. Reconstitution and characterization of the (1-->3)-beta-D-glucan-sensitive serine protease cascade. *J Biol Chem* **270**: 892-897

Nakamura T, Morita T, & Iwanaga S (1986) Lipopolysaccharide-sensitive serine-protease zymogen (factor C) found in Limulus hemocytes. Isolation and characterization. *Eur J Biochem* **154**: 511-521

Nakamura T, Tokunaga F, Morita T, & Iwanaga S (1988a) Interaction between lipopolysaccharide and intracellular serine protease zymogen, factor C, from horseshoe crab (*Tachypleus tridentatus*) hemocytes. *J Biochem* **103**: 370-374

Nakamura T, Tokunaga F, Morita T, Iwanaga S, Kusumoto S, Shiba T, Kobayashi T, & Inoue K (1988b) Intracellular serine-protease zymogen, factor C, from horseshoe crab hemocytes. Its activation by synthetic lipid A analogues and acidic phospholipids. *Eur J Biochem* **176**: 89-94

Riddiford LM (2008) Juvenile hormone action: a 2007 perspective. *J Insect Physiol* **54**: 895-901

Riddiford LM (1993) Hormone receptors and the regulation of insect metamorphosis. *Receptor* **3**: 203-209

Riddiford LM, Hiruma K, Zhou X, & Nelson CA (2003) Insights into the molecular basis of the hormonal control of molting and metamorphosis from *Manduca sexta* and *Drosophila melanogaster*. *Insect Biochem Mol Biol* **33**: 1327-1338

Salvesen G (2004) New perspectives on proteases. In *Horizon Symposia*, Anonymous Nature Publishing Group, http://www.nature.com/horizon/proteases/summary.hmtl

Silverman GA, Bird PI, Carrell RW, Church FC, Coughlin PB, Gettins PG, Irving JA, Lomas DA, Luke CJ, Moyer RW, Pemberton PA, Remold-O'Donnell E, Salvesen GS, Travis J, & Whisstock JC (2001) The serpins are an expanding superfamily of structurally similar but functionally diverse proteins. Evolution, mechanism of inhibition, novel functions, and a revised nomenclature. *J Biol Chem* **276**: 33293-33296

Sim RB & Laich A (2000) Serine proteases of the complement system. *Biochem Soc Trans* **28**: 545-550

Sim RB & Tsiftsoglou SA (2004) Proteases of the complement system. *Biochem Soc Trans* **32**: 21-27

Vorup-Jensen T, Petersen SV, Hansen AG, Poulsen K, Schwaeble W, Sim RB, Reid KB, Davis SJ, Thiel S, & Jensenius JC (2000) Distinct pathways of mannan-binding lectin (MBL)- and C1-complex autoactivation revealed by reconstitution of MBL with recombinant MBL-associated serine protease-2. *J Immunol* **165**: 2093-2100

Wang Y & Jiang H (2007) Reconstitution of a branch of the *Manduca sexta* prophenoloxidase activation cascade in vitro: snake-like hemolymph proteinase 21 (HP21) cleaved by HP14 activates prophenoloxidase-activating proteinase-2 precursor. *Insect Biochem Mol Biol* **37**: 1015-1025

Wang Y & Jiang H (2006) Interaction of beta-1,3-glucan with its recognition protein activates hemolymph proteinase 14, an initiation enzyme of the prophenoloxidase activation system in *Manduca sexta*. *J Biol Chem* **281**: 9271-9278

Wang Y & Jiang H (2004) Prophenoloxidase (proPO) activation in *Manduca sexta*: an analysis of molecular interactions among proPO, proPO-activating proteinase-3, and a cofactor. *Insect Biochem Mol Biol* **34**: 731-742

Wang Y, Zou Z, & Jiang H (2006) An expansion of the dual clip-domain serine proteinase family in *Manduca sexta*: gene organization, expression, and evolution of prophenoloxidase-activating proteinase-2, hemolymph proteinase 12, and other related proteinases. *Genomics* **87**: 399-409

Zou Z, Wang Y, & Jiang H (2005) *Manduca sexta* prophenoloxidase activating proteinase-1 (PAP-1) gene: organization, expression, and regulation by immune and hormonal signals. *Insect Biochem Mol Biol* **35**: 627-636

Figures

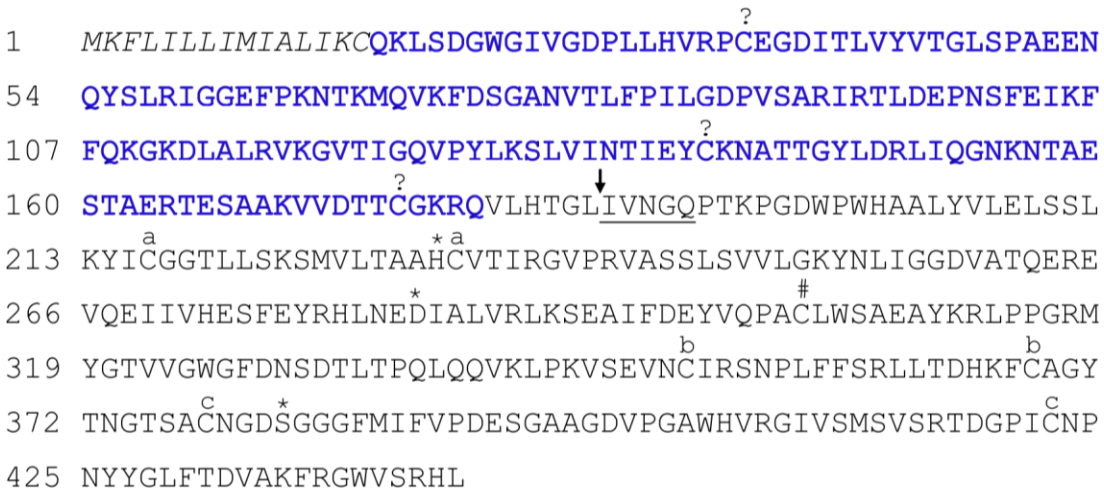

Figure 2-1. Amino acid sequence of *Manduca sexta* hemolymph proteinase 16 (AAV91013). The amino-terminal signal peptide is italicized. The putative activation site is marked by a solid arrow. Residues of the catalytic triad are identified by * located above the one-letter amino acid code. The paired letters (a-a, b-b, c-c) indicate predicted disulfide bonds in the catalytic domain (based on alignment with bovine chymotrysinogen). Cysteines that may be involved in an interdomain disulfide bond are marked with # in the catalytic domain and ? in the amino-terminal domain. The underlined sequence, IVNGQ, was identified by Edman degradation to be the amino-terminus of the catalytic domain of HP16 in a sample of recombinant HP16. Residues in blue were inserted into the expression vector, pProExHTb, for expression and purification of NT16 in *Escherichia coli*.

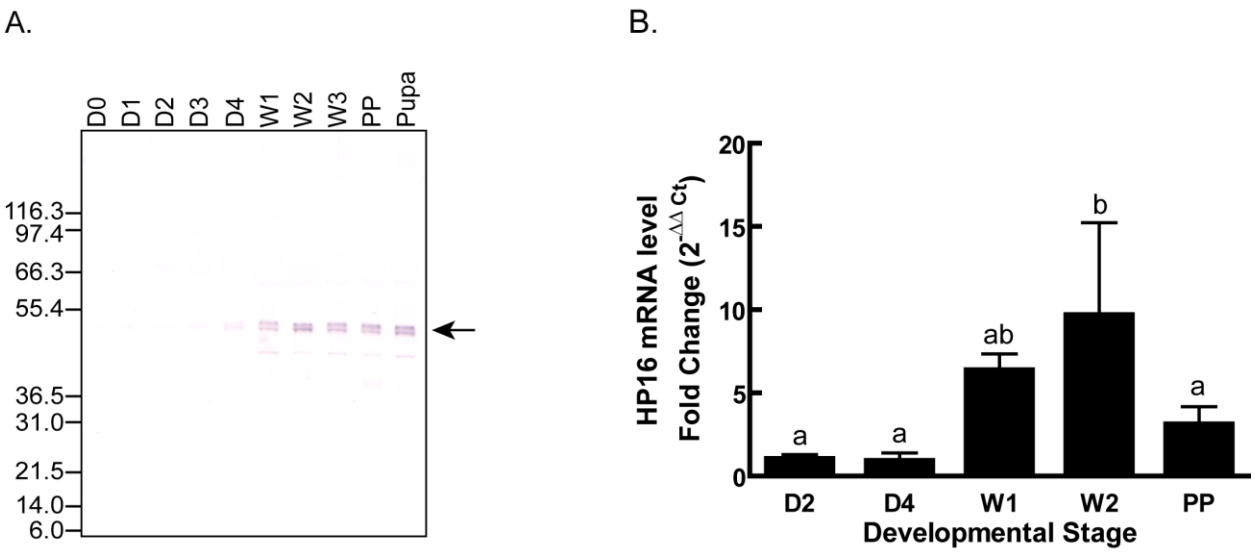

Figure 2-2. Fluctuations in HP16 protein levels in plasma correlate with changes in HP16 mRNA levels in fat body during larval development.

A) Plasma samples from naïve *Manduca sexta* larvae (0.2 µL) were treated with sample buffer containing β-mercaptoethanol and separated by SDS-PAGE (4-12% Bis-Tris gel) followed by immunoblotting with HP16 antibody. D0-D4 = day 0-day 4 5th instar larvae (feeding), W1-W3 = day 1-day 3 wandering larvae (non-feeding), PP = prepupa. An arrow indicates the position of proHP16.

B) Fat body samples were collected from day 2 and day 4 5th instar larvae, day 1 and day 2 wandering larvae, and prepupae. RNA samples were prepared from each insect, and relative mRNA levels for HP16 were determined by quantitative RT-PCR. Bars represent the mean fold change and standard deviation (n = 3). Data were analyzed using a one-way ANOVA followed by the Newman-Keuls Multiple Comparison Test. Means with the same letter are not significantly different ($p > 0.05$).

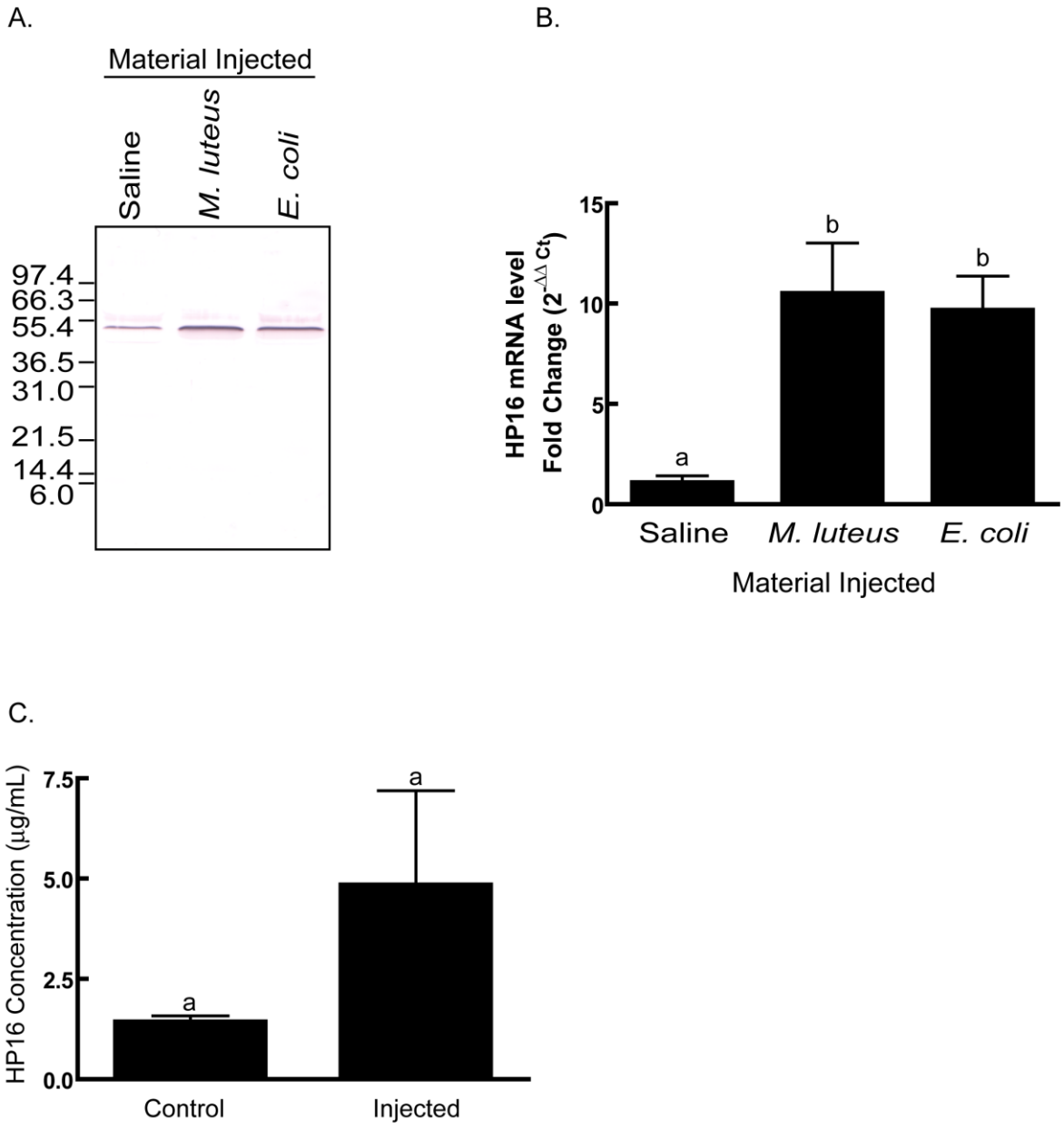

Figure 2-3. Immune stimulation elicits HP16 protein expression in plasma and HP16 mRNA levels in fat body.

A) Fifth-instar day 2 larvae were injected with 0.85% NaCl (saline), 10^8 cells of *E. coli*, or 500 µg *M. luteus*. Hemolymph and fat body were collected 24 h post-injection. Plasma (6 µL) was mixed with sample buffer containing β-mercaptoethanol and separated by SDS-PAGE (10%) followed by immunoblotting with HP16 antibody.

B) RNA was extracted from insects described in (A), and HP16 mRNA levels were determined by quantitative RT-RCR. Bars represent mean fold change and standard deviation for each

treatment (n = 3). Data were analyzed using a one-way ANOVA followed by the Newman-Keuls Multiple Comparison Test. Means with the same letter are not significantly different ($p > 0.05$). C) HP16 concentration in hemolymph of control (= naïve) and injected (= *M. luteus*) larvae. Bars represent mean HP16 concentration and standard deviation for each treatment (n = 3). Data were analyzed using an unpaired t-test with a two-tailed p-value. As indicated by the same letter, mean HP16 concentrations were not significantly different ($p = 0.0651$).

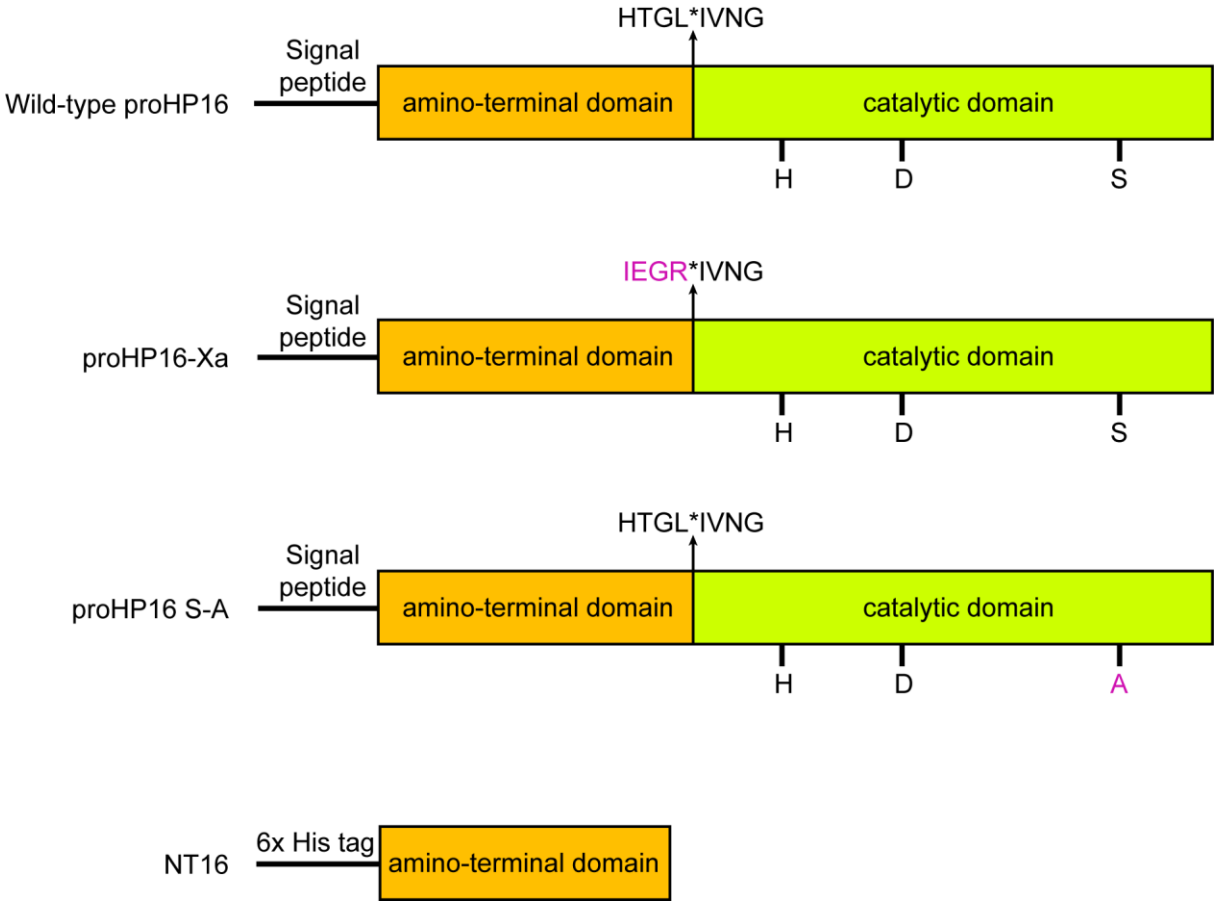

Figure 2-4. Schematic representation of wild-type HP16 and HP16 mutants.

For proHP16-Xa, the predicted activation site of proHP16 was changed from HTGL to IEGR by site-directed mutagenesis. IEGR is the cleavage site for bovine factor Xa. An inactive proteinase, proHP16 S-A, was produced by mutating the active site Ser to Ala. NT16 contains residues 1-165 of the amino-terminal domain of HP16 and a 6 x histidine tag.

A. Wild-type HP16

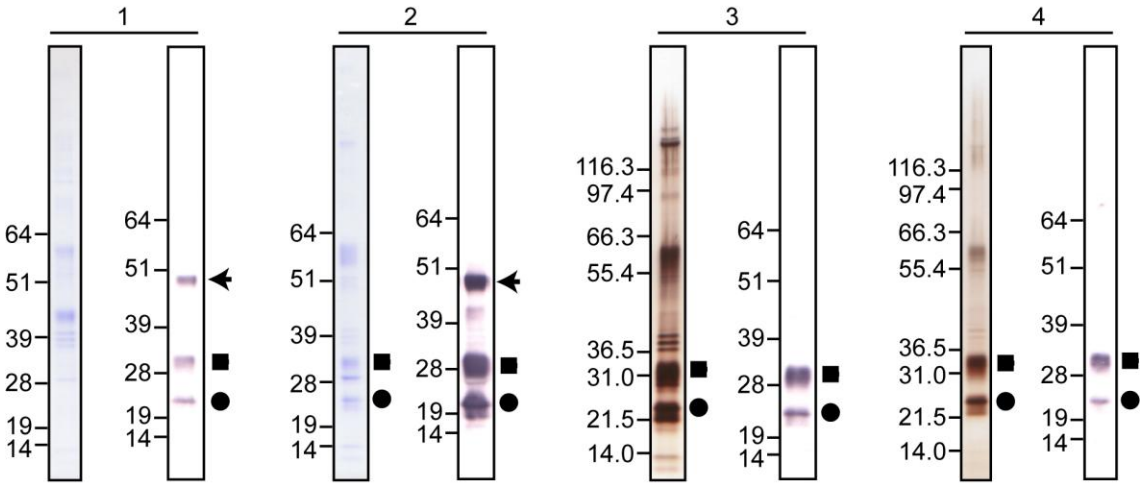

B. HP16-Xa

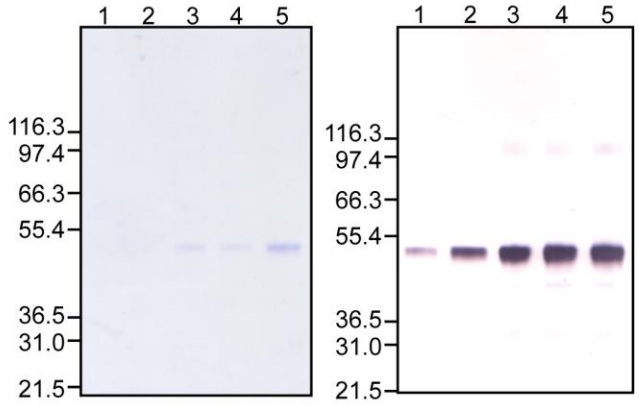

C. HP16 S-A

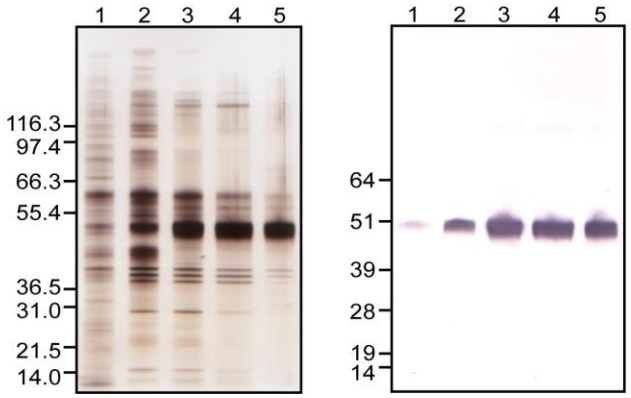

Figure 2-5. SDS-PAGE and immunoblot analysis of recombinant wild-type HP16 and HP16 mutants.

A) Wild-type HP16 was expressed as a recombinant protein in *Spodoptera frugiperda* Sf-9 cells, using a baculovirus vector. Protein secreted into the media was enriched by ConA sepharose (lane 1), followed by Q sepharose chromatography (lane 2), hydrophobic interaction chromatography (lane 3), and gel permeation chromatography with Sephacryl S100 (lane 4). Protein samples (10 μL) were treated with sample buffer containing β-mercaptoethanol and separated by SDS-PAGE (4-12% Bis-Tris gel) followed by Coomassie or silver staining (left) or immunoblotting with HP16 antibody (right). HP16 zymogen bands are marked by an arrow while the catalytic domain is marked by a square and the amino-terminal domain by a circle.

B) A mutant (named HP16-Xa) at the putative activation site of HP16 with residues HTGL changed to IEAR by site directed mutagenesis was expressed and purified as a recombinant protein from Sf-9 cells. For each purification step, 400 ng (left) or 200 ng (right) of total protein was mixed with sample buffer containing β-mercaptoethanol and separated by SDS-PAGE (4-12% Bis-Tris gel) followed by Coomassie staining (left) or immunoblotting with HP16 antibody (right). Media post-dialysis (lane 1), after ConA sepharose and dialysis (lane 2), after Q sepharose (lane 3), after ammonium sulfate precipitation (lane 4), after gel permeation chromatography (lane 5).

C) HP16 S-A is a mutant in which the active site serine was changed to alanine by site directed mutagenesis. Recombinant protein was obtained by expression and purification from Sf-9 cells. 200 ng of total protein was mixed with sample buffer containing β-mercaptoethanol and separated by SDS-PAGE (4-12% Bis-Tris gel) for analysis by silver staining (left) or immunoblotting (right). Media post-dialysis (lane 1), after ConA sepharose and dialysis (lane 2), after Q sepharose (lane 3), after hydrophobic interaction chromatography (lane 4), after gel permeation chromatography (lane 5).

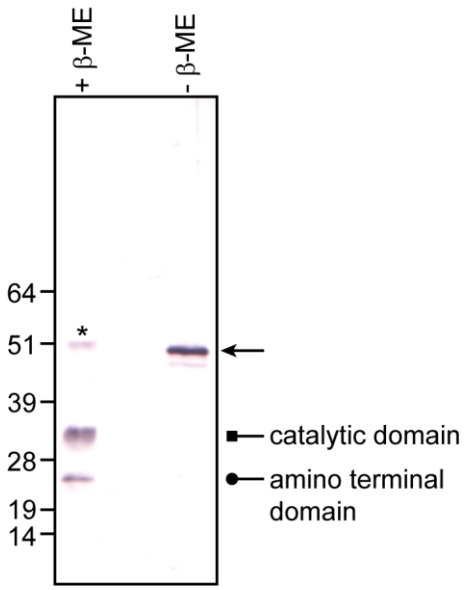

Figure 2-6. A disulfide bond connects the catalytic and amino-terminal domains of purified recombinant HP16.

Partially purified wild-type HP16 (ConA Sepharose and Q-Sepharose only; ~20 ng) samples were mixed with 2 µL of 6X SDS-sample buffer with or without β-mercaptoethanol and separated by SDS-PAGE (4-12% Bis-Tris gel) followed by immunoblot analysis with HP16 antibody. HP16 zymogen is marked by * while the catalytic domain is marked by an arrow with a square head and the amino-terminal domain by an arrow with a circle head. In absence of reducing agent, HP16 is marked by a solid arrow.

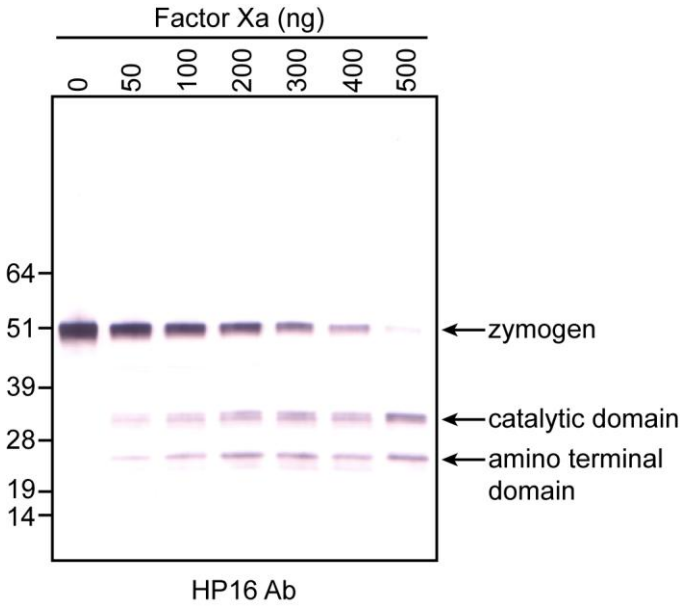

Figure 2-7. Cleavage of HP16-Xa by bovine factor Xa.

After incubation of recombinant HP16-Xa (100 ng) with different amounts of bovine factor Xa in the presence of bovine serum albumin (1000 ng), the mixtures were separated by SDS-PAGE (4-12% Bis-Tris gel) followed by immunoblot analysis with HP16 antibody.

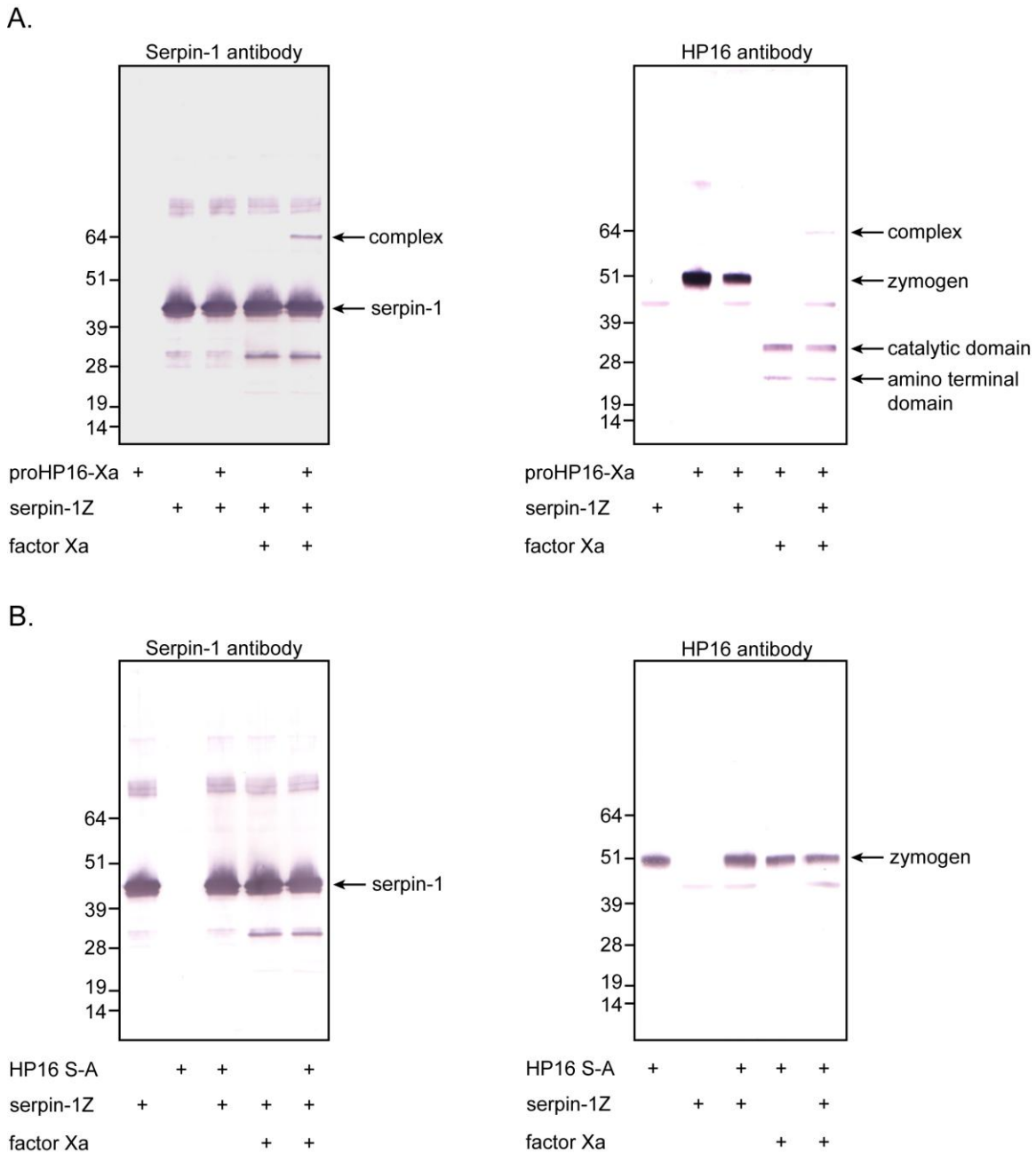

Figure 2-8. Active HP16-Xa, but not recombinant HP16 S-A, forms a covalent complex with serpin-1Z.

(A) proHP16-Xa or (B) HP16 S-A (100 ng = 2 pmol) was incubated with bovine factor Xa (500 ng) and BSA (1000 ng) for 1 h at 37°C. Recombinant serpin-1Z (880 ng = 20.2 pmol) was added to the activated mixture and incubated for 10 min at room temperature. Mixtures were subjected to SDS-PAGE under reducing conditions followed by immunoblot analysis with serpin-1 and HP16 antibodies.

A.

QKLSDGWGIVGDPLLHVRP<u>C</u>EGDITLVYVTGLSPAEENQYSLRIGGEFPKNTKMQVKFDSGANV
TLFPILGDPVSARIRTLDEPNSFEIKFFQKGKDLALRVKGVTIGQVPYLKSLVINTIEY<u>C</u>KNAT
TGYLDRLIQGNKNTAESTAERTESAAKVVDTT<u>C</u>GKRQ

20 124 161

B.

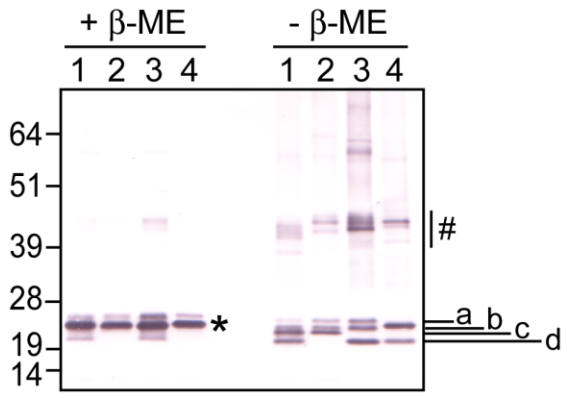

Figure 2-9. Amino acid sequence of NT16 and immunoblot analysis of recombinant wild-type NT16 and NT16 mutants.

(A) Full-length sequence of wild-type NT16. Cysteine residues mutated to serine are underlined and numbered 1-3.

(B) Protein samples (10 µL) were mixed with sample buffer with or without β-mercaptoethanol and separated by SDS-PAGE (4-12% Bis-Tris gel) followed by immunoblotting with HP16 antibody. A single band, marked with a star, is the expected size (~21.4 kDa) of NT16. Labeled bands (a-d) detected under non-reducing conditions may represent different disulfide bond arrangements that occur upon mutation of each Cys residue. Multiple bands marked by # represent potential dimer formation for each recombinant protein. Wild-type NT16 (lane 1), NT16 C20S (lane 2), NT16 C124S (lane 3), NT16 C161S (lane 4).

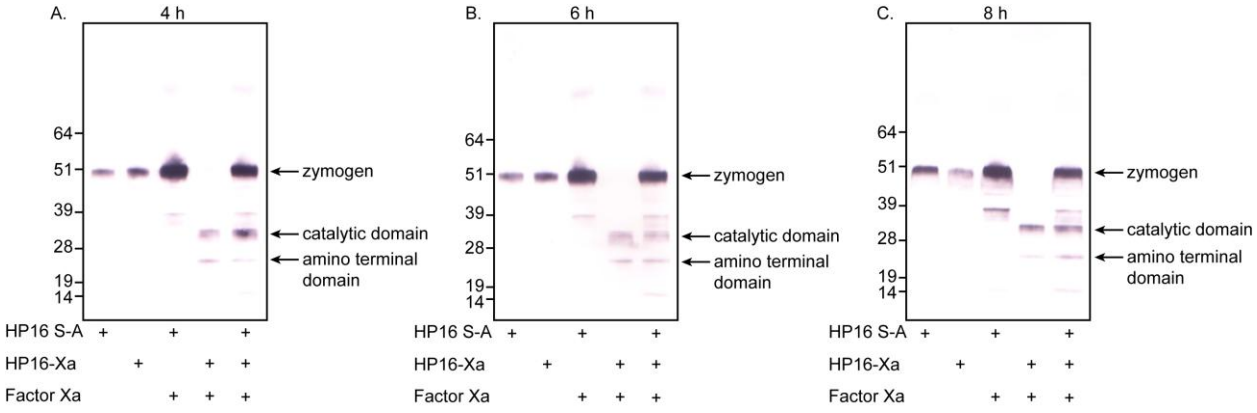

Figure 2-10. Lack of evidence for autoactivation of HP16.

Purified recombinant HP16-Xa (100 ng) or HP16 S-A (200 ng) were either incubated alone or in the presence of 100 ng bovine factor Xa (New England Biolabs) in buffer (20 mM Tris-HCl, 150 mM NaCl, pH 8.4) plus $CaCl_2$ (final concentration = 2 mM) and Tween-20 (final concentration = 0.002%) for 2 h at 25°C. Mixtures containing HP16-Xa and bovine factor Xa were mixed with recombinant HP16 S-A (200 ng) and incubated at 25°C for an additional 2, 4, or 6 h (= 4, 6, or 8 h total). Samples were subjected to SDS-PAGE (4-12% Bis-Tris gel) under reducing conditions followed by immunoblot analysis using antiserum against HP16 as the primary antibody.

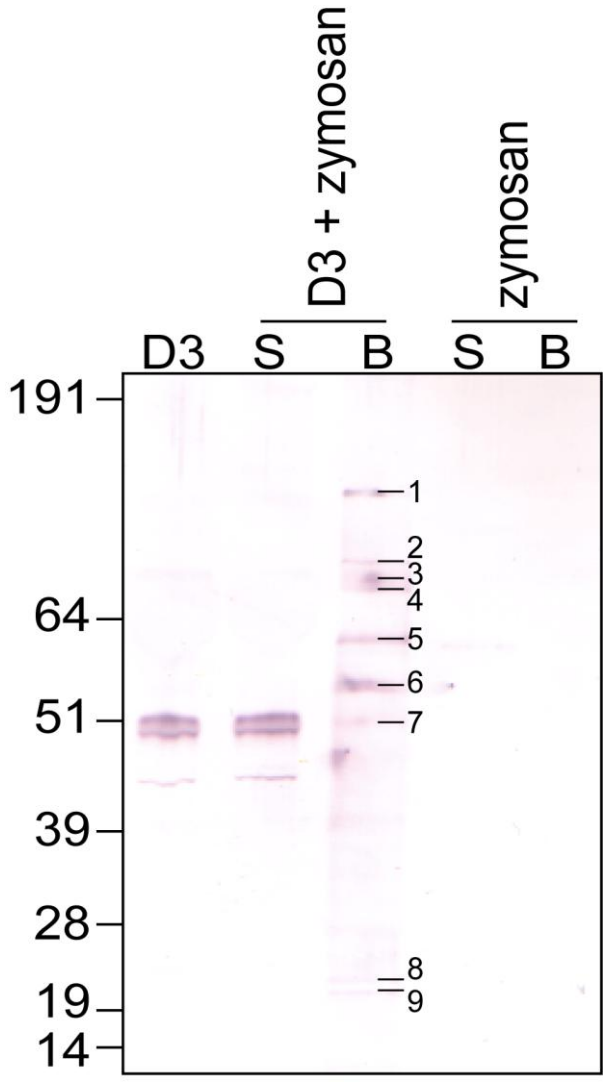

Figure 2-11. Activation of proHP16 in plasma incubated with zymosan.

Plasma from day three, fifth instar larvae (30 µL) was incubated alone or with 0.4 mg of zymosan A from *Saccharomyces cerevisiae* for 1 h at 25°C. As a control, zymosan A was incubated in 30 µL of 20 mM Tris-HCl, 150 mM NaCl, pH 8.0. After centrifugation and washing, supernatant (S) and bound (B) samples were subjected to SDS-PAGE under reducing conditions followed by immunoblot analysis using HP16 antibody. To speculate what bands 1-9 might be, a standard curve (log molecular weight vs. distance) was constructed. Using point-to-point analysis, a line of best fit was determined and used to calculate the molecular weight of each band. Putative identification of bands: Band 1 = unknown, Bands 2-4 = serpin-HP16 complexes, Bands 5-6 = cleaved serpin-HP16 complexes, Band 7 = proHP16, Band 8-9 = amino-terminal domain of HP16.

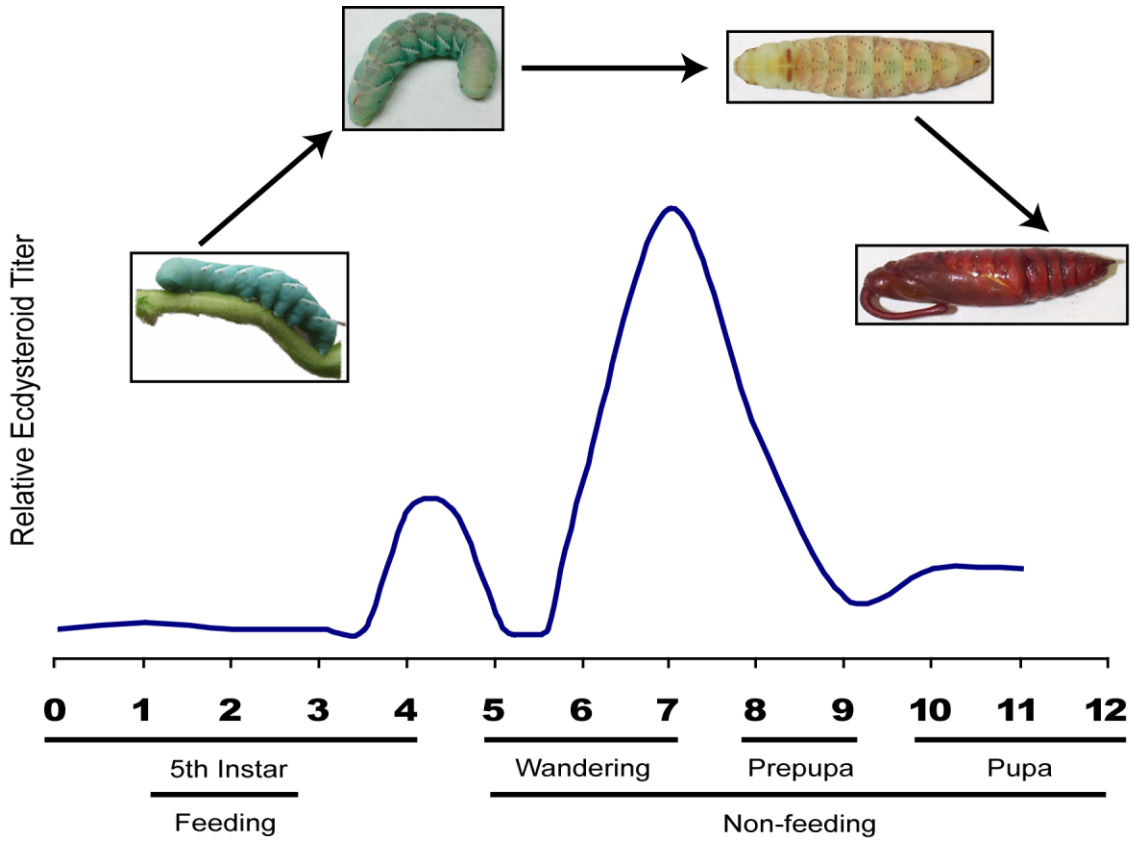

Figure 2-12. Ecdysteroid titer changes during larval to pupal transition in *M. sexta*. Stages represented are day 0-day 4 5th larval instar (0-4), day 1- day 3 wandering larvae (5-7), prepupa (PP), and pupa. Increase in ecdysteroid level around day 4, 5th instar triggers a behavioral change from feeding larvae to non-feeding, wandering larvae. The increase observed around day 7 triggers molting. Ecdysteroid titer data adapted from Bollenbacher *et al*., 1981. Photos courtesy of Drs. Emily Ragan, Neal Dittmer, and Adam Sparks.

CHAPTER 3 - IDENTIFICATION OF COMPLEXES OF SERPIN-3 WITH PROTEINASES IN PLASMA FROM *MANDUCA SEXTA*

Introduction

Humoral immune responses in insects include the production of antimicrobial peptides, prophenoloxidase activation that leads to melanization, and production of reactive intermediate oxygen or nitrogen species (Lavine and Strand, 2002; Jiravanichpaisal et al., 2006; Marmaras and Lampropoulou, 2009; Cerenius et al., 2010). Synthesis of antimicrobial peptides by the Toll pathway and activation of prophenoloxidase are stimulated in response to foreign invaders (e.g. bacteria, fungi, and other pathogens). Once a foreign invader is recognized, extracellular serine proteinase cascades are put into motion to remove the invader from the insect's system (Kanost and Clarke, 2005; Cerenius et al., 2010). Because active proteinases can be detrimental to the host, precise regulation is critical. One regulatory mechanism is the production of proteinases as zymogens. Zymogens remain inactive until activated by proteolytic cleavage by another proteinase. Another regulatory mechanism is the inhibition of proteinases by proteinase inhibitors.

Serine proteinase inhibitors, or serpins, belong to a superfamily of proteins that inhibit serine proteinases through a suicide inhibition mechanism. Serpins consist of a single chain of 350-400 amino acid residues and share a highly conserved structure composed of β-sheets and α-helices (Silverman et al., 2001). Between β-sheets A and C, is a flexible region termed the reactive center loop (RCL) that contains the P1 residue. It is the sequence of the RCL that determines serpin specificity. Inhibition of the target proteinase begins with the formation of a noncovalent complex between the serpin and the serine proteinase. However, once the proteinase cleaves the serpin at the P1 residue of the RCL, a covalent ester linkage is formed. Once cleaved, the serpin undergoes a dramatic conformational change. The RCL is inserted into β-sheet A, causing a 70Å translocation and active site distortion of the proteinase (Schulze et al., 1994; Wright, 1996; Silverman et al., 2001).

Serpins have a role in regulating prophenoloxidase activation in *Aedes aegypti* (Zou et al., 2010), *Anopheles gambiae* (Abraham et al., 2005; Michel et al., 2006; An et al., 2010a), *Tenebrio molitor* (Jiang et al., 2009; Park et al., 2011), *Drosophila melanogaster* (Ligoxygakis et

al., 2002; De Gregorio et al., 2002; Scherfer et al., 2008; Tang et al., 2008), and *Manduca sexta* (Jiang et al., 2003; Zhu et al., 2003b; Wang and Jiang, 2004; Tong and Kanost, 2005; Tong et al., 2005; Zou and Jiang, 2005; Wang and Jiang, 2006; An and Kanost, 2010). Regulation of the Toll pathway by serpins has also been observed in *Ae. aegypti* (Shin et al., 2006), *T. molitor* (Jiang et al., 2009; Park et al., 2011), *D. melanogaster* (Levashina et al., 1999; Ahmad et al., 2009), and *M. sexta* (Zou and Jiang, 2005; An and Kanost, 2010; An et al., 2011).

At present, seven serpins have been found in *M. sexta* (Kanost, 2007), but the endogenous proteinase targets for only some of the serpins have been identified. Of the twelve serpin-1 isoforms (Jiang et al., 1994; Jiang and Kanost, 1997), proteinase targets for only serpin-1I and serpin-1J have been determined. Serpin-1I inhibits prophenoloxidase activation, and recombinant serpin-1I can form a complex with purified hemolymph proteinase 14 (Wang and Jiang, 2006). Serpin-1J can form a complex with prophenoloxidase-activating proteinase-3 (Jiang et al., 2003). Serpin-1J also inhibits hemolymph proteinase 8 to regulate the expression of antimicrobial peptides (An et al., 2011). Serpin-3 inhibits prophenoloxidase-activating proteinase activity to block prophenoloxidase activation (Zhu et al., 2003b). Serpin-4 and serpin-5 regulate prophenoloxidase activation at steps prior to the prophenoloxidase-activating proteinases. Serpin-4 inhibits hemolymph proteinase 21, whereas serpin-5 inhibits hemolymph proteinase 6 (Tong and Kanost, 2005; Tong et al., 2005). Hemolymph proteinase 6 also stimulates the activation of the Toll pathway, and antimicrobial expression is regulated by serpin-5 (An and Kanost, 2010). Serpin-6 inhibits prophenoloxidase-activating proteinase-3 to regulate prophenoloxidase activation (Wang and Jiang, 2004; Zou and Jiang, 2005) and can form a complex with hemolymph proteinase 8 (Zou and Jiang, 2005).

Previous studies to identify the PAPs as proteinase targets of serpin-3 (Zhu et al., 2003b) were completed prior to obtaining sequences of many hemolymph proteinases (Jiang et al., 2005; Wang et al., 2006). It is reasonable to hypothesize that additional proteinases are also endogenous targets of serpin-3.

In this study, a serpin-3 immunoaffinity column was used to purify serpin-3-proteinase complexes from *M. sexta* plasma. Proteinase components identified by immunoblot analysis and analysis of tryptic peptides by mass spectrometry indicated that a serpin-3-HP8 complex was present in plasma. Inhibitory activity of serpin-3 for HP8 was investigated by using purified recombinant proteins. Identification of serpin-3-proteinase complexes in plasma provides insight

into some of the proteinase targets of serpin-3 and extends the understanding of the functions of serpins and proteinases in the immune response of *M. sexta* and other insects.

Materials and Methods

Insects

Manduca sexta eggs were originally obtained from Carolina Biological Supply and used to establish a laboratory colony. The colony has been maintained by feeding larvae on an artificial diet as previously described by Dunn and Drake (1983).

Preparation of plasma samples from bacteria injected larvae

Hemolymph was collected from thirty-three day 3 fifth instar larvae 24 h after injection with 100 µg *Micrococcus luteus* (injected as day 2 fifth instar larvae) into two 50 mL polypropylene centrifuge tubes containing diethyldithiocarbamic acid (final concentration of 2.25 mg/mL) to prevent melanization. Each tube contained ~15 mL of pooled hemolymph (tube 1: 18 larvae and tube 2: 15 larvae). Hemocytes were removed by centrifugation at 9000 × g for 15 min at 4°C. Aliquots (700 µL) of each pooled sample were saved and stored at -80°C. The remainder of each pooled sample was mixed together and used for immunoaffinity purification as described later.

Preparation of plasma from naïve larvae

Day 2 fifth instar larvae were chilled on ice for at least 20 min. Hemolymph was collected into individual microcentrifuge tubes by clipping the dorsal horn with scissors. Hemocytes were removed by centrifugation at 8000 × g for 7.5 min at 4°C. The samples were screened for endogenous phenoloxidase activity as described by Tong and Kanost (2005) with some modification. Plasma (4 µL) from each larva was incubated with Nuclease-free water (2 µL; Ambion) or *M. luteus* (2 µL of a 1 µg/µL stock) for 10 min at room temperature. Samples were transferred to a 96-well plate, and 200 µL of 2 mM dopamine in 50 mM sodium phosphate buffer, pH 6.5 were added to each well as substrate. Absorbance at 470 nm was monitored for 15 min with a read every 30 sec in a BioTek Power Wave XS plate reader. One unit of PO activity was defined as a change in A_{470} of 0.001/min. Plasma samples that exhibited low phenoloxidase

activity that could be increased significantly after addition of bacteria were pooled and stored at -80°C.

Expression and purification of recombinant hemolymph proteinase 8 mutant (HP8-Xa)

A HP8-Xa stable cell line prepared by Dr. Chunju An in 2007 and stored in liquid nitrogen was used to initiate a cell culture for the expression and purification of HP8-Xa, a mutant of HP8 that can be activated by bovine factor Xa (An et al., 2009; An et al., 2010b; An et al., 2011). Six flasks (225 cm^2) containing Schneider's *Drosophila* media (Invitrogen) plus heat-inactivated fetal bovine serum (Atlanta Biologicals; final concentration = 10%) were seeded with 1.8×10^6 cells/mL in 60 mL. After cells were incubated for 3 h at 28°C, HP8-Xa expression was induced by the addition of 500 mM copper sulfate (final concentration = 500 µM). Media (365 mL) was collected 48 h after induction by centrifugation at 500 × g for 10 min at 4°C. HP8-Xa was secreted into the medium under the control of its own signal peptide and purified by sequential chromatography steps including Affi-gel Blue Gel (150-300 µm; Bio-Rad 153-7301), Concanavalin A Sepharose 4B (GE Healthcare) affinity, Q-Sepharose™ Fast Flow (GE Healthcare) anion exchange, and Sephacryl-S100 High Resolution (GE Healthcare) gel permeation as described by An et al. (2009; 2010b) with some modification.

Cell-free media collected as described above was placed in a 1 L flask along with phenylmethylsulfonyl fluoride, a proteinase inhibitor (Sigma P-7626; final concentration = 1 mM). Approximately 22 mL of Affi-gel Blue gel beads pre-equilibrated in 20 mM Tris-HCl, pH 7.5 were added to the flask and incubated at 4°C with shaking (150 rpm) for 13 h. Supernatant, containing proHP8-Xa, was removed from the beads in two ways. First, the beads were allowed to settle on ice for 30 min and most of the supernatant was removed by pipette and placed in a 1 L flask. Second, the slurry was applied to a 2.5 × 10 cm column and allowed to drain. The resulting flow through was added to the 1 L flask containing most of the supernatant.

Concanavalin A-Sepharose 4B (GE Healthcare) that had been equilibrated in ConA binding buffer (20 mM Tris-HCl, 0.5 M NaCl, pH 7.5) and phenylmethylsulfonyl fluoride (final concentration = 1 mM) were added to the 1 L flask containing the supernatant from Affi-gel Blue gel affinity. After shaking at 150 rpm for 8 h at 4°C, the slurry was applied to a 2.5 × 10 cm column and allowed to drain. The column was washed four times with 35 mL of ConA binding buffer at 4°C. Once the A_{280} reading was below 0.06, 35 mL ConA elution buffer (ConA binding

buffer and 0.5 M methyl-α-D-mannopyranoside) was added to elute bound proteins. The column was rotated overnight at 4°C. After collection of the first elution fraction, a fresh 35 mL of ConA elution buffer was added to the column and rotated for an additional 5 h at 4°C. The second 35 mL elution fraction was collected and followed by four, 10 mL elutions with ConA elution buffer. Immunoblotting using an antibody specific to HP8 (OSU 3) was used to analyze the eluted fractions.

Fractions containing HP8-Xa were pooled and dialyzed against Q-Sepharose start buffer (20 mM Tris, 20 mM NaCl, pH 8.0; 3.5 L for at least 6 h at 4°C, two times). The dialyzed sample was applied to a Q-Sepharose™ Fast Flow column (GE Healthcare; 1 x 10 cm) equilibrated with Q-Sepharose start buffer at 1 mL/min. The column was washed with Q-Sepharose start buffer at 1 mL/min until the A_{280} reading was less than 0.025. Proteins bound to the column were eluted with a 50 mL linear gradient of 20-700 mM NaCl in 20 mM Tris-HCl, pH 8.0 at 1 mL/min. Fractions of 1 mL each were collected and analyzed by immunoblotting.

Q-Sepharose fractions containing HP8-Xa were pooled and used for further purification by gel permeation chromatography. Partially purified HP8-Xa (4 mL) was loaded at 1 mL/min onto a Sephacryl-S100 High Resolution (GE Healthcare) 1.5 × 100 cm column equilibrated with gel filtration buffer (20 mM Tris-HCl, 150 mM NaCl, pH 8.0). Proteins were eluted from the column with the gel filtration buffer at 1 mL/min. The first eleven fractions were collected at 4 mL/tube as this was determined to be the void volume by running blue dextran (Sigma) through the column. After the void volume, 2 mL fractions were collected. Selected fractions were analyzed by SDS-PAGE and immunoblotting. Fractions containing the most HP8-Xa and the least contaminating proteins were pooled and stored at -80°C.

Expression and purification of recombinant serpin-3

Manduca sexta serpin-3 was expressed in *Escherichia coli* BL21 DE3 cells using the pET28a expression vector, which encodes an amino-terminal 6 x histidine tag. A single colony harboring the recombinant plasmid was inoculated into 50 mL of sterile LB containing 50 µL of 50 mg/mL kanamycin in a 250 mL flask and incubated overnight at 37°C with shaking at 250 rpm. Ten milliliters of the overnight culture were transferred to four, 2 L flasks containing 500 mL LB and kanamycin (0.5 mL of 50 mg/mL). Flasks were incubated at 37°C with shaking at 250 rpm until OD_{600} was 0.8 to 1.0. Cultures were transferred to a 20°C incubator with shaking

at 150 rpm and expression of serpin-3 was induced by adding 1 M isopropyl-β-D-thiogalactoside (IPTG) to a final concentration of 1 mM for 10 h. After storage at 4°C overnight, the bacteria were harvested by centrifugation at 4000 × g for 20 min at 4°C. Pellets were resuspended in cold lysis buffer (300 mM NaCl, 10 mM imidazole in 0.5 M sodium phosphate buffer, pH 8.0) at 4 mL lysis buffer/g cells (48 mL total). Proteinase inhibitor cocktail for His-tagged proteins (Sigma P8849) was also added at 50 µL inhibitor/g cells (600 µL total). Samples were transferred to a 50 mL polypropylene centrifuge tubes (Fisher Scientific) and placed in an ice-water bath. Cells were sonicated for 10 × 30 seconds with a 1 min rest between bursts using a Vibra Cell Sonics and Materials Sonicator that was set on level 5 and 50% duty cycle. After sonication, the lysed cell sample was centrifuged at 10,000 × g for 30 min at 4°C.

The soluble serpin-3 was first purified by nickel-affinity chromatography (Ni^{2+}-NTA). Clear lysate (~46 mL) was incubated with Ni^{2+}-NTA agarose (Qiagen) at 1 mL agarose for every 4 mL clear lysate in two 50 mL polypropylene centrifuge tubes with rotation for 1 h at 4°C. This mixture was poured into a 1.5 cm diameter column. The column was washed twice with 46 mL of wash buffer (300 mM NaCl, 20 mM imidazole in 0.5 M sodium phosphate buffer, pH 8.0). Recombinant serpin-3 was eluted 4 times with 5 mL of elution buffer (300 mM NaCl, 250 mM imidazole in 0.5 M sodium phosphate buffer, pH 8.0). Fractions were analyzed by SDS-PAGE under reducing conditions and Coomassie Blue staining. To further purify serpin-3, fractions containing relatively pure recombinant serpin-3 were pooled and dialyzed against dialysis buffer (20 mM Tris-HCl, pH 8.0). Serpin-3 was added to two 3-12 mL Slide-A-Lyzer 3.5 K Dialysis Cassettes (~8 mL/cassette; Thermo Scientific) and dialyzed in 2 L dialysis buffer (twice, for at least 6 h) at 4°C. The dialyzed sample (~23 mL) was applied to an equilibrated Q-Sepharose™ Fast Flow column (1 × 10 cm) at 1 mL/min. Dialysis buffer (25 mL total) was used to wash the column until A_{280} readings were near zero. Proteins bound to the column were eluted with a 60 mL linear gradient of 0-500 mM NaCl in 20 mM Tris-HCl, pH 8.0 at 1 mL/min. Fractions of 1 mL each were collected and analyzed by SDS-PAGE under reducing conditions and Coomassie Blue staining. Fractions containing serpin-3 were pooled and stored at 4°C.

SDS-PAGE and immunoblotting

SDS-polyacrylamide gel electrophoresis (SDS-PAGE) was performed using NuPAGE 4-12% Bis-Tris gels (Invitrogen). Proteins were treated with sample loading buffer containing SDS

and β-mercaptoethanol. Samples were heated at 95°C for 5 min and briefly centrifuged. Gels were run in an XCell SureLock™ Electrophoresis Cell (Invitrogen; Novex Mini-Cell) at a constant voltage of 200 V. Gels were stained for 30-60 min in 0.2% (w/v) Coomassie Blue R-250 in 50% (v/v) methanol and 12% (v/v) acetic acid, followed by destaining with 30% (v/v) methanol and 10% (v/v) acetic acid. Alternatively, when expected protein concentrations were low, gels were stained using the SilverXpress® Silver Staining Kit (Invitrogen). Gels were placed in a gel drying solution (20% (v/v) ethanol, 5% (v/v) glycerol) for 30 min and dried between two cellophane membranes (14 × 14 cm; Fisher).

For immunoblotting, proteins were transferred from SDS-PAGE gels to 0.45 µm nitrocellulose membranes using a Trans-Blot SD Semi-Dry Transfer Cell (Bio-Rad). Membranes were blocked for 1 h with 3% dry milk dissolved in TTBS (1X Tris-buffered saline plus 0.05% Tween-20), washed for 5 min with TTBS, and incubated for 2 h with an appropriate primary antiserum diluted 1:2000 (unless otherwise specified) in 3% dry milk in TTBS (5 µL antiserum:10 mL 3% dry milk in TTBS). After three, 5 min washes with TTBS, membranes were incubated for 1 h with a secondary antibody (Goat Anti-Rabbit IgG (H+L)-alkaline phosphatase conjugate; Bio-Rad) diluted 1:3000 in 3% dry milk in TTBS (4 µL antibody: 12 mL 3% dry milk in TTBS). Membranes were washed twice with TTBS and once with TBS (25 mM Tris-HCl, 137 mM NaCl, 2.7 mM KCl, pH 7.4), followed by development using an Alkaline Phosphatase Conjugate Substrate Kit (Bio-Rad). Primary antisera to *M. sexta* serpin-1I (Jiang and Kanost, 1997; Ragan et al., 2010), serpin-3 (Zhu et al., 2003b), serpin-4 (Tong and Kanost, 2005), serpin-5 (Tong and Kanost, 2005), serpin-6 (Zou and Jiang, 2005), hemolymph proteinase 8 (Jiang et al., 2005), and prophenoloxidase-activating proteinases 1-3 (Wang et al., 2001; Ji et al., 2003, Jiang et al., 2003) were previously prepared.

Protein concentration assay

Protein concentrations were determined with the Coomassie Plus™ Protein Assay Reagent (Pierce) using bovine serum albumin (Pierce) as the standard. Alternatively, some samples of purified protein were analyzed by SDS-PAGE together with several bovine serum albumin samples of known amounts to account for the presence of contaminating proteins. This was followed by Coomassie Blue staining and determination of protein concentration by comparison of band intensity with the standards.

Immunoaffinity purification of serpin-proteinase complexes from induced plasma

Serpin-3 (KSU 114) or HP8 (OSU 3) antibodies were coupled to Protein-A Sepharose CL-4B (Sigma P3391) according to Harlow and Lane (1988) with some modification. Protein-A Sepharose CL-4B beads (0.5 g) were hydrated in ~6 mL of 1X phosphate buffered saline (PBS) for 2 h at room temperature and then at 4°C overnight. Beads were resuspended and aliquoted (3 mL) into two 15 mL polypropylene centrifuge tubes (Fisher Scientific). After centrifugation at 1000 × g for 2 min, the pre-swollen beads were washed three times with PBS (10 mL/wash). About 1 mL of beads was resuspended in 3 mL of PBS and mixed by rotation with 2 mL of serpin-3 or HP8 antiserum by rotation for 2 h at room temperature. Then, the serpin-3 or HP8 antibody beads were washed three times with PBS (10 mL/wash) and twice with 0.2 M sodium borate, pH 9.0 (10 mL/wash). After resuspension in 10 mL of 0.2 M sodium borate, pH 9.0 buffer, solid dimethylpimelimidate (Sigma D388) was added to a final concentration of 20 mM and rotated for 4 h at room temperature. Beads were centrifuged for 2 min at 1000 x g, washed once with 0.2 M ethanolamine-HCl, pH 8.0 (10 mL), resupended in 10 mL 0.2 M ethanolamine-HCl, pH 8.0, and rotated overnight at 4°C. Centrifugation of the beads at 1000 × g for 2 min at room temperature was followed by washing the beads once with PBS (10 mL) and resuspension of the beads in 10 mL of PBS. Beads were stored at 4°C overnight. Serpin-3 or HP8 antibody beads were poured into a 1 cm glass column and washed five times with 5 mL of 100 mM glycine-HCl (pH 2.5) plus 10% ethylene glycol (25 mL total) to remove any uncoupled antibody. Antibody-coupled beads were equilibrated with 50 mL of PBS, resuspended in 2.5 mL of PBS, and stored at 4°C until use.

Serpin-proteinase complexes were purified from hemolymph according to Tong et al. (2005), with some modification. Hemolymph (30 mL) was collected into two 50 mL polypropylene centrifuge tubes (15 mL/tube) from day 3 fifth instar larvae 24 h after injection with 100 µg *Micrococcus luteus* (injected as day 2 fifth instar larvae). Tubes contained diethyldithiocarbamic acid (final concentration of 2.25 mg/mL) to prevent melanization. Hemocytes were removed by centrifugation at 9000 × g for 15 min at 4°C. The resulting plasma was mixed with phenylthiourea to 1 mM and *M. luteus* to stimulate proteinase activation to a final concentration of 1 µg/µL for 30 min at room temperature with rocking. Phenylmethylsulfonyl fluoride (Sigma P-7626; final concentration = 4 mM) and protease inhibitor cocktail (Sigma P8849; 1 mL to 30 mL plasma) were then added to the plasma mixture

and incubated for 10 min at room temperature with rocking. The plasma mixture was centrifuged at 5000 × g for 15 min at 4°C to remove debris. The supernatant was added to 1 mL of antibody-coupled beads in 2.5 mL of PBS and rotated horizontally at 4°C overnight. The plasma plus antibody-coupled bead mixture was applied to a 1 cm glass column. Beads were washed with 20 mL of 1 M NaCl followed by 10 mL of 10 mM sodium phosphate buffer, pH 6.5. Bound proteins were eluted with twenty 1 mL aliquots of 100 mM glycine-HCl (pH 2.5), 10% ethylene glycol. Elution fractions were collected into 1.5 microcentrifuge tubes and neutralized with 100 µL of 1 M sodium phosphate buffer, pH 8.0. The fractions were analyzed by SDS-PAGE followed by Coomassie Blue staining and immunoblot analysis.

As a control, Protein-A Sepharose CL-4B (Sigma P3391) beads without antibody-coupling were prepared. Protein-A Sepharose CL-4B beads (0.5 g) were hydrated in ~6 mL of 1X phosphate buffered saline (PBS) for 2 h at room temperature and then at 4°C overnight. Beads were resuspended and aliquoted (3 mL) into two 15 mL polypropylene centrifuge tubes (Fisher Scientific). After centrifugation at 1000 × g for 2 min, the pre-swollen beads were washed three times with PBS (10 mL/wash). About 1 mL of beads was resuspended in 3 mL of PBS, poured into a 1 cm glass column, and washed five times with 5 mL of 100 mM glycine-HCl (pH 2.5) plus 10% ethylene glycol (25 mL total). Beads were equilibrated with 50 mL of PBS, resuspended in 2.5 mL of PBS, and stored at 4°C until use. Isolation of proteins from hemolymph that bound to the Protein-A Sepharose CL-4B utilized the same method as described above for the purification of serpin-proteinase complexes. Starting amount of plasma was 12 mL instead of 15 mL, and proteins were eluted with sixteen 1 mL aliquots of 100 mM glycine-HCl (pH 2.5), 10% ethylene glycol. Neutralized elution fractions were subjected to SDS-PAGE followed by Coomassie Blue staining.

Protein identification by matrix assisted laser desorption ionization (MALDI) mass spectrometry

Thirty microliters (6.9 µg) of a sample of plasma proteins that bound to a serpin-3 antibody-coupled immunoaffinity column were treated with 6X SDS sample buffer containing β-mercaptoethanol and were subjected to SDS-PAGE using a NuPAGE 4-12% Bis-Tris gel (Invitrogen). The gel was washed three times in deionized water (200 mL/wash) for 5 min, covered with Bio-Safe Coomassie G-250 stain (Bio-Rad 161-0786) for 1 h, and destained with

deionized water (200 mL) for at least 30 min. Bands of interest were excised with a clean razor blade and placed in individual 1.5 mL microcentrifuge tubes containing ~100 µL deionized water. Samples were sent to the Nevada Proteomics Center at the University of Nevada-Reno for analysis.

Spots were digested using a previously described protocol with some modifications (Rosenfeld et al., 1992). Samples were washed twice with 25 mM ammonium bicarbonate and 100% acetonitrile, reduced and alkylated using 10 mM dithiothreitol and 100 mM iodoacetamide and incubated with 75 ng sequencing grade modified porcine trypsin (Promega) in 25 mM ammonium bicarbonate for 6 hours at 37^{o}C. Samples were spotted onto a MALDI target with ZipTipµ-C18 (Millipore Corp., MA). Samples were eluted with 70% acetonitrile, 0.2% formic acid and overlaid with 0.5 µl 5 mg/ml MALDI matrix (α-Cyano-4 hydroxycinnamic acid 10 mM ammonium phosphate). All mass spectrometric data were collected using an ABI 4700 Proteomics Analyzer MALDI TOF/TOF mass spectrometer (Applied Biosystems, CA), using their 4000 Series Explorer software v. 3.6. The peptide masses were acquired in reflectron positive mode (1-keV accelerating voltage) from a mass range of 700 – 4000 Daltons, 1250 laser shots were averaged for each mass spectrum. Each sample was internally calibrated on trypsin's autolysis peaks 842.51 and 2211.10 to within 20 ppm. Any sample failing to internally calibrate was analyzed under default plate calibration conditions of 150 ppm. Raw spectrum filtering/peak detection settings were S/N threshold of 3, and cluster area S/N optimization enabled at S/N threshold 10, baseline subtraction enabled at peak width 50. The twenty most intense ions from the MS analysis, which were not on the exclusion list, were subjected to MS/MS. The MS/MS exclusion list included known trypsin masses: 842.51, 870.54, 1045.56, 1126.56, 1420.72, 1531.84, 1940.94, 2003.07, 2211.10, 2225.12, 2239.14, 2283.18, 2299.18, 2678.38, 2807.31, 2914.51, 3094.62, 3337.76, and 3353.75. For MS/MS analysis the mass range was 70 to precursor ion with a precursor window resolution of -1 to +4 Da with an average 2500 laser shots for each spectrum, CID on, metastable suppressor on. Raw spectrum filtering/peak detection settings were S/N threshold of 5, and cluster area S/N optimization enabled at S/N threshold 6, baseline subtraction enabled at peak width 50. The data was then stored in an Oracle database (Oracle database schema v. 3.19.0 Data version 3.90.0).

The data were extracted from the Oracle database and a peak list was created by GPS Explorer software v 3.6 (Applied Biosystems) from the raw data generated from the ABI 4700.

Analyses were performed as combination MS + MS/MS. MS peak filtering included mass range 700-4000 Da, minimum S/N filter 10. A peak density filter of 50 peaks per 200 Da with a maximum number of peaks set to 65. MS/MS peak filtering included mass range of 60 Da to 20 Da below each precursor mass. Minimum S/N filter 10, peak density filter of 50 peaks per 200 Da, cluster area filter used with maximum number of peaks 65. The filtered data were searched by Mascot v 1.9.05 (Matrix Science) using NCBI nr database (NCBI 20090915), containing 9,694,989 sequences. Searches were performed without restriction to protein species, M_r, or pI and with variable oxidation of methionine residues and carbamidomethylation of cysteines. Maximum missed cleavage was set to 1 and limited to trypsin cleavage sites. Precursor mass tolerance and fragment mass tolerance were set to 20 ppm and ± 0.2 Da, respectively.

Two-dimensional electrophoresis

Plasma proteins that bound to a serpin-3 antibody-coupled immunoaffinity column and from the control column of Protein-A Sepharose CL-4B beads without antibody were separated by two-dimensional electrophoresis at Kendrick Laboratories, Inc. (Madison, WI). The sample (200 µL = 46 µg) of plasma proteins that bound to a serpin-3 antibody-coupled immunoaffinity column was precipitated with trichloroacetic acid, redissolved in 25 µL of SDS Boiling Buffer (5% sodium dodecyl sulfate, 5% β-mercaptoethanol, 10% glycerol and 60 mM Tris, pH 6.8), heated in a boiling water bath for 3 min, and diluted with 25 µL of Urea Sample Buffer (9.5 M urea, 2% (w/v) Nonidet P-40, 5% β-mercaptoethanol, and 2% ampholines consisting of 2% pH 2-11 (Servalytes, Serva, Heidelberg Germany)) before loading. The sample of plasma proteins that bound to a control column of Protein-A Sepharose CL-4B beads without antibody was treated similarly. For both samples, 46 µg of protein in 50 µL was used for the two-dimensional separation.

Two-dimensional electrophoresis was performed according to the carrier ampholine method of isoelectric focusing (O'Farrell, 1975; Burgess-Cassler et al., 1989) at Kendrick Laboratories. Isoelectric focusing (IEF) was carried out in a glass tube of 2.3 mm (inner diameter) using a 2% pH 3.5-10 mix 4 L ampholines (GE Healthcare, Piscataway, NJ; Serva, Heidelberg, Germany) for 9600 volt-hrs. One microgram of an IEF internal standard, tropomyosin, was added to the sample. Tropomyosin migrates as a doublet and the lower polypeptide spot has a molecular weight of 33,000 and a pI of 5.2.

After equilibration for 10 min in 10% glycerol, 50 mM dithiothreitol, 2.3% SDS, 0.0625 M Tris, pH 6.8, each tube gel was sealed to the top of a stacking gel on top of a 10% acrylamide slab gel (0.75 mm thick). SDS slab gel electrophoresis was carried out for about 4 h at 12.5 mA/gel (serpin-3 immunoaffinity sample) or 15 mA/gel (control sample). Myosin (220,000), phosphorylase A (94,000), catalase (60,000), actin (43,000), carbonic anhydrase (29,000), and lysozyme (14,000) were used as molecular weight standards (Sigma Chemical Co., St. Louis, MO). Gels were stained with Coomassie Blue and shipped in dilute acetic acid.

Electrospray ionization tandem mass spectrometry

Gel spots excised from the two-dimensional gels were incubated a few times for 10 min in 100 μL of 50% acetonitrile at 30°C, followed by the addition of 50 μl of 100% acetonitrile for 10 min. After discarding the solvent, the gel pieces were dried by speed vacuum concentrator and incubated with 200 ng of sequencing grade trypsin (Trypsin Gold, Promega, Madison, WI) in 20 mM ammonium bicarbonate (total volume = 20 μL). An additional 20 μL of 20 mM ammonium bicarbonate and 10% acetonitrile were added to gel pieces upon rehydration, followed by incubation at 30°C for 17 h. Tryptic peptides were recovered from gel plugs by extraction with 100 μL of 50% acetonitrile in 2% trifluoroacetic acid for 30 min at 30°C. Extracted peptides were concentrated by speed vacuum concentrator and added to 100 μL of 2% acetonitrile in 0.1% formic acid.

Automatic nano-high performance liquid chromatography (nano-HPLC) was performed using a microcolumn switching device (Switchos, LC Packings) coupled to an autosampler (Famos, LC Packings) and a nanogradient generator (UltiMate Nano HPLC, LC Packings). Peptide solution (30 μL) was loaded on a C18 reversed-phase capillary column (75 μm inner diameter × 15 cm; PepMap, Dionex) in conjunction with an Acclaim C18 PepMap trapping column (300 μm inner diameter × 10 mm, Dionex). Peptides were separated by a nanoflow linear acetonitrile gradient using buffer A (0.1% formic acid, 2% acetonitrile) and buffer B (0.1% formic acid, 80% acetonitrile) starting from 5% buffer B to 60% over 45 min at a flow rate of 200 nL/min. Then, the column was washed with 95% buffer B for 5 min. This process was controlled by the system control software, Hystar 3.2. Eluted peptides were injected into an HCT Ultra Ion Trap Mass Spectrometer (Bruker Daltronics). The mass spectrometer was set up in the data dependent MS/MS mode to alternatively acquire full scans (*m*/*z* acquisition range from 300

to 1700 Da). The four most intense peaks in any full scan were selected as precursor ions and fragmented by collision energy. MS/MS spectra were interpreted and peak lists were generated by DataAnalysis 3.4 and Biotools 3.0 software (Bruker Daltronics).

Peptide masses were searched by Mascot v 2.3.02 (Matrix Science) using NCBI nr database (NCBI 20110319), containing 13,254,464 sequences. After applying a taxonomy filter to include sequences from *Manduca sexta* only, 772 sequences were searched. Additionally, *M. sexta* ESTs (181,602) from NCBI and a pyrosequencing project (Zou et al., 2008; Zhang et al., 2011) were searched for positive identifications. Searches were performed without restriction to M_r or pI, and with variable oxidation of methionine residues and dehydro of cysteine residues (indicates S-S linkage). Maximum missed cleavage was set to 2 and limited to trypsin cleavage sites. The peptide mass tolerance and fragment mass tolerance were set to ±1.2 Da and ±0.6 Da, respectively. A threshold of 0.05 was used to determine positive protein identifications and peptides scoring <20 were automatically rejected, ensuring that all protein identifications were based on reliable peptide identifications.

Antibacterial activity assay

Day 2 fifth instar larvae were injected with recombinant serpin-3, *M. luteus*, or with various control materials, as described in the figure legend. After 24 h, hemolymph was collected on ice and centrifuged at 7000 × g for 25 min at 4°C to remove hemocytes. Aliquots (200-300 µL) of each plasma sample were heated at 95°C for 5 min, followed by centrifugation at 10000 × g for 8 min to remove large proteins. Supernatants were placed at -20°C until use.

An overnight culture (3 mL) of *E. coli* strain XL1-Blue was started by inoculating a single colony from a streak plate into LB without antibiotics. The culture was grown at 37°C with shaking at 275 rpm. Fresh LB (3 mL) was inoculated with 60 µL of the overnight culture and grown at 37°C with shaking at 275 rpm for 4 h. To create a good bacterial lawn, 50 µL of *E. coli* was added to 20 mL of LB plus 1% agar held at 47°C and poured into a petri dish. Plates were held at room temperature for 10 min and then placed at 4°C for 30 min. Wells were made in the LB agar plates using a metal tool with a 4 mm diameter opening and removing the agar plug with a sterile toothpick. Liquid was removed from each well and 15 µL of each sample to be tested was added. Water was used as a negative control and plasma samples from larvae injected with *M. luteus* (100 µg) only were used as a positive control. Plates were placed in a 37°C

incubator for 19-21 h and were not inverted. The diameter of each zone of inhibition was measured three times, averaged, and divided by 2 to obtain the radius. The radius was used to calculate the area ($A = \pi r^2$) of the zone of inhibition (= area of entire circle – area of sample well).

Results

Formation of serpin-proteinase complexes in plasma

Injection of bacteria into larvae 24 h prior to hemolymph collection increases the synthesis and hemolymph concentration of many immune related proteins (Kanost et al., 2004), and the incubation of plasma with bacteria after collection stimulates activation of hemolymph proteinases that interact with each other and are inhibited by serpins (Kanost, 2007; Ragan et al., 2009). To investigate if exposure of plasma to bacteria led to the activation of plasma proteinases and the formation of serpin-proteinase complexes, plasma collected from larvae 24 h after injection with *M. luteus* was incubated with filter-sterlized water or with *M. luteus*, followed by immunoblot analysis. Serpin-3, HP8, PAP-1, and PAP-3 antibodies detected bands in plasma, representing intact serpin-3 (~50 kDa), proHP8 (~42 kDa), proPAP-1 (~40 kDa), and proPAP-3 (~44 kDa) (Figure 3-1). A band representing a potential serpin-proteinase complex (~70 kDa) was also observed for serpin-3, HP8, and PAP-1, and is most likely present due to spontaneous proteinase activation or activation caused by the injury of hemolymph collection. Smaller bands detected by serpin-3 antibody are consistent with cleaved serpin. After incubation of plasma with *M. luteus*, the intensity of the 50 kDa serpin-3 band was reduced, while an increase was observed for bands representing cleaved serpin, and two higher molecular weight bands (~70 kDa), consistent with the sizes of serpin-proteinase complexes, were detected by serpin-3 antibody. This result indicates that plasma proteinases were activated by exposure to bacteria and inhibited by serpin-3 to form SDS-stable serpin-3-proteinase complexes, which are larger than either the serpin or proteinase alone. The zymogen form of HP8 and PAP-3 completely disappeared, while the zymogen form of PAP-1 was reduced in intensity in plasma incubated with *M. luteus*. In addition, the PAP-3 antibody recognized a band representing the clip domain of this protein. In conjunction with these changes, a higher molecular weight band (~70 kDa) was observed for each proteinase. These results indicate that proHP8, proPAP-1, and proPAP-3 were activated by

the exposure to bacteria and then inhibited by an unidentified serpin to form an SDS-stable serpin-proteinase complex.

Purification and identification of serpin-HP8 complexes in plasma

To identify serpins that may inhibit HP8, complexes were purified from plasma by immunoaffinity chromatography using HP8 antibody. Proteins that bound to the column were analyzed by immunoblot using HP8, serpin-1, serpin-3, serpin-4, serpin-5, and serpin-6 antibodies (Figure 3-2). Antibodies to HP8 recognized two bands with sizes (~70 kDa) consistent with that expected for a serpin-proteinase complex. This result suggests that HP8 may be inhibited by more that one serpin. Putative serpin-proteinase complexes were detected with serpin-1, serpin-3, and serpin-6 antibodies, but not with serpin-4 or serpin-5 antibodies in the sample purified using HP8 antibody. These results suggest that serpin-1, serpin-3, and serpin-6 can form a SDS-stable serpin-proteinase complex with HP8 in plasma.

Purification and identification of serpin-3-proteinase complexes in plasma

To further investigate serpin-3 as an inhibitor of HP8 or other plasma proteinases, immunoaffinity chromatography was conducted using serpin-3 antibody to isolate serpin-3-proteinase complexes found in plasma. Immunoblot analysis of plasma proteins that bound to the serpin-3 antibody column was carried out using antibodies to serpin-3, HP8, PAP-1, PAP-2, and PAP-3 (Figure 3-3A). Antibodies to serpin-3 recognized a band with a size (~70 kDa) consistent with that expected for a serpin-proteinase complex. Bands between 51 and 64 kDa recognized by the antibody may be cleaved serpin-proteinase complexes, while the band at ~50 kDa is intact serpin-3, and the band located below 50 kDa probably represents cleaved serpin-3. Bands at the sizes expected for serpin-proteinase complexes were detected with HP8, PAP-1, PAP-2, and PAP-3 antibodies (Figure 3-3A). The zymogen form of HP8 and PAP-1 observed in naïve plasma was not detected in the immunopurified sample. In addition, the PAP-1, PAP-2, and PAP-3 antibodies recognized a band representing the clip domain of these proteins. These results suggest that proHP8, proPAP-1, proPAP-2, and proPAP-3 activated in plasma by exposure to bacteria were inhibited by serpin-3. Antibodies specific for HP6, HP9, HP10, HP12, HP13, HP14, HP15, HP16, HP17, HP18, HP19, and HP21 were also tested, but no serpin-3-proteinase complexes were detected (data not shown).

To further identify plasma proteins isolated by serpin-3 immunoaffinity, proteins separated by SDS-PAGE were digested with trypsin and analyzed by MALDI-TOF/TOF. Resulting peptide masses for each sample were searched against the NCBInr protein sequence database using Mascot. Protein identifications are listed in Table 3-1. Each band number corresponds with bands excised from a one-dimensional gel (Figure 3-3B). Serpin-3 (~51 kDa) was identified in band 4. Matching peptides were distributed over the entire sequence (covering 65%) and included peptides on the C-terminal side of the P1 Lys residue in the reactive center loop, all consistent with this band representing unmodified serpin-3. Band 2 contained tryptic peptides from PAP-3 and serpin-3. Identified tryptic peptides from PAP-3 covered 19% of the sequence and were located in the catalytic domain of the proteinase (none in the clip domain). This is consistent with the expectation that PAP-3 was activated by cleavage between the clip domain and catalytic domain prior to reacting with serpin-3. Moreover, no tryptic peptides were identified from serpin-3 after the P1 Lys residue, suggesting that serpin-3 was cleaved at this position by PAP-3, resulting in formation of the SDS-stable serpin-proteinase complex. Band 5, which only contained tryptic peptides from serpin-3, may be cleaved serpin-3. No tryptic peptides C-terminal to the P1 Lys residue were detected. Serpin-3 was also found in band 3, slightly smaller than the serpin-3-PAP-3 complex, and is predicted to be a cleaved serpin-3-proteinase complex. No tryptic peptides for any proteinase were identified in band 3. However, band 3 did contain prophenoloxidase subunit 1 and prophenoloxidase subunit 2.

A band at 200 kDa was apolipophorin-1, a subunit of a plasma lipid transfer protein (Figure 3-3B, band 1) (Kanost et al., 1990; Ryan and van der Horst, 2000). Intense bands (6 and 7) between 28 and 39 kDa were identified as immulectins (Yu and Kanost, 2008). Band 6 contains immulectin-2 and serine proteinase homolog-1. Band 7 included immulectin-3, -4, and -III. Immulectins are pattern recognition proteins that associate with prophenoloxidase and serine proteinase homologs (Yu et al., 2003). To understand the difference between immulectin-3 and immulectin-III, a nucleotide blast (NCBI: BLASTN 2.2.25+) was completed using the nucleotide sequence for immulectin-III (AM293329.1) as the query. Immulectin-III was 96% identical to immulectin-4 (AY768812.2), suggesting that immulectin-III could be an allele of the same gene. Alternatively, immulectin-III could be encoded by a highly similar gene that arose from gene duplication. Antimicrobial peptides (Kanost et al., 2004; Ragan et al., 2009) were detected in

bands 8 and 9. Band 8 contained attacin-1, while attacin-II and gloverin (dVG-AP3-2) were detected in band 9.

To gain higher resolution for protein identification, plasma proteins that bound to the serpin-3 antibody column (Figure 3-4A; Table 3-2) were separated by two-dimensional electrophoresis followed by electrospray ionization tandem mass spectrometry. As a control, plasma proteins eluting from a Protein-A Sepharose CL-4B column lacking antibody were similarly analyzed (Figure 3-4B, Table 3-3). Table 3-2 lists the top Mascot hits after searching the NCBI protein database restricted to sequences from *M. sexta*. Protein scores are a sum of individual ion scores that had a score greater than 22 (significant identity; $p < 0.05$). Only proteins with two or more MS/MS spectra are included in this table (MS/MS results are listed in Table B-2).

Spots 22-26 (Figure 3-4A) are apparently intact serpin-3, and all of these spots contain peptides on the C-terminal side of the P1 Lys residue in the reactive center loop. Since plasma from 15-18 larvae was used for immunoaffinity purification, multiple spots of serpin-3 with small changes in pI are likely due to allelic variation.

Serpin-3-proteinase complexes are expected to have a molecular weight of ~94 kDa. Spots 1-5 and 37-39 are good candidates for putative complexes (Figure 3-4A). Spot 1 contained serpin-3 and two peptides from the catalytic domain of HP8 (Figure 3-5). Both serpin-3 and PAP-3 were present in spots 2, 3, 4, and 39. No peptides C-terminal to the P1 Lys residue of serpin-3 were detected and only peptides in the catalytic domain of PAP-3 were identified (Figures 3-6, 3-7, 3-8, and 3-10). PAP-1 and serpin-3 were present in spot 5. Like the serpin-3-PAP-3 complexes, no peptides were found after the P1 Lys residue of serpin-3 and only peptides from the catalytic domain of PAP-1 were detected (Figure 3-9). Percent sequence coverage was calculated by Mascot based on sequences in the NCBI database. In regard to proteinases, this means the zymogen sequence. However, proteinases are processed by activation cleavage before interacting with a serpin. This means that only the catalytic domain should be present in a serpin-proteinase complex. Therefore, the percent sequence coverage for each proteinase in complex was recalculated using the residues in the catalytic domain only (Table 3-2; values in parentheses). Spots 37 and 38 are located at a molecular weight that is consistent with a serpin-proteinase complex. The spots clearly contained serpin-3, but no proteinase was identified. These may represent proteinases in plasma that have not yet been discovered.

Spots 15-19, 43, and 52 all contained serpin-3 (Figure 3-4A; Table 3-2), and are at molecular weights that are consistent with cleaved serpin-proteinase complexes. In addition to serpin-3, spot 17 contained seven peptides from a protein similar to a gram-negative binding protein (Wang et al., 2011). Unexpectedly, serpin-3 in spots 16, 17, and 43 contained peptides C-terminal to the P1 Lys residue, indicating that serpin-3a in these spots was not cleaved in the RCL.

Spots 27-30 were located at a size smaller than intact serpin-3, but contained serpin-3 peptides (Figure 3-4A; Table 3-2). These spots, with the exception of 27 did not contain peptides C-terminal to the P1 Lys residue, suggesting that they were cleaved in the RCL, but reacted as substrate rather than inhibitor. These spots also contained peptides from serine proteinase homologs 1b (spots 27, 30) and 4 (28-30).

Other immune related proteins were also identified. Immulectins (2, 2a, 3, III, and 4), were found in spots 3, 4, 13, 15, 67, and in a series of very intensely stained spots 54-61. Serine proteinase homologs (1b, 2, and 4), which are necessary for prophenoloxidase activation, were found in spots 20-22, 27-30, 33-35, and 56. Prophenoloxidase subunit 1 was found in spots 7-9, and prophenoloxidase subunit 2 was found in spots 6, 10-14, 30, and 51. Attacin-1, an antimicrobial peptide, was in spots 66-68. Hemolymph proteinase 14, known to initiate a prophenoloxidase pathway, was identified in spot 41.

To find additional proteins that do not have sequences in the NCBI protein database, the ESI-MS/MS data was searched against *M. sexta* expressed sequence tags (ESTs) compiled from NCBI and a new pyrosequencing EST project (Zou et al., 2008; Zhang et al., 2011). Table 3-4 lists the top Mascot hits, and protein scores composed of individual ion scores that had a score greater than 46 were considered to have significant identity ($p < 0.05$). Identification of ESTs based on BLAST searches against the NCBI database was consistent with results obtained by searching the NCBI protein database restricted to *M. sexta*. Additional protein identifications were made for several spots. Two peptides for alpha tubulin from *Bombyx mori* and *M. sexta* were matched from spot 19. Eukaryotic initiation factor-4a from *M. sexta* was identified in spots 22 and 26; however, this identification was based on one peptide. Protein scores were 78 and 80, respectively. Inter-alpha trypsin inhibitor was identified by four peptides in spot 32 (protein score = 445) and a Kazal family serine proteinase inhibitor was detected by one peptide in spot

51. The latter match had a protein score of 47, which is just above the significance threshold of 46.

To investigate the potential for plasma proteins to non-specifically interact with serpin-3, a control column of Protein-A Sepharose CL-4B without antibody was prepared. Plasma proteins that bound to the control column were identified by using Mascot to search the NCBI protein database restricted to sequences from *M. sexta* (Figure 3-4B; Table 3-3). Protein scores are a sum of individual ion scores that had a score greater than 22 (significant identity; $p < 0.05$). Detailed MS/MS data are included in Table B-3.

Immulectins (2b, 3, III, and 4) were very prominent proteins that bound to the Protein-A Sepharose CL-4B beads lacking antibody (Table 3-3; Figure 3-4B). Spots containing immulectins included 1c-6c, 12c-21c, and 23c-30c. Identification of immulectins in spots 12c-14c are most likely a separation artifact as their location is not consistent with the expected pI of immulectin-2b (pI = 5.76) or immulectin-3 (pI = 5.86). However, spot 13c also contained immulectin-III, which has a pI of 9.23. Prophenoloxidase subunit 2 was found in spot 11c, but prophenoloxidase subunit 1 was not identified. Serine proteinase homologs were present in spots 22c (SPH-2) and 28c (SPH-1b). Four peptides for endochitinase were found in spot 10c and one peptide was found for serpin-1 in spot 9c and scolexin A in spot 17c. No protein match was found for spots 7c and 8c.

These ESI-MS/MS data were also searched against *M. sexta* expressed sequence tags (ESTs) compiled from NCBI and a new pyrosequencing EST project (Zou et al., 2008; Zhang et al., 2011) to find additional proteins that do not have sequences in the NCBI protein database. Table 3-5 lists the top Mascot hits, and protein scores composed of individual ion scores that had a score greater than 46 were considered to have significant identity ($p < 0.05$). Identification of ESTs was based on BLAST searches against the NCBI database. Protein identification for spots 1c-6c, 9c, 11-13c, 15c, 17c-18c, and 23c-30c (Tables 3-4 and 3-5) were similar to those obtained by searching the NCBI protein database restricted to sequences from *M. sexta*. Spots 7c-8c, 10c, 14c, 16c, 19c-22c did not have an EST hit (Table 3-5).

Purification of recombinant HP8-Xa

To investigate potential inhibition of HP8 by serpin-3, I prepared a recombinant form of HP8 mutated to permit activation by bovine factor Xa as previously described (An et al., 2009;

An et al., 2010b; An et al., 2011). Recombinant HP8-Xa expressed in *Drosophila* S2 cells was secreted into the culture medium utilizing its own secretion signal peptide. Medium was incubated with Affi-gel Blue Gel beads to remove bovine serum albumin and then applied to a column of concanavalin A-Sepharose 4B. Protein eluted from the concanavalin A column was further purified by anion exchange chromatography using a Q-Sepharose^{TM} Fast Flow column followed by gel permeation chromatography on a Sephacryl-S100 High Resolution column. Analysis by SDS-PAGE followed by silver staining or immunoblot indicated that two forms of HP8-Xa were present, a full-length (42 kDa) and truncated protein (37 kDa) in approximately equal amounts (Figure 3-11). Previous analysis of the 37 kDa band by Edman degradation revealed that HP8-Xa had been cleaved after Arg^{59} (An et al., 2010b). A total of 26.5 µg of protein was purified from a starting culture volume of 365 mL.

Complex formation between purified, recombinant HP8 and serpin-3

After recombinant serpin-3 was mixed with activated HP8-Xa, immunoblot analysis detected the appearance of a higher molecular weight complex (~70 kDa) using antisera to serpin-3 or HP8 (Figure 3-13). When serpin-3 was mixed with proHP8-Xa, anti-HP8 antibodies recognized only the 42 kDa proHP8-Xa zymogen and 37 kDa truncated form of HP8. After incubation with factor Xa, the proHP8-Xa zymogen disappeared, and the 34 kDa HP8 catalytic domain was detected. Mixing serpin-3 with active HP8-Xa resulted in decreased intensity of the 34 kDa catalytic domain and the appearance of a new immunoreactive band at 70 kDa, consistent with the expected size for a serpin-proteinase complex. This serpin-proteinase complex band was absent in lanes for negative controls containing only serpin-3, proHP8 plus serpin-3, serpin-3 plus factor Xa, or proHP8-Xa plus factor Xa. These results indicate that serpin-3 forms a covalent complex with active HP8-Xa and that HP8-Xa was activated by bovine factor Xa.

Inhibition of HP8 by serpin-3 in plasma

Two different pooled samples of naïve plasma were used to investigate the hypothesis that more serpin-3-HP8 complex would be observed when exogenous recombinant serpin-3 was added to plasma in which proteinases were activated by treatment with curdlan. In plasma sample 1, some serpin-HP8 complex was observed in all samples (Figure 3-12), and the expected catalytic domain of HP8 (~34 kDa) was observed in plasma incubated with curdlan. After plasma was pre-incubated with recombinant serpin-3 followed by incubation with curdlan, HP8

antibody recognized two putative complex bands, and the intensity of these bands was greater than that in lanes not containing recombinant serpin-3. This increased band intensity indicates greater inhibition of HP8. The lack of glycosylation in recombinant serpin-3 may explain the detection of two complex bands (one containing natural serpin-3 and one with recombinant serpin-3). In addition, the band representing the catalytic domain disappeared in samples pre-incubated with serpin-3, indicating that active HP8 was in complex with serpin-3. Observation of the catalytic domain in plasma not activated by curdlan was surprising and is best explained by spontaneous activation of HP8 during the collection of this hemolymph sample.

The expected HP8 zymogen (~42 kDa) was observed in the second plasma sample (6 larvae; Figure 3-12). When curdlan was added to this plasma, the HP8 zymogen disappeared, the catalytic domain was observed, and some serpin-HP8 complex was detected. HP8 zymogen, but not the catalytic domain of HP8, was detected in plasma pre-incubated with recombinant serpin-3. However, after stimulation by curdlan, the zymogen form of HP8 was reduced, and a higher molecular weight band corresponding to a serpin-3-HP8 complex was observed. These results indicate that HP8 activated by curdlan in plasma was inhibited by serpin-3.

Production of antimicrobial peptides is not inhibited by injection of serpin-3

To determine if serpin-3 could regulate Spätzle activation by serving as a biologically relevant inhibitor of HP8, I injected larvae with purified recombinant serpin-3 followed by injection with bacteria to stimulate proteinase cascade activation, and assayed the plasma for antibacterial activity. If serpin-3 regulates the activity of HP8 *in vivo*, I expected samples from insects injected with exogenous serpin-3 to have higher levels of antibacterial activity than controls. However, plasma samples from larvae with enhanced serpin-3 concentration did not differ in antibacterial activity from larvae injected with bovine serum albumin as a control (Figure 3-14, panels A/B). Plasma samples from larvae injected with serpin-3 did not exhibit melanization, whereas plasma from control larvae melanized within a few hours (Figure 3-14C). This confirmed that the activity of serpin-3 to inhibit PAP-1, PAP-2, and PAP-3 effectively regulates melanization of hemolymph (Zhu et al., 2003b).

Discussion

Previous studies to identify proteinase targets of serpin-3 (Zhu et al., 2003b) were completed prior to obtaining sequences of many hemolymph proteinases (Jiang et al., 2005; Wang et al., 2006). PAP-1 and PAP-3 were identified as targets of serpin-3 by immunoaffinity chromatography followed by immunoblot analysis (Zhu et al., 2003b). In the current study, I re-analyzed serpin-3 and its proteinase targets by purifying serpin-3-proteinase complexes from plasma activated by treatment with bacteria, using a serpin-3 immunoaffinity column. Proteinase components were identified by immunoblot analysis and analysis of tryptic peptides by MALDI-TOF/TOF or ESI-MS/MS after separation by one- or two-dimensional SDS-PAGE. Both of these strategies have been utilized to identify proteinase targets of other *M. sexta* serpins (Tong et al., 2005; Ragan et al., 2010). One-dimensional SDS-PAGE followed by immunoblot and MALDI-TOF analysis was used to identify serpin-4 or serpin-5-proteinase complexes in plasma. Serpin-4 formed a complex with HP1, HP6, and HP21, whereas serpin-5 formed a complex with HP1 and HP6 (Tong et al., 2005). Two-dimensional SDS-PAGE followed by immunoblot and MALDI-TOF/TOF analysis identified serpin-1A, -1E, and -1J in complex with HP8, and an unidentified serpin-1 isoform complexed with HP1 (Ragan et al., 2010).

Serpin-3-proteinase complexes identified in plasma

Results in this study demonstrated that serpin-3 formed complexes in plasma with four proteinases, HP8, PAP-1, PAP-2, and PAP-3. These are all clip domain serine proteinases with at least one amino-terminal clip domain and a C-terminal serine proteinase domain (Jiang et al., 2005). Since all have predicted trypsin-like specificity (Jiang et al., 2005) and the P1 residue of serpin-3 is a Lys residue (Zhu et al., 2003b), it is not surprising that all four proteinases interacted with serpin-3. All four complexes were confirmed by immunoblot analysis using appropriate antibodies. Identification of serpin-3-PAP-1 and serpin-3-PAP-3 complexes by immunoblot analysis is consistent with results obtained by Zhu et al. (2003b). One-dimensional SDS-PAGE followed by trypsin digestion and MALDI-TOF/TOF analysis of selected bands identified tryptic peptides of both serpin-3 and PAP-3 in the same band; however, tryptic peptides for HP8, PAP-1, or PAP-2 were not identified by this method. To achieve better separation, two-dimensional SDS-PAGE was performed and followed by ESI-MS/MS analysis. In two-dimensional SDS-PAGE, proteins are first separated by electric charge differences

(isoelectic focusing) and then by molecular weight. Eight spots (1-5, 37-39) were consistent with the size of a serpin-3 proteinase complex. Two to five tryptic peptides for the catalytic domain of PAP-3 were found in spots 2, 3, 4, and 39 along with serpin-3. A total of six tryptic peptides for PAP-1 were found with serpin-3 in spot 5. Spot 1 contained serpin-3 and two tryptic peptides from the catalytic domain of HP8. Although immunoblot analysis detected a serpin-3-PAP-2 complex in plasma, no tryptic peptides from PAP-2 were detected by mass spectrometry. Detection of six or fewer peptides from proteinases found in the same spot as serpin-3 indicated that not all potential tryptic peptides in the catalytic domain of each proteinase were detected. Lack of detection could be due to the size of the tryptic peptides. If a peptide was too small or too large, it would not be identified by mass spectrometry. Spots 37 and 38 contained serpin-3, but no proteinase components were identified. These may represent proteinases in plasma that have not yet been identified. I hypothesize that other clip domain proteinases exhibiting predicted trypsin-like specificity (e.g. HP1, 2, 6, 12, 13, 15, 17, 18, and 22-24 (Jiang et al., 2005; Wang et al., 2006)) might be regulated by serpin-3. Such complexes were not identified by immunoblot analysis or using the database search parameters described in the materials and methods section (i.e. peptide mass tolerance and fragment mass tolerance were set to ±1.2 Da and ±0.6 Da, respectively). However, if I were to change these parameters, additional serpin-3-proteinase complex identifications might be made and significance would be determined based on a set identity threshold.

Other proteins identified in plasma by mass spectrometry

Full-length serpin-3 was identified in spots 22-26 (2D gel) and spot 4 (1D gel). Allelic variation involving charged amino acids is one possible explanation for the five distinct serpin-3 spots observed after two-dimensional SDS-PAGE. Another possible explanation is changes in post-translational modifications such as N-linked glycosylation. Differences in glycosylation were shown to change the pI, but not the apparent molecular weight of glycoproteins found in human plasma (Packer et al., 1996).

Immulectins, prophenoloxidase subunits 1 and 2, and serine proteinase homologs co-purified with serpin-3-proteinase complexes. These proteins are all known components of the prophenoloxidase activation pathway. A large amount of immulectin-2 and smaller amounts of immulectin-3, -III, and -4 were purified from the serpin-3 immunoaffinity column. This result is

consistent with immunoaffinity purification of serpin-4 or -5-proteinase complexes (Tong et al., 2005). Immulectin-2 binds to lipopolysaccharide from gram-negative bacteria and stimulates the activation of prophenoloxidase (Yu and Kanost, 2000). Tong et al. (2005) speculated that immulectin-2 might recognize carbohydrates on the surface of bacteria or function as a linker to localize components of the prophenoloxidase activation system. Serine proteinase homologs bind to immulectin-2 and prophenoloxidase (Yu et al., 2003) suggesting the formation of proteinase complexes, including proteinases inhibited by serpins, held together by their interaction with serine proteinase homologs and immulectins (Tong et al., 2005). As a control, I ran a column of Protein-A Sepharose CL-4B beads without antibody to determine what proteins in plasma bound. The most prominent bound protein was immulectin-2 with lesser amounts of immulectins-3, -III, and -4. Prophenoloxidase subunit 2 was found in two spots while serine proteinase homologs 1 and 2 were each found in one spot. These results do not support the hypothesis presented by Tong et al. (2005). They suggest that immulectins bind to carbohydrates present on the Protein-A Sepharose CL-4B beads and that serine proteinase homologs and prophenoloxidase interact with bound immulectins and that the binding of those components to the column is independent of interaction with serpins of serpin-proteinase complexes.

Seven tryptic peptides corresponding to a gram-negative binding protein, named microbe binding protein, were detected in spot 17. Microbe binding protein is a new member of the β-1,3-glucanase-related protein superfamily (Wang et al., 2011). The sequence of microbe binding protein is 61% identical to *B. mori* gram-negative binding protein and 34-36% identical to *M. sexta* β-1,3-glucan recognition protein-1 and -2. Microbe binding protein bound to a variety of microbial cells and cell surface components which indicates that microbe binding protein serves as a pattern recognition protein during infection. In addition, the ability of microbe binding protein to enhance proPO activation indicates that this protein works in concert with other defense molecules to stimulate the activation of proPO (Wang et al., 2011).

Three tryptic peptides from HP14 were found in spot 41. HP14 consists of five low-density lipoprotein receptor class A domains, a Sushi domain, a cysteine-rich region (Wonton), and C-terminal serine proteinase domain (Ji et al., 2004). HP14 autoactivates in the presence of peptidoglycan (Ji et al., 2004) or β-1,3-glucan and βGRP2 to stimulate the activation of prophenoloxidase (Wang and Jiang, 2006). However, all tryptic peptides were found in the amino-terminal region of HP14 and the molecular size of this spot is consistent with that of

HP14 zymogen (~73 kDa), suggesting that HP14 was not cleaved. The low-density lipoprotein receptor class A, Sushi, and Wonton domains of HP14 all bound to Lys-type peptidoglycan while the Sushi and Wonton domains also bound to β-1,3-glucan recognition protein-1 (Wang and Jiang, 2010). This knowledge leads me to speculate that HP14 may bind to microbe binding protein described above. Alternatively, the detection of HP14 could be due to a non-specific interaction with other identified proteins.

Attacin-1 was identified in spots 66-68 (2D gel) and spot 8 (1D gel) while attacin-II and gloverin were found in spot 9 (1D gel). Attacin and gloverin are both immune-inducible glycine-rich antibacterial peptides. These antibacterial peptides inhibit the synthesis of outer membrane components, which increases the permeability of the outer membrane (Engström et al., 1984; Carlsson et al., 1991; Axén et al., 1997). Detection of antibacterial peptides was unexpected. It is likely that these peptides were detected due to interactions with other proteins as I do not expect an interaction with serpin-3.

Spot 32 contained serpin-3 and inter-α-trypsin inhibitor heavy chain from *M. sexta*. Inter-α-trypsin inhibitor was originally identified in *M. sexta* by substractive suppression hybridization (Zhu et al., 2003a). It is similar to mouse and human inter-α-trypsin inhibitor heavy chain 4 (Cai et al., 1998), which is thought to function in inflammatory responses (Salier et al., 1996). This inhibitor is a member of the inter-α-inhibitor family, which belongs to the Kunitz-type proteinase inhibitor superfamily (Salier, 1990). In *M. sexta*, expression of inter-α-trypsin inhibitor, detected by Northern blot analysis, was dramatically increased after exposure to bacteria (Zhu et al., 2003a).

An interesting match to a Kazal family serine proteinase inhibitor was found by EST search of spot 51. Kazal family serine proteinase inhibitors contain one or more Kazal-type domains, which are 40-60 amino acid residues in length. A typical Kazal domain is recognized by the general amino acid sequence C-X_a-C-X_b-PVCG-X_c-Y-X_d-C-X_e-C-X_f-C where subscript letters represent an integral number of amino acid residues, and the six cysteine residues form three intradomain disulfide bonds (Rimphanitchayakit and Tassanakajon, 2010). Substractive suppression hybridization identified this proteinase inhibitor in *M. sexta* (Zhu et al., 2003a) and BLAST results indicated that it is similar to rhodniin from *Rhodnius prolixus* (Friedrich et al., 1993). Rhodniin prevents blood clotting by inhibiting thrombin to facilitate the insect's ability to take a blood meal. Other insects, including *Drosophila melanogaster* (Niimi et al., 1999),

Galleria mellonella (Nirmala et al., 2001), *Triatoma infestans* (Campos et al., 2004), *Bombyx mori* (Zheng et al., 2007), and *Aedes aegypti* (Watanabe et al., 2010) possess Kazal-type inhibitors. Kazal-type inhibitors from *T. infestans* inhibit thrombin and factor XIIa to control blood coagulation during blood feeding (Campos et al., 2004), and silk proteinase inhibitor 1 from *G. mellonella* inhibits subtilisin and proteinase K to prevent the destruction of silk proteins for cocoon formation by microbial invaders (Nirmala et al., 2001). Kazal family serine proteinase inhibitors are also found in crayfish (Johansson et al., 1994) and shrimp (Somprasong et al., 2006). Subtilisin was inhibited by Kazal-type inhibitors from both organisms, while chymotrypsin and elastase were inhibited by inhibitors from crayfish and shrimp, respectively (Johansson et al., 1994; Somprasong et al., 2006).

Interaction of serpin-3 and HP8

After identifying HP8 as a proteinase target for serpin-3, my goal was to biochemically characterize the interaction between the two proteins. The first step towards this goal was the production of purified recombinant HP8-Xa in *Drosophila* S2 cells and serpin-3 in *E.coli*. Both proteins were successfully purified, but the concentration of HP8-Xa was very low and a truncated version of HP8-Xa was present (An et al., 2010b). Due to the low concentration and stability of the protein, I was only able to conduct one experiment with purified HP8-Xa. Formation of an SDS-stable complex is a hallmark feature of a serpin-proteinase interaction and was tested by incubating recombinant serpin-3 with active HP8-Xa. I determined that serpin-3 and HP8 form a complex *in vitro*. Samples containing factor Xa alone did not result in complex formation, indicating that the observed complex was due to the interaction of serpin-3 with active HP8-Xa and not factor Xa. Similar *in vitro* complexes have been detected for serpin-1J and PAP-3 (Jiang et al., 2003), serpin-3 and PAP-1/PAP-3 (Zhu et al., 2003b), serpins-4 and -5 with PAP-1 (Tong and Kanost, 2005), serpin-1I and HP14 (Wang and Jiang, 2006), serpin-6 and PAP-3 (Zou and Jiang, 2005), serpin-4 and HP21 (Wang and Jiang, 2007), serpins-4 and -5 with HP6 (An and Kanost., 2010), and serpin-1J and HP8 (An et al., 2011). This result further supports the hypothesis that serpin-3 might be a biologically relevant inhibitor of HP8 in hemolymph.

Next, I determined that exogenous purified recombinant serpin-3 could form a complex with endogenous HP8 in plasma when curdlan was used as an elicitor to stimulate proteinase

activation. Two different pooled plasma samples were used in this experiment. With pooled plasma sample #1, a serpin-3-HP8 complex was detected by HP8 antibody in all samples, and the intensity of the detected complex was greater in samples containing exogenous serpin-3. Mixtures lacking active HP8 (lanes without curdlan) were not expected to exhibit complex formation. The best explanation for this result is that spontaneous activation of HP8 in plasma took place in this sample during the collection of hemolymph (i.e. wounding from clipping the posterior horn). In pooled plasma sample #2, HP8 was not activated in the absence of curdlan. When this plasma was incubated with curdlan, serpin-3-HP8 complexes were observed in the presence and absence of exogenous serpin-3. In the presence of serpin-3, less HP8 zymogen was converted to active HP8. This suggests that serpin-3 may inhibit activation of HP8. In mixtures containing exogenous serpin-3, two bands corresponding to the serpin-3-HP8 complex observed are likely due to differences in glycosylation. Serpin-3 in plasma undergoes post-translational modification (N-linked glycosylation) while serpin-3 expressed in *E. coli* does not.

HP6 activates HP8 to stimulate the production of antimicrobial peptides (An et al., 2009; An et al., 2010b). Knowing this and discovering that serpin-3 inhibits HP8, I hypothesized that serpin-3 may be a biologically relevant inhibitor of HP8 and could regulate Spätzle activation. If my hypothesis was correct, serpin-3 should inhibit HP8, and a decrease in antibacterial activity should be observed. However, there was no difference in antibacterial activity in plasma samples from insects with or without injected recombinant serpin-3 (Figure 3-14, panels A/B). One possible explanation is that serpin-3 inhibited HP8, but additional unknown proteinases with redundant function in antimicrobial production were activated and are not regulated by serpin-3. Another possibility is that serpin-3 is not an efficient inhibitor of HP8 (i.e. stoichiometry of inhibition is high), but this remains to be tested. I observed that plasma samples from larvae injected with serpin-3 did not melanized, whereas plasma from control larvae melanized within a few hours (Figure 3-14C). This *in vivo* result confirms that serpin-3 is an efficient regulator of melanization through its inhibition of prophenoloxidase-activating proteinases (Zhu et al., 2003b). Taken together, the results of these experiments indicate that serpin-3 plays a significant role in the inhibition of prophenoloxidase activation, but do not indicate that inhibition of HP8 by serpin-3 regulates the production of antimicrobial peptides.

Bacterial challenge stimulates the formation of serpin-proteinase complexes in plasma

Serine proteinase cascade pathways are involved in innate immune responses of vertebrates and invertebrates, and promote rapid, non-specific responses to infection and wounding (Krem and Di Cera, 2002; Kanost and Clarke, 2005; Cerenius et al., 2010). After active proteinases perform their functions, they are inactivated by serpins to prevent damage to the organism (Silverman et al., 2001; Gettins, 2002). In insects, serpins have a role in regulating serine proteinases involved in the Toll pathway (Levashina et al., 1999; Zou and Jiang, 2005; Shin et al., 2006; Ahmad et al., 2009; Jiang et al., 2009; An and Kanost, 2010; An et al., 2011; Park et al., 2011). Regulation of prophenoloxidase activation by serpins, including two orthologs to *M. sexta* serpin-3 (*Drosophila* serpin-27A (De Gregorio et al., 2002; Ligoxygakis et al., 2002) and *Anopheles gambiae* serpin-2 (An et al., 2010a)), in insects has also been observed (Jiang et al., 2003; Zhu et al., 2003b; Wang and Jiang, 2004; Abraham et al., 2005; Tong and Kanost, 2005; Tong et al., 2005; Zou and Jiang, 2005; Michel et al., 2006; Wang and Jiang, 2006; Scherfer et al., 2008; Tang et al., 2008; Jiang et al., 2009; An and Kanost, 2010; Zou et al., 2010; Park et al., 2011).

Synthesis and hemolymph concentration of many immune related proteins increase after injection of bacteria into larvae 24 h prior to hemolymph collection (Kanost et al., 2004). The incubation of plasma with bacteria after collection stimulates activation of hemolymph proteinases that interact with each other and are inhibited by serpins (Kanost, 2007; Ragan et al., 2009). Inhibition of a proteinase by a serpin is characterized by cleavage of the serpin, resulting in the formation of an SDS-stable serpin-proteinase complex. In this study, serpin-proteinase complexes were detected with serpin-3, HP8, PAP-1, and PAP-3 antibodies, suggesting that the hemolymph proteinases were activated by bacterial challenge and then interacted with serpins to form a stable serpin-proteinase complex (Figure 3-1).

In previous studies, PAP-3 was inhibited by serpin-1J (Jiang et al., 2003), serpin-3 (Zhu et al., 2003b), and serpin-6 (Wang and Jiang, 2004; Zou and Jiang, 2005) to regulate prophenoloxidase activation, indicating that key proteinases in a serine proteinase cascade may be regulated by multiple serpins (Zou and Jiang, 2005). This also suggests that the serpin-PAP-3 complex detected by immunoblot, in the current study, could represent PAP-3 with any one of these serpins. In addition, serpin-3 inhibited PAP-1 (Zhu et al., 2003b), suggesting that serpin-3

may inhibit more than one proteinase. Detection of two bands (~70 kDa) by serpin-3 antibody in this study further supports inhibition of multiple proteinases by one serpin.

Future Directions

Two-dimensional SDS-PAGE, ESI-MS/MS, and immunoblot analysis strategies used to identify serpin-3-proteinase complexes in the the hemolymph of *M. sexta* confirmed serpin-3-PAP-1 and serpin-3-PAP-3 complexes identified in previous studies and identified a previously undiscovered complex between serpin-3 and HP8. The next step in understanding the inhibitor relationship between serpin-3 and HP8 is to investigate the inhibitory activity of serpin-3 against HP8 by biochemical experiments using purified recombinant proteins. Specific goals and questions to be answered are as follows:

(1) There is a need for a substantially improved expression system to produce recombinant HP8-Xa.
(2) What is the stoichiometry of inhibition?
(3) What is the association rate constant of inhibition for HP8?

When producing recombinant proteinases, including HP8-Xa, the goal is to obtain protein of expected size and of high purity. Although recombinant HP8-Xa was successfully purified from *Drosophila* S2 cells, analysis by SDS-PAGE followed by immunoblot indicated that two forms of HP8-Xa were present, a full-length (42 kDa) and truncated protein (37 kDa) in approximately equal amounts (Figure 3-11). Previous analysis of the 37 kDa band by Edman degradation revealed that HP8-Xa had been cleaved after Arg^{59} (An et al., 2010b). Therefore, to use HP8-Xa in future experiments, the search for a new expression system has started, with the goal to find an expression system that will not result in truncated HP8-Xa and will produce a usable amount of highly pure protein.

Efficiency of the inhibition of HP8 by serpin-3 will be characterized by deterimining the stoichiometry of inhibition and the association rate constant of inhibition of HP8. The stoichiometry of inhibition indicates if the serpin is acting as an inhibitor or substrate. Strong inhibitors exhibit a stoichiometry of inhibition close to one, while serpins acting as substrates have a stoichiometry of inhibition greater than one (Schick et al., 1997) in which the predominant reaction is cleavage of the serpin reactive center loop without formation of a stable

complex and inhibition of the proteinase. The association rate constant will indicate how fast complex formation occurs between serpin-3 and HP8 (Schick et al., 1997). If complex formation between serpin-3 and HP8 occurs quickly, the association rate constant should be large. Results obtained from these two experiments will further indicate if serpin-3 is a relevant inhibitor of HP8.

Acknowledgements

I would like to thank Rebekah Woolsey from the Nevada Proteomics Center for sample digestion and MALDI-TOF/TOF. The Nevada Proteomics Center is supported by NIH Grant Number P20 RR-016464 from the INBRE Program of the National Center for Research Resources. I also thank Yasuaki Hiromasa from the Biotechnology Core/Proteomics Facility at Kansas State University for ESI-MS/MS. This work was supported by NIH Grant GM41247.

References

Abraham EG, Pinto SB, Ghosh A, Vanlandingham DL, Budd A, Higgs S, Kafatos FC, Jacobs-Lorena M, & Michel K (2005) An immune-responsive serpin, SRPN6, mediates mosquito defense against malaria parasites. *Proc Natl Acad Sci USA* **102**: 16327-16332

Ahmad ST, Sweeney ST, Lee JA, Sweeney NT, & Gao FB (2009) Genetic screen identifies serpin5 as a regulator of the toll pathway and CHMP2B toxicity associated with frontotemporal dementia. *Proc Natl Acad Sci USA* **106**: 12168-12173

An C, Budd A, Kanost MR, & Michel K (2010a) Characterization of a regulatory unit that controls melanization and affects longevity of mosquitoes. *Cell Mol Life Sci*, doi: 10.1007/s00018-010-0543-z

An C, Ishibashi J, Ragan EJ, Jiang H, & Kanost MR (2009) Functions of *Manduca sexta* hemolymph proteinases HP6 and HP8 in two innate immune pathways. *J Biol Chem* **284**: 19716-19726

An C, Jiang H, & Kanost MR (2010b) Proteolytic activation and function of the cytokine Spätzle in the innate immune response of a lepidopteran insect, *Manduca sexta*. *FEBS J* **277**: 148-162

An C & Kanost MR (2010) *Manduca sexta* serpin-5 regulates prophenoloxidase activation and the Toll signaling pathway by inhibiting hemolymph proteinase HP6. *Insect Biochem Mol Biol* **40**: 683-689

An C, Ragan EJ, & Kanost MR (2011) Serpin-1 splicing isoform J inhibits the proSpätzle-activating proteinase HP8 to regulate expression of antimicrobial hemolymph proteins in *Manduca sexta*. *Dev Comp Immunol* **35**: 135-141

Axén A, Carlsson A, Engström A, & Bennich H (1997) Gloverin, an antibacterial protein from the immune hemolymph of *Hyalophora* pupae. *Eur J Biochem* **247**: 614-619

Burgess-Cassler A, Johansen JJ, Santek DA, Ide JR, & Kendrick NC (1989) Computerized quantitative analysis of coomassie-blue-stained serum proteins separated by two-dimensional electrophoresis. *Clin Chem* **35**: 2297-2304

Cai T, Yu P, Monga SP, Mishra B, & Mishra L (1998) Identification of mouse itih-4 encoding a glycoprotein with two EF-hand motifs from early embryonic liver. *Biochim Biophys Acta* **1398**: 32-37

Campos IT, Tanaka-Azevedo AM, & Tanaka AS (2004) Identification and characterization of a novel factor XIIa inhibitor in the hematophagous insect, *Triatoma infestans* (Hemiptera: Reduviidae). *FEBS Lett* **577**: 512-516

Carlsson A, Engström P, Palva ET, & Bennich H (1991) Attacin, an antibacterial protein from *Hyalophora cecropia*, inhibits synthesis of outer membrane proteins in *Escherichia coli* by interfering with *omp* gene transcription. *Infect Immun* **59**: 3040-3045

Cerenius L, Kawabata S, Lee BL, Nonaka M, & Söderhäll K (2010) Proteolytic cascades and their involvement in invertebrate immunity. *Trends Biochem Sci* **35**: 575-583

De Gregorio E, Han SJ, Lee WJ, Baek MJ, Osaki T, Kawabata S, Lee BL, Iwanaga S, Lemaitre B, & Brey PT (2002) An immune-responsive serpin regulates the melanization cascade in *Drosophila*. *Dev Cell* **3**: 581-592

Dunn PE & Drake D (1983) Fate of bacteria injected into naive and immunized larvae of the tobacco hornworm, *Manduca sexta*. *J Invertebr Pathol* **41**: 77-85

Engström P, Carlsson A, Engström A, Tao ZJ, & Bennich H (1984) The antibacterial effect of attacins from the silk moth *Hyalophora cecropia* is directed against the outer membrane of *Escherichia coli*. *EMBO J* **3**: 3347-3351

Friedrich T, Kröger B, Bialojan S, Lemaire HG, Höffken HW, Reuschenbach P, Otte M, & Dodt J (1993) A Kazal-type inhibitor with thrombin specificity from *Rhodnius prolixus*. *J Biol Chem* **268**: 16216-16222

Gettins PG (2002) Serpin structure, mechanism, and function. *Chem Rev* **102**: 4751-4804

Ji C, Wang Y, Guo X, Hartson S, & Jiang H (2004) A pattern recognition serine proteinase triggers the prophenoloxidase activation cascade in the tobacco hornworm, *Manduca sexta*. *J Biol Chem* **279**: 34101-34106

Ji C, Wang Y, Ross J, & Jiang H (2003) Expression and in vitro activation of *Manduca sexta* prophenoloxidase-activating proteinase-2 precursor (proPAP-2) from baculovirus-infected insect cells. *Protein Expr Purif* **29**: 235-243

Jiang H & Kanost MR (1997) Characterization and functional analysis of 12 naturally occurring reactive site variants of serpin-1 from *Manduca sexta*. *J Biol Chem* **272**: 1082-1087

Jiang H, Wang Y, Gu Y, Guo X, Zou Z, Scholz F, Trenczek TE, & Kanost MR (2005) Molecular identification of a bevy of serine proteinases in *Manduca sexta* hemolymph. *Insect Biochem Mol Biol* **35**: 931-943

Jiang H, Wang Y, & Kanost MR (1994) Mutually exclusive exon use and reactive center diversity in insect serpins. *J Biol Chem* **269**: 55-58

Jiang H, Wang Y, Yu XQ, Zhu Y, & Kanost M (2003) Prophenoloxidase-activating proteinase-3 (PAP-3) from *Manduca sexta* hemolymph: a clip-domain serine proteinase regulated by serpin-1J and serine proteinase homologs. *Insect Biochem Mol Biol* **33**: 1049-1060

Jiang R, Kim EH, Gong JH, Kwon HM, Kim CH, Ryu KH, Park JW, Kurokawa K, Zhang J, Gubb D, & Lee BL (2009) Three pairs of protease-serpin complexes cooperatively regulate the insect innate immune responses. *J Biol Chem* **284**: 35652-35658

Jiravanichpaisal P, Lee BL, & Söderhäll K (2006) Cell-mediated immunity in arthropods: hematopoiesis, coagulation, melanization and opsonization. *Immunobiology* **211**: 213-236

Johansson MW, Keyser P, & Söderhäll K (1994) Purification and cDNA cloning of a four-domain Kazal proteinase inhibitor from crayfish blood cells. *Eur J Biochem* **223**: 389-394

Kanost MR (2007) Serpins in a lepidopteran insect, *Manduca sexta*. In *The Serpinopathies: Molecular and Cellular Aspects of Serpins and their Disorders,* Silverman GA & Lomas DA (eds) pp 229-242. World Scientific Publishing Co.: Hackensack, NJ

Kanost MR & Clarke T (2005) Proteases. In *Comprehensive Molecular Insect Science,* Gilbert LI, Iatrou K, Gill SS (eds) pp 247-265. Elsevier

Kanost MR, Jiang H, & Yu XQ (2004) Innate immune responses of a lepidopteran insect, *Manduca sexta*. *Immunol Rev* **198**: 97-105

Kanost MR, Kawooya JK, Law JH, Ryan RO, Van Heusden MC, Ziegler R (1990) Insect haemolymph proteins. In *Advances in Insect Physiology,* Evans PD & Wigglesworth VB (eds) pp 299-396. Academic Press: San Diego

Krem MM & Di Cera E (2002) Evolution of enzyme cascades from embryonic development to blood coagulation. *Trends Biochem Sci* **27**: 67-74

Lavine MD & Strand MR (2002) Insect hemocytes and their role in immunity. *Insect Biochem Mol Biol* **32**: 1295-1309

Levashina EA, Langley E, Green C, Gubb D, Ashburner M, Hoffmann JA, & Reichhart JM (1999) Constitutive activation of toll-mediated antifungal defense in serpin-deficient *Drosophila*. *Science* **285**: 1917-1919

Ligoxygakis P, Pelte N, Ji C, Leclerc V, Duvic B, Belvin M, Jiang H, Hoffmann JA, & Reichhart JM (2002) A serpin mutant links Toll activation to melanization in the host defence of *Drosophila*. *EMBO J* **21**: 6330-6337

Marmaras VJ & Lampropoulou M (2009) Regulators and signalling in insect haemocyte immunity. *Cell Signal* **21**: 186-195

Michel K, Suwanchaichinda C, Morlais I, Lambrechts L, Cohuet A, Awono-Ambene PH, Simard F, Fontenille D, Kanost MR, & Kafatos FC (2006) Increased melanizing activity in *Anopheles gambiae* does not affect development of *Plasmodium falciparum*. *Proc Natl Acad Sci USA* **103**: 16858-16863

Niimi T, Yokoyama H, Goto A, Beck K, & Kitagawa Y (1999) A *Drosophila* gene encoding multiple splice variants of Kazal-type serine protease inhibitor-like proteins with potential destinations of mitochondria, cytosol and the secretory pathway. *Eur J Biochem* **266**: 282-292

Nirmala X, Kodrik D, Zurovec M, & Sehnal F (2001) Insect silk contains both a Kunitz-type and a unique Kazal-type proteinase inhibitor. *Eur J Biochem* **268**: 2064-2073

O'Farrell PH (1975) High resolution two-dimensional electrophoresis of proteins. *J Biol Chem* **250**: 4007-4021

Packer NH, WIlkins MR, Golaz O, Lawson MA, Gooley AA, Hochstrasser DF, Redmond JW, & Williams KL (1996) Characterization of human plasma glycoproteins separated by two-dimensional gel electrophoresis. *Biotechnology (NY)* **14**: 66-70

Park SH, Jiang R, Piao S, Zhang B, Kim EH, Kwon HM, Jin XL, Lee BL, & Ha NC (2011) Structural and functional characterization of a highly specific serpin in the insect innate immunity. *J Biol Chem* **286**: 1567-1575

Ragan EJ, An C, Jiang H, Kanost MR (2009) Roles of haemolymph proteins in antimicrobial defences of *Manduca sexta*. In *Insect Infection and Immunity,* Rolff J & Reynolds SE (eds) pp 34-48. Oxford University Press

Ragan EJ, An C, Yang CT, & Kanost MR (2010) Analysis of mutually exclusive alternatively spliced serpin-1 isoforms and identification of serpin-1 proteinase complexes in *Manduca sexta* hemolymph. *J Biol Chem* **285**: 29642-29650

Rimphanitchayakit V & Tassanakajon A (2010) Structure and function of invertebrate Kazal-type serine proteinase inhibitors. *Dev Comp Immunol* **34**: 377-386

Ryan RO & van der Horst DJ (2000) Lipid transport biochemistry and its role in energy production. *Annu Rev Entomol* **45**: 233-260

Rosenfeld J, Capdevielle J, Guillemot JC, & Ferrara P (1992) In-gel digestion of proteins for internal sequence analysis after one- or two-dimensional gel electrophoresis. *Anal Biochem* **203**: 173-179

Salier JP (1990) Inter-alpha-trypsin inhibitor: emergence of a family within the Kunitz-type protease inhibitor superfamily. *Trends Biochem Sci* **15**: 435-439

Salier JP, Rouet P, Raguenez G, & Daveau M (1996) The inter-alpha-inhibitor family: from structure to regulation. *Biochem J* **315 (Pt 1)**: 1-9

Scherfer C, Tang H, Kambris Z, Lhocine N, Hashimoto C, & Lemaitre B (2008) *Drosophila* Serpin-28D regulates hemolymph phenoloxidase activity and adult pigmentation. *Dev Biol* **323**: 189-196

Schick C, Kamachi Y, Bartuski AJ, Cataltepe S, Schechter NM, Pemberton PA, & Silverman GA (1997) Squamous cell carcinoma antigen 2 is a novel serpin that inhibits the chymotrypsin-like proteinases cathepsin G and mast cell chymase. *J Biol Chem* **272**: 1849-1855

Schulze AJ, Huber R, Bode W, & Engh RA (1994) Structural aspects of serpin inhibition. *FEBS Lett* **344**: 117-124

Shin SW, Bian G, & Raikhel AS (2006) A toll receptor and a cytokine, Toll5A and Spz1C, are involved in toll antifungal immune signaling in the mosquito *Aedes aegypti*. *J Biol Chem* **281**: 39388-39395

Silverman GA, Bird PI, Carrell RW, Church FC, Coughlin PB, Gettins PG, Irving JA, Lomas DA, Luke CJ, Moyer RW, Pemberton PA, Remold-O'Donnell E, Salvesen GS, Travis J, & Whisstock JC (2001) The serpins are an expanding superfamily of structurally similar but functionally diverse proteins. Evolution, mechanism of inhibition, novel functions, and a revised nomenclature. *J Biol Chem* **276**: 33293-33296

Somprasong N, Rimphanitchayakit V, & Tassanakajon A (2006) A five-domain Kazal-type serine proteinase inhibitor from black tiger shrimp *Penaeus monodon* and its inhibitory activities. *Dev Comp Immunol* **30**: 998-1008

Tang H, Kambris Z, Lemaitre B, & Hashimoto C (2008) A serpin that regulates immune melanization in the respiratory system of *Drosophila*. *Dev Cell* **15**: 617-626

Tong Y, Jiang H, & Kanost MR (2005) Identification of plasma proteases inhibited by *Manduca sexta* serpin-4 and serpin-5 and their association with components of the prophenol oxidase activation pathway. *J Biol Chem* **280**: 14932-14942

Tong Y & Kanost MR (2005) *Manduca sexta* serpin-4 and serpin-5 inhibit the prophenol oxidase activation pathway: cDNA cloning, protein expression, and characterization. *J Biol Chem* **280**: 14923-14931

Wang Y & Jiang H (2010) Binding properties of the regulatory domains in *Manduca sexta* hemolymph proteinase-14, an initiation enzyme of the prophenoloxidase activation system. *Dev Comp Immunol* **34**: 316-322

Wang Y & Jiang H (2007) Reconstitution of a branch of the *Manduca sexta* prophenoloxidase activation cascade in vitro: snake-like hemolymph proteinase 21 (HP21) cleaved by HP14 activates prophenoloxidase-activating proteinase-2 precursor. *Insect Biochem Mol Biol* **37**: 1015-1025

Wang Y & Jiang H (2006) Interaction of beta-1,3-glucan with its recognition protein activates hemolymph proteinase 14, an initiation enzyme of the prophenoloxidase activation system in *Manduca sexta*. *J Biol Chem* **281**: 9271-9278

Wang Y & Jiang H (2004) Purification and characterization of *Manduca sexta* serpin-6: a serine proteinase inhibitor that selectively inhibits prophenoloxidase-activating proteinase-3. *Insect Biochem Mol Biol* **34**: 387-395

Wang Y, Jiang H, & Kanost MR (2001) Expression and purification of *Manduca sexta* prophenoloxidase-activating proteinase precursor (proPAP) from baculovirus-infected insect cells. *Protein Expr Purif* **23**: 328-337

Wang Y, Sumathipala N, Rayaprolu S, & Jiang H (2011) Recognition of microbial molecular patterns and stimulation of prophenoloxidase activation by a beta-1,3-glucanase-related protein in *Manduca sexta* larval plasma. *Insect Biochem Mol Biol* **41**: 322-331

Wang Y, Zou Z, & Jiang H (2006) An expansion of the dual clip-domain serine proteinase family in *Manduca sexta*: gene organization, expression, and evolution of prophenoloxidase-activating proteinase-2, hemolymph proteinase 12, and other related proteinases. *Genomics* **87**: 399-409

Watanabe RM, Soares TS, Morais-Zani K, Tanaka-Azevedo AM, Maciel C, Capurro ML, Torquato RJ, & Tanaka AS (2010) A novel trypsin Kazal-type inhibitor from *Aedes aegypti* with thrombin coagulant inhibitory activity. *Biochimie* **92**: 933-939

Wright HT (1996) The structural puzzle of how serpin serine proteinase inhibitors work. *Bioessays* **18**: 453-464

Yu XQ, Jiang H, Wang Y, & Kanost MR (2003) Nonproteolytic serine proteinase homologs are involved in prophenoloxidase activation in the tobacco hornworm, *Manduca sexta*. *Insect Biochem Mol Biol* **33**: 197-208

Yu X & Kanost MR (2008) Activation of lepidopteran insect innate immune responses by C-type immulectins. In *Animal lectins: A functional view,* Ahmed HA & Vasta GR (eds) pp 383-395. CRC Press: Boca Raton

Yu XQ & Kanost MR (2000) Immulectin-2, a lipopolysaccharide-specific lectin from an insect, *Manduca sexta,* is induced in response to gram-negative bacteria. *J Biol Chem* **275**: 37373-37381

Zhang S, Gunaratna RT, Zhang X, Najar F, Wang Y, Roe B, & Jiang H (2011) Pyrosequencing-based expression profiling and identification of differentially regulated genes from *Manduca sexta*, A lepidopteran model insect. *Insect Biochem Mol Biol*, doi:10.1016/j.ibmb.2011.05.005

Zheng QL, Chen J, Nie ZM, Lv ZB, Wang D, & Zhang YZ (2007) Expression, purification and characterization of a three-domain Kazal-type inhibitor from silkworm pupae (*Bombyx mori*). *Comp Biochem Physiol B Biochem Mol Biol* **146**: 234-240

Zhu Y, Johnson TJ, Myers AA, & Kanost MR (2003a) Identification by subtractive suppression hybridization of bacteria-induced genes expressed in *Manduca sexta* fat body. *Insect Biochem Mol Biol* **33**: 541-559

Zhu Y, Wang Y, Gorman MJ, Jiang H, & Kanost MR (2003b) *Manduca sexta* serpin-3 regulates prophenoloxidase activation in response to infection by inhibiting prophenoloxidase-activating proteinases. *J Biol Chem* **278**: 46556-46564

Zou Z & Jiang H (2005) *Manduca sexta* serpin-6 regulates immune serine proteinases PAP-3 and HP8. cDNA cloning, protein expression, inhibition kinetics, and function elucidation. *J Biol Chem* **280**: 14341-14348

Zou Z, Najar F, Wang Y, Roe B, & Jiang H (2008) Pyrosequence analysis of expressed sequence tags for *Manduca sexta* hemolymph proteins involved in immune responses. *Insect Biochem Mol Biol* **38**: 677-682

Zou Z, Shin SW, Alvarez KS, Kokoza V, & Raikhel AS (2010) Distinct melanization pathways in the mosquito *Aedes aegypti*. *Immunity* **32**: 41-53

Figures

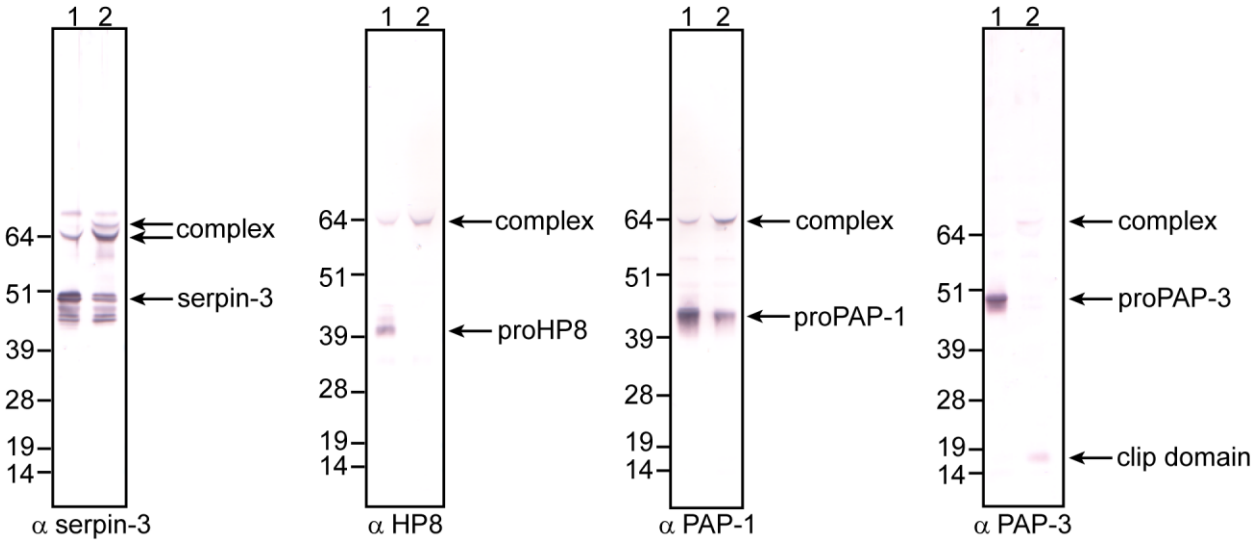

Figure 3-1. Treatment of plasma with bacteria promotes formation of serpin-proteinase complexes.

Plasma (8 µL) obtained from larvae 24 h post-injection of *M. luteus* (100 µg) was incubated with 2 µL of filter-sterilized water (lane 1) or 2 µL *M. luteus* (lane 2; final concentration = 0.1 µg/µL) for 1 h at room temperature. Samples were prepared so that an equivalent of 1 µL of plasma was loaded in each lane and were subjected to SDS-PAGE under reducing conditions followed by immunoblot analysis with antibodies to serpin-3, HP8, PAP-1, or PAP-3. Antibodies were used at a 1:2000 dilution except for PAP-3, which was used at a 1:750 dilution.

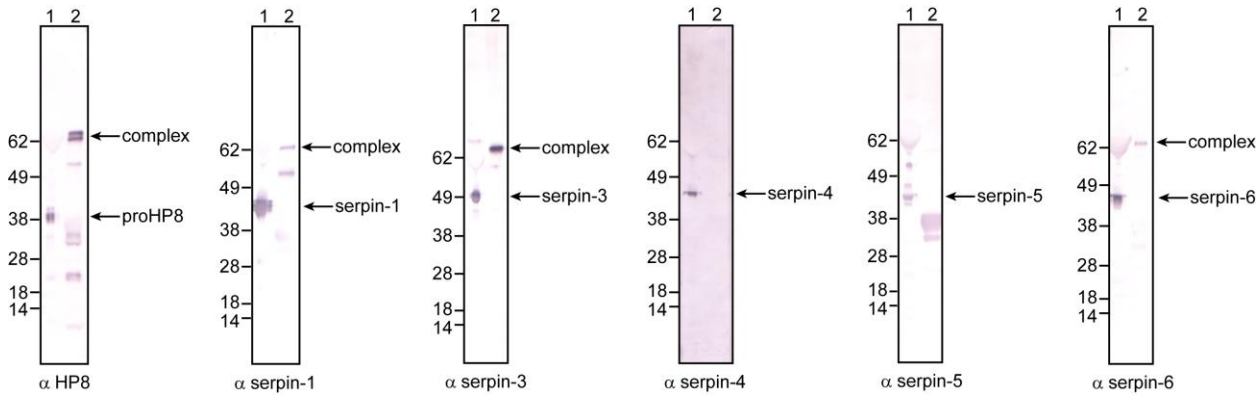

Figure 3-2. Complex formation between HP8 and serpin-1, serpin-3, and serpin-6 in plasma.

Naïve plasma (lane 1) and a sample of plasma proteins that bound to a HP8 antibody affinity column (lane 2) were subjected to SDS-PAGE under reducing conditions followed by immunoblot analysis with HP8, serpin-1, serpin-3, serpin-4, serpin-5, or serpin-6 antibodies. Work by Dr. Chunju An.

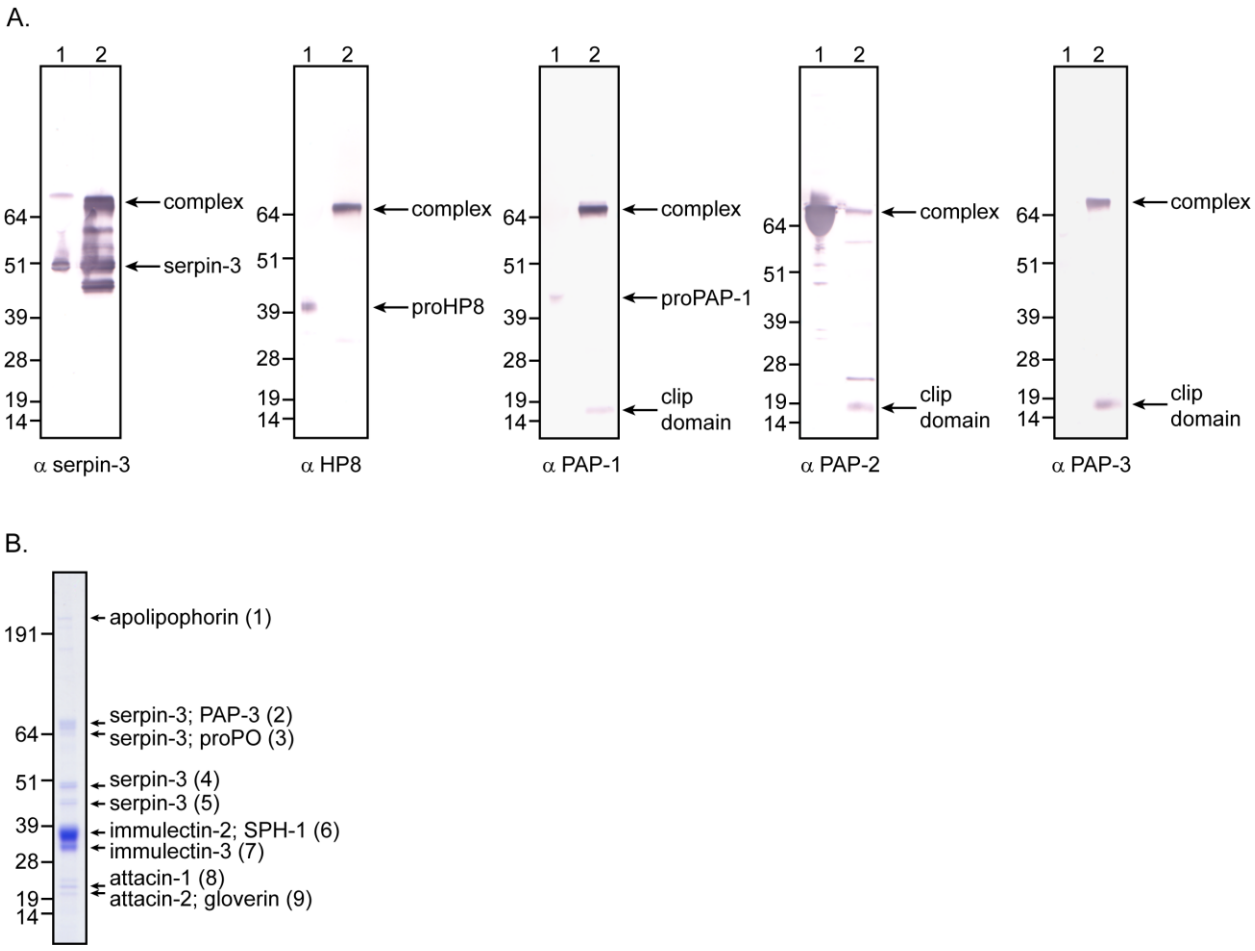

Figure 3-3. Complex formation between serpin-3 and HP8, PAP-1, PAP-2, and PAP-3 in plasma.

Fifth-instar, day 3 naïve plasma (lane 1) and a sample of plasma proteins that bound to a serpin-3 antibody affinity column (lane 2) were subjected to SDS-PAGE under reducing conditions followed by immunoblot analysis with serpin-3, HP8, PAP-1, PAP-2, and PAP-3 antibodies (A) and Coomassie Blue staining (B). Coomassie Blue stained bands were excised for trypsin digestion followed by MALDI-TOF and MALDI-TOF/TOF mass spectrometry analysis. Numbers in parentheses correspond to the band number in Table 3-1.

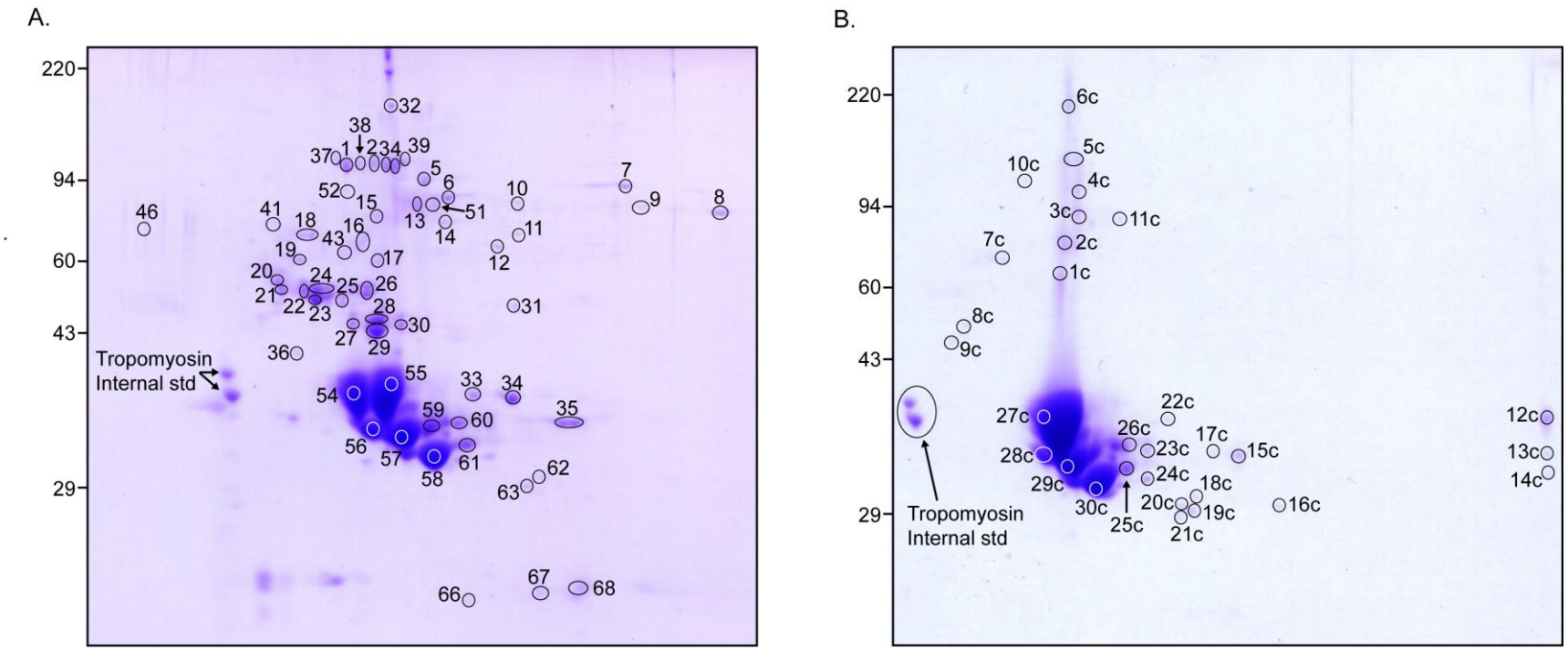

Figure 3-4. Serpin-3 forms a covalent complex with HP8, PAP-1, and PAP-3 in plasma.

A sample of plasma proteins that bound to a serpin-3 antibody-coupled immunoaffinity column (A) and a control column of Protein-A Sepharose CL-4B beads without antibody (B) was separated by two-dimensional gel electrophoresis, using a pH range of 3.5-10 for isoelectric focusing (tropomyosin: pI = 5.2) and a 10% acrylamide slab gel for molecular weight separation. Numbers indicate selected Coomassie Blue stained spots that were subjected to trypsin digestion followed by ESI-MS/MS mass spectrometry (Tables 3-2, 3-3, 3-4, 3-5). Spots 22-26 contain unprocessed serpin-3. Spot 1 contains serpin-3 and HP8, spots 2, 3, 4, and 39 contain serpin-3 and PAP-3, spot 5 contains serpin-3 and PAP-1. Spots 37 and 38 contain serpin-3, but no peptides for known *M. sexta* proteinases.

Serpin 3

1 *MTSTIYFAFF VAPLLLCSLA* DDVDPNTLRA VFGYSALDQA ALVGAESNKQ
51 AATVTPDNGT LVDPDYWDTE EFQPSTADYD IFDWVLTKRV ASTSNANFLL
101 SPLGLKLALA ILTEAATGST RSELASALGF GLDRTEVRRK FSTIIESLKR
151 ESPDYILNLG SRIYMGEGVQ PRQRFAAIAQ EFYKTELKTT NFFKPEVAAR
201 EINNWVSNAT QGKIPNLVEA DDVADVILLI LNTLYFKGTW RHQFAPNATK
251 PGPFYVSPQL QKTVPFMNVK DNFYYVDSSR FDAKILRLPY RGNKYAMYIV
301 VPNSLTGLPR VLNNLSELRT EMIYLQERLV DVILPKFQFE YMSRLEGVLR
351 EMGVREAFED TASFPGIARG QLLYQRLRVS KVFQRTGIEV NELGSVAFSA
401 TQIGIQN**K**FG EDSDINYEVV ANKPFMFFIQ EESTRQTLFT GRVSDPALVD
451 GAFKA

Hemolymph proteinase 8

1 *MNILYVKTTV VTCILVITFS NVVG*QSCNGG ADCIALDKCS GLYRQLQKGS
51 TPALTRLLRS LHCGFENANM PKICCPPEFL AQRGAFGNDQ GSARENPLAL
101 LPNRRECGIQ NNDRIVGGIQ TEIDEHPWMV LLRYDKPSGW GFYCGGVLIS
151 SKYVLTAAHC VKGSDLPPNW KLSQVRLGEW NTSSQVDCVG DDCSQPVQDI
201 RIEQIVAHES YDPEDNNQQN DIALLRLAQN VHLNDFVKPI CLPTTEDLRD
251 SNFDGLEMEV AGWGKTETRT ESDVKLKVRV PVVSRRLCKS VYERVERLIT
301 DKQLCAGGVE GKDSCRGDSG GALMGQAPSA NNWLVVGVVS YGPSPCGTPG
351 WPGVYTRVGA FMDWILSKLR P

Figure 3-5. Complex spot 1 contains serpin-3 and hemolymph proteinase 8.

Sequence coverage of serpin-3 and hemolymph proteinase 8 from spot 1 (Figure 3-4A). Tryptic peptides identified by mass spectrometry are shown in red letters. The serpin-3 P1 residue is bold and underlined and the activation site of hemolymph proteinase 8 is highlighted in cyan. Signal peptides of each protein are italicized.

Serpin 3

1 *MTSTIYFAFF VAPLLLCSLA* DDVDPNTLRA VFGYSALDQA ALVGAESNKQ
51 AATVTPDNGT LVDPDYWDTE EFQPSTADYD IFDWVLTKRV ASTSNANFLL
101 SPLGLKLALA ILTEAATGST RSELASALGF GLDRTEVRRK FSTIIESLKR
151 ESPDYILNLG SRIYMGEGVQ PRQRFAAIAQ EFYKTELKTT NFFKPEVAAR
201 EINNWVSNAT QGKIPNLVEA DDVADVILLI LNTLYFKGTW RHQFAPNATK
251 PGPFYVSPQL QKTVPFMNVK DNFYYVDSSR FDAKILRLPY RGNKYAMYIV
301 VPNSLTGLPR VLNNLSELRT EMIYLQERLV DVILPKFQFE YMSRLEGVLR
351 EMGVREAFED TASFPGIARG QLLYQRLRVS KVFQRTGIEV NELGSVAFSA
401 TQIGIQN**K**FG EDSDINYEVV ANKPFMFFIQ EESTRQTLFT GRVSDPALVD
451 GAFKA

Prophenoloxidase-activating proteinase-3

1 *MANLVYVLLL ASYFCFVSGQ* SCTTPNNGKG TCKSIYECEE LLKLVYKKDR
51 TQQDTDYLKK SQCGFMGNTP TVCCPNPCIT PQGEPGQCVS IYECTNLANL
101 LKPPITADTY NYVQKSRCQG ADQYSVCCGS APNFPSTGDC KASVSAFPPD
151 PKSKCCGVDS RVGNKIIGGN ATDVDQYPWL TIIEYVKTGP IKLLCGGVLI
201 SGKYVLTAGH CLTGPVLQIG TPTNVRLGEY NTKNDGADCV TVEAGGMDCT
251 EGAVIVPIEK TIPHPEYNPI SRTRRNDIGL IRLKEMAPFT DFIRPICLPS
301 LDLTQAPPVN FTLYAAGWGA VSTSQPSSNV KLHVQLPFIS YERCQPSYAV
351 QNRQIELWEK QVCAGGEAGK DSCKGDSGGP LMYENGQTYE VIGIVSFGPT
401 PCGMQDIPGV YTKVHSYKDW IISNIKP

Figure 3-6. Complex spot 2 contains serpin-3 and prophenoloxidase-activating proteinase-3.

Sequence coverage of serpin-3 and prophenoloxidase-activating proteinase-3 from spot 2 (Figure 3-4A). Tryptic peptides identified by mass spectrometry are shown in red letters. The P1 residue of serpin-3 is bold and underlined and the activation site of prophenoloxidase-activating proteinase-3 is highlighted in cyan. Signal peptides for both proteins are italicized.

Serpin 3

1 *MTSTIYFAFF VAPLLLCSLA* DDVDPNTLRA VFGYSALDQA ALVGAESNKQ
51 AATVTPDNGT LVDPDYWDTE EFQPSTADYD IFDWVLTKRV ASTSNANFLL
101 SPLGLKLALA ILTEAATGST RSELASALGF GLDRTEVRRK FSTIIESLKR
151 ESPDYILNLG SRIYMGEGVQ PRQRFAAIAQ EFYKTELKTT NFFKPEVAAR
201 EINNWVSNAT QGKIPNLVEA DDVADVILLI LNTLYFKGTW RHQFAPNATK
251 PGPFYVSPQL QKTVPFMNVK DNFYYVDSSR FDAKILRLPY RGNKYAMYIV
301 VPNSLTGLPR VLNNLSELRT EMIYLQERLV DVILPKFQFE YMSRLEGVLR
351 EMGVREAFED TASFPGIARG QLLYQRLRVS KVFQRTGIEV NELGSVAFSA
401 TQIGIQN**K**FG EDSDINYEVV ANKPFMFFIQ EESTRQTLFT GRVSDPALVD
451 GAFKA

Prophenoloxidase-activating proteinase-3

1 *MANLVYVLLL ASYFCFVSGQ* SCTTPNNGKG TCKSIYECEE LLKLVYKKDR
51 TQQDTDYLKK SQCGFMGNTP TVCCPNPCIT PQGEPGQCVS IYECTNLANL
101 LKPPITADTY NYVQKSRCQG ADQYSVCCGS APNFPSTGDC KASVSAFPPD
151 PKSKCCGVDS RVGNKIIGGN ATDVDQYPWL TIIEYVKTGP IKLLCGGVLI
201 SGKYVLTAGH CLTGPVLQIG TPTNVRLGEY NTKNDGADCV TVEAGGMDCT
251 EGAVIVPIEK TIPHPEYNPI SRTRRNDIGL IRLKEMAPFT DFIRPICLPS
301 LDLTQAPPVN FTLYAAGWGA VSTSQPSSNV KLHVQLPFIS YERCQPSYAV
351 QNRQIELWEK QVCAGGEAGK DSCKGDSGGP LMYENGQTYE VIGIVSFGPT
401 PCGMQDIPGV YTKVHSYKDW IISNIKP

Figure 3-7. Complex spot 3 contains serpin-3 and prophenoloxidase-activating proteinase-3.

Sequence coverage of serpin-3 and prophenoloxidase-activating proteinase-3 from spot 3 (Figure 3-4A). Tryptic peptides identified by mass spectrometry are shown in red letters. The P1 residue of serpin-3 is bold and underlined and the activation site of prophenoloxidase-activating proteinase-3 is highlighted in cyan. Signal peptides for both proteins are italicized.

Serpin 3

1 *MTSTIYFAFF VAPLLLCSLA* DDVDPNTLRA VFGYSALDQA ALVGAESNKQ
51 AATVTPDNGT LVDPDYWDTE EFQPSTADYD IFDWVLTKRV ASTSNANFLL
101 SPLGLKLALA ILTEAATGST RSELASALGF GLDRTEVRRK FSTIIESLKR
151 ESPDYILNLG SRIYMGEGVQ PRQRFAAIAQ EFYKTELKTT NFFKPEVAAR
201 EINNWVSNAT QGKIPNLVEA DDVADVILLI LNTLYFKGTW RHQFAPNATK
251 PGPFYVSPQL QKTVPFMNVK DNFYYVDSSR FDAKILRLPY RGNKYAMYIV
301 VPNSLTGLPR VLNNLSELRT EMIYLQERLV DVILPKFQFE YMSRLEGVLR
351 EMGVREAFED TASFPGIARG QLLYQRLRVS KVFQRTGIEV NELGSVAFSA
401 TQIGIQN**K**FG EDSDINYEVV ANKPFMFFIQ EESTRQTLFT GRVSDPALVD
451 GAFKA

Prophenoloxidase-activating proteinase-3

1 *MANLVYVLLL ASYFCFVSGQ* SCTTPNNGKG TCKSIYECEE LLKLVYKKDR
51 TQQDTDYLKK SQCGFMGNTP TVCCPNPCIT PQGEPGQCVS IYECTNLANL
101 LKPPITADTY NYVQKSRCQG ADQYSVCCGS APNFPSTGDC KASVSAFPPD
151 PKSKCCGVDS RVGNKIIGGN ATDVDQYPWL TIIEYVKTGP IKLLCGGVLI
201 SGKYVLTAGH CLTGPVLQIG TPTNVRLGEY NTKNDGADCV TVEAGGMDCT
251 EGAVIVPIEK TIPHPEYNPI SRTRRNDIGL IRLKEMAPFT DFIRPICLPS
301 LDLTQAPPVN FTLYAAGWGA VSTSQPSSNV KLHVQLPFIS YERCQPSYAV
351 QNRQIELWEK QVCAGGEAGK DSCKGDSGGP LMYENGQTYE VIGIVSFGPT
401 PCGMQDIPGV YTKVHSYKDW IISNIKP

Figure 3-8. Complex spot 4 contains serpin-3 and prophenoloxidase-activating proteinase-3.

Sequence coverage of serpin-3 and prophenoloxidase-activating proteinase-3 from spot 4 (Figure 3-4A). Tryptic peptides identified by mass spectrometry are shown in red letters. The P1 residue of serpin-3 is bold and underlined and the activation site of prophenoloxidase-activating proteinase-3 is highlighted in cyan. Signal peptides for both proteins are italicized.

Serpin 3

1 *MTSTIYFAFF VAPLLLCSLA* DDVDPNTLRA VFGYSALDQA ALVGAESNKQ
51 AATVTPDNGT LVDPDYWDTE EFQPSTADYD IFDWVLTKRV ASTSNANFLL
101 SPLGLKLALA ILTEAATGST RSELASALGF GLDRTEVRRK FSTIIESLKR
151 ESPDYILNLG SRIYMGEGVQ PRQRFAAIAQ EFYKTELKTT NFFKPEVAAR
201 EINNWVSNAT QGKIPNLVEA DDVADVILLI LNTLYFKGTW RHQFAPNATK
251 PGPFYVSPQL QKTVPFMNVK DNFYYVDSSR FDAKILRLPY RGNKYAMYIV
301 VPNSLTGLPR VLNNLSELRT EMIYLQERLV DVILPKFQFE YMSRLEGVLR
351 EMGVREAFED TASFPGIARG QLLYQRLRVS KVFQRTGIEV NELGSVAFSA
401 TQIGIQN**K**FG EDSDINYEVV ANKPFMFFIQ EESTRQTLFT GRVSDPALVD
451 GAFKA

Prophenoloxidase-activating proteinase-1

1 *MKNHTVFIVF AVYWTCVFSQ* SCTTPQGVDS NCISLYECPQ LLSAFEQRPL
51 PSPVVNYLRK SQCGFDGYTP RVCCGPLPQQ ASRPQPTPAP VPTRAPPVNP
101 GGVDPTYDED SSPAPRNQCG VDMNGDRIYG GQITDLDEFP WMALLGYLTR
151 TGSTTYQCGG VLINQRYVLT AAHCTIGAVE REVGKLITVR LGEYDTQNSV
201 DCVDDVCADP PQNIPIEVAY PHSGYSDNNK NRKDDIALVR LTRRAQYTYY
251 VKPICLANNN ERLATGNDVF VAGWGKTLSG KSSPIKLKLG MPIFDKSDCA
301 SKYRNLGAEL TDKQICAGGV FAKDTCRGDS GGPLMQRRPE GIWEVVGIVS
351 FGNRCGLDGW PGVYSSVAGY SDWILSTLRS TNV

Figure 3-9. Complex spot 5 contains serpin-3 and prophenoloxidase-activating proteinase-1.

Sequence coverage of serpin-3 and prophenoloxidase-activating proteinase-1 from spot 5 (Figure 3-4A). Tryptic peptides identified by mass spectrometry are shown in red letters. The P1 residue of serpin-3 is bold and underlined and the activation site of prophenoloxidase-activating proteinase-1 is highlighted in cyan. Signal peptides for both proteins are italicized.

Serpin 3

1 *MTSTIYFAFF VAPLLLCSLA* DDVDPNTLRA VFGYSALDQA ALVGAESNKQ
51 AATVTPDNGT LVDPDYWDTE EFQPSTADYD IFDWVLTKRV ASTSNANFLL
101 SPLGLKLALA ILTEAATGST RSELASALGF GLDRTEVRRK FSTIIESLKR
151 ESPDYILNLG SRIYMGEGVQ PRQRFAAIAQ EFYKTELKTT NFFKPEVAAR
201 EINNWVSNAT QGKIPNLVEA DDVADVILLI LNTLYFKGTW RHQFAPNATK
251 PGPFYVSPQL QKTVPFMNVK DNFYYVDSSR FDAKILRLPY RGNKYAMYIV
301 VPNSLTGLPR VLNNLSELRT EMIYLQERLV DVILPKFQFE YMSRLEGVLR
351 EMGVREAFED TASFPGIARG QLLYQRLRVS KVFQRTGIEV NELGSVAFSA
401 TQIGIQN**K**FG EDSDINYEVV ANKPFMFFIQ EESTRQTLFT GRVSDPALVD
451 GAFKA

Prophenoloxidase-activating proteinase-3

1 *MANLVYVLLL ASYFCFVSGQ* SCTTPNNGKG TCKSIYECEE LLKLVYKKDR
51 TQQDTDYLKK SQCGFMGNTP TVCCPNPCIT PQGEPGQCVS IYECTNLANL
101 LKPPITADTY NYVQKSRCQG ADQYSVCCGS APNFPSSGDC KASVSAFPPD
151 PKSKCCGVDS RVGNKIIGGN ATDVDQYPWL TIIEYVKTGP IKLLCGGVLI
201 SGKYVLTAGH CLTGPVLQIG TPTNVRLGEY NTKNDGADCV TVEAGGMDCT
251 EGAVIVPIEK TIPHPEYNPI SRTRRNDIGL IRLKEMAPFT DFIRPICLPS
301 LDLTQAPPVN FTLYAAGWGA VSTSQPSSNV KLHVQLPFIS YERCQPSYAV
351 QNRQIELWEK QVCAGGEAGK DSCKGDSGGP LMFENGQTYE VIGIVSFGPT
401 PCGMQDIPGV YTKVHSYKDW IISNIKP

Figure 3-10. Complex spot 39 contains serpin-3 and prophenoloxidase-activating proteinase-3.

Sequence coverage of serpin-3 and prophenoloxidase-activating proteinase-3 from spot 39 (Figure 3-4A). Tryptic peptides identified by mass spectrometry are shown in red letters. The P1 residue of serpin-3a is bold and underlined and the activation site of prophenoloxidase-activating proteinase-3 is highlighted in cyan. Signal peptides for both proteins are italicized.

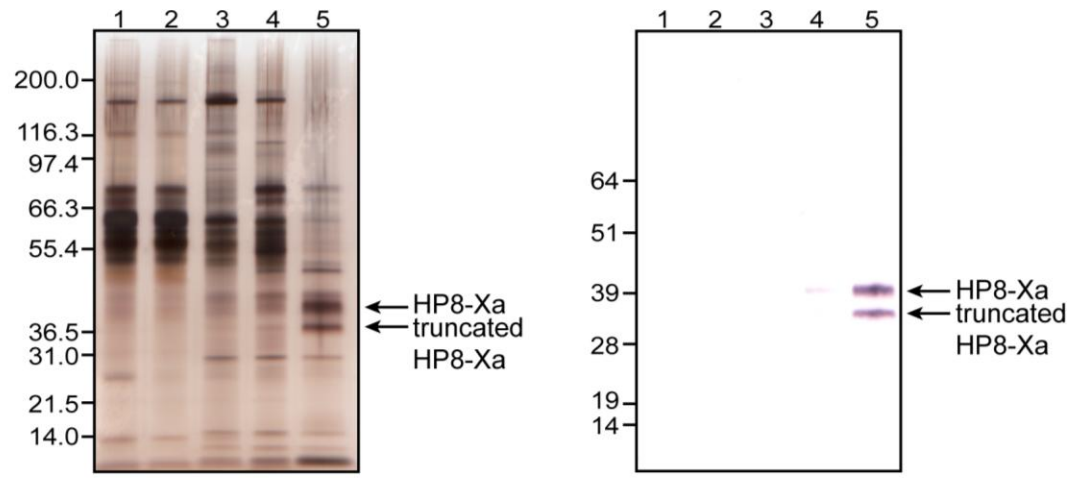

Figure 3-11. Analysis of recombinant HP8-Xa.

A mutant (named HP8-Xa) at the putative activation site of HP8 with residues NNDR[90] changed to IEAR[90] by site directed mutagenesis was expressed in S2 cells and purified (An et al., 2009; An et al., 2010b). For each purification step, 100 ng of total protein was mixed with sample buffer containing β-mercaptoethanol and separated by SDS-PAGE (4-12% Bis-Tris gel), followed by silver staining (left) and immunoblotting with HP8 antibody (right). Media post-dialysis (lane 1), after Affi-gel Blue Gel (lane 2), after ConA sepharose and dialysis (lane 3), after Q sepharose (lane 4), after gel permeation chromatography (lane 5).

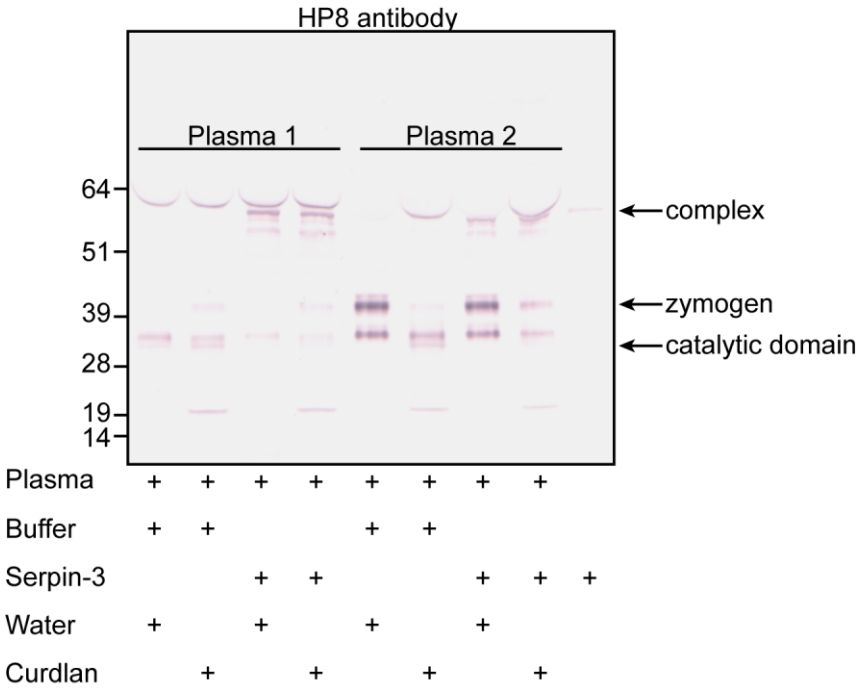

Figure 3-12. Active HP8 in plasma forms a complex with serpin-3.

Samples of plasma pooled from 7 (#1) or 6 naïve larvae (#2) were incubated with or without recombinant serpin-3 (final concentration = 0.1 µg/µL) in buffer (20 mM Tris-HCl, 250 mM NaCl, pH 8.0) containing diethyldithiocarbamic acid (final concentration = 2.25 mg/mL) for 5 min, followed by incubation with filter-sterilized water or curdlan (20 µg) for 1 h at room temperature. An equivalent of 1 µL of plasma loaded in each lane was subjected to SDS-PAGE under reducing conditions followed by immunoblot analysis with HP8 antibody (OSU 3; 1:2000 dilution). The bands of proHP8 (zymogen), catalytic domain, and putative serpin complexes are indicated by solid arrows.

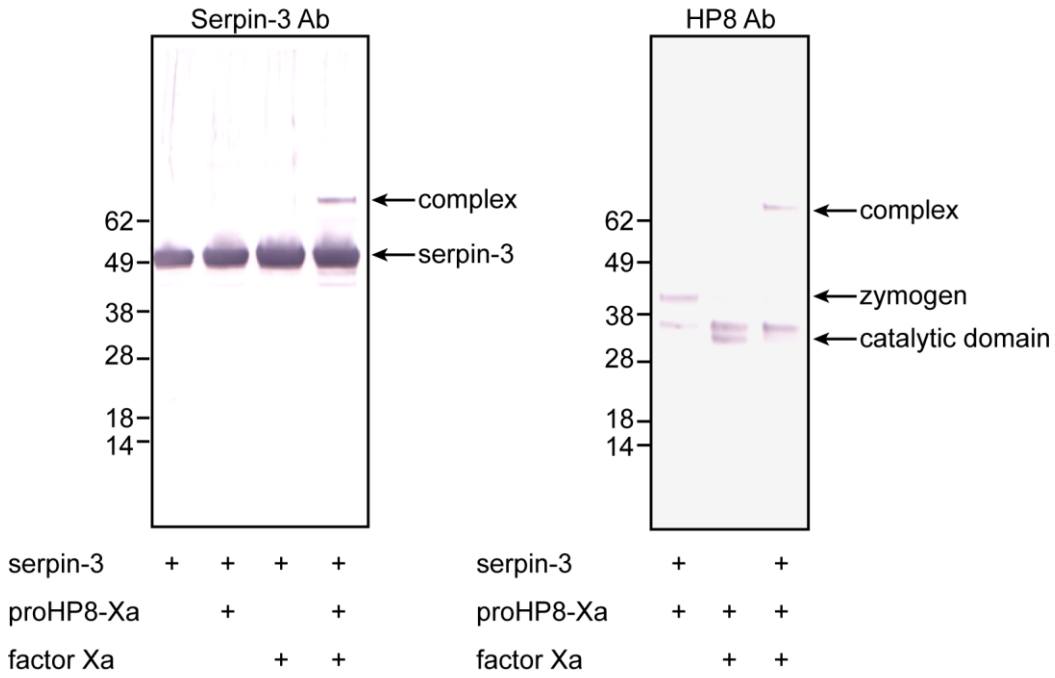

Figure 3-13. Recombinant HP8-Xa and serpin-3 form a complex *in vitro*.

Recombinant proHP8-Xa (50 ng=1.3 pmol) was incubated with bovine factor Xa (100 ng) and 0.05% Tween-20 (final concentration = 0.005%) in 20 mM Tris-HCl, 150 mM NaCl, pH 8.0 for 23.5 h at 37 °C. Recombinant serpin-3 (636.3 ng=13 pmol) was added to the activated mixture and incubated for 10 min at room temperature. Mixtures were subjected to SDS-PAGE under reducing conditions followed by immunoblot analysis with serpin-3 (KSU 114) and HP8 (OSU 3) antibodies.

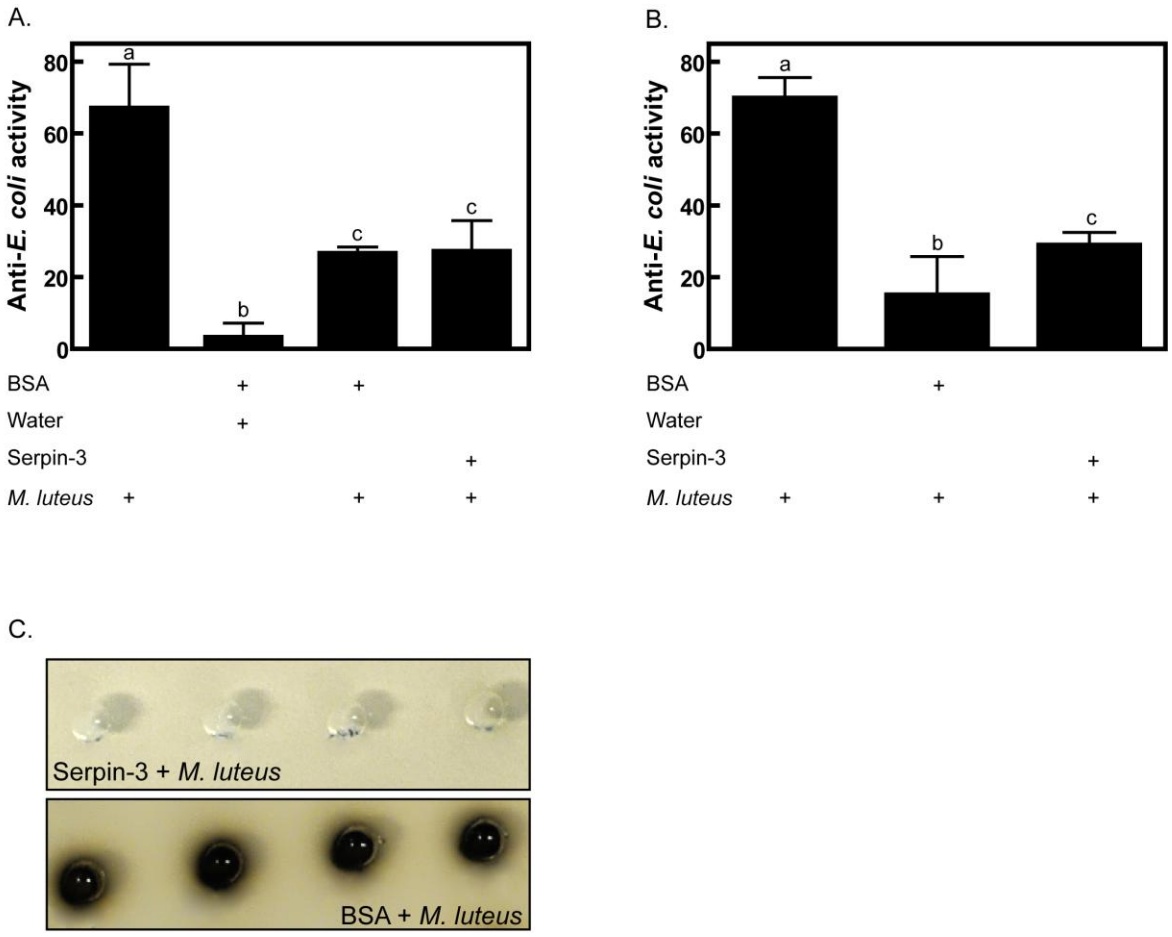

Figure 3-14. Production of antimicrobial peptides is not inhibited by injection of serpin-3. Antimicrobial activity of plasma assayed against *E. coli*. (A) Plasma from larvae injected with BSA (200 µg in 200 µL) or serpin-3 (200 µg in 200 µL) followed by filter sterilized water (50 µL) or *M. luteus* (100 ng in 50 µL). (B) Plasma from larvae injected with BSA (200 µg in 200 µL) or serpin-3 (200 µg in 200 µL) followed by filter sterilized water (50 µL) or *M. luteus* (3000 ng in 50 µL). Larvae were held at room temperature for 25 min and placed on ice for 5 min before the second injection. In panels A and B, the positive control was plasma injected with *M. luteus* (100 µg) only. (C) Non-heated plasma samples from larvae described in panel A after 2 h of incubation at 37°C. The bars represent mean ± SD (n = 9 (A); n = 6 (B)). Bars labeled with different letters are significantly different (Analysis of Variance and Newman-Keuls test, $p < 0.05$).

Tables

Table 3-1. NCBInr database identification of plasma proteins that bound to a serpin-3 antibody-coupled immunoaffinity column separated by 1D gel electrophoresis.

Bands as marked in Figure 3-3. List of top Mascot PMF hits from the NCBInr database for bands identified as *M. sexta* protein. Mascot scores are for the entire protein sequences, CI% is the confidence interval. Sequence coverages are based on the entire sequence in the database. MS/MS results listed in more detail in Table B-1.

Band	Protein name	GenInfo identifier	Protein score	Protein score C.I.%	Peptide count	Total ion score	Total ion score C.I.%	% sequence coverage
1	apolipophorin-1	gi|2498144	178	100	38	21	0	12
2	serpin-3a	gi|27733415	857	100	21	678	100	54
2	PAP-3	gi|60299972	164	100	8	130	100	19
3	serpin-3a	gi|27733415	594	100	18	460	100	45
3	proPO-p2	gi|75038472	199	100	18	105	100	25
3	proPO-p1	gi|74763772	85	97.0	12	29	0	17
4	serpin-3a	gi|27733415	1240	100	26	981	100	65
5	serpin-3a	gi|27733415	1050	100	22	841	100	54
6	immulectin-2	gi|237869126	351	100	11	285	100	44
6	immulectin-2a	gi|224381229	330	100	11	262	100	44
6	SPH-1	gi|242351233	59	0	6	42	5.2	12
7	immulectin-3	gi|55139125	626	100	15	489	100	70
7	immulectin-4	gi|237861314	76	73.9	7	44	50.3	18
7	immulectin-III	gi|110649250	68	0	7	44	50.3	19
8	attacin-1	gi|67906420	423	100	14	286	100	54
9	attacin-II	gi|110649242	163	100	10	59	97.6	55
9	dVG-AP3-2 (gloverin)	gi|110649228	112	99.9	7	29	0	57

PAP-3 = prophenoloxidase-activating proteinase-3; proPO-p2 = prophenoloxidase subunit 2; proPO-p1 = prophenoloxidase subunit 1; SPH-1 = serine proteinase homolog-1

Table 3-2. ESI-MS/MS results using Mascot and NCBI database restricted to *Manduca sexta* for plasma proteins that bound to a serpin-3 antibody-coupled immunoaffinity column separated by 2D-PAGE.

List of top Mascot hits for spots marked in Figure 3-4A. Percent sequence coverage values in parentheses are calculated by using the residues in the catalytic domain of the proteinase only. Protein scores (sum of ion scores) > 22 indicate significant identity ($p < 0.05$). MS/MS results listed in more detail in Table B-2.

Spot	Protein name	GenInfo identifier	Protein MW	Protein score	Peptide count	% sequence coverage
1	serpin 3a	gi|27733415	51096	1311	19	45.7
	HP8	gi|56418397	40710	122	2	6.7 (9.7)
2	serpin 3a	gi|27733415	51096	1390	22	54.1
	PAP-3	gi|35277829	46240	119	2	4.7 (7.3)
3	serpin 3a	gi|27733415	51096	1459	22	52.5
	immulectin-2b	gi|224381231	37069	190	4	11.9
	PAP-3	gi|35277829	46240	180	4	9.6 (15.3)
4	serpin 3a	gi|27733415	51096	1462	23	52.7
	immulectin-2b	gi|224381231	37069	249	6	19.6
	PAP-3	gi|35277829	46240	200	5	10.5 (17.2)
	immulectin-2a	gi|224381229	37179	171	5	15.3
5	serpin 3a	gi|27733415	51096	1495	23	56
	PAP-1	gi|60299968	42785	356	6	13.3 (19.9)
6	proPO-p2	gi|75038472	80010	1297	22	31.9
	serpin 3a	gi|27733415	51096	401	5	15.2
7	proPO-p1	gi|74763772	78915	1270	23	34
8	proPO-p1	gi|74763772	78915	1232	24	32.7
9	proPO-p1	gi|74763772	78915	864	15	27.6
10	proPO-p2	gi|75038472	80010	809	14	22.4
	serpin 3a	gi|27733415	51096	551	9	26.2
11	proPO-p2	gi|75038472	80010	781	13	21.9
	serpin 3a	gi|27733415	51096	104	2	8.1
12	proPO-p2	gi|75038472	80010	890	16	24.9
13	serpin 3a	gi|27733415	51096	607	10	24.6
	proPO-p2	gi|75038472	80010	239	5	8.3
14	serpin 3a	gi|27733415	51096	870	14	37.4
	proPO-p2	gi|75038472	80010	260	5	7.3
15	serpin 3a	gi|27733415	51096	715	12	35.8
16	serpin 3a	gi|27733415	51096	1489	22	46.8
17	serpin 3a	gi|27733415	51096	1491	23	53.8
	GNBP-like protein	gi|315142915	53653	323	7	12.7
18	serpin 3a	gi|27733415	51096	229	4	13.2
19	serpin 3a	gi|27733415	51096	179	4	7.5
20	beta-1-tubulin	gi|12585365	50198	169	3	8.1
	SPH-1b	gi|242351233	45594	114	4	8.2
21	SPH-1b	gi|242351233	45594	252	6	12
22	serpin 3a	gi|27733415	51096	1212	19	36.7
	SPH-1b	gi|242351233	45594	147	5	9.6
23	serpin 3a	gi|27733415	51096	1329	21	43.7
24	serpin 3a	gi|27733415	51096	1380	21	42
25	serpin 3a	gi|27733415	51096	1110	17	34.3

Spot	Protein name	GenInfo identifier	Protein MW	Protein score	Peptide count	% sequence coverage
26	serpin 3a	gi|27733415	51096	1244	19	38.7
27	serpin 3a	gi|27733415	51096	1087	17	36.7
	SPH-1b	gi|242351233	45594	104	3	6.7
28	serpin 3a	gi|27733415	51096	954	15	33.6
	SPH-4	gi|56418466	43122	156	5	6.7
29	serpin 3a	gi|27733415	51096	1204	19	40.9
	SPH-4	gi|56418466	43122	160	5	6.7
30	serpin 3a	gi|27733415	51096	899	15	32.1
	proPO-p2	gi|75038472	80010	120	2	2.9
	serpin-4a	gi|45594224	46452	102	2	4.7
	SPH-1b	gi|242351233	45594	74	2	4.6
	SPH-4	gi|56418466	43122	56	2	4.6
31	serpin 3a	gi|27733415	51096	286	6	13
32	serpin 3a	gi|27733415	51096	317	7	14.3
33	SPH-2	gi|21630233	43461	414	9	17.8
34	SPH-2	gi|21630233	43461	457	10	20.4
35	SPH-4	gi|56418466	43122	254	6	11.1
36	serpin 3a	gi|27733415	51096	176	4	8.8
37	serpin 3a	gi|27733415	51096	935	16	33.4
38	serpin 3a	gi|27733415	51096	1291	21	46.2
39	serpin 3a	gi|27733415	51096	873	15	28.8
	PAP-3	gi|35277829	46240	79	2	4.4 (7.3)
41	PRSP (HP14)	gi|39655053	73623	100	3	3.8
43	serpin 3a	gi|27733415	51096	476	8	19.6
51	proPO-p2	gi|75038472	80010	140	3	4.2
	serpin 3a	gi|27733415	51096	119	2	4.6
52	serpin 3a	gi|27733415	51096	589	10	22.2
54	immulectin-2b	gi|224381231	37069	432	7	22.9
	immulectin-2a	gi|224381229	37179	377	6	19.9
55	immulectin-2b	gi|224381231	37069	452	7	27.8
56	immulectin-2b	gi|224381231	37069	211	5	19.6
	immulectin-2a	gi|224381229	37069	211	5	19.6
	SPH-1b	gi|242351233	45594	204	4	7
	immulectin III	gi|110649250	34789	80	2	4.6
57	immulectin-4	gi|237861314	35559	279	5	15.4
	immulectin III	gi|110649250	34789	277	4	11.1
	immulectin-2b	gi|224381231	37069	114	3	10.4
	dVA-AP7	gi|110649220	16486	106	2	14
58	immulectin-3	gi|55139125	33846	139	3	10.6
59	immulectin III	gi|110649250	34789	210	4	11.1
	immulectin-2a	gi|224381229	37179	141	3	10.4
	immulectin-2b	gi|224381231	37069	131	3	10.4
60	immulectin-2b	gi|224381231	37069	168	4	13.8
61	PAP-1	gi|60299968	42785	182	2	5.7
	immulectin-3	gi|55139125	33846	65	2	6.1
66	attacin-1	gi|67906420	24232	96	3	13.8
67	immulectin-2b	gi|224381231	37069	215	5	16.2
	attacin-1	gi|67906420	24232	147	3	17.8
68	attacin-1	gi|67906420	24232	406	8	34.2

*Spots are listed in sequential order. Gaps between numbers indicate that no *M. sexta* protein was identified in those spots (data also excluded from Figure 3-4A).
HP = hemolymph proteinase; PAP = prophenoloxidase-activating proteinase; proPO = prophenoloxidase; GNBP = gram-negative binding protein; SPH = serine proteinase homolog; PRSP = pattern recognition serine proteinase

Table 3-3. ESI-MS/MS results using Mascot and NCBI database restricted to *Manduca sexta* for plasma proteins that bound to a control column of Protein-A Sepharose CL-4B beads without antibody separated by 2D-PAGE.

List of top Mascot hits for spots marked in Figure 3-4B. Protein scores (sum of ion scores) > 22 indicate significant identity ($p < 0.05$). MS/MS results listed in more detail in Table B-3.

Spot	Protein name	GenInfo identifier	Protein MW	Protein score	Peptide count	% sequence coverage
1c	immulectin-2b	gi|224381231	37069	377	7	22.9
2c	immulectin-2b	gi|224381231	37069	265	5	17.7
3c	immulectin-2b	gi|224381231	37069	296	6	19
4c	immulectin-2b	gi|224381231	37069	87	2	6.1
5c	immulectin-2b	gi|224381231	37069	201	4	15
6c	immulectin-2b	gi|224381231	37069	85	2	6.7
7c	no match					
8c	no match					
9c	serpin-1	gi|134436	43483	50	1	3.3
10c	endochitinase	gi|544013	62164	163	4	7.4
11c	proPO-p2	gi|75038472	80010	300	5	7.6
12c	immulectin-2b	gi|224381231	37069	231	4	18.7
13c	immulectin-2b	gi|224381231	37069	84	2	6.7
	immulectin III	gi|110649250	34789	66	2	6.5
	immulectin-3	gi|55139125	33846	25	1	3.9
14c	immulectin-3	gi|55139125	33846	55	2	6.1
	immulectin-2b	gi|224381231	37069	42	1	3.1
15c	immulectin-2b	gi|224381231	37069	221	5	18.7
16c	immulectin-2b	gi|224381231	37069	86	2	6.7
17c	immulectin-2b	gi|224381231	37069	182	4	13.8
	scolexin A	gi|4262357	30353	47	1	3.2
18c	immulectin-3	gi|55139125	33846	24	1	2.3
19c	proPO-p2	gi|75038472	80010	38	1	1
	immulectin-3	gi|55139125	33846	31	1	2.3
20c	immulectin-3	gi|55139125	33846	36	1	2.3
21c	immulectin-3	gi|55139125	33846	27	1	2.3
22c	SPH-2	gi|21630233	43461	102	3	8.5
23c	immulectin-2b	gi|224381231	37069	190	4	13.8
	immulectin-3	gi|55139125	33846	31	1	2.3
24c	immulectin-3	gi|55139125	33846	27	1	2.3
25c	immulectin-2b	gi|224381231	37069	119	2	9.8
	immulectin-3	gi|55139125	33846	75	2	6.1
26c	immulectin-2b	gi|224381231	37069	172	4	13.8
	immulectin III	gi|110649250	34789	94	2	6.5
	immulectin-3	gi|55139125	33846	64	2	6.1
27c	immulectin-2b	gi|224381231	37069	424	7	27.8
28c	immulectin-2b	gi|224381231	37069	250	5	17.4
	SPH-1b	gi|242351233	45594	99	3	10.3
29c	immulectin III	gi|110649250	34789	219	4	11.1
	immulectin-4	gi|237861314	35559	201	4	11
	immulectin-3	gi|55139125	33846	27	1	3.9
30c	immulectin-3	gi|55139125	33846	69	2	6.1

proPO = prophenoloxidase; SPH = serine proteinase homolog

Table 3-4. EST database identification of plasma proteins bound to a serpin-3 antibody-coupled immunoaffinity column separated by 2D-PAGE.

The Mascot program was used to search ESI-MS/MS data against compiled *M. sexta* ESTs from NCBI and a pyrosequencing EST project (Haobo Jiang). Identification of the ESTs is based on BLAST searches against the NCBI database (tblastx = no highlight, nucleotide collection; blastn = light purple highlight, non-mouse and non-human EST entries).

Spot	Protein name	Contig/GenInfo identifier	Protein score[a]	Peptide count	% sequence coverage	Other[b]
1	serpin-3a/3b	contig09983	1309	14	37.2	
	HP8	contig00781	122	1	7.4	
	HP8	contig10728	90	1	9.2	
	unknown protein (*Bombyx mori*)	contig01320	50	1	3.1	gi|29533080
2	serpin-3a/3b	contig09983	1386	17	44	
	PAP-3	contig00625	93	1	2.8	
	HP8	contig10728	53	1	6.5	
	unknown protein (*B. mori*)	contig01320	50	1	3.1	gi|29533080
3	serpin-3a/3b	contig09983	1453	18	42.8	
	immulectin-2	contig00874	190	3	9.5	
	PAP-3	contig00625	178	1	6.1	
4	serpin-3a/3b	contig09983	1458	20	42.9	
	immulectin-2	contig00874	249	2	15.6	
	PAP-3	contig00625	198	1	6.7	
5	serpin-3a/3b	contig09983	1491	18	45.6	
	PAP-1	contig00173	355	4	10.3	
	unknown protein (*B. mori*)	contig01320	50	1	3.1	gi|29533080
6	proPO	gi|119434460	402	5	26.3	
	serpin-3a/3b	contig09983	401	5	12.3	
	proPO	contig21993	175	1	51.1	
	proPO	contig20740	159	1	29.2	
	proPO	contig24654	142	2	28.4	
	proPO	contig19763	109	1	36.6	
	proPO	gi|119434509	56	1	4.3	

Spot	Protein name	Contig/GenInfo identifier	Protein score[a]	Peptide count	% sequence coverage	Other[b]
7	proPO-p1	contig21092	149	1	41.3	
	proPO-p1	contig09675	139	2	34.3	
	proPO-p1	contig20765	124	1	50	
	proPO-p1	contig19861	122	2	30.2	
	proPO-p1	contig18477	99	1	16.3	
	proPO-p1	contig18610	65	1	24.3	
	proPO-p1	contig19396	62	1	34.3	
	unknown protein (*Antheraea assama*)	contig00018	57	1	10.8	gi|188459103
8	proPO-p1	contig20765	126	1	50	
	proPO-p1	contig09675	115	1	34.3	
	proPO-p1	contig19861	113	2	30.2	
	proPO-p1	contig21092	109	1	41.3	
	proPO-p1	contig18477	100	2	16.3	
	proPO-p1	contig18610	66	1	24.3	
	proPO-p1	contig19396	64	1	34.3	
	proPO	contig05761	58	1	2.8	
9	proPO-p1	contig20765	126	1	50	
	proPO-p1	contig19861	99	1	30.2	
	proPO-p1	contig09675	98	1	34.3	
	proPO-p1	contig19396	70	1	34.3	
	proPO-p1	contig18610	59	1	24.3	
	proPO-p1	contig18610	59	1	24.3	
	proPO-p1	contig21092	58	1	41.3	
	proPO-p1	contig18477	57	1	9.2	
10	serpin-3a/3b	contig09983	549	8	21.3	
	proPO	gi|119434460	367	3	25.9	
	unknown protein (*B. mori*)	contig10237	111	1	6.7	gi|91833685
	unknown protein (*Antheraea assama*)	contig10239	91	1	11.1	gi|189551604
	proPO	contig19763	87	1	36.6	
	proPO	contig19763	87	1	36.6	
	proPO	contig20740	68	1	11.5	
	proPO	gi|119434509	57	1	4.3	

Spot	Protein name	Contig/GenInfo identifier	Protein score[a]	Peptide count	% sequence coverage	Other[b]
11	proPO	gi|119434460	329	3	25.9	
	unknown protein (*Antheraea assama*)	contig10239	150	2	20	gi|189551604
	serpin-3a/3b	contig09983	104	1	6.6	
	proPO	contig19763	85	1	36.6	
	proPO	contig24654	70	1	15.8	
	proPO	contig20740	70	1	11.5	
	proPO	contig10922	48	1	5.3	
12	proPO	gi|119434460	282	3	21.5	
	proPO	contig19763	113	1	36.6	
	proPO	contig20740	97	1	19.2	
	proPO	contig21993	84	1	36.2	
	proPO	contig24654	68	1	15.8	
	proPO	gi|119434509	52	1	4.3	
13	serpin-3a/3b	contig09983	605	7	20	
	proPO	gi|119434460	156	2	14.9	
	immulectin-3	contig18028	107	1	14.3	
	PAP-1	contig00173	93	1	2.8	
	unknown protein (*Choristoneura fumiferana*)	contig10840	83	1	2.6	gi|282377349
14	serpin-3a/3b	contig09983	868	11	30.4	
	proPO	gi|119434460	216	2	18	
	PAP-1	contig00173	98	1	2.8	
15	serpin-3a/3b	contig09983	713	9	29.2	
	unknown protein (*Raphanus raphanistrum*)	contig11562	223	1	19.4	gi|167500278
	unknown protein (*Manduca sexta*)	contig14828	141	1	9.9	gi|255978320
	immulectin-2	contig00874	52	1	2.4	
	ubiquitin/ribosomal protein S27A	contig15324	51	1	5.3	
16	serpin-3a/3b	contig09983	1485	16	38.1	
	unknown protein (*B. mori*)	contig01320	50	1	3.1	gi|29533080
17	serpin-3a/3b	contig09983	1485	18	43.8	
	GNBP-like protein	contig06029	323	3	12.5	
18	serpin-3a/3b	contig09983	227	4	10.7	

Spot	Protein name	Contig/GenInfo identifier	Protein score[a]	Peptide count	% sequence coverage	Other[b]
19	alpha tubulin (*B. mori*)	contig09663	222	2	8.9	gi|112983500
	serpin-3a/3b	contig09983	179	1	6.1	
	alpha tubulin (*M. sexta*)	gi|3827974	152	2	18	gi|3827974
	unknown protein (*M. sexta*)	gi|255980816	118	1	14.1	gi|255980816
	SPH-1b	contig00488	59	1	2.5	
20	beta-1 tubulin	gi|10763921	134	2	10.6	
21	SPH-1b	contig00488	252	1	9.5	
	beta-1 tubulin	contig10459	59	1	5.9	
22	serpin-3a/3b	contig09983	1208	14	29.9	
	serpin-3a/3b	gi|14860734	320	3	28.2	
	eukaryotic initiation factor-4a (*M. sexta*)	contig00160	78	1	2.3	gi|10763918
23	serpin-3a/3b	contig09983	1325	16	35.6	
	serpin-3a/3b	gi|14860734	390	4	31.3	
	hypothetical protein (*Choristoneura fumiferana*)	contig15079	62	1	0.8	gi|282363237
	unknown protein (*B. mori*)	contig01320	50	1	3.1	gi|29533080
24	serpin-3a/3b	contig09983	1376	17	34.2	
	serpin-3a/3b	gi|14860734	486	5	37.4	
25	serpin-3a/3b	contig09983	1106	13	27.9	
	SPH-1b	contig00488	63	1	2.5	
26	serpin-3a/3b	contig09983	1240	16	31.5	
	eukaryotic initiation factor-4a (*M. sexta*)	contig00160	80	1	2.3	gi|10763918
27	serpin-3a/3b	contig09983	1083	15	29.9	
	serpin-3a/3b	gi|14860734	247	3	27.6	
	SPH-1b	contig00488	104	1	5.3	
	proPO	gi|119434509	65	1	4.3	
28	serpin-3a/3b	contig09983	950	12	27.4	
29	serpin-3a/3b	contig09983	1200	14	33.3	
	proPO	contig19763	51	1	14.1	

Spot	Protein name	Contig/GenInfo identifier	Protein score[a]	Peptide count	% sequence coverage	Other[b]
29	unknown protein (*B. mori*)	contig01320	50	1	3.1	gi|29533080
30	serpin-3a/3b	contig09983	895	11	26.1	
	serpin-4a/4b	contig07207	74	1	1.3	
	proPO	contig19763	67	1	14.1	
	proPO	contig19763	67	1	14.1	
	unknown protein (*B. mori*)	contig01320	63	1	3.1	gi|29533080
	proPO	gi|119434509	53	1	4.3	
31	serpin-3a/3b	contig09983	286	4	10.6	
32	inter-alpha trypsin inhibitor (*M. sexta*)	contig10831	445	4	10.4	gi|14860668
	serpin-3a/3b	contig09983	315	2	11.6	
33	SPH-2	contig09999	412	3	13.6	
34	SPH-2	contig09999	455	3	15.5	
35	SPH-4	contig09788	254	1	7.7	
36	serpin-3a/3b	contig09983	176	1	7.2	
37	serpin-3a/3b	contig09983	931	10	27.2	
	unknown protein (*M. sexta*)	contig15549	55	1	2.5	gi|119435450
	unknown protein (*B. mori*)	contig01320	50	1	3.1	gi|29533080
38	serpin-3a/3b	contig09983	1285	16	37.6	
	unknown protein (*M. sexta*)	contig15549	51	1	2.5	gi|119435450
	unknown protein (*B. mori*)	contig01320	50	1	3.1	gi|29533080
39	serpin-3a/3b	contig09983	869	11	23.4	
	unknown protein (*Spodoptera frugiperda*)	contig02455	57	1	2.8	gi|295265638
	no BLAST hit	contig19330	57	1	12.9	
	unknown protein (*M. sexta*)	contig15549	51	1	2.5	gi|119435450
43	serpin-3a/3b	contig09983	453	5	14.5	
	unknown protein (*B. mori*)	contig01320	50	1	3.1	gi|29533080

Spot	Protein name	Contig/GenInfo identifier	Protein score[a]	Peptide count	% sequence coverage	Other[b]
46	unknown protein (*M. sexta*)	contig15297	165	2	7.9	gi|285007385
	unknown protein (*M. sexta*)	contig18435	131	1	16	gi|285007385
51	proPO	gi|119434460	142	1	12.7	
	serpin-3a/3b	contig09983	117	2	3.8	
	Kazal family serine proteinase inhibitor (*M. sexta*)	contig14641	47	1	2.1	gi|14860836
52	serpin-3a/3b	contig09983	587	8	18.1	
	unknown protein (*B. mori*)	contig01320	63	1	3.1	gi|29533080
	PRSP (HP14)	contig10343	60	1	3.2	
	unknown protein (*M. sexta*)	contig15549	56	1	2.5	gi|119435450
54	immulectin-2	contig00874	432	7	18.3	
	PAP-3	contig00625	51	1	1.3	
55	immulectin-2	contig00874	452	7	22.2	
56	immulectin-3	contig13019	218	3	22.2	
	immulectin-2	contig00874	211	2	15.6	
	SPH-1b	contig00488	204	2	5.5	
	immulectin-4	gi|14863326	80	1	14.3	
57	immulectin-4	contig14268	382	3	18.3	
	immulectin-3	contig18028	131	2	14.3	
	immulectin-3	contig12030	55	1	6.1	
58	immulectin-3	contig10887	139	1	5.3	
	immulectin-3	contig12425	84	1	11.1	
59	immulectin-4	contig14268	207	2	9	
	immulectin-3	contig18028	131	2	14.3	
60	immulectin-2	contig00874	168	1	11	
	immulectin-3	contig18028	146	2	14.3	
61	PAP-1	contig00173	182	2	4.4	
	immulectin-3	contig12425	65	1	11.1	
62	immulectin-3	contig13019	67	1	7.9	
63	immulectin-3	contig13019	48	1	7.9	
66	attacin-1	contig00567	155	1	17.5	

Spot	Protein name	Contig/GenInfo identifier	Protein score[a]	Peptide count	% sequence coverage	Other[b]
66	ferritin heavy chain-like protein	contig11084	75	1	2.2	
67	immulectin-2	contig00874	215	2	13	
	attacin-1	gi|14860782	147	2	22	
68	attacin-1	gi|14860782	275	3	24.7	
	attacin-1	contig00567	257	3	22	
	attacin-1	contig12089	195	2	59.8	
68	attacin-2	contig14717	132	2	19.3	
	attacin-1	contig11045	131	1	37.2	
	attacin-1	contig10503	121	1	37.1	
	attacin-1	contig17095	119	1	64	

a: Sum of individual ion scores excluding duplicate matches. Scores > 46 indicate significant identity ($p < 0.05$)
b: GenInfo identifier of protein identifications made by BLAST searching non-mouse and non-human EST entries in NCBI or the nucleotide collection database (for alpha tubulin from *B. mori* in spot 19 only).

HP = hemolymph proteinase; PAP = prophenoloxidase-activating proteinase; proPO = prophenoloxidase; GNBP = gram-negative binding protein; SPH = serine proteinase homolog; PRSP = pattern recognition serine proteinase

Table 3-5. EST database identification of plasma proteins that bound to a control column of Protein-A Sepharose CL-4B beads without antibody separated by 2D-PAGE.

The Mascot program was used to search ESI-MS/MS data against compiled *M. sexta* ESTs from NCBI and a pyrosequencing EST project (Haobo Jiang). Identification of the ESTs is based on BLAST searches against the NCBI database (tblastx = no highlight, nucleotide collection; blastn = light purple highlight, non-mouse and non-human EST entries).

Spot	Protein name	Contig/GenInfo identifier	Protein score[a]	Peptide count	% sequence coverage	Other[b]
1c	immulectin-2	contig00874	377	4	18.3	
2c	immulectin-2	contig00874	265	4	14.2	
3c	immulectin-2	contig00874	296	3	15.2	
4c	immulectin-2	contig00874	87	1	4.9	
5c	immulectin-2	contig00874	201	2	12	
	unknown protein (*Spodoptera littoralis*)	contig06962	48	1	0.7	gi|300744602
6c	unknown protein (*Caenorhabditis remanei*)	contig19852	126	1	16.3	gi|68276617
	immulectin-2	contig00874	85	1	5.4	
	zinc finger protein (*Glycine max*)	contig20460	50	1	8.2	gi|7795340
7c		no EST hit				
8c		no EST hit				
9c	serpin-1	contig10071	50	1	3.5	
10c		no EST hit				
11c	proPO	gi|119434460	195	2	13.2	
	proPO	contig19763	62	1	14.1	
12c	immulectin-2	contig00874	231	4	14.9	
13c	immulectin-2	contig00874	84	1	5.4	
14c		no EST hit				
15c	immulectin-2	contig00874	221	1	14.9	
16c		no EST hit				
17c	immulectin-2	contig00874	182	2	11	
18c	immulectin-3	contig18028	51	1	6.4	
19c		no EST hit				
20c		no EST hit				
21c		no EST hit				
22c		no EST hit				

Spot	Protein name	Contig/GenInfo identifier	Protein score[a]	Peptide count	% sequence coverage	Other[b]
23c	immulectin-2	contig00874	190	2	11	
24c	immulectin-3	contig18028	55	1	6.4	
25c	immulectin-2	contig00874	119	2	7.8	
26c	immulectin-2	contig00874	172	2	11	
	immulectin-3	contig18028	117	1	14.3	
	immulectin-4	contig14268	94	1	5.3	
27c	immulectin-2	contig00874	424	7	22.2	
28c	immulectin-3	contig13019	330	4	24.1	
	immulectin-2	contig00874	250	3	13.9	
29c	immulectin-4	contig14268	238	3	12.2	
	immulectin-3	contig18028	134	2	14.3	
30c	immulectin-3	contig13019	61	1	7.9	

a: Sum of individual ion scores excluding duplicate matches. Scores > 46 indicate significant identity ($p < 0.05$)
b: GenInfo identifier of protein identifications made by BLAST searching non-mouse and non-human EST entries in NCBI.

proPO = prophenoloxidase

Appendix A - HP16: Unexpected Results from a Hypothesis Tested

Prophenoloxidase Activation by HP16 and NT16

Upon invasion by bacteria or other pathogens, the activation of two proteinase cascades (prophenoloxidase or Toll) can be stimulated. Hemolymph proteinase 16 protein and mRNA levels increased upon injection of larvae with *M. luteus* or *E.coli*, which suggested that HP16 might be involved in the activation of one or both of these pathways. I hypothesized that HP16 might be a component of a proteinase cascade involved in prophenoloxidase activation, and I tested this hypothesis by conducting a prophenoloxidase activation assay.

Materials and methods

To prepare a plasma sample suitable to test for prophenoloxidase activation, thirty day 2 fifth instar larvae (naïve) were checked for low basal levels of PO activity that dramatically increased after incubation with *M. luteus* as described by Tong and Kanost (2005), with modification. Larvae were chilled on ice for at least 20 min and wiped off with 70% ethanol. Hemolymph was collected on ice into individual 1.5 mL microcentrifuge tubes by clipping the posterior horn. Tubes were centrifuged at 8,000 × g for 7.5 min at 4°C to remove hemocytes and the resulting plasma was placed into a new 1.5 mL microcentrifuge tubes. All plasma was frozen at -80°C except for a 15 µL aliquot to be tested for PO activity. Plasma (4 µL) was incubated in 0.6 mL microcentrifuge tubes with Nuclease free water (2 µL) or *M. luteus* (2 µL of 1 µg/µL) for 10 min at room temperature and then transferred to a 96-well plate. PO activity was measured by adding 200 µL of 2 mM dopamine in 50 mM sodium phosphate buffer, pH 6.5 and monitoring absorbance at 470 nm for 15 min in a PowerWave XS plate reader (BioTek). One unit of PO activity was defined as a change in A_{470} of 0.001/min. Plasma samples with low endogenous PO activity, but high PO activity after incubation with *M. luteus* were pooled and stored at -80°C.

When necessary, purified recombinant HP16-Xa (100 ng) was incubated in the presence of 100 ng bovine factor Xa (New England Biolabs) in buffer (20 mM Tris-HCl, 150 mM NaCl, pH 8.4) plus $CaCl_2$ (final concentration = 2 mM) for 4 h at 25°C. Details of the reaction mixtures are provided in the figure and corresponding figure legend (Figures A-1). After incubation for 10 min at room temperature, PO activity was measured by adding 200 µL of 2 mM dopamine in 50

mM sodium phosphate buffer, pH 6.5 and monitoring absorbance at 470 nm for 30 min in a PowerWave XS plate reader (BioTek). One unit of PO activity was defined as a change in A_{470} of 0.001/min.

Results and conclusions

The addition of HP16-Xa activated by bovine factor Xa abolished PO activity in the presence of *M. luteus*, while addition of proHP16-Xa or factor Xa had no impact when compared to plasma mixed with *M. luteus* (Figure A-1A). To see if I could explain what looked like inhibition of PO activity or activation, I tested the effect of salt concentration on PO activity because samples containing active HP16-Xa had a higher salt concentration (37 mM NaCl) than controls (17, 14.4, 27.4, and 14.4 mM NaCl). It is obvious that the gel filtration buffer (20 mM Tris-HCl, 150 mM NaCl, pH 8.0) used in the activation mixture of HP16-Xa resulted in low levels of PO activity (Figure A-1B). NaCl concentrations were 10, 49, and 53 mM, respectively. Morever, PO activity decreased with increasing NaCl concentration (Figure A-1C). PO activity decreased by ~50% with the addition of 20 mM NaCl and ~83% with the addition of 27 mM NaCl. Therefore, I concluded that the NaCl concentration of the gel filtration buffer was responsible for the inhibition of PO activation and PAP-3 activation (data not shown), not HP16-Xa activated by bovine factor Xa.

I also tested the effect of NT16 on prophenoloxidase activation (Figure A-2) in the presence of *M. luteus* or zymosan. Plasma mixed with NT16 alone or plasma incubated with *M. luteus* in the presence or absence of NT16 did not increase PO activity when compared to plasma alone. Using zymosan as an elicitor instead of *M. luteus* produced high levels of PO activity in the presence or absence of NT16. Therefore, I concluded that zymosan is a good elicitor of PO activity and that NT16 does not impact prophenoloxidase activation in plasma.

References

Tong Y, Jiang H, & Kanost MR (2005) Identification of plasma proteases inhibited by *Manduca sexta* serpin-4 and serpin-5 and their association with components of the prophenol oxidase activation pathway. *J Biol Chem* **280**: 14932-14942

Figures

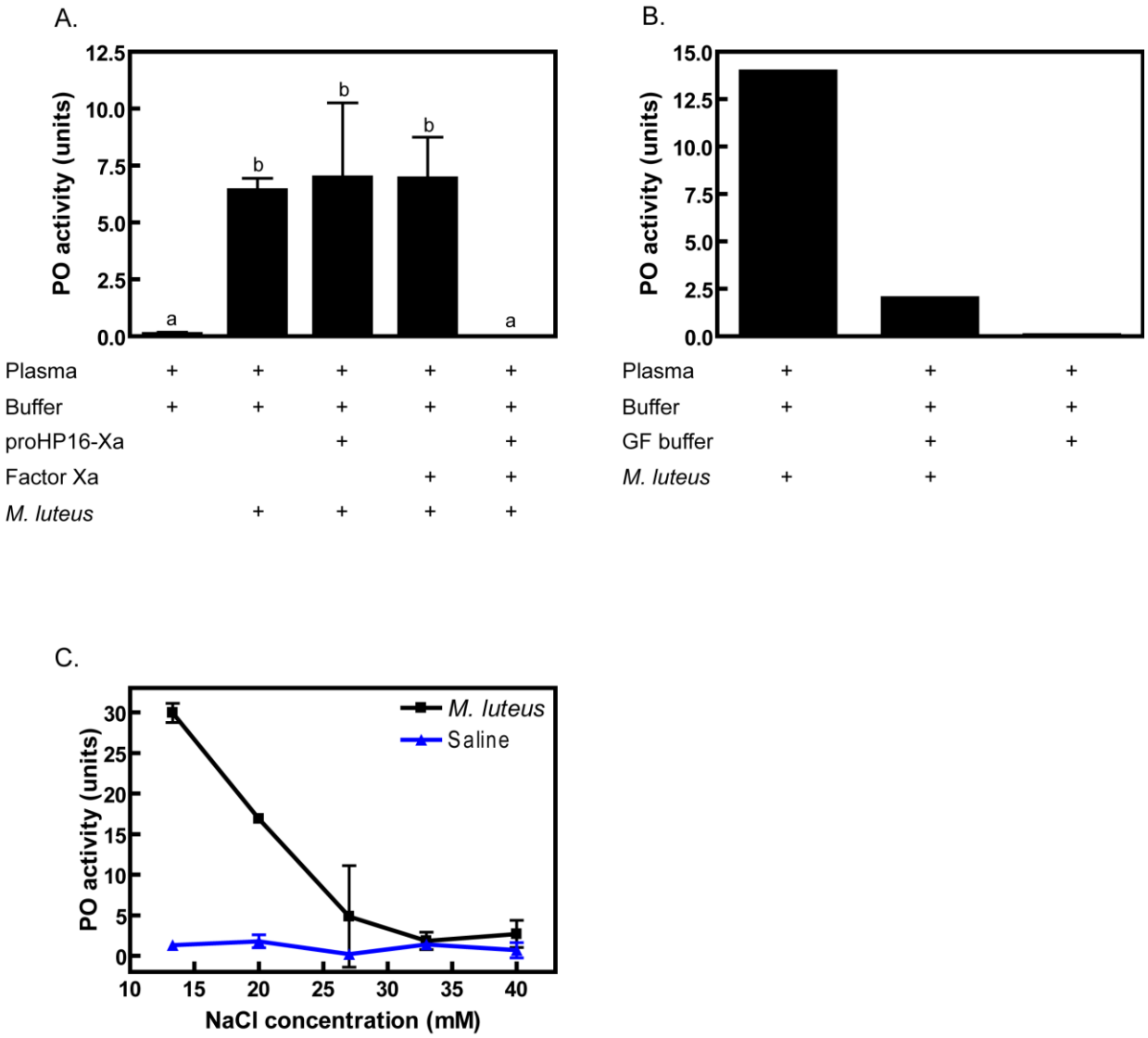

Figure A-1. Involvement of HP16 in prophenoloxidase activation.

A) Samples of plasma (3 µL) were mixed with buffer (20 mM Tris-HCl, 20 mM NaCl, 6.7 mM $CaCl_2$, pH 7.5), *M. luteus* (2 µg), or with *M. luteus* plus proHP16-Xa (100 ng), factor Xa (100 ng), or HP16-Xa (100 ng) activated by factor Xa (100 ng). After incubation for 10 min at room temperature, PO activity was measured as described under "Materials and methods." The bars represent mean ± SD (n = 2). Bars labeled with different letters are significantly different (Analysis of Variance and Newman-Keuls test, $p < 0.05$).

B) Plasma samples (3 µL) were mixed with *M. luteus* (2 µg), GF buffer (20 mM Tris-HCl, 150 mM NaCl, pH 8.0), or *M. luteus* plus GF buffer. Mixtures were incubated and assayed for PO activity as described under "Materials and methods." Buffer = 20 mM Tris-HCl, 20 mM NaCl, 6.7 mM $CaCl_2$, pH 7.5, GF = gel filtration buffer

C) Plasma samples (2 µL) were mixed with buffer (20 mM Tris-HCl, 20 mM NaCl, 6.7 mM $CaCl_2$, pH 7.5), *M. luteus* (2 µg) or saline, and different concentrations of NaCl. After incubation for 10 min at room temperature, PO activity was measured as described under "Materials and methods." Each point represents mean ± SD (n = 3 for *M. luteus*; n = 2 for saline). Work completed by Dr. Di Wu.

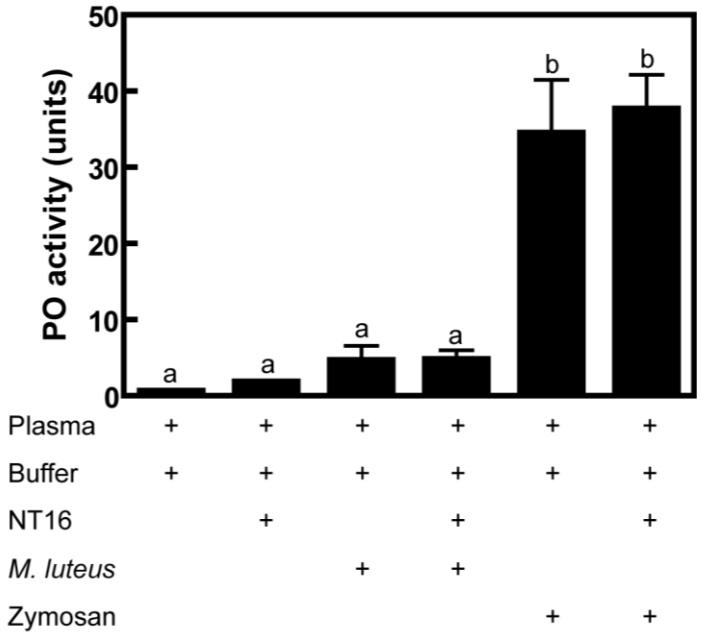

Figure A-2. Prophenoloxidase activation assay conducted with NT16.

Samples of plasma (3 µL) were mixed with buffer (20 mM Tris-HCl, 20 mM NaCl, 6.7 mM $CaCl_2$, pH 7.5), *M. luteus* (2 µg), zymosan (2 µg), NT16 (100 ng), *M. luteus* plus NT16, or zymosan plus NT16. After incubation for 10 min at room temperature, PO activity was measured as described under "Materials and methods." The bars represent mean ± SD (n = 3). Bars labeled with different letters are significantly different (Analysis of Variance and Newman-Keuls test, $p < 0.05$).

Appendix B - Serpin-3

Antibacterial Activity Assay

HP8 cleaves the cytokine precursor proSpätzle to stimulate the production of antimicrobial peptides (An et al., 2009), and serpin-1J inhibits HP8 to regulate this process (An et al., 2011). In addition, results presented in this dissertation revealed that serpin-3 also forms a complex with HP8 (Figures 3-2 and 3-3). Therefore, I tested the hypothesis that serpin-3 might be a biologically relevant inhibitor of HP8.

Materials and methods

Day 2 fifth instar larvae (8 larvae/treatment) were injected with antiserum to serpin-3 (50 µL), 0.85% NaCl (saline; 50 µL), or pre-immune serpin-3 serum as a control (50 µL) Larvae were held at room temperature for 25 min, placed on ice for 5 min, and then injected with *M. luteus* (100 ng in 50 µL) or filter sterilized water (50 µL). After 24 h, hemolymph was collected on ice and centrifuged at 7000 × g for 25 min at 4°C to remove hemocytes. Aliquots (200-300 µL) of each plasma sample were heated at 95°C for 5 min, followed by centrifugation at 10000 × g for 8 min to remove large proteins. Supernatants were placed at -20°C until use.

An overnight culture (3 mL) of *E. coli* strain XL1-Blue was started by inoculating a single colony from a streak plate into LB without antibiotics. The culture was grown at 37°C with shaking at 275 rpm. Fresh LB (3 mL) was inoculated with 60 µL of the overnight culture and grown at 37°C with shaking at 275 rpm for 4 h. To create a good bacterial lawn, 50 µL of *E. coli* was added to 20 mL of LB plus 1% agar held at 47°C and poured into a petri dish. Plates were held at room temperature for 10 min and then placed at 4°C for 30 min. Wells were made in the LB agar plates using a metal tool with a 4 mm diameter opening and removing the agar plug with a sterile toothpick. Liquid was removed from each well and 15 µL of each sample to be tested was added. Water was used as a negative control and plasma samples from larvae injected with *M. luteus* (100 µg) only were used as a positive control. Plates were placed in a 37°C incubator for 19-21 h and were not inverted. The diameter of each zone of inhibition was measured three times, averaged, and divided by 2 to obtain the radius. The radius was used to calculate the area ($A = \pi r^2$) of the zone of inhibition (= area of entire circle – area of sample well).

Results and conclusions

Injection of serpin-3 antibody was based on the idea that the antibody should inactivate serpin-3 protein in the hemolymph, which might result in increased antimicrobial activity due to poor regulation of HP8. However, there was no difference in plasma samples from larvae injected with serpin-3 antibody or pre-immune serum in anti-*E. coli* activity (Figure B-1). To test whether the serpin-3 antibody recognizes native serpin-3 protein in plasma, I used the Ouchterlony method to analyze the interaction of serpin-3 antiserum with recombinant serpin-3 and serpin-3 in plasma. There was no detectable precipitin line for serpin-3 interaction with antibody, even though this antibody binds to denatured serpin-3. This result indicates that this antiserum probably does not inactivate serpin-3 and thus, the *in vivo* experiment with injection of serpin-3 antiserum cannot be interpreted.

Impact of Heparin on the Inhibitory Activity of Serpin-3

Heparin increases the inhibitory activity of antithrombin against thrombin to regulate the blood coagulation cascade in vertebrates (Olson et al., 2010). Upon binding of heparin pentasaccharide to antithrombin, antithrombin undergoes a conformational change to expose the hinge region of the reactive center loop from β-sheet A, which makes the P1-P1' site accessible for recognition and cleavage by thrombin (Li et al., 2004). Like antithrombin, SPN48 from *Tenebrio molitor* contains a partially inserted reactive center loop, and the addition of full-length heparin, but not the pentasaccharide unit of heparin, enhanced the reactivity of SPN48 with Spätzle-processing enzyme (Park et al., 2011). Although it is not known if the hinge region of serpin-3 is partially inserted into β-sheet A, I designed experiments to investigate the hypothesis that the addition of heparin may enhance the inhibitory activity of serpin-3 against PAP-1 and PAP-3.

Materials and methods-PAP-1/PAP-3

For PAP-1 a molar ratio of 1:1 (0.63 pmol serpin-3/0.63 pmol PAP-1) was used while a molar ratio of 0.5:1 (0.77 pmol serpin-3/1.5 pmol PAP-3) was used for PAP-3. Regardless of the proteinase under investigation, serpin-3 was incubated with 250 ng of heparin (Sigma H3393-50KU) in buffer (20 mM Tris-HCl, 250 mM NaCl, pH 8.0) for 10 min at room temperature, followed by the addition of bovine serum albumin (2 µg) and PAP-1/PAP-3 and incubation for

another 10 min. All mixtures were in a total volume of 11.6 µL for PAP-1 and 22.3 µL for PAP-3 (adjusted with 20 mM Tris-HCl, 250 mM NaCl, pH 8.0 before incubation). Samples were spotted into a 96-well plate and 200 µL of 50 µM IEAR*p*Na in 0.1 M Tris-HCl, 0.1 M NaCl, 5 mM $CaCl_2$, pH 8.0. Absorbance at 405 nm was measured continuously for 30 min in a PowerWave XS plate reader (BioTek). One unit of activity was defined as a change in A_{405} of 0.001/min. Percent inhibition was determined using the following formula: [1 – (slope serpin-3/slope PAP-1/PAP-3 only)]*100 and residual PAP-1 or PAP-3 activity (%) was calculated as 100 – percent inhibition.

Results and conclusions

At a molar ratio of 1:1, serpin-3 inhibited PAP-1 amidase activity by 64-80% which resulted in an average residual activity of 28% (Figure B-2A). When serpin-3 was pre-incubated with heparin before addition of PAP-1, percent inhibition by serpin-3 was 38-40% and average residual PAP-1 activity was 61%. Similar results were obtained when the proteinase was changed from PAP-1 to PAP-3 (Figure B-2B). At a molar ratio of 0.5:1, serpin-3 inhibited PAP-3 amidase activity by 89-94% which resulted in an average residual PAP-3 activity of 8.5%. Incubation of serpin-3 with heparin before the addition of PAP-3 resulted in lower levels of inhibition by serpin-3 (57-70%) and higher levels of average residual PAP-3 activity (37.5%). Although these results suggest that heparin does not increase the efficiency of serpin-3 as an inhibitor of PAP-1 or PAP-3, kinetic experiments (e.g. determination of the association rate constant with and without heparin) are needed to provide a conclusive answer to the hypothesis tested (Huang et al., 2011).

References

An C, Ishibashi J, Ragan EJ, Jiang H, & Kanost MR (2009) Functions of *Manduca sexta* hemolymph proteinases HP6 and HP8 in two innate immune pathways. *J Biol Chem* **284**: 19716-19726

An C, Ragan EJ, & Kanost MR (2011) Serpin-1 splicing isoform J inhibits the proSpätzle-activating proteinase HP8 to regulate expression of antimicrobial hemolymph proteins in *Manduca sexta*. *Dev Comp Immunol* **35**: 135-141

Huang X, Rezaie AR, Broze GJ,Jr, & Olson ST (2011) Heparin is a major activator of the anticoagulant serpin, protein Z-dependent protease inhibitor. *J Biol Chem* **286**: 8740-8751

Li W, Johnson DJ, Esmon CT, & Huntington JA (2004) Structure of the antithrombin-thrombin-heparin ternary complex reveals the antithrombotic mechanism of heparin. *Nat Struct Mol Biol* **11**: 857-862

Olson ST, Richard B, Izaguirre G, Schedin-Weiss S, & Gettins PG (2010) Molecular mechanisms of antithrombin-heparin regulation of blood clotting proteinases. A paradigm for understanding proteinase regulation by serpin family protein proteinase inhibitors. *Biochimie* **92**: 1587-1596

Park SH, Jiang R, Piao S, Zhang B, Kim EH, Kwon HM, Jin XL, Lee BL, & Ha NC (2011) Structural and functional characterization of a highly specific serpin in the insect innate immunity. *J Biol Chem* **286**: 1567-1575

Figures

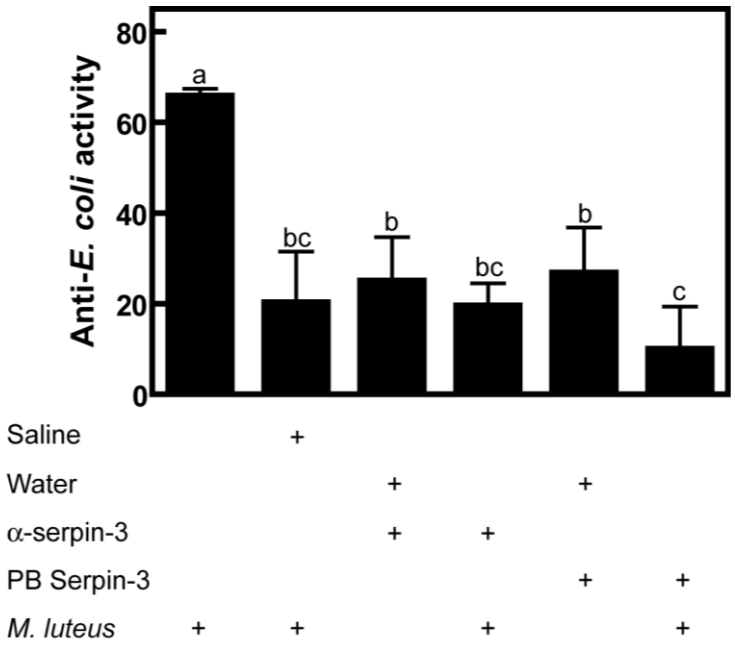

Figure B-1. Production of antimicrobial peptides is not stimulated by injection of antiserum to serpin-3.

Antimicrobial activity of plasma assayed against *E. coli*. Plasma from larvae injected with 0.85% NaCl (saline; 50 µL), antiserum to serpin-3 (50 µL), or pre-immune serpin-3 serum (50 µL) followed by filter sterilized water (50 µL) of *M. luteus* (100 ng in 50 µL). The positive control was plasma injected with *M. luteus* (100 µg) only. The bars represent mean ± SD (n = 8). Bars labeled with different letters are significantly different (Analysis of Variance and Newman-Keuls test, $p < 0.05$). PB = pre-immune serum

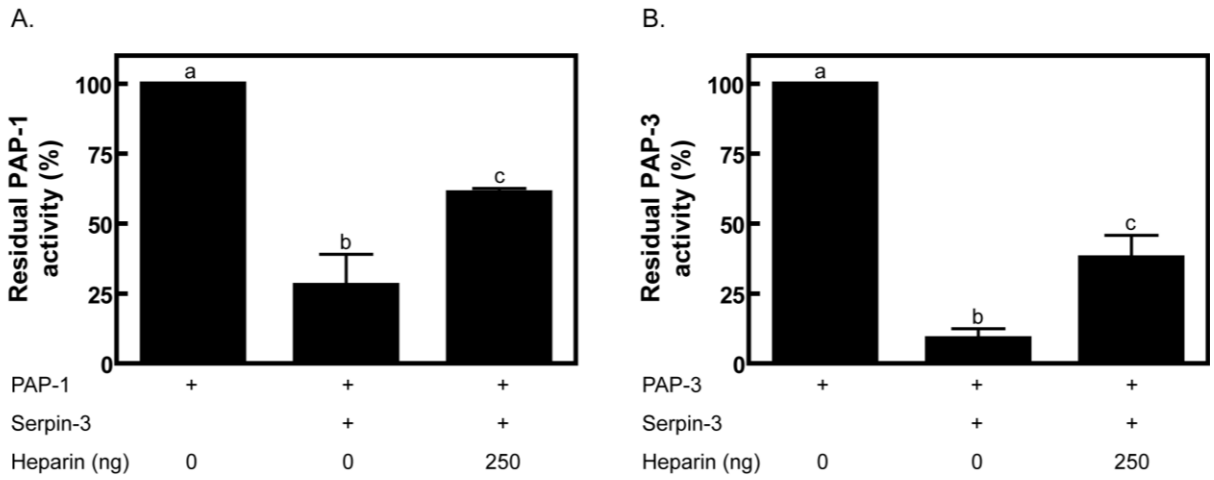

Figure B-2. Residual PAP-1 and PAP-3 activity in the presence of serpin-3 and heparin. Residual PAP-1 (A) or PAP-3 (B) activity was measured with serpin-3 (1:1 or 0.5:1 molar ratio, respectively), BSA (2 µg), and with heparin (250 ng). PAP-1 or PAP-3 alone was used as a control. Serpin-3 and heparin were incubated for 10 min followed by incubation with PAP-1 or PAP-3 for another 10 min. Samples were mixed with 200 µL of 50 µM IEAR*p*Na in 0.1 M Tris-HCl, 0.1 M NaCl, 5 mM $CaCl_2$, pH 8.0. Absorbance at 405 nm was measured continuously for 30 min in a PowerWave XS plate reader (BioTek). One unit of activity was defined as a change in A_{405} of 0.001/min. Percent inhibition was determined using the following formula: [1 – (slope serpin-3/slope PAP-1/PAP-3 only)]*100 and residual PAP-1 or PAP-3 activity (%) was calculated as 100 – percent inhibition. The bars represent mean ± SD (n = 2). Bars labeled with different letters are significantly different (Analysis of Variance and Newman-Keuls test, $p < 0.05$).

Tables

Table B-1. MS/MS results for immunoaffinity purified proteins identified in Table 3-1.

Band	Protein name	Peptide count	Calc. mass	Obsrv. mass	± da	± ppm	Start	End	Peptide sequence	Ion score	C. I. %
1	apolipophorin-1	38	675.3209	675.3332	0.0123	18	2428	2432	AEWNR		
			696.3715	696.3672	-0.0043	-6	2415	2420	AAPYFK		
			749.4192	749.4098	-0.0094	-13	1200	1205	INFDLK		
			758.4155	758.4235	0.008	11	1255	1260	NNLEIR		
			800.4624	800.4606	-0.0018	-2	1121	1127	IDGQVIR		
			907.4631	907.4647	0.0016	2	2421	2427	KVEDNFR		
			917.4686	917.4824	0.0138	15	2407	2414	DVEAVTQR		
			949.5717	949.5607	-0.011	-12	1233	1240	ITFSQILK		
			952.4669	952.4696	0.0027	3	2291	2297	TQQCLFR		
			987.5621	987.5593	-0.0028	-3	3051	3059	VFLVGHTSK		
			999.5945	999.5973	0.0028	3	809	818	LNLIGAATAR	16	0
			1037.5626	1037.5737	0.0111	11	1616	1624	NLQSTFSLK		
			1037.5779	1037.5737	-0.0042	-4	3085	3092	YDRIPFVK		
			1126.5851	1126.6042	0.0191	17	1578	1588	RGSGASTISYK		
			1129.6212	1129.6255	0.0043	4	819	828	LDVATNIDIR		
			1160.6058	1160.6061	0.0003	0	829	838	QIFQSPQNAK		
			1192.6361	1192.6287	-0.0074	-6	1347	1356	YELSGFVLHK		
			1215.652	1215.6569	0.0049	4	2204	2214	AVAEIGFFHPK		
			1226.6237	1226.634	0.0103	8	2103	2112	DEVSDRRPPR		
			1243.6178	1243.6294	0.0116	9	1085	1095	LGFSVQGNEHR		
			1258.6313	1258.6445	0.0132	10	1698	1707	YLDDYTLTVR	21	0
			1344.6655	1344.6671	0.0016	1	1962	1972	RLEFHATNDNK		
			1433.7131	1433.7307	0.0176	12	1312	1324	ANLNNANLEAFSR	6	0
			1435.7903	1435.7817	-0.0086	-6	1535	1547	AHTVAELVLPTER		
			1438.7583	1438.7559	-0.0024	-2	484	496	LVHCAVDNNVKAR		
			1474.7577	1474.7802	0.0225	15	3060	3071	HPYPILYDTDLK		
			1500.7805	1500.7858	0.0053	4	2113	2124	FTLDLHINKEDR		
			1500.7845	1500.7858	0.0013	1	2377	2388	ENFNYFLNALKK		
			1535.6431	1535.6671	0.024	16	2881	2893	ICSSESEFGNSYR		
			1539.839	1539.8508	0.0118	8	3256	3268	QFIQTAAHNIIQR		
			1615.8439	1615.8401	-0.0038	-2	1185	1199	GSDVVLAFNNQLNPK		
			1638.8962	1638.881	-0.0152	-9	1357	1371	TKPNDVNVGFIGHLK		

Band	Protein name	Peptide count	Calc. mass	Obsrv. mass	± da	± ppm	Start	End	Peptide sequence	Ion score	C. I. %
1	apolipophorin-1		1652.9119	1652.9178	0.0059	4	2355	2369	NIAHGALFLQDNLVK		
			1659.8601	1659.8726	0.0125	8	2735	2749	AVVVNGQHIFTFDGR	10	0
			1703.8018	1703.8121	0.0103	6	2237	2252	IESSASLCHSALGTDR		
			1704.83	1704.829	-0.001	-1	2276	2290	AIDVEGSFNVNQQQR		
			1793.8817	1793.8896	0.0079	4	1874	1889	AHPVLDIQYHSPSSDK		
			1851.0083	1851.0197	0.0114	6	1518	1534	RTEVNIHQDGILAVTGK		
2	serpin-3a	21	686.4195	686.4189	-0.0006	-1	345	350	LEGVLR	36	0
			877.489	877.491	0.002	2	370	376	GQLLYQR	31	0
			896.5815	896.5709	-0.0106	-12	329	336	LVDVILPK		
			935.5018	935.4923	-0.0095	-10	263	270	TVPFMNVK		
			1057.6	1057.604	0.004	4	311	319	VLNNLSELR	41	0
			1107.4928	1107.5018	0.009	8	337	344	FQFEYMSR	39	0
			1149.5721	1149.5765	0.0044	4	163	172	IYMGEGVQPR	34	0
			1182.5824	1182.5845	0.0021	2	320	328	TEMIYLQER		
			1187.6095	1187.6061	-0.0034	-3	175	184	FAAIAQEFYK		
			1193.6888	1193.6949	0.0061	5	141	150	FSTIIESLKR	35	0
			1265.5433	1265.548	0.0047	4	271	280	DNFYYVDSSR	73	99.896
			1335.6903	1335.6964	0.0061	5	122	134	SELASALGFGLDR	91	99.999
			1363.6852	1363.6908	0.0056	4	151	162	ESPDYILNLGSR	56	95.632
			1380.7271	1380.7319	0.0048	3	189	200	TTNFFKPEVAAR	44	22.858
			1460.7128	1460.723	0.0102	7	201	213	EINNWVSNATQGK		
			1487.8428	1487.8501	0.0073	5	107	121	LALAILTEAATGSTR	66	99.544
			1510.7173	1510.7234	0.0061	4	356	369	EAFEDTASFPGIAR	70	99.791
			1731.9639	1731.96	-0.0039	-2	90	106	VASTSNANFLLSPLGLK	61	98.496
			1793.9618	1793.9669	0.0051	3	295	310	YAMYIVVPNSLTGLPR		
			2011.0131	2011.0067	-0.0064	-3	30	49	AVFGYSALDQAALV GAESNK		
			2376.2405	2376.2366	-0.0039	-2	386	408	TGIEVNELGSVAFSAT QIGIQNK		
	PAP-3	8	800.4624	800.4647	0.0023	3	276	282	NDIGLIR	32	0
			945.504	945.4991	-0.0049	-5	354	360	QIELWEK		
			956.5635	956.5653	0.0018	2	275	282	RNDIGLIR	28	0
			1116.6445	1116.6364	-0.0081	-7	193	203	LLCGGVLISGK		
			1222.5634	1222.5707	0.0073	6	344	353	CQPSYAVQNR	37	0
			1423.7329	1423.741	0.0081	6	261	272	TIPHPEYNPISR	32	0
			1501.8162	1501.824	0.0078	5	332	343	LHVQLPFISYER		

Band	Protein name	Peptide count	Calc. mass	Obsrv. mass	± da	± ppm	Start	End	Peptide sequence	Ion score	C. I. %
2	PAP-3		2467.3125	2467.2949	-0.0176	-7	204	226	YVLTAGHCLTGPVLQI GTPTNVR		
3	serpin-3a	18	686.4195	686.4183	-0.0012	-2	345	350	LEGVLR	23	0
			877.489	877.4916	0.0026	3	370	376	GQLLYQR	25	0
			951.4968	951.4933	-0.0035	-4	263	270	TVPFMNVK		
			1057.6	1057.6083	0.0083	8	311	319	VLNNLSELR	42	0
			1107.4928	1107.5112	0.0184	17	337	344	FQFEYMSR		
			1165.567	1165.5691	0.0021	2	163	172	IYMGEGVQPR	18	0
			1182.5824	1182.5913	0.0089	8	320	328	TEMIYLQER		
			1187.6095	1187.6122	0.0027	2	175	184	FAAIAQEFYK	60	98.144
			1193.6888	1193.6975	0.0087	7	141	150	FSTIIESLKR		
			1265.5433	1265.5508	0.0075	6	271	280	DNFYYVDSSR	70	99.789
			1335.6903	1335.7009	0.0106	8	122	134	SELASALGFGLDR	57	96.537
			1363.6852	1363.6947	0.0095	7	151	162	ESPDYILNLGSR	39	0
			1380.7271	1380.7345	0.0074	5	189	200	TTNFFKPEVAAR	35	0
			1487.8428	1487.8552	0.0124	8	107	121	LALAILTEAATGSTR	41	0
			1510.7173	1510.7258	0.0085	6	356	369	EAFEDTASFPGIAR	50	80.254
			1731.9639	1731.962	-0.0019	-1	90	106	VASTSNANFLLSPLGLK		
			1809.9568	1809.9602	0.0034	2	295	310	YAMYIVVPNSLTGLPR		
			2011.0131	2011.0167	0.0036	2	30	49	AVFGYSALDQAALV GAESNK		
	proPO-p2	18	662.362	662.3708	0.0088	13	476	481	GPVYAR		
			688.4391	688.4264	-0.0127	-18	509	514	IFIAPK		
			708.3828	708.3824	-0.0004	-1	202	206	LAYWR		
			809.3787	809.3787	0	0	469	475	GLDFSDR		
			809.5243	809.522	-0.0023	-3	183	189	TPIIIPR	18	0
			844.3987	844.4012	0.0025	3	401	406	DPFFYR		
			1067.464	1067.4773	0.0133	12	52	60	FGDEEEVSR		
			1087.5378	1087.5468	0.009	8	567	576	DLSIQGSDPR		
			1127.5691	1127.5687	-0.0004	0	682	691	LSDVTEPNPR		
			1199.6167	1199.6123	-0.0044	-4	519	528	NLPWALSDQR		
			1279.6681	1279.67	0.0019	1	149	159	VQNYAEIFPAK		
			1311.6692	1311.6791	0.0099	8	160	170	FLDSQVFTQAR	46	46.485
			1324.7021	1324.7091	0.007	5	482	491	FTHLNHRPFR	6	0
			1478.6394	1478.6515	0.0121	8	190	201	DYTATDLEEEHR		
			1503.8165	1503.8278	0.0113	8	537	550	FVVPLSAGENTITR		
			1745.8486	1745.855	0.0064	4	305	319	RPVDGLNVTIDDMER		

Band	Protein name	Peptide count	Calc. mass	Obsrv. mass	± da	± ppm	Start	End	Peptide sequence	Ion score	C. I. %
3	proPO-p2		1870.9181	1870.9237	0.0056	3	551	566	QSTESSLTIPFEQTFR	41	0
			1897.9119	1897.9202	0.0083	4	267	281	FSDWREPIPEAYYPK		
	proPO-p1	12	656.3514	656.3579	0.0065	10	284	288	TWPPR		
			783.4147	783.4184	0.0037	5	289	295	FAGSVFR	29	0
			803.4409	803.4422	0.0013	2	428	434	LDFPGVR	15	0
			805.4202	805.4252	0.005	6	462	468	GLDFTPR		
			844.3987	844.4012	0.0025	3	399	404	DPFFYR		
			1127.5587	1127.5687	0.01	9	96	104	LIDIFMGMR		
			1259.6306	1259.6298	-0.0008	-1	408	417	FVDDVFNIYK		
			1352.6692	1352.6796	0.0104	8	546	557	SVDSSVTIPYER		
			1417.7434	1417.7543	0.0109	8	450	461	TLWQQSTVELGR		
			1555.855	1555.8632	0.0082	5	435	449	VSSVGIEGARPNTLR		
			1754.8683	1754.8617	-0.0066	-4	232	245	GELFYYMHQQIIGR		
			2190.0496	2190.0586	0.009	4	177	195	MPVNVPINYTANTTEPEQR		
4	serpin-3a	26	686.4195	686.4213	0.0018	3	345	350	LEGVLR	32	0
			822.4468	822.4508	0.004	5	436	442	QTLFTGR	56	94.945
			877.489	877.4942	0.0052	6	370	376	GQLLYQR	36	0
			896.5815	896.5745	-0.007	-8	329	336	LVDVILPK		
			935.5018	935.4984	-0.0034	-4	263	270	TVPFMNVK		
			1037.5878	1037.5886	0.0008	1	141	149	FSTIIESLK		
			1057.6	1057.6075	0.0075	7	311	319	VLNNLSELR	42	0
			1107.4928	1107.5023	0.0095	9	337	344	FQFEYMSR	51	86.946
			1149.5721	1149.5814	0.0093	8	163	172	IYMGEGVQPR	17	0
			1182.5824	1182.5909	0.0085	7	320	328	TEMIYLQER		
			1187.6095	1187.6112	0.0017	1	175	184	FAAIAQEFYK		
			1193.6888	1193.6973	0.0085	7	141	150	FSTIIESLKR	35	0
			1218.6365	1218.6389	0.0024	2	443	454	VSDPALVDGAFK		
			1265.5433	1265.5524	0.0091	7	271	280	DNFYYVDSSR	76	99.959
			1289.6736	1289.6711	-0.0025	-2	443	455	VSDPALVDGAFKA		
			1335.6903	1335.7021	0.0118	9	122	134	SELASALGFGLDR	96	100
			1363.6852	1363.6971	0.0119	9	151	162	ESPDYILNLGSR	72	99.888
			1380.7271	1380.7406	0.0135	10	189	200	TTNFFKPEVAAR	56	95.161
			1460.7128	1460.7164	0.0036	2	201	213	EINNWVSNATQGK		
			1487.8428	1487.8572	0.0144	10	107	121	LALAILTEAATGSTR	59	97.586
			1510.7173	1510.7324	0.0151	10	356	369	EAFEDTASFPGIAR	75	99.947
			1731.9639	1731.9697	0.0058	3	90	106	VASTSNANFLLSPLGLK	108	100
			1809.9568	1809.9647	0.0079	4	295	310	YAMYIVVPNSLTGLPR	26	0

Band	Protein name	Peptide count	Calc. mass	Obsrv. mass	± da	± ppm	Start	End	Peptide sequence	Ion score	C. I. %
4	serpin-3a		2011.0131	2011.0197	0.0066	3	30	49	AVFGYSALDQAALV GAESNK	143	100
			2376.2405	2376.2456	0.0051	2	386	408	TGIEVNELGSVAFSAT QIGIQNK		
			3228.4829	3228.4836	0.0007	0	409	435	FGEDSDINYEVVANKPFM FFIQEESTR		
5	serpin-3a	22	686.4195	686.4189	-0.0006	-1	345	350	LEGVLR	35	0
			877.489	877.4921	0.0031	4	370	376	GQLLYQR	36	0
			896.5815	896.5699	-0.0116	-13	329	336	LVDVILPK		
			951.4968	951.4894	-0.0074	-8	263	270	TVPFMNVK	15	0
			1037.5878	1037.5834	-0.0044	-4	141	149	FSTIIESLK		
			1057.6	1057.6055	0.0055	5	311	319	VLNNLSELR	43	0.839
			1107.4928	1107.5028	0.01	9	337	344	FQFEYMSR	26	0
			1165.567	1165.5658	-0.0012	-1	163	172	IYMGEGVQPR	13	0
			1182.5824	1182.5892	0.0068	6	320	328	TEMIYLQER		
			1187.6095	1187.6093	-0.0002	0	175	184	FAAIAQEFYK	45	32.026
			1193.6888	1193.6957	0.0069	6	141	150	FSTIIESLKR		
			1265.5433	1265.5499	0.0066	5	271	280	DNFYYVDSSR	83	99.991
			1335.6903	1335.6995	0.0092	7	122	134	SELASALGFGLDR	85	99.993
			1363.6852	1363.6936	0.0084	6	151	162	ESPDYILNLGSR	76	99.951
			1380.7271	1380.7372	0.0101	7	189	200	TTNFFKPEVAAR	63	98.918
			1460.7128	1460.7144	0.0016	1	201	213	EINNWVSNATQGK		
			1487.8428	1487.8544	0.0116	8	107	121	LALAILTEAATGSTR	56	95.042
			1510.7173	1510.7286	0.0113	7	356	369	EAFEDTASFPGIAR	75	99.931
			1731.9639	1731.9664	0.0025	1	90	106	VASTSNANFLLSPLGLK	83	99.989
			1809.9568	1809.965	0.0082	5	295	310	YAMYIVVPNSLTGLPR	30	0
			2011.0131	2011.0162	0.0031	2	30	49	AVFGYSALDQAALV GAESNK	94	100
			2376.2405	2376.2458	0.0053	2	386	408	TGIEVNELGSVAFSAT QIGIQNK		
6	immulectin-2	11	1174.5669	1174.5679	0.001	1	71	80	FAMASMMILK		
			1239.6078	1239.621	0.0132	11	30	39	YLDVIDGWMK		
			1308.6833	1308.6892	0.0059	5	97	108	GDFFSVEGIPLK		
			1436.7783	1436.7878	0.0095	7	97	109	GDFFSVEGIPLKK	38	0
			1450.7438	1450.7612	0.0174	12	84	96	QSVFTGIHATFSR	57	96.743

Band	Protein name	Peptide count	Calc. mass	Obsrv. mass	± da	± ppm	Start	End	Peptide sequence	Ion score	C. I. %
6	immulectin-2		1472.7394	1472.7573	0.0179	12	40	51	LHEIPANWHEAR	45	49.896
			1513.645	1513.6583	0.0133	9	141	152	SCSATFNYICYK	23	0
			1822.948	1822.9462	-0.0018	-1	54	70	CHLEGAVLASPLNSNLK	56	95.586
			1990.9844	1991.0005	0.0161	8	217	233	EIFAQHLPASMVGNFWK	19	0
			2091.9724	2091.9841	0.0117	6	192	210	AYMTCAAEGGYLTIINSEK		
			2408.0923	2408.094	0.0017	1	304	324	DPNSLLCDPTSDSFDDIIDIR	47	69.46
	immulectin-2a	11	1225.5922	1225.6074	0.0152	12	30	39	YLDVVDGWMK		
			1308.6833	1308.6892	0.0059	5	97	108	GDFFSVEGIPLK		
			1436.7783	1436.7878	0.0095	7	97	109	GDFFSVEGIPLKK	38	0
			1450.7438	1450.7612	0.0174	12	84	96	QSVFTGIHATFSR	57	96.743
			1472.7394	1472.7573	0.0179	12	40	51	LHEIPANWHEAR	45	49.896
			1539.697	1539.7148	0.0178	12	141	152	LCSATFNYICYK		
			1822.948	1822.9462	-0.0018	-1	54	70	CHLEGAVLASPLNSNLK	56	95.586
			1990.9844	1991.0005	0.0161	8	217	233	EIFAQHLPASMVGNFWK	19	0
			2091.9724	2091.9841	0.0117	6	192	210	AYMTCAAEGGYLTIINSEK		
			2408.0923	2408.094	0.0017	1	304	324	DPNSLLCDPTSDSFDDIIDIR	47	69.46
			2944.5457	2944.501	-0.0447	-15	54	80	CHLEGAVLASPLNSNLKF AMSSIMILK		
	SPH-1b	6	926.5305	926.5455	0.015	16	310	317	IEVPVVDR		
			1054.6255	1054.6426	0.0171	16	309	317	KIEVPVVDR		
			1067.4792	1067.4946	0.0154	14	227	234	EPYPYQDR	42	5.186
			1468.6914	1468.7181	0.0267	18	172	184	IEPVNENEPDGQK		
			1524.7078	1524.7241	0.0163	11	227	238	EPYPYQDRDVSR		
			1865.8334	1865.85	0.0166	9	353	369	GDGGSPLVCPSEYEKDR		
7	immulectin-3	15	766.4093	766.4072	-0.0021	-3	168	174	GYQLSAK		
			791.4661	791.4618	-0.0043	-5	221	227	YPTGLIK	45	56.882
			892.4596	892.4558	-0.0038	-4	292	298	VPFICEK	42	17.651
			1163.5361	1163.5365	0.0004	0	281	291	SGQLDDIGCAK	42	14.953
			1361.6631	1361.6565	-0.0066	-5	299	310	HPNNIMPVPNNV	37	0
			1541.6823	1541.6815	-0.0008	-1	154	167	TAELSMTECGTVDK		
			1736.8907	1736.8969	0.0062	4	181	194	FHNYGLPWSLAYLR	34	0
			1802.7108	1802.7159	0.0051	3	115	129	DMFTEEYSSGPHCAR	56	96.455
			2059.8596	2059.8618	0.0022	1	113	129	TRDMFTEEYSSGPHCAR	20	0
			2156.1379	2156.1387	0.0008	0	195	215	CIAEGGQLAVINSAV EANVLK	96	100
			2305.0686	2305.0789	0.0103	4	154	174	TAELSMTECGTVDKG YQLSAK		

Band	Protein name	Peptide count	Calc. mass	Obsrv. mass	± da	± ppm	Start	End	Peptide sequence	Ion score	C. I. %
7	immulectin-3		2352.0693	2352.0681	-0.0012	-1	228	248	GGYAGGAFLGFHDWN NNNVWR	67	99.73
			2454.2043	2454.2114	0.0071	3	130	151	LIPQEGLVAGSCSDALP YICYK	51	87.848
			3560.5803	3560.5903	0.01	3	249	280	TVNGQTLEEAGYANWGV TQPDSSVQNCGQMFR		
			3676.981	3676.9377	-0.0433	-12	78	112	IEHLSTGVHTGVHNTISPVV FNSIEGVPLSALPVR		
	immulectin-4	7	739.3555	739.3571	0.0016	2	127	131	QYCLR		
			1041.457	1041.4591	0.0021	2	280	287	QYHGAMYR		
			1131.5542	1131.5597	0.0055	5	244	252	DLNQSNVWR	44	50.266
			1365.7274	1365.7318	0.0044	3	38	49	LHLVPATWSDAR		
			1387.6384	1387.6451	0.0067	5	143	153	CSEALPYICFK		
			1420.7583	1420.765	0.0067	5	231	243	GSEPVNVIFVGFR		
			1548.8533	1548.8633	0.01	6	230	243	KGSEPVNVIFVGFR		
	immulectin-III	7	739.3555	739.3571	0.0016	2	123	127	QYCLR		
			1041.457	1041.4591	0.0021	2	269	276	QYHGAMYR		
			1131.5542	1131.5597	0.0055	5	233	241	DLNQSNVWR	44	50.266
			1420.7583	1420.765	0.0067	5	220	232	GSEPVNVIFVGFR		
			1428.6318	1428.6302	-0.0016	-1	112	122	GIYYEQYDYSK		
			1548.8533	1548.8633	0.01	6	219	232	KGSEPVNVIFVGFR		
			1658.76	1658.7272	-0.0328	-20	1	13	MNRCLGWTCVFSK		
8	attacin-1	14	662.3984	662.3971	-0.0013	-2	185	189	LNLFR	33	0
			848.4148	848.4221	0.0073	9	57	64	VPFAGDDK		
			928.4232	928.4226	-0.0006	-1	204	210	FEMPNFK		
			1056.5183	1056.5178	-0.0005	0	203	210	KFEMPNFK	33	0
			1274.59	1274.5928	0.0028	2	192	202	TTSLDFNADYK		
			1348.7107	1348.7158	0.0051	4	65	77	NVFSAIGGLDLDK		
			1485.7008	1485.7021	0.0013	1	211	223	SDWTPNIGFSFSK	37	0
			1499.7601	1499.7688	0.0087	6	162	176	VGASASAAHTPLFDR	64	99.229
			1517.7118	1517.7067	-0.0051	-3	190	202	DKTTSLDFNADYK	22	0
			1678.8296	1678.8342	0.0046	3	118	131	LNVFHNDNHNLDVK	76	99.951
			1742.882	1742.8871	0.0051	3	160	176	DKVGASASAAHTPLFDR	4	0
			2178.1077	2178.1094	0.0017	1	57	77	VPFAGDDKNVFSAI GGLDLDK	1	0
			2320.1316	2320.1331	0.0015	1	162	184	VGASASAAHTPLFDRN DYSVGGK	2	0

Band	Protein name	Peptide count	Calc. mass	Obsrv. mass	± da	± ppm	Start	End	Peptide sequence	Ion score	C. I. %
8	attacin-1		2589.1423	2589.1633	0.021	8	137	159	TMPDIPHAPDFNTFGG GVDYMFK		
9	attacin-II	10	662.3984	662.4	0.0016	2	169	173	LNLFR	20	0
			718.3882	718.3918	0.0036	5	41	47	VPFGGNK		
			929.4185	929.4253	0.0068	7	188	194	FDTPFMR	4	0
			1057.5135	1057.5251	0.0116	11	187	194	KFDTPFMR	1	0
			1387.7539	1387.7654	0.0115	8	65	78	LSSATAGVALDNIR	30	0
			1397.6696	1397.6749	0.0053	4	174	186	NPSTSLDFNAGFK		
			1528.7866	1528.7988	0.0122	8	146	160	VGASLGAAHTDFINR		
			1751.8711	1751.8807	0.0096	5	79	95	GHGLSLTDTHIPGFGDK		
			1789.8616	1789.8688	0.0072	4	48	64	NNIFSAIGGADFNANHK		
			2183.074	2183.0752	0.0012	1	102	120	LNLFHNNNHDLTANAFATR	1	0
9	dVG-AP3-2	7	662.3984	662.4	0.0016	2	100	104	LNLFR	20	0
	(gloverin)		929.4185	929.4253	0.0068	7	119	125	FDTPFMR	4	0
			1057.5135	1057.5251	0.0116	11	118	125	KFDTPFMR	1	0
			1397.6696	1397.6749	0.0053	4	105	117	NPSTSLDFNAGFK		
			1528.7866	1528.7988	0.0122	8	77	91	VGASLGAAHTDFINR	28	0
			1751.8711	1751.8807	0.0096	5	10	26	GHGLSLTDTHIPGFGDK		
			2183.074	2183.0752	0.0012	1	33	51	LNLFHNNNHDLTANAFATR	1	0

Table B-2. MS/MS results for immunoaffinity purified proteins identified in Table 3-2.

Spot	Protein name	Peptide count	Calc. mass	Obsrv. mass	Peptide delta	Start	End	Peptide sequence	Ion score*	E-value
1	serpin 3a	19	685.4123	685.7074	0.2952	345	350	LEGVLR	31.54	0.0056
			876.4817	876.6934	0.2117	370	376	GQLLYQR	44.45	0.00034
			895.5742	895.8234	0.2492	329	336	LVDVILPK	60.32	9.20E-06
			1036.5804	1036.7894	0.209	141	149	FSTIIESLK	41.5	0.00096
			1056.5927	1056.8774	0.2847	311	319	VLNNLSELR	69.51	1.20E-06
			1148.5648	1148.8834	0.3186	163	172	IYMGEGVQPR	76.34	3.20E-07
			1186.6022	1186.9194	0.3172	175	184	FAAIAQEFYK	58.45	1.60E-05
			1192.6815	1192.9734	0.2919	141	150	FSTIIESLKR	46.88	0.00018
			1197.5699	1197.8434	0.2735	320	328	TEMIYLQER	65.48	3.60E-06
			1264.536	1264.8214	0.2854	271	280	DNFYYVDSSR	71.35	1.10E-06
			1320.7765	1321.5442	0.7677	140	150	KFSTIIESLKR	31.67	0.0071
			1334.683	1335.0754	0.3924	122	134	SELASALGFGLDR	83.79	3.50E-08
			1362.6779	1363.5894	0.9115	151	162	ESPDYILNLGSR	77.48	1.60E-07
			1459.7055	1460.0834	0.3779	201	213	EINNWVSNATQGK	78.05	1.70E-07
			1486.8355	1487.6754	0.84	107	121	LALAILTEAATGSTR	103.34	6.00E-10
			1509.71	1510.1354	0.4255	356	369	EAFEDTASFPGIAR	59.45	1.00E-05
			1730.9567	1731.8314	0.8748	90	106	VASTSNANFLLSPLGLK	84.34	3.60E-08
			1808.9495	1810.0254	1.076	295	310	YAMYIVVPNSLTGLPR	84.41	3.20E-08
			2010.0058	2011.0214	1.0156	30	49	AVFGYSALDQAAL VGAESNK	124.9	5.00E-12
	HP8	2	1012.4978	1012.6834	0.1857	163	171	GSDLPPNWK	27.66	0.024
			1769.7567	1770.2454	0.4888	250	265	DSNFDGLEMEVAGWGK	94.12	4.60E-09
2	serpin 3a	22	685.4123	685.6494	0.2372	345	350	LEGVLR	28.92	0.011
			876.4817	876.6874	0.2057	370	376	GQLLYQR	42.05	0.0006
			895.5742	895.8094	0.2352	329	336	LVDVILPK	60.21	9.40E-06
			1036.5804	1036.8074	0.227	141	149	FSTIIESLK	35.93	0.0035
			1056.5927	1056.8814	0.2887	311	319	VLNNLSELR	70.28	1.00E-06
			1106.4855	1106.6694	0.1839	337	344	FQFEYMSR	34.82	0.0039
			1148.5648	1148.7714	0.2066	163	172	IYMGEGVQPR	78.63	2.00E-07
			1186.6022	1186.9614	0.3592	175	184	FAAIAQEFYK	50.18	0.00011
			1192.6815	1193.2852	0.6036	141	150	FSTIIESLKR	29.19	0.0087
			1197.5699	1197.7854	0.2155	320	328	TEMIYLQER	62.55	7.50E-06
			1264.536	1264.7834	0.2474	271	280	DNFYYVDSSR	51.57	0.00011
			1334.683	1335.0294	0.3464	122	134	SELASALGFGLDR	80.83	7.20E-08
			1362.6779	1363.0294	0.3515	151	162	ESPDYILNLGSR	77.52	1.50E-07
			1379.7197	1380.5234	0.8037	189	200	TTNFFKPEVAAR	57.52	2.40E-05

Spot	Protein name	Peptide count	Calc. mass	Obsrv. mass	Peptide delta	Start	End	Peptide sequence	Ion score*	E-value
2	serpin 3a		1459.7055	1459.9834	0.2779	201	213	EINNWVSNATQGK	72.68	6.00E-07
			1486.8355	1487.1334	0.298	107	121	LALAILTEAATGSTR	103.31	6.00E-10
			1509.71	1510.3974	0.6875	356	369	EAFEDTASFPGIAR	60.09	8.20E-06
			1730.9567	1731.9154	0.9588	90	106	VASTSNANFLLSPLGLK	93.71	4.00E-09
			1808.9495	1809.9854	1.036	295	310	YAMYIVVPNSLTGLPR	81.12	7.00E-08
			1819.9428	1820.7472	0.8044	122	138	SELASALGFGLDRTEVR	54.68	4.80E-05
			2010.0058	2011.0234	1.0176	30	49	AVFGYSALDQAALV GAESNK	104.97	4.90E-10
			2375.2332	2376.3322	1.0989	386	408	TGIEVNELGSVAFSAT QIGIQNK	60.73	9.00E-06
	PAP-3	2	799.4552	799.5854	0.1303	276	282	NDIGLIR	36.69	0.0031
			1500.8089	1501.8472	1.0383	332	343	LHVQLPFISYER	58.43	2.10E-05
3	serpin 3a	22	685.4123	685.6314	0.2192	345	350	LEGVLR	26.81	0.018
			876.4817	876.6514	0.1697	370	376	GQLLYQR	47.48	0.00018
			895.5742	895.7914	0.2172	329	336	LVDVILPK	60.36	9.10E-06
			1036.5804	1036.7834	0.203	141	149	FSTIIESLK	39.24	0.0016
			1056.5927	1056.8414	0.2487	311	319	VLNNLSELR	72.26	6.60E-07
			1148.5648	1148.8514	0.2866	163	172	IYMGEGVQPR	78.41	2.00E-07
			1181.575	1181.8494	0.2744	320	328	TEMIYLQER	67.57	1.80E-06
			1186.6022	1186.9934	0.3912	175	184	FAAIAQEFYK	52.05	6.90E-05
			1192.6815	1193.0034	0.3219	141	150	FSTIIESLKR	47.34	0.00016
			1264.536	1264.8614	0.3254	271	280	DNFYYVDSSR	71.41	1.00E-06
			1320.7765	1321.6642	0.8877	140	150	KFSTIIESLKR	54.59	3.60E-05
			1334.683	1335.6414	0.9584	122	134	SELASALGFGLDR	93.96	3.90E-09
			1362.6779	1363.0654	0.3875	151	162	ESPDYILNLGSR	77.51	1.50E-07
			1379.7197	1379.8954	0.1757	189	200	TTNFFKPEVAAR	47.08	0.00023
			1459.7055	1460.1314	0.4259	201	213	EINNWVSNATQGK	80.75	9.20E-08
			1486.8355	1487.1254	0.29	107	121	LALAILTEAATGSTR	103.37	6.00E-10
			1509.71	1509.9354	0.2255	356	369	EAFEDTASFPGIAR	63.41	4.20E-06
			1730.9567	1731.8452	0.8885	90	106	VASTSNANFLLSPLGLK	69.05	1.80E-06
			1808.9495	1810.0934	1.144	295	310	YAMYIVVPNSLTGLPR	65.65	2.50E-06
			1819.9428	1821.0352	1.0924	122	138	SELASALGFGLDRTEVR	65.23	3.90E-06
			2010.0058	2010.3594	0.3537	30	49	AVFGYSALDQAALV GAESNK	122.16	6.90E-12
			2375.2332	2376.1874	0.9542	386	408	TGIEVNELGSVAFSAT QIGIQNK	56.76	1.80E-05
	immulectin-2b	4	851.3926	851.5694	0.1769	170	175	YVHYDR	40.2	0.00076

Spot	Protein name	Peptide count	Calc. mass	Obsrv. mass	Peptide delta	Start	End	Peptide sequence	Ion score*	E-value
3	immulectin-2b		1157.5647	1157.8334	0.2688	71	80	FAMASMMILK	48.97	0.00016
			1238.6005	1238.8854	0.2849	30	39	YLDVIDGWMK	51.52	7.70E-05
			1449.7365	1450.4542	0.7177	84	96	QSVFTGIHATFSR	49.01	0.0001
	PAP-3	4	799.4552	799.6554	0.2003	276	282	NDIGLIR	36.35	0.0034
			1084.5917	1084.9154	0.3238	419	427	DWIISNIKP	32.68	0.0055
			1422.7255	1423.0354	0.3099	261	272	TIPHPEYNPISR	38.52	0.0012
			1500.8089	1501.6702	0.8613	332	343	LHVQLPFISYER	50.58	0.00013
4	serpin 3a	23	685.4123	685.6214	0.2092	345	350	LEGVLR	29.98	0.0085
			876.4817	876.6874	0.2057	370	376	GQLLYQR	44.36	0.00035
			895.5742	895.8534	0.2792	329	336	LVDVILPK	54.51	3.50E-05
			1036.5804	1036.8814	0.301	141	149	FSTIIESLK	30.46	0.012
			1056.5927	1056.8654	0.2727	311	319	VLNNLSELR	68.26	1.60E-06
			1148.5648	1148.8254	0.2606	163	172	IYMGEGVQPR	81.16	1.10E-07
			1181.575	1181.8434	0.2684	320	328	TEMIYLQER	62.25	6.10E-06
			1186.6022	1186.9454	0.3432	175	184	FAAIAQEFYK	53.14	5.40E-05
			1192.6815	1192.9834	0.3019	141	150	FSTIIESLKR	54.89	2.80E-05
			1264.536	1264.9054	0.3694	271	280	DNFYYVDSSR	71.4	9.80E-07
			1320.7765	1321.4842	0.7077	140	150	KFSTIIESLKR	50.24	9.60E-05
			1334.683	1334.9694	0.2864	122	134	SELASALGFGLDR	89.09	1.10E-08
			1362.6779	1363.0654	0.3875	151	162	ESPDYILNLGSR	77.57	1.50E-07
			1379.7197	1380.5554	0.8357	189	200	TTNFFKPEVAAR	50.13	0.00014
			1459.7055	1460.0154	0.3099	201	213	EINNWVSNATQGK	70.99	9.00E-07
			1486.8355	1487.1634	0.328	107	121	LALAILTEAATGSTR	103.41	5.80E-10
			1509.71	1509.9154	0.2055	356	369	EAFEDTASFPGIAR	57.55	1.60E-05
			1730.9567	1731.2474	0.2908	90	106	VASTSNANFLLSPLGLK	88.44	1.40E-08
			1808.9495	1809.1374	0.188	295	310	YAMYIVVPNSLTGLPR	56.85	2.20E-05
			1819.9428	1820.8042	0.8614	122	138	SELASALGFGLDRTEVR	50.64	0.00012
			1887.0578	1888.1632	1.1054	89	106	RVASTSNANFLLSPLGLK	54	5.90E-05
			2010.0058	2010.9994	0.9937	30	49	AVFGYSALDQAALV GAESNK	108.61	2.10E-10
			2375.2332	2376.3202	1.0869	386	408	TGIEVNELGSVAFSAT QIGIQNK	57.26	2.00E-05
	immulectin-2b	6	851.3926	851.5594	0.1669	170	175	YVHYDR	35.75	0.0021
			1141.5697	1141.9034	0.3337	71	80	FAMASMMILK	52.19	6.60E-05
			1254.5955	1254.9374	0.342	30	39	YLDVIDGWMK	51.23	7.80E-05
			1435.7711	1435.9374	0.1663	97	109	GDFFSVEGIPLKK	35.16	0.0038
			1449.7365	1450.6192	0.8827	84	96	QSVFTGIHATFSR	36.23	0.0023

Spot	Protein name	Peptide count	Calc. mass	Obsrv. mass	Peptide delta	Start	End	Peptide sequence	Ion score*	E-value
4	immulectin-2b		1471.732	1472.1982	0.4662	40	51	LHEIPANWHEAR	38	0.0017
	PAP-3	5	799.4552	799.6594	0.2043	276	282	NDIGLIR	30.34	0.014
			1084.5917	1084.9814	0.3898	419	427	DWIISNIKP	40.6	0.00085
			1422.7255	1423.7294	1.0039	261	272	TIPHPEYNPISR	44.82	0.00031
			1500.8089	1501.8234	1.0146	332	343	LHVQLPFISYER	60.74	1.00E-05
			1698.9093	1699.6012	0.6919	414	427	VHSYKDWIISNIKP	23.76	0.042
	immulectin-2a	5	769.3871	769.5814	0.1943	182	187	FHDVPR	25.81	0.022
			851.3926	851.5594	0.1669	170	175	YVHYDR	35.75	0.0021
			1435.7711	1435.9374	0.1663	97	109	GDFFSVEGIPLKK	35.16	0.0038
			1449.7365	1450.6192	0.8827	84	96	QSVFTGIHATFSR	36.23	0.0023
			1471.732	1472.1982	0.4662	40	51	LHEIPANWHEAR	38	0.0017
5	serpin 3a	23	685.4123	685.5994	0.1872	345	350	LEGVLR	32.5	0.0047
			876.4817	876.6634	0.1817	370	376	GQLLYQR	44.61	0.00034
			895.5742	895.8074	0.2332	329	336	LVDVILPK	52.12	6.00E-05
			1036.5804	1036.7574	0.177	141	149	FSTIIESLK	42.29	0.00081
			1056.5927	1056.7954	0.2027	311	319	VLNNLSELR	66.08	2.90E-06
			1106.4855	1106.6734	0.1879	337	344	FQFEYMSR	28.96	0.015
			1148.5648	1148.7654	0.2006	163	172	IYMGEGVQPR	86.3	3.50E-08
			1186.6022	1186.9574	0.3552	175	184	FAAIAQEFYK	51.14	8.60E-05
			1192.6815	1193.7194	1.0379	141	150	FSTIIESLKR	31.78	0.0069
			1197.5699	1197.7754	0.2055	320	328	TEMIYLQER	62.57	7.40E-06
			1264.536	1264.7674	0.2314	271	280	DNFYYVDSSR	71.4	1.10E-06
			1320.7765	1321.4932	0.7167	140	150	KFSTIIESLKR	51.5	7.20E-05
			1334.683	1335.0654	0.3824	122	134	SELASALGFGLDR	83.81	3.60E-08
			1362.6779	1363.0414	0.3635	151	162	ESPDYILNLGSR	77.53	1.50E-07
			1379.7197	1379.8954	0.1757	189	200	TTNFFKPEVAAR	50.15	0.00011
			1459.7055	1459.9894	0.2839	201	213	EINNWVSNATQGK	77.38	2.00E-07
			1486.8355	1487.2454	0.41	107	121	LALAILTEAATGSTR	103.4	5.90E-10
			1509.71	1510.2774	0.5675	356	369	EAFEDTASFPGIAR	62.69	4.30E-06
			1730.9567	1731.8314	0.8748	90	106	VASTSNANFLLSPLGLK	101.55	6.80E-10
			1808.9495	1810.0714	1.122	295	310	YAMYIVVPNSLTGLPR	58.35	1.30E-05
			1819.9428	1820.8852	0.9424	122	138	SELASALGFGLDRTEVR	57.87	2.20E-05
			2010.0058	2010.2154	0.2097	30	49	AVFGYSALDQAALV GAESNK	121.71	7.90E-12
			2375.2332	2376.3802	1.1469	386	408	TGIEVNELGSVAFSAT QIGIQNK	61.63	7.00E-06
	PAP-1	6	928.5342	928.7254	0.1913	233	240	KDDIALVR	51.03	8.80E-05

Spot	Protein name	Peptide count	Calc. mass	Obsrv. mass	Peptide delta	Start	End	Peptide sequence	Ion score*	E-value
5	PAP-1		935.4786	935.7094	0.2308	289	296	LGMPIFDK	55.93	2.70E-05
			959.4924	959.7374	0.2451	305	313	NLGAELTDK	32.41	0.0067
			1016.4709	1016.6114	0.1405	328	337	GDSGGPLMQR	74.42	5.20E-07
			1198.6782	1199.1712	0.493	231	240	NRKDDIALVR	42.05	0.00089
			1433.7303	1434.9234	1.1931	263	276	LATGNDVFVAGWGK	103.89	5.70E-10
6	proPO-p2	22	613.4527	613.5934	0.1408	61	65	KIILK	32.75	0.0059
			687.4319	687.7394	0.3075	509	514	IFIAPK	33.82	0.0051
			808.5171	808.7014	0.1844	183	189	TPIIIPR	41.19	0.00092
			861.4556	861.7114	0.2559	282	289	LDSLTSAR	35.1	0.0055
			956.4096	956.6414	0.2319	530	536	MFIEMDR	39.21	0.002
			1066.4567	1066.6274	0.1707	52	60	FGDEEEVSR	65.96	3.40E-06
			1086.5305	1086.7294	0.1989	567	576	DLSIQGSDPR	47.21	0.00027
			1126.5618	1126.7594	0.1976	682	691	LSDVTEPNPR	56.03	3.30E-05
			1198.6095	1198.7674	0.158	519	528	NLPWALSDQR	46.89	0.00032
			1199.655	1199.8994	0.2444	66	75	NLDKIPEFPK	56.62	2.90E-05
			1278.6608	1279.0514	0.3906	149	159	VQNYAEIFPAK	69.74	8.70E-07
			1310.6619	1311.0854	0.4235	160	170	FLDSQVFTQAR	87.72	1.70E-08
			1326.7044	1327.0194	0.315	519	529	NLPWALSDQRK	55	3.60E-05
			1451.7157	1452.3262	0.6104	469	481	GLDFSDRGPVYAR	40.28	0.00075
			1477.6321	1477.8674	0.2354	190	201	DYTATDLEEEHR	80.89	8.20E-08
			1502.8093	1503.6334	0.8242	537	550	FVVPLSAGENTITR	97.16	1.80E-09
			1590.7831	1591.0634	0.2804	407	419	VHAWVDDIFQSFK	63.2	4.50E-06
			1695.9043	1696.3114	0.4072	323	338	NIEEAIATGNVILPDK	78.59	1.50E-07
			1744.8414	1745.0254	0.184	305	319	RPVDGLNVTIDDMER	72.32	8.30E-07
			1869.9109	1870.3554	0.4446	551	566	QSTESSLTIPFEQTFR	61.86	7.10E-06
			1896.9046	1897.9162	1.0116	267	281	FSDWREPIPEAYYPK	33.25	0.0055
			2012.0789	2012.9032	0.8242	323	341	NIEEAIATGNVILPDKSTK	69.21	1.50E-06
	serpin 3a	5	1148.5648	1148.7674	0.2026	163	172	IYMGEGVQPR	76.22	3.50E-07
			1334.683	1334.9934	0.3104	122	134	SELASALGFGLDR	86.18	2.20E-08
			1486.8355	1487.0214	0.186	107	121	LALAILTEAATGSTR	91.9	8.50E-09
			1509.71	1509.9274	0.2175	356	369	EAFEDTASFPGIAR	63.83	3.80E-06
			1730.9567	1732.0334	1.0768	90	106	VASTSNANFLLSPLGLK	82.78	5.00E-08
7	proPO-p1	23	782.4075	782.6154	0.2079	289	295	FAGSVFR	43.7	0.00059
			802.4337	802.6314	0.1977	428	434	LDFPGVR	39.26	0.002
			804.413	804.6114	0.1984	462	468	GLDFTPR	41.1	0.0015
			921.4668	921.6474	0.1806	52	59	FGNEATKR	47.77	0.00023

Spot	Protein name	Peptide count	Calc. mass	Obsrv. mass	Peptide delta	Start	End	Peptide sequence	Ion score*	E-value
7	proPO-p1		990.5094	990.6634	0.154	43	51	SLSNTLSNR	33.02	0.0049
			1090.5659	1090.7594	0.1936	316	324	DQFLEAIQK	55	4.70E-05
			1094.5616	1094.8514	0.2898	96	104	LIDIFMGMR	65.05	3.00E-06
			1145.604	1145.8154	0.2114	166	176	EVSNVVISGSR	61.85	8.30E-06
			1350.5874	1351.5934	1.006	509	520	VDDNGQPMSFNK	61.53	7.70E-06
			1372.7423	1372.9494	0.2072	164	176	AREVSNVVISGSR	59.94	1.10E-05
			1416.7361	1417.1374	0.4013	450	461	TLWQQSTVELGR	83.17	4.90E-08
			1459.7896	1460.6692	0.8796	531	543	FSQALRPGTNTIR	34.37	0.0055
			1507.7631	1508.2612	0.4981	545	557	RSVDSSVTIPYER	29.32	0.02
			1515.7609	1515.9274	0.1665	408	419	FVDDVFNIYKEK	59.83	1.30E-05
			1554.8478	1555.8622	1.0144	435	449	VSSVGIEGARPNTLR	43.3	0.00059
			1730.8086	1731.7372	0.9285	635	648	KYPDKQAMGYPFDR	29.13	0.017
			1753.861	1754.5762	0.7152	232	245	GELFYYMHQQIIGR	33.95	0.0043
			1764.7923	1765.6972	0.9048	383	398	HLEQFGVMGDSATAMR	79.37	1.40E-07
			1769.8559	1770.4612	0.6053	232	245	GELFYYMHQQIIGR	40.64	0.0011
			1780.7873	1781.4142	0.6269	383	398	HLEQFGVMGDSATAMR	70.79	8.90E-07
			1925.957	1926.9472	0.9902	231	245	RGELFYYMHQQIIGR	56.44	2.90E-05
			2092.0193	2092.1872	0.1678	650	668	MANDAATLSDFLRPN MAVR	49.72	0.00013
			2189.0423	2190.1134	1.0712	177	195	MPVNVPINYTANTTE PEQR	148.67	1.10E-14
8	proPO-p1	24	782.4075	782.6254	0.2179	289	295	FAGSVFR	47.6	3.30E-05
			802.4337	802.6354	0.2017	428	434	LDFPGVR	42.05	0.0011
			804.413	804.6274	0.2144	462	468	GLDFTPR	43.42	0.00087
			921.4668	921.9052	0.4384	52	59	FGNEATKR	26.66	0.019
			1083.4808	1083.7574	0.2767	640	648	QAMGYPFDR	29.2	0.011
			1090.5659	1090.7794	0.2136	316	324	DQFLEAIQK	52.25	8.80E-05
			1094.5616	1094.8194	0.2578	96	104	LIDIFMGMR	65.52	2.70E-06
			1145.604	1145.8174	0.2134	166	176	EVSNVVISGSR	61.45	9.10E-06
			1227.5706	1227.8594	0.2888	640	649	QAMGYPFDRK	22.19	0.06
			1258.6234	1259.0214	0.3981	408	417	FVDDVFNIYK	73.78	5.30E-07
			1351.662	1351.7254	0.0635	546	557	SVDSSVTIPYER	40.16	0.0011
			1366.5823	1367.4354	0.8531	509	520	VDDNGQPMSFNK	64.18	3.40E-06
			1372.7423	1373.7374	0.9952	164	176	AREVSNVVISGSR	51.98	6.50E-05
			1416.7361	1417.0814	0.3453	450	461	TLWQQSTVELGR	83.01	5.40E-08
			1459.7896	1460.5402	0.7506	531	543	FSQALRPGTNTIR	34.69	0.0052
			1507.7631	1507.8874	0.1244	545	557	RSVDSSVTIPYER	26.44	0.02

Spot	Protein name	Peptide count	Calc. mass	Obsrv. mass	Peptide delta	Start	End	Peptide sequence	Ion score*	E-value
8	proPO-p1		1507.7631	1508.2582	0.4951	545	557	RSVDSSVTIPYER	36.61	0.0037
			1515.7609	1516.5142	0.7532	408	419	FVDDVFNIYKEK	40.75	0.00088
			1554.8478	1555.8772	1.0294	435	449	VSSVGIEGARPNTLR	44.58	0.00044
			1714.8137	1715.6182	0.8045	635	648	KYPDKQAMGYPFDR	37.4	0.0022
			1748.7974	1749.8542	1.0567	383	398	HLEQFGVMGDSATAMR	88.21	1.60E-08
			1769.8559	1770.8962	1.0403	232	245	GELFYYMHQQIIGR	40.33	0.0014
			2092.0193	2092.6672	0.6478	650	668	MANDAATLSDFLRPN MAVR	69.05	1.10E-06
			2173.0473	2174.0994	1.0521	177	195	MPVNVPINYTANTTE PEQR	109.39	1.30E-10
9	proPO-p1	15	802.4337	802.6214	0.1877	428	434	LDFPGVR	35.24	0.0052
			804.413	804.5774	0.1644	462	468	GLDFTPR	43.05	0.001
			1090.5659	1090.7314	0.1656	316	324	DQFLEAIQK	57.48	2.80E-05
			1094.5616	1094.8674	0.3058	96	104	LIDIFMGMR	59.37	1.10E-05
			1145.604	1145.7874	0.1834	166	176	EVSNVVISGSR	61.84	8.40E-06
			1258.6234	1258.9594	0.3361	408	417	FVDDVFNIYK	73.75	5.40E-07
			1350.5874	1350.7414	0.154	509	520	VDDNGQPMSFNK	69.77	1.50E-06
			1372.7423	1373.0422	0.2999	164	176	AREVSNVVISGSR	37.54	0.002
			1416.7361	1417.0874	0.3513	450	461	TLWQQSTVELGR	82.94	5.40E-08
			1459.7896	1460.7502	0.9606	531	543	FSQALRPGTNTIR	27.49	0.026
			1554.8478	1555.8292	0.9814	435	449	VSSVGIEGARPNTLR	38.53	0.0018
			1753.861	1754.4262	0.5652	232	245	GELFYYMHQQIIGR	21.2	0.077
			1780.7873	1781.3572	0.5699	383	398	HLEQFGVMGDSATAMR	82.21	6.40E-08
			2108.0143	2108.9032	0.8889	650	668	MANDAATLSDFLRPN MAVR	55.89	3.60E-05
			2189.0423	2190.2002	1.1579	177	195	MPVNVPINYTANTTE PEQR	57.7	1.90E-05
10	proPO-p2	14	797.4647	797.6854	0.2208	171	178	EAAAVIPK	45.31	0.00033
			808.5171	808.7054	0.1884	183	189	TPIIIPR	30.6	0.01
			1086.5305	1087.6594	1.1289	567	576	DLSIQGSDPR	24.91	0.04
			1126.5618	1126.7574	0.1956	682	691	LSDVTEPNPR	57.1	2.60E-05
			1199.655	1199.8394	0.1844	66	75	NLDKIPEFPK	47.25	0.00025
			1278.6608	1279.0034	0.3426	149	159	VQNYAEIFPAK	66.03	2.10E-06
			1310.6619	1311.0274	0.3655	160	170	FLDSQVFTQAR	79.13	1.20E-07
			1451.7157	1452.3562	0.6404	469	481	GLDFSDRGPVYAR	33.27	0.0038
			1477.6321	1477.8474	0.2154	190	201	DYTATDLEEEHR	77.75	1.70E-07

Spot	Protein name	Peptide count	Calc. mass	Obsrv. mass	Peptide delta	Start	End	Peptide sequence	Ion score*	E-value
10	proPO-p2		1502.8093	1503.0914	0.2822	537	550	FVVPLSAGENTITR	95.18	3.10E-09
			1695.9043	1697.0122	1.1079	323	338	NIEEAIATGNVILPDK	39.42	0.0012
			1728.8465	1729.7932	0.9467	305	319	RPVDGLNVTIDDMER	68.43	1.60E-06
			1869.9109	1870.8814	0.9706	551	566	QSTESSLTIPFEQTFR	62.23	8.70E-06
			2012.0789	2013.0892	1.0102	323	341	NIEEAIATGNVILPDKSTK	64.58	3.90E-06
	serpin 3a	9	1056.5927	1056.8254	0.2327	311	319	VLNNLSELR	63.27	5.30E-06
			1164.5597	1164.8894	0.3297	163	172	IYMGEGVQPR	68.8	1.10E-06
			1264.536	1264.5094	-0.0266	271	280	DNFYYVDSSR	52.67	8.60E-05
			1334.683	1335.0194	0.3364	122	134	SELASALGFGLDR	72.16	5.40E-07
			1362.6779	1362.9054	0.2275	151	162	ESPDYILNLGSR	70.24	8.80E-07
			1459.7055	1459.9354	0.2299	201	213	EINNWVSNATQGK	60.32	1.00E-05
			1486.8355	1487.0794	0.244	107	121	LALAILTEAATGSTR	43.79	0.00054
			1509.71	1509.8474	0.1375	356	369	EAFEDTASFPGIAR	53.14	4.50E-05
			2375.2332	2376.1642	0.9309	386	408	TGIEVNELGSVAFSAT QIGIQNK	70.94	8.90E-07
11	proPO-p2	13	687.4319	687.7054	0.2735	509	514	IFIAPK	29.44	0.014
			797.4647	797.6594	0.1948	171	178	EAAAVIPK	37.97	0.0017
			808.5171	808.7054	0.1884	183	189	TPIIIPR	43.63	0.00052
			1199.655	1199.8914	0.2364	66	75	NLDKIPEFPK	48.49	0.00019
			1278.6608	1279.0114	0.3506	149	159	VQNYAEIFPAK	69.75	8.80E-07
			1310.6619	1311.0274	0.3655	160	170	FLDSQVFTQAR	87.73	1.70E-08
			1451.7157	1452.4732	0.7574	469	481	GLDFSDRGPVYAR	48.38	0.00014
			1477.6321	1478.1802	0.5481	190	201	DYTATDLEEEHR	41.51	0.00091
			1502.8093	1503.1174	0.3082	537	550	FVVPLSAGENTITR	89.12	1.20E-08
			1695.9043	1696.2194	0.3152	323	338	NIEEAIATGNVILPDK	69.88	1.20E-06
			1744.8414	1745.8192	0.9778	305	319	RPVDGLNVTIDDMER	69.52	1.00E-06
			1869.9109	1870.9894	1.0786	551	566	QSTESSLTIPFEQTFR	62.62	7.80E-06
			2012.0789	2013.1342	1.0552	323	341	NIEEAIATGNVILPDKSTK	66.42	2.60E-06
	serpin 3a	2	1509.71	1510.1294	0.4195	356	369	EAFEDTASFPGIAR	39.93	0.00093
			2375.2332	2376.0562	0.8229	386	408	TGIEVNELGSVAFSAT QIGIQNK	64.18	4.30E-06
12	proPO-p2	16	687.4319	687.6714	0.2395	509	514	IFIAPK	28.97	0.016
			797.4647	797.7554	0.2908	171	178	EAAAVIPK	34.49	0.0039
			808.5171	808.7054	0.1884	183	189	TPIIIPR	39.05	0.0015
			1086.5305	1086.7054	0.1749	567	576	DLSIQGSDPR	33.45	0.0066
			1126.5618	1126.7474	0.1856	682	691	LSDVTEPNPR	51.93	8.60E-05

Spot	Protein name	Peptide count	Calc. mass	Obsrv. mass	Peptide delta	Start	End	Peptide sequence	Ion score*	E-value
12	proPO-p2		1205.5968	1206.6574	1.0606	272	281	EPIPEAYYPK	25.03	0.054
			1278.6608	1278.8354	0.1746	149	159	VQNYAEIFPAK	53.15	5.10E-05
			1310.6619	1311.1894	0.5275	160	170	FLDSQVFTQAR	74.58	3.60E-07
			1326.7044	1326.9854	0.281	519	529	NLPWALSDQRK	54.54	4.00E-05
			1451.7157	1452.3832	0.6674	469	481	GLDFSDRGPVYAR	43.73	0.00036
			1477.6321	1477.8614	0.2294	190	201	DYTATDLEEEHR	80.85	8.30E-08
			1502.8093	1503.6894	0.8802	537	550	FVVPLSAGENTITR	96.98	1.80E-09
			1695.9043	1696.2614	0.3572	323	338	NIEEAIATGNVILPDK	67.85	1.90E-06
			1728.8465	1729.0534	0.207	305	319	RPVDGLNVTIDDMER	73.95	4.60E-07
			1744.8414	1745.7952	0.9538	305	319	RPVDGLNVTIDDMER	68.6	1.20E-06
			1869.9109	1870.9054	0.9946	551	566	QSTESSLTIPFEQTFR	79.8	1.50E-07
13	serpin 3a	10	895.5742	895.7774	0.2032	329	336	LVDVILPK	43.54	0.00044
			1148.5648	1148.7374	0.1726	163	172	IYMGEGVQPR	89.67	1.70E-08
			1181.575	1181.7834	0.2084	320	328	TEMIYLQER	54.74	3.70E-05
			1186.6022	1186.7474	0.1452	175	184	FAAIAQEFYK	49.37	0.00015
			1192.6815	1193.7982	1.1166	141	150	FSTIIESLKR	33.79	0.0032
			1288.6663	1288.9674	0.3011	443	455	VSDPALVDGAFKA	43.33	0.00064
			1334.683	1335.1154	0.4324	122	134	SELASALGFGLDR	83.42	3.80E-08
			1362.6779	1362.9694	0.2915	151	162	ESPDYILNLGSR	77.52	1.60E-07
			1459.7055	1459.8594	0.1539	201	213	EINNWVSNATQGK	69.14	1.40E-06
			1509.71	1509.9174	0.2075	356	369	EAFEDTASFPGIAR	64.42	3.30E-06
	proPO-p2	5	1126.5618	1126.7374	0.1756	682	691	LSDVTEPNPR	47.82	0.00023
			1278.6608	1278.7834	0.1226	149	159	VQNYAEIFPAK	56.86	2.40E-05
			1310.6619	1311.0794	0.4175	160	170	FLDSQVFTQAR	70.9	8.00E-07
			1477.6321	1478.4772	0.8451	190	201	DYTATDLEEEHR	27.95	0.021
			1502.8093	1502.9974	0.1882	537	550	FVVPLSAGENTITR	35.9	0.0028
14	serpin 3a	14	876.4817	876.6334	0.1517	370	376	GQLLYQR	47.09	0.00021
			895.5742	895.8374	0.2632	329	336	LVDVILPK	60.21	9.30E-06
			1056.5927	1056.7834	0.1907	311	319	VLNNLSELR	63.15	5.70E-06
			1164.5597	1164.7034	0.1437	163	172	IYMGEGVQPR	80.73	9.00E-08
			1181.575	1181.7794	0.2044	320	328	TEMIYLQER	49.88	0.00011
			1186.6022	1186.7854	0.1832	175	184	FAAIAQEFYK	48.34	0.00018
			1192.6815	1193.2372	0.5556	141	150	FSTIIESLKR	26.44	0.016
			1334.683	1335.0034	0.3204	122	134	SELASALGFGLDR	83.62	3.90E-08
			1362.6779	1363.0054	0.3275	151	162	ESPDYILNLGSR	73.94	3.60E-07
			1459.7055	1459.9114	0.2059	201	213	EINNWVSNATQGK	82.62	6.20E-08

Spot	Protein name	Peptide count	Calc. mass	Obsrv. mass	Peptide delta	Start	End	Peptide sequence	Ion score*	E-value
14	serpin 3a		1486.8355	1487.8394	1.004	107	121	LALAILTEAATGSTR	76.92	2.60E-07
			1509.71	1509.8974	0.1875	356	369	EAFEDTASFPGIAR	59.66	9.90E-06
			1730.9567	1731.1114	0.1548	90	106	VASTSNANFLLSPLGLK	84.15	4.00E-08
			2375.2332	2376.1672	0.9339	386	408	TGIEVNELGSVAFSAT QIGIQNK	36.7	0.0024
	proPO-p2	5	808.5171	808.6554	0.1384	183	189	TPIIIPR	39.85	0.0013
			1126.5618	1126.7114	0.1496	682	691	LSDVTEPNPR	46.02	0.00012
			1278.6608	1278.8934	0.2326	149	159	VQNYAEIFPAK	69.52	1.10E-06
			1310.6619	1311.1454	0.4835	160	170	FLDSQVFTQAR	82.27	6.10E-08
			1477.6321	1477.7752	0.1431	190	201	DYTATDLEEEHR	24.22	0.048
15	serpin 3a	12	876.4817	876.6954	0.2137	370	376	GQLLYQR	29.62	0.01
			895.5742	895.7474	0.1732	329	336	LVDVILPK	51.98	6.20E-05
			1056.5927	1056.8234	0.2307	311	319	VLNNLSELR	69.34	1.30E-06
			1148.5648	1149.3234	0.7586	163	172	IYMGEGVQPR	55.04	3.80E-05
			1181.575	1181.8094	0.2344	320	328	TEMIYLQER	26.06	0.026
			1186.6022	1186.8754	0.2732	175	184	FAAIAQEFYK	51.04	9.20E-05
			1192.6815	1193.1772	0.4956	141	150	FSTIIESLKR	25.69	0.019
			1334.683	1335.0514	0.3684	122	134	SELASALGFGLDR	85.72	2.30E-08
			1362.6779	1362.9214	0.2435	151	162	ESPDYILNLGSR	77.5	1.70E-07
			1459.7055	1459.9034	0.1979	201	213	EINNWVSNATQGK	78.78	1.50E-07
			1509.71	1509.9054	0.1955	356	369	EAFEDTASFPGIAR	50.17	8.90E-05
			1730.9567	1731.7234	0.7668	90	106	VASTSNANFLLSPLGLK	71.92	6.20E-07
16	serpin 3a	22	685.4123	685.6214	0.2092	345	350	LEGVLR	33.58	0.0037
			876.4817	876.6514	0.1697	370	376	GQLLYQR	47.35	0.00019
			895.5742	895.7754	0.2012	329	336	LVDVILPK	47.08	0.00019
			1036.5804	1036.7494	0.169	141	149	FSTIIESLK	39.76	0.0015
			1056.5927	1056.7614	0.1687	311	319	VLNNLSELR	70.34	1.10E-06
			1122.4804	1122.6514	0.171	337	344	FQFEYMSR	27.76	0.022
			1164.5597	1164.7394	0.1797	163	172	IYMGEGVQPR	87.75	1.70E-08
			1186.6022	1186.9474	0.3452	175	184	FAAIAQEFYK	58.42	1.60E-05
			1192.6815	1192.9094	0.2279	141	150	FSTIIESLKR	50.67	7.60E-05
			1197.5699	1197.7434	0.1735	320	328	TEMIYLQER	65.59	3.80E-06
			1217.6292	1217.8334	0.2042	443	454	VSDPALVDGAFK	94.12	4.20E-09
			1264.536	1264.7834	0.2474	271	280	DNFYYVDSSR	71.41	1.10E-06
			1288.6663	1289.0734	0.4071	443	455	VSDPALVDGAFKA	79.15	1.60E-07
			1320.7765	1321.4872	0.7107	140	150	KFSTIIESLKR	49.83	0.00011

Spot	Protein name	Peptide count	Calc. mass	Obsrv. mass	Peptide delta	Start	End	Peptide sequence	Ion score*	E-value
16	serpin 3a		1334.683	1335.0434	0.3604	122	134	SELASALGFGLDR	83.83	3.60E-08
			1362.6779	1363.0514	0.3735	151	162	ESPDYILNLGSR	77.5	1.50E-07
			1379.7197	1380.5254	0.8057	189	200	TTNFFKPEVAAR	47.85	0.00022
			1459.7055	1460.2534	0.5479	201	213	EINNWVSNATQGK	82.95	5.10E-08
			1486.8355	1487.1094	0.274	107	121	LALAILTEAATGSTR	103.31	6.00E-10
			1509.71	1510.7274	1.0175	356	369	EAFEDTASFPGIAR	77.24	2.30E-07
			1730.9567	1731.8614	0.9048	90	106	VASTSNANFLLSPLGLK	93.49	4.30E-09
			1819.9428	1820.7382	0.7954	122	138	SELASALGFGLDRTEVR	62.39	8.10E-06
17	serpin 3a	23	685.4123	685.5714	0.1592	345	350	LEGVLR	35.6	0.0022
			876.4817	876.6434	0.1617	370	376	GQLLYQR	44.37	0.00037
			895.5742	895.7474	0.1732	329	336	LVDVILPK	60.34	9.10E-06
			950.4895	950.6654	0.1759	263	270	TVPFMNVK	26.45	0.036
			1056.5927	1056.7554	0.1627	311	319	VLNNLSELR	70.39	1.10E-06
			1106.4855	1106.6954	0.2099	337	344	FQFEYMSR	33.24	0.0024
			1164.5597	1164.7294	0.1697	163	172	IYMGEGVQPR	87.87	1.60E-08
			1181.575	1181.8434	0.2684	320	328	TEMIYLQER	62.22	6.10E-06
			1186.6022	1186.7574	0.1552	175	184	FAAIAQEFYK	53.58	5.70E-05
			1192.6815	1193.0254	0.3439	141	150	FSTIIESLKR	54.95	2.70E-05
			1264.536	1264.7534	0.2174	271	280	DNFYYVDSSR	79.43	1.80E-07
			1288.6663	1288.9214	0.2551	443	455	VSDPALVDGAFKA	76.09	3.40E-07
			1320.7765	1321.5082	0.7317	140	150	KFSTIIESLKR	48.82	0.00013
			1334.683	1335.6054	0.9224	122	134	SELASALGFGLDR	80	9.70E-08
			1362.6779	1362.9814	0.3035	151	162	ESPDYILNLGSR	77.54	1.60E-07
			1379.7197	1380.5314	0.8117	189	200	TTNFFKPEVAAR	46.32	0.00032
			1459.7055	1459.9694	0.2639	201	213	EINNWVSNATQGK	69.81	1.20E-06
			1486.8355	1487.1174	0.282	107	121	LALAILTEAATGSTR	94.44	4.70E-09
			1509.71	1510.2254	0.5155	356	369	EAFEDTASFPGIAR	62.89	4.30E-06
			1730.9567	1731.8714	0.9148	90	106	VASTSNANFLLSPLGLK	68.19	1.50E-06
			1808.9495	1809.1374	0.188	295	310	YAMYIVVPNSLTGLPR	65.32	3.10E-06
			1819.9428	1820.8882	0.9454	122	138	SELASALGFGLDRTEVR	60.07	1.30E-05
			2010.0058	2010.9454	0.9396	30	49	AVFGYSALDQAALV GAESNK	118.8	2.00E-11
	GNBP-like protein	7	864.4593	864.5834	0.1242	472	478	LEVDYVK	29.25	0.018
			928.4978	928.6194	0.1217	381	389	VEPTASGLR	34.03	0.0049
			1013.5692	1013.7734	0.2043	398	405	QLPQMLLR	39.24	0.0016
			1023.5237	1023.5794	0.0558	109	117	DNLSFTVTK	43.71	0.00042

Spot	Protein name	Peptide count	Calc. mass	Obsrv. mass	Peptide delta	Start	End	Peptide sequence	Ion score*	E-value
17	GNBP-like		1214.6507	1215.5934	0.9428	61	72	NDVGTIAGEVLK	50.86	9.30E-05
	protein		1460.6572	1460.7254	0.0683	314	325	QLYYGPNDYSNK	51.22	0.00011
			1626.8941	1627.1154	0.2214	57	72	GINKNDVGTIAGEVLK	78.15	1.70E-07
18	serpin 3a	4	1148.5648	1148.7174	0.1526	163	172	IYMGEGVQPR	75.72	4.20E-07
			1362.6779	1362.9714	0.2935	151	162	ESPDYILNLGSR	47.3	0.00017
			1486.8355	1487.0234	0.188	107	121	LALAILTEAATGSTR	52.98	6.60E-05
			2375.2332	2376.2302	0.9969	386	408	TGIEVNELGSVAFSAT QIGIQNK	52.65	6.00E-05
19	serpin 3a	4	876.4817	876.7074	0.2257	370	376	GQLLYQR	33.47	0.0043
			895.5742	895.8274	0.2532	329	336	LVDVILPK	35.39	0.0028
			1056.5927	1056.6994	0.1067	311	319	VLNNLSELR	42.81	0.00066
			1148.5648	1148.7794	0.2146	163	172	IYMGEGVQPR	67.81	2.40E-06
20	beta-1-tubulin	3	1313.6252	1313.8734	0.2483	47	58	INVYYNEASGGK	69.09	1.60E-06
			1334.6904	1334.9454	0.255	163	174	IMNTYSVVPSPK	64.63	3.20E-06
			1459.6977	1459.8714	0.1738	325	336	EVDEQMLNIQNK	35.75	0.003
	SPH-1b	4	762.464	762.6594	0.1955	303	308	YQVILK	28.01	0.011
			1053.6182	1053.7454	0.1272	309	317	KIEVPVVDR	24.4	0.038
			1098.6186	1099.0462	0.4276	239	247	IVVHKDFNK	27.72	0.013
			1141.5152	1142.0992	0.5839	217	226	AGEWDTQHAK	34.17	0.0038
21	SPH-1b	6	762.464	762.6574	0.1935	303	308	YQVILK	29.93	0.0073
			890.5589	890.7574	0.1985	303	309	YQVILKK	36.77	0.0027
			1053.6182	1053.8194	0.2012	309	317	KIEVPVVDR	47.95	0.00017
			1141.5152	1141.7734	0.2582	217	226	AGEWDTQHAK	36.67	0.0026
			1467.6841	1467.9254	0.2413	172	184	IEPVNENEPDGQK	46.95	0.00022
			1523.7005	1524.5014	0.801	227	238	EPYPYQDRDVSR	33.09	0.0051
22	serpin 3a	19	876.4817	876.6834	0.2017	370	376	GQLLYQR	42.26	0.00058
			895.5742	895.8194	0.2452	329	336	LVDVILPK	60.44	8.90E-06
			950.4895	950.6674	0.1779	263	270	TVPFMNVK	26.77	0.033
			1036.5804	1036.8234	0.243	141	149	FSTIIESLK	42.34	0.00078
			1056.5927	1056.8754	0.2827	311	319	VLNNLSELR	71.77	7.30E-07
			1106.4855	1106.7234	0.2379	337	344	FQFEYMSR	33.27	0.0052
			1148.5648	1148.8494	0.2846	163	172	IYMGEGVQPR	92.99	7.00E-09
			1186.6022	1187.0194	0.4172	175	184	FAAIAQEFYK	48.58	0.00015

Spot	Protein name	Peptide count	Calc. mass	Obsrv. mass	Peptide delta	Start	End	Peptide sequence	Ion score*	E-value
22	serpin 3a		1192.6815	1192.9954	0.3139	141	150	FSTIIESLKR	50.56	7.50E-05
			1197.5699	1197.8514	0.2815	320	328	TEMIYLQER	76.11	3.10E-07
			1217.6292	1217.9254	0.2962	443	454	VSDPALVDGAFK	94.18	4.10E-09
			1264.536	1264.8654	0.3294	271	280	DNFYYVDSSR	79.4	1.60E-07
			1288.6663	1289.0154	0.3491	443	455	VSDPALVDGAFKA	67.53	2.40E-06
			1320.7765	1321.6132	0.8367	140	150	KFSTIIESLKR	39.06	0.0013
			1334.683	1334.9774	0.2944	122	134	SELASALGFGLDR	86.97	1.80E-08
			1362.6779	1363.0514	0.3735	151	162	ESPDYILNLGSR	77.49	1.50E-07
			1379.7197	1379.8914	0.1717	189	200	TTNFFKPEVAAR	67.05	2.30E-06
			1459.7055	1459.9694	0.2639	201	213	EINNWVSNATQGK	81.2	8.40E-08
			1509.71	1509.8794	0.1695	356	369	EAFEDTASFPGIAR	77.52	1.60E-07
	SPH-1b	5	762.464	762.6074	0.1435	303	308	YQVILK	23.82	0.031
			925.5233	925.7294	0.2062	310	317	IEVPVVDR	23.4	0.044
			1053.6182	1053.8834	0.2652	309	317	KIEVPVVDR	38.18	0.0016
			1467.6841	1468.3312	0.647	172	184	IEPVNENEPDGQK	25.17	0.038
			1523.7005	1524.5092	0.8087	227	238	EPYPYQDRDVSR	36.22	0.0032
23	serpin 3a	21	876.4817	876.6614	0.1797	370	376	GQLLYQR	42.28	0.00059
			895.5742	895.8054	0.2312	329	336	LVDVILPK	54.48	3.50E-05
			950.4895	950.7054	0.2159	263	270	TVPFMNVK	25.65	0.041
			1036.5804	1036.7734	0.193	141	149	FSTIIESLK	40.63	0.0012
			1056.5927	1056.8854	0.2927	311	319	VLNNLSELR	71.96	6.80E-07
			1122.4804	1122.6594	0.179	337	344	FQFEYMSR	26.65	0.028
			1164.5597	1164.7734	0.2137	163	172	IYMGEGVQPR	93.1	4.50E-09
			1186.6022	1186.9254	0.3232	175	184	FAAIAQEFYK	50.29	0.00011
			1192.6815	1192.9734	0.2919	141	150	FSTIIESLKR	47.32	0.00016
			1197.5699	1197.8314	0.2615	320	328	TEMIYLQER	64.16	4.80E-06
			1217.6292	1217.9154	0.2862	443	454	VSDPALVDGAFK	94.13	4.20E-09
			1264.536	1264.7594	0.2234	271	280	DNFYYVDSSR	76.61	3.40E-07
			1288.6663	1289.0294	0.3631	443	455	VSDPALVDGAFKA	73.46	6.10E-07
			1320.7765	1321.5622	0.7857	140	150	KFSTIIESLKR	46.2	0.00025
			1334.683	1335.0714	0.3884	122	134	SELASALGFGLDR	83.76	3.60E-08
			1362.6779	1363.0654	0.3875	151	162	ESPDYILNLGSR	77.52	1.50E-07
			1379.7197	1380.4874	0.7677	189	200	TTNFFKPEVAAR	58.2	1.90E-05
			1459.7055	1460.4314	0.7259	201	213	EINNWVSNATQGK	78.16	1.80E-07
			1486.8355	1487.1714	0.336	107	121	LALAILTEAATGSTR	90.51	1.10E-08
			1509.71	1510.8214	1.1115	356	369	EAFEDTASFPGIAR	55.39	3.60E-05

Spot	Protein name	Peptide count	Calc. mass	Obsrv. mass	Peptide delta	Start	End	Peptide sequence	Ion score*	E-value
23	serpin 3a		1730.9567	1731.9314	0.9748	90	106	VASTSNANFLLSPLGLK	84.02	3.80E-08
24	serpin 3a	21	876.4817	876.6374	0.1557	370	376	GQLLYQR	35.07	0.0032
			895.5742	895.7974	0.2232	329	336	LVDVILPK	60.29	9.20E-06
			1036.5804	1036.7714	0.191	141	149	FSTIIESLK	40.7	0.0012
			1056.5927	1056.8714	0.2787	311	319	VLNNLSELR	71.69	7.40E-07
			1122.4804	1122.6374	0.157	337	344	FQFEYMSR	27.72	0.022
			1164.5597	1164.7154	0.1557	163	172	IYMGEGVQPR	87.91	1.70E-08
			1164.6754	1165.0754	0.4	140	149	KFSTIIESLK	38.39	0.0012
			1181.575	1181.8394	0.2644	320	328	TEMIYLQER	58.69	1.40E-05
			1186.6022	1186.9794	0.3772	175	184	FAAIAQEFYK	53.1	5.40E-05
			1192.6815	1192.9754	0.2939	141	150	FSTIIESLKR	63.93	3.50E-06
			1217.6292	1217.9094	0.2802	443	454	VSDPALVDGAFK	94.16	4.20E-09
			1264.536	1264.7154	0.1794	271	280	DNFYYVDSSR	73.99	6.60E-07
			1288.6663	1289.0334	0.3671	443	455	VSDPALVDGAFKA	80.85	1.10E-07
			1320.7765	1321.5142	0.7377	140	150	KFSTIIESLKR	62	6.50E-06
			1334.683	1335.0454	0.3624	122	134	SELASALGFGLDR	83.73	3.60E-08
			1362.6779	1363.0874	0.4095	151	162	ESPDYILNLGSR	77.54	1.50E-07
			1379.7197	1379.9794	0.2597	189	200	TTNFFKPEVAAR	58.05	1.80E-05
			1459.7055	1460.1954	0.4899	201	213	EINNWVSNATQGK	78.89	1.30E-07
			1486.8355	1487.1174	0.282	107	121	LALAILTEAATGSTR	98.35	1.90E-09
			1509.71	1510.4914	0.7815	356	369	EAFEDTASFPGIAR	68.1	1.30E-06
			1730.9567	1731.3714	0.4148	90	106	VASTSNANFLLSPLGLK	72.21	5.40E-07
25	serpin 3a	17	685.4123	685.6594	0.2472	345	350	LEGVLR	29.14	0.0098
			876.4817	876.6554	0.1737	370	376	GQLLYQR	35.79	0.0027
			895.5742	895.8014	0.2272	329	336	LVDVILPK	55.75	2.60E-05
			1036.5804	1036.7414	0.161	141	149	FSTIIESLK	42.27	0.00082
			1056.5927	1056.8834	0.2907	311	319	VLNNLSELR	68.21	1.60E-06
			1164.5597	1164.7614	0.2017	163	172	IYMGEGVQPR	87.91	1.50E-08
			1186.6022	1186.9634	0.3612	175	184	FAAIAQEFYK	50.08	0.00011
			1192.6815	1193.5914	0.9099	141	150	FSTIIESLKR	51.87	6.90E-05
			1197.5699	1197.8194	0.2495	320	328	TEMIYLQER	76.12	3.10E-07
			1217.6292	1217.8954	0.2662	443	454	VSDPALVDGAFK	94.06	4.30E-09
			1264.536	1264.7834	0.2474	271	280	DNFYYVDSSR	71.42	1.10E-06
			1288.6663	1289.0054	0.3391	443	455	VSDPALVDGAFKA	83.68	5.80E-08
			1334.683	1334.9154	0.2324	122	134	SELASALGFGLDR	94.05	3.80E-09

Spot	Protein name	Peptide count	Calc. mass	Obsrv. mass	Peptide delta	Start	End	Peptide sequence	Ion score*	E-value
25	serpin 3a		1362.6779	1363.0474	0.3695	151	162	ESPDYILNLGSR	77.49	1.50E-07
			1379.7197	1380.4534	0.7337	189	200	TTNFFKPEVAAR	47.83	0.0002
			1459.7055	1460.4814	0.7759	201	213	EINNWVSNATQGK	80.93	1.00E-07
			1509.71	1509.9334	0.2235	356	369	EAFEDTASFPGIAR	67.44	1.70E-06
26	serpin 3a	19	876.4817	876.6674	0.1857	370	376	GQLLYQR	44.41	0.00036
			895.5742	895.8154	0.2412	329	336	LVDVILPK	52.06	6.10E-05
			1036.5804	1036.7934	0.213	141	149	FSTIIESLK	41.82	0.00089
			1056.5927	1056.7534	0.1607	311	319	VLNNLSELR	66.42	2.70E-06
			1148.5648	1148.7254	0.1606	163	172	IYMGEGVQPR	89.58	1.70E-08
			1164.6754	1164.9574	0.282	140	149	KFSTIIESLK	37.18	0.0015
			1181.575	1181.8194	0.2444	320	328	TEMIYLQER	62.25	6.10E-06
			1186.6022	1186.9654	0.3632	175	184	FAAIAQEFYK	49.89	0.00011
			1192.6815	1193.0034	0.3219	141	150	FSTIIESLKR	47.58	0.00015
			1217.6292	1217.9134	0.2842	443	454	VSDPALVDGAFK	79.49	1.20E-07
			1264.536	1264.8414	0.3054	271	280	DNFYYVDSSR	71.43	1.00E-06
			1288.6663	1289.0354	0.3691	443	455	VSDPALVDGAFKA	74.24	5.10E-07
			1320.7765	1321.5082	0.7317	140	150	KFSTIIESLKR	48.6	0.00014
			1334.683	1335.0414	0.3584	122	134	SELASALGFGLDR	86.97	1.70E-08
			1362.6779	1363.0834	0.4055	151	162	ESPDYILNLGSR	77.58	1.50E-07
			1379.7197	1379.9014	0.1817	189	200	TTNFFKPEVAAR	62.31	6.80E-06
			1459.7055	1460.2174	0.5119	201	213	EINNWVSNATQGK	80.96	8.30E-08
			1509.71	1510.5994	0.8895	356	369	EAFEDTASFPGIAR	70.21	1.00E-06
			1730.9567	1732.0074	1.0508	90	106	VASTSNANFLLSPLGLK	84.3	3.60E-08
27	serpin 3a	17	876.4817	876.6494	0.1677	370	376	GQLLYQR	44.6	0.00035
			895.5742	895.7634	0.1892	329	336	LVDVILPK	60.35	9.10E-06
			1036.5804	1036.8994	0.319	141	149	FSTIIESLK	42.42	0.00075
			1056.5927	1056.7794	0.1867	311	319	VLNNLSELR	66.01	3.00E-06
			1164.5597	1164.7174	0.1577	163	172	IYMGEGVQPR	83.03	5.10E-08
			1181.575	1181.8494	0.2744	320	328	TEMIYLQER	68.04	1.60E-06
			1186.6022	1186.9374	0.3352	175	184	FAAIAQEFYK	53.45	5.10E-05
			1192.6815	1193.0094	0.3279	141	150	FSTIIESLKR	47.19	0.00016
			1217.6292	1217.8014	0.1722	443	454	VSDPALVDGAFK	74.66	3.60E-07
			1264.536	1264.8534	0.3174	271	280	DNFYYVDSSR	71.41	1.00E-06
			1288.6663	1288.9654	0.2991	443	455	VSDPALVDGAFKA	64.25	5.20E-06
			1334.683	1335.0094	0.3264	122	134	SELASALGFGLDR	89.62	9.70E-09

Spot	Protein name	Peptide count	Calc. mass	Obsrv. mass	Peptide delta	Start	End	Peptide sequence	Ion score*	E-value
27	serpin 3a		1362.6779	1363.0114	0.3335	151	162	ESPDYILNLGSR	77.48	1.60E-07
			1379.7197	1379.9074	0.1877	189	200	TTNFFKPEVAAR	53.89	4.70E-05
			1459.7055	1460.4494	0.7439	201	213	EINNWVSNATQGK	72.4	7.00E-07
			1509.71	1509.9474	0.2375	356	369	EAFEDTASFPGIAR	53.83	4.00E-05
			1730.9567	1731.0114	0.0548	90	106	VASTSNANFLLSPLGLK	67.87	6.40E-07
	SPH-1b	3	762.464	762.6434	0.1795	303	308	YQVILK	26.94	0.015
			1053.6182	1053.7994	0.1812	309	317	KIEVPVVDR	27.85	0.017
			1467.6841	1467.8794	0.1953	172	184	IEPVNENEPDGQK	49.28	0.00013
28	serpin 3a	15	876.4817	876.6254	0.1437	370	376	GQLLYQR	47.36	0.0002
			895.5742	895.8174	0.2432	329	336	LVDVILPK	60.2	9.40E-06
			1036.5804	1036.8654	0.285	141	149	FSTIIESLK	32.9	0.0068
			1056.5927	1056.8494	0.2567	311	319	VLNNLSELR	69.61	1.20E-06
			1122.4804	1122.6774	0.197	337	344	FQFEYMSR	30.51	0.011
			1164.5597	1164.7114	0.1517	163	172	IYMGEGVQPR	85.25	3.10E-08
			1181.575	1181.8034	0.2284	320	328	TEMIYLQER	62.25	6.20E-06
			1186.6022	1186.9894	0.3872	175	184	FAAIAQEFYK	51.93	7.10E-05
			1192.6815	1192.9834	0.3019	141	150	FSTIIESLKR	58.85	1.10E-05
			1264.536	1264.9294	0.3934	271	280	DNFYYVDSSR	79.39	1.50E-07
			1334.683	1335.0054	0.3224	122	134	SELASALGFGLDR	80.67	7.70E-08
			1362.6779	1363.0754	0.3975	151	162	ESPDYILNLGSR	77.51	1.50E-07
			1379.7197	1379.9034	0.1837	189	200	TTNFFKPEVAAR	66.85	2.40E-06
			1459.7055	1460.6074	0.9019	201	213	EINNWVSNATQGK	78.12	2.20E-07
			1509.71	1509.8974	0.1875	356	369	EAFEDTASFPGIAR	54.37	3.30E-05
	SPH-4	5	762.464	762.6454	0.1815	275	280	YQVILK	23.98	0.029
			890.5589	890.6754	0.1165	275	281	YQVILKK	34.76	0.0044
			925.5233	925.6774	0.1542	282	289	IEVPVVDR	26.56	0.02
			1053.6182	1053.7994	0.1812	281	289	KIEVPVVDR	38.17	0.0016
			1292.7452	1293.5392	0.794	98	108	RPEVTPKPELK	32.05	0.012
29	serpin 3a	19	876.4817	876.6354	0.1537	370	376	GQLLYQR	44.64	0.00036
			895.5742	895.8114	0.2372	329	336	LVDVILPK	60.18	9.50E-06
			950.4895	950.6694	0.1799	263	270	TVPFMNVK	25.39	0.046
			1036.5804	1036.7794	0.199	141	149	FSTIIESLK	42.62	0.00075
			1056.5927	1056.8354	0.2427	311	319	VLNNLSELR	70.16	1.10E-06
			1106.4855	1106.6254	0.1399	337	344	FQFEYMSR	26.87	0.025
			1148.5648	1148.7754	0.2106	163	172	IYMGEGVQPR	81.23	1.10E-07

Spot	Protein name	Peptide count	Calc. mass	Obsrv. mass	Peptide delta	Start	End	Peptide sequence	Ion score*	E-value
29	serpin 3a		1186.6022	1186.9074	0.3052	175	184	FAAIAQEFYK	50.16	0.00011
			1192.6815	1193.2462	0.5646	141	150	FSTIIESLKR	31.25	0.0054
			1197.5699	1197.8094	0.2395	320	328	TEMIYLQER	62.56	7.00E-06
			1264.536	1264.7454	0.2094	271	280	DNFYYVDSSR	80.04	1.60E-07
			1320.7765	1321.6012	0.8247	140	150	KFSTIIESLKR	46.81	0.00022
			1334.683	1335.0574	0.3744	122	134	SELASALGFGLDR	83.77	3.60E-08
			1362.6779	1362.9794	0.3015	151	162	ESPDYILNLGSR	79.48	1.00E-07
			1379.7197	1379.9234	0.2037	189	200	TTNFFKPEVAAR	62.18	6.90E-06
			1459.7055	1460.2234	0.5179	201	213	EINNWVSNATQGK	84.07	4.00E-08
			1486.8355	1487.0554	0.22	107	121	LALAILTEAATGSTR	95.01	4.10E-09
			1509.71	1510.5154	0.8055	356	369	EAFEDTASFPGIAR	67.69	1.60E-06
			1730.9567	1731.8794	0.9228	90	106	VASTSNANFLLSPLGLK	84.16	3.70E-08
	SPH-4	5	762.464	762.7054	0.2415	275	280	YQVILK	24.44	0.025
			890.5589	890.6674	0.1085	275	281	YQVILKK	36.09	0.0033
			925.5233	925.6874	0.1642	282	289	IEVPVVDR	29.93	0.0097
			1053.6182	1053.8154	0.1972	281	289	KIEVPVVDR	41.65	0.00071
			1292.7452	1293.4312	0.686	98	108	RPEVTPKPELK	28.19	0.029
30	serpin 3a	15	685.4123	685.6134	0.2012	345	350	LEGVLR	32.02	0.0053
			876.4817	876.6834	0.2017	370	376	GQLLYQR	44.46	0.00035
			895.5742	895.7934	0.2192	329	336	LVDVILPK	60.33	9.10E-06
			1036.5804	1036.7974	0.217	141	149	FSTIIESLK	44.35	0.0005
			1056.5927	1056.8374	0.2447	311	319	VLNNLSELR	69.56	1.20E-06
			1122.4804	1122.6514	0.171	337	344	FQFEYMSR	27.31	0.024
			1148.5648	1148.7754	0.2106	163	172	IYMGEGVQPR	80.1	1.40E-07
			1181.575	1181.7874	0.2124	320	328	TEMIYLQER	71.28	8.20E-07
			1186.6022	1186.9874	0.3852	175	184	FAAIAQEFYK	53.5	4.90E-05
			1192.6815	1192.9354	0.2539	141	150	FSTIIESLKR	65.19	2.60E-06
			1264.536	1264.7334	0.1974	271	280	DNFYYVDSSR	71.45	1.20E-06
			1362.6779	1363.0294	0.3515	151	162	ESPDYILNLGSR	77.44	1.60E-07
			1379.7197	1379.8734	0.1537	189	200	TTNFFKPEVAAR	50.1	0.00011
			1459.7055	1459.9354	0.2299	201	213	EINNWVSNATQGK	68.22	1.70E-06
			1509.71	1509.9854	0.2755	356	369	EAFEDTASFPGIAR	63.52	4.10E-06
	proPO-p2	2	1086.5305	1086.7014	0.1709	567	576	DLSIQGSDPR	67.09	1.20E-06
			1126.5618	1126.7214	0.1596	682	691	LSDVTEPNPR	52.6	7.60E-05
	serpin-4a	2	1086.6073	1086.9434	0.3361	98	106	EISNWLVVK	27.72	0.021
			1241.5533	1241.8494	0.2962	217	226	IGEVNMMYNR	74.38	4.30E-07

Spot	Protein name	Peptide count	Calc. mass	Obsrv. mass	Peptide delta	Start	End	Peptide sequence	Ion score*	E-value
30	SPH-1b	2	762.464	762.6154	0.1515	303	308	YQVILK	28.23	0.011
			1467.6841	1467.9474	0.2633	172	184	IEPVNENEPDGQK	45.89	0.00028
	SPH-4	2	762.464	762.6154	0.1515	275	280	YQVILK	28.23	0.011
			1497.696	1498.8262	1.1301	199	210	EPYPHQDRDVSR	27.77	0.017
31	serpin 3a	6	895.5742	895.7814	0.2072	329	336	LVDVILPK	51.47	7.00E-05
			1056.5927	1056.7334	0.1407	311	319	VLNNLSELR	54.06	4.70E-05
			1164.5597	1164.8834	0.3237	163	172	IYMGEGVQPR	63.63	3.60E-06
			1186.6022	1186.7074	0.1052	175	184	FAAIAQEFYK	24.5	0.049
			1197.5699	1197.0874	-0.4825	320	328	TEMIYLQER	30.72	0.0097
			1459.7055	1459.9414	0.2359	201	213	EINNWVSNATQGK	65.93	2.80E-06
32	serpin 3a	7	876.4817	876.5934	0.1117	370	376	GQLLYQR	28.71	0.015
			895.5742	895.9454	0.3712	329	336	LVDVILPK	43.97	0.00035
			1056.5927	1057.7374	1.1447	311	319	VLNNLSELR	26.05	0.03
			1148.5648	1148.7094	0.1446	163	172	IYMGEGVQPR	91.14	1.30E-08
			1181.575	1181.5794	0.0044	320	328	TEMIYLQER	25.68	0.029
			1264.536	1264.8894	0.3534	271	280	DNFYYVDSSR	24.4	0.049
			1362.6779	1362.8334	0.1555	151	162	ESPDYILNLGSR	77.3	2.00E-07
33	SPH-2	9	813.4708	813.7494	0.2786	235	241	NDIALLR	40.56	0.001
			946.5488	947.1652	0.6164	227	234	DFKPLSLK	28.69	0.017
			1093.6131	1093.8214	0.2083	218	226	DVQEILIHK	43.54	0.00049
			1105.4716	1105.6454	0.1738	389	398	WGYGSSTYSV	41.6	0.00068
			1171.508	1171.7494	0.2414	380	388	HWVDENMNK	66.98	8.20E-07
			1196.5608	1197.0382	0.4774	293	302	VEQDMVPHSR	29.52	0.01
			1324.6558	1324.7514	0.0957	292	302	KVEQDMVPHSR	69.19	1.90E-06
			1521.8039	1522.5772	0.7733	114	127	DPSEVVKPKPDPSK	42.58	0.00067
			1862.0513	1862.9272	0.8759	111	127	VLKDPSEVVKPKPDPSK	56.21	2.70E-05
34	SPH-2	10	813.4708	813.6774	0.2066	235	241	NDIALLR	42.14	0.00072
			946.5488	947.0512	0.5024	227	234	DFKPLSLK	26.41	0.029
			1093.6131	1093.8534	0.2403	218	226	DVQEILIHK	45.23	0.00033
			1105.4716	1105.7794	0.3078	389	398	WGYGSSTYSV	42.24	0.00062
			1147.5509	1147.7034	0.1525	200	209	AGEWDTQTIK	41.66	0.00096
			1171.508	1171.7934	0.2854	380	388	HWVDENMNK	66.94	2.40E-06
			1196.5608	1197.2032	0.6424	293	302	VEQDMVPHSR	44.12	0.00036

Spot	Protein name	Peptide count	Calc. mass	Obsrv. mass	Peptide delta	Start	End	Peptide sequence	Ion score*	E-value
34	SPH-2		1324.6558	1324.7834	0.1277	292	302	KVEQDMVPHSR	72.36	9.00E-07
			1521.8039	1522.5082	0.7043	114	127	DPSEVVKPKPDPSK	26.42	0.026
			1862.0513	1862.8942	0.8429	111	127	VLKDPSEVVKPKPDPSK	54.5	4.10E-05
35	SPH-4	6	762.464	762.4627	-0.0012	275	280	YQVILK	32.54	0.0064
			868.4767	868.6174	0.1408	116	123	NPEGVVVR	61.73	8.60E-06
			890.5589	890.6454	0.0865	275	281	YQVILKK	33.49	0.006
			925.5233	925.6714	0.1482	282	289	IEVPVVDR	25.63	0.025
			1053.6182	1053.8294	0.2112	281	289	KIEVPVVDR	41.69	0.00071
			1098.6186	1099.1572	0.5386	211	219	IVVHKDFNK	34.21	0.0028
36	serpin 3a	4	895.5742	895.8054	0.2312	329	336	LVDVILPK	36.54	0.0022
			1056.5927	1056.6154	0.0227	311	319	VLNNLSELR	36.48	0.0031
			1164.5597	1164.7054	0.1457	163	172	IYMGEGVQPR	66.97	2.10E-06
			1459.7055	1459.7714	0.0659	201	213	EINNWVSNATQGK	39.64	0.0012
37	serpin 3a	16	685.4123	685.6874	0.2752	345	350	LEGVLR	25.98	0.02
			876.4817	876.6734	0.1917	370	376	GQLLYQR	55.48	2.80E-05
			895.5742	895.8134	0.2392	329	336	LVDVILPK	46.24	0.00023
			1036.5804	1036.7334	0.153	141	149	FSTIIESLK	33.62	0.0061
			1056.5927	1056.7814	0.1887	311	319	VLNNLSELR	53.36	5.40E-05
			1164.5597	1164.7274	0.1677	163	172	IYMGEGVQPR	86.25	2.40E-08
			1164.6754	1164.9414	0.266	140	149	KFSTIIESLK	37.29	0.0015
			1186.6022	1186.9134	0.3112	175	184	FAAIAQEFYK	51.94	7.30E-05
			1192.6815	1192.8854	0.2039	141	150	FSTIIESLKR	40.03	0.0009
			1197.5699	1197.7574	0.1875	320	328	TEMIYLQER	65.6	3.80E-06
			1264.536	1264.7094	0.1734	271	280	DNFYYVDSSR	71.35	1.20E-06
			1334.683	1335.0394	0.3564	122	134	SELASALGFGLDR	89.28	1.00E-08
			1362.6779	1362.9714	0.2935	151	162	ESPDYILNLGSR	77.46	1.60E-07
			1379.7197	1379.8734	0.1537	189	200	TTNFFKPEVAAR	45.47	0.00033
			1459.7055	1459.8574	0.1519	201	213	EINNWVSNATQGK	87.44	2.00E-08
			1509.71	1509.8574	0.1475	356	369	EAFEDTASFPGIAR	51.97	5.80E-05
38	serpin 3a	21	685.4123	685.7114	0.2992	345	350	LEGVLR	36.26	0.0019
			876.4817	876.6754	0.1937	370	376	GQLLYQR	50.71	8.30E-05
			895.5742	895.8294	0.2552	329	336	LVDVILPK	60.26	9.20E-06
			1036.5804	1036.7374	0.157	141	149	FSTIIESLK	31.06	0.011

Spot	Protein name	Peptide count	Calc. mass	Obsrv. mass	Peptide delta	Start	End	Peptide sequence	Ion score*	E-value
38	serpin 3a		1056.5927	1056.8374	0.2447	311	319	VLNNLSELR	69.65	1.20E-06
			1122.4804	1122.7094	0.229	337	344	FQFEYMSR	25.61	0.033
			1164.5597	1164.7414	0.1817	163	172	IYMGEGVQPR	82.24	5.90E-08
			1186.6022	1186.9274	0.3252	175	184	FAAIAQEFYK	53.09	5.50E-05
			1192.6815	1192.9194	0.2379	141	150	FSTIIESLKR	51.07	6.90E-05
			1197.5699	1197.7674	0.1975	320	328	TEMIYLQER	62.49	7.60E-06
			1217.6292	1217.7994	0.1702	443	454	VSDPALVDGAFK	71.22	8.00E-07
			1264.536	1264.7654	0.2294	271	280	DNFYYVDSSR	79.42	1.80E-07
			1288.6663	1288.9154	0.2491	443	455	VSDPALVDGAFKA	70.78	1.20E-06
			1320.7765	1321.1542	0.3777	140	150	KFSTIIESLKR	37.95	0.0015
			1334.683	1335.6654	0.9824	122	134	SELASALGFGLDR	89.62	1.10E-08
			1362.6779	1362.9734	0.2955	151	162	ESPDYILNLGSR	77.56	1.60E-07
			1379.7197	1380.5794	0.8597	189	200	TTNFFKPEVAAR	39.12	0.0018
			1459.7055	1459.9214	0.2159	201	213	EINNWVSNATQGK	78.01	1.80E-07
			1509.71	1509.9174	0.2075	356	369	EAFEDTASFPGIAR	64.76	3.10E-06
			1730.9567	1731.7554	0.7988	90	106	VASTSNANFLLSPLGLK	73.45	4.20E-07
			2010.0058	2010.8854	0.8797	30	49	AVFGYSALDQAALV GAESNK	70.16	1.50E-06
39	serpin 3a	15	685.4123	685.6654	0.2532	345	350	LEGVLR	32.99	0.004
			876.4817	876.6654	0.1837	370	376	GQLLYQR	50.71	8.40E-05
			895.5742	895.7974	0.2232	329	336	LVDVILPK	60.25	9.30E-06
			1036.5804	1036.7494	0.169	141	149	FSTIIESLK	41.78	0.00092
			1056.5927	1056.7834	0.1907	311	319	VLNNLSELR	67.7	2.00E-06
			1164.5597	1164.7394	0.1797	163	172	IYMGEGVQPR	87.99	1.60E-08
			1186.6022	1186.8794	0.2772	175	184	FAAIAQEFYK	50.1	0.00011
			1192.6815	1193.6394	0.9579	141	150	FSTIIESLKR	51	8.40E-05
			1197.5699	1197.7514	0.1815	320	328	TEMIYLQER	75.99	3.40E-07
			1264.536	1264.7674	0.2314	271	280	DNFYYVDSSR	79.41	1.80E-07
			1320.7765	1321.7722	0.9957	140	150	KFSTIIESLKR	32.13	0.0064
			1362.6779	1363.0494	0.3715	151	162	ESPDYILNLGSR	77.46	1.50E-07
			1379.7197	1380.5614	0.8417	189	200	TTNFFKPEVAAR	42.14	0.00087
			1459.7055	1459.9114	0.2059	201	213	EINNWVSNATQGK	69.39	1.30E-06
			1509.71	1509.9154	0.2055	356	369	EAFEDTASFPGIAR	59.65	1.00E-05
	PAP-3	2	799.4552	799.7174	0.2623	276	282	NDIGLIR	41.09	0.0011
			1422.7255	1422.8594	0.1339	261	272	TIPHPEYNPISR	37.95	0.0018

Spot	Protein name	Peptide count	Calc. mass	Obsrv. mass	Peptide delta	Start	End	Peptide sequence	Ion score*	E-value
41	PRSP (HP14)	3	711.3955	711.6474	0.2519	178	183	FIAAYK	28.65	0.011
			989.4818	989.6534	0.1717	327	334	EHVSVEYK	28.31	0.013
			1404.6674	1404.7514	0.0841	363	373	KPNYYSETTFR	43.47	0.00078
43	serpin 3a	8	895.5742	895.8534	0.2792	329	336	LVDVILPK	50.45	8.80E-05
			1056.5927	1056.8134	0.2207	311	319	VLNNLSELR	78.22	1.70E-07
			1164.5597	1164.8054	0.2457	163	172	IYMGEGVQPR	75.89	2.30E-07
			1186.6022	1186.8014	0.1992	175	184	FAAIAQEFYK	42.85	0.00064
			1197.5699	1197.8294	0.2595	320	328	TEMIYLQER	62.43	7.20E-06
			1264.536	1264.7514	0.2154	271	280	DNFYYVDSSR	36.24	0.0038
			1288.6663	1288.8254	0.1591	443	455	VSDPALVDGAFKA	66.14	3.60E-06
			1362.6779	1363.0294	0.3515	151	162	ESPDYILNLGSR	44.25	0.00033
51	proPO-p2	3	808.5171	808.6834	0.1664	183	189	TPIIIPR	38.36	0.0018
			1278.6608	1278.8834	0.2226	149	159	VQNYAEIFPAK	33.77	0.0041
			1310.6619	1310.9094	0.2475	160	170	FLDSQVFTQAR	70.25	9.80E-07
	serpin 3a	2	1056.5927	1056.7814	0.1887	311	319	VLNNLSELR	60.27	1.10E-05
			1362.6779	1362.9614	0.2835	151	162	ESPDYILNLGSR	58.62	1.30E-05
52	serpin 3a	10	876.4817	876.6734	0.1917	370	376	GQLLYQR	55.7	2.60E-05
			895.5742	895.8134	0.2392	329	336	LVDVILPK	49.93	0.0001
			1056.5927	1056.7694	0.1767	311	319	VLNNLSELR	58.14	1.80E-05
			1122.4804	1122.6654	0.185	337	344	FQFEYMSR	24.77	0.042
			1164.5597	1164.7274	0.1677	163	172	IYMGEGVQPR	87.79	1.70E-08
			1186.6022	1186.8714	0.2692	175	184	FAAIAQEFYK	58.47	1.70E-05
			1192.6815	1193.0872	0.4056	141	150	FSTIIESLKR	24.39	0.026
			1197.5699	1197.8774	0.3075	320	328	TEMIYLQER	60.48	1.10E-05
			1264.536	1264.7034	0.1674	271	280	DNFYYVDSSR	68.89	2.10E-06
			1362.6779	1362.9574	0.2795	151	162	ESPDYILNLGSR	77.42	1.70E-07
54	immulectin-2b	7	1173.5596	1173.5174	-0.0421	71	80	FAMASMMILK	55.77	3.30E-05
			1254.5955	1254.6914	0.096	30	39	YLDVIDGWMK	53.93	5.40E-05
			1307.6762	1307.6974	0.0213	97	108	GDFFSVEGIPLK	74.04	4.00E-07
			1435.7711	1435.8274	0.0563	97	109	GDFFSVEGIPLKK	73.13	5.80E-07
			1449.7365	1449.7074	-0.029	84	96	QSVFTGIHATFSR	51.97	3.00E-05
			1471.732	1471.7294	-0.0026	40	51	LHEIPANWHEAR	59.63	1.10E-05
			1989.9771	1990.7392	0.7621	217	233	EIFAQHLPASMVGNFWK	63.86	4.30E-06

Spot	Protein name	Peptide count	Calc. mass	Obsrv. mass	Peptide delta	Start	End	Peptide sequence	Ion score*	E-value
54	immulectin-2a	6	1240.5798	1240.5714	-0.0084	30	39	YLDVVDGWMK	54.64	4.10E-05
			1307.6762	1307.6974	0.0213	97	108	GDFFSVEGIPLK	74.04	4.00E-07
			1435.7711	1435.8274	0.0563	97	109	GDFFSVEGIPLKK	73.13	5.80E-07
			1449.7365	1449.7074	-0.029	84	96	QSVFTGIHATFSR	51.97	3.00E-05
			1471.732	1471.7294	-0.0026	40	51	LHEIPANWHEAR	59.63	1.10E-05
			1989.9771	1990.7392	0.7621	217	233	EIFAQHLPASMVGNFWK	63.86	4.30E-06
55	immulectin-2b	7	1157.5647	1157.5334	-0.0312	71	80	FAMASMMILK	72.37	6.90E-07
			1254.5955	1254.6414	0.046	30	39	YLDVIDGWMK	57.28	2.50E-05
			1307.6762	1307.7654	0.0893	97	108	GDFFSVEGIPLK	64.61	3.50E-06
			1435.7711	1435.7594	-0.0117	97	109	GDFFSVEGIPLKK	58.72	1.60E-05
			1449.7365	1450.1302	0.3937	84	96	QSVFTGIHATFSR	55.22	2.40E-05
			1471.732	1471.7074	-0.0246	40	51	LHEIPANWHEAR	59.7	1.10E-05
			1989.9771	1990.7872	0.8101	217	233	EIFAQHLPASMVGNFWK	65.98	2.80E-06
56	immulectin-2b	5	1254.5955	1254.5934	-0.002	30	39	YLDVIDGWMK	54.06	5.40E-05
			1307.6762	1307.7694	0.0933	97	108	GDFFSVEGIPLK	56.44	2.30E-05
			1449.7365	1450.4992	0.7627	84	96	QSVFTGIHATFSR	29.04	0.011
			1471.732	1472.0512	0.3192	40	51	LHEIPANWHEAR	25.17	0.031
			1989.9771	1990.9852	1.0081	217	233	EIFAQHLPASMVGNFWK	46.39	0.00026
	immulectin-2b	5	1240.5798	1240.6314	0.0516	30	39	YLDVVDGWMK	54.02	4.80E-05
			1307.6762	1307.7694	0.0933	97	108	GDFFSVEGIPLK	56.44	2.30E-05
			1449.7365	1450.4992	0.7627	84	96	QSVFTGIHATFSR	29.04	0.011
			1471.732	1472.0512	0.3192	40	51	LHEIPANWHEAR	25.17	0.031
			1989.9771	1990.9852	1.0081	217	233	EIFAQHLPASMVGNFWK	46.39	0.00026
	SPH-1b	4	925.5233	925.4854	-0.0378	310	317	IEVPVVDR	55.39	2.70E-05
			1053.6182	1053.6594	0.0412	309	317	KIEVPVVDR	38.37	0.0014
			1066.472	1066.5314	0.0595	227	234	EPYPYQDR	41.32	0.001
			1452.7475	1452.6474	-0.1001	160	171	FGEFPWMVAILK	69.22	1.50E-06
	immulectin III	2	1419.7511	1419.7834	0.0324	220	232	GSEPVNVIFVGFR	55.46	2.70E-05
			1547.846	1547.7532	-0.0929	219	232	KGSEPVNVIFVGFR	24.28	0.052
57	immulectin-4	5	1130.5469	1130.5954	0.0486	244	252	DLNQSNVWR	37.43	0.0025
			1364.7201	1364.7374	0.0174	38	49	LHLVPATWSDAR	33.91	0.0047
			1419.7511	1420.4494	0.6984	231	243	GSEPVNVIFVGFR	73.82	3.80E-07
			1547.846	1548.5954	0.7494	230	243	KGSEPVNVIFVGFR	99.56	1.40E-09
			1788.8293	1789.4212	0.5918	183	196	FHEYAMSWSLAYLR	34.39	0.0032

Spot	Protein name	Peptide count	Calc. mass	Obsrv. mass	Peptide delta	Start	End	Peptide sequence	Ion score*	E-value
57	immulectin III	4	1130.5469	1130.5954	0.0486	233	241	DLNQSNVWR	37.43	0.0025
			1419.7511	1420.4494	0.6984	220	232	GSEPVNVIFVGFR	73.82	3.80E-07
			1427.6245	1428.1754	0.551	112	122	GIYYEQYDYSK	66.29	2.80E-06
			1547.846	1548.5954	0.7494	219	232	KGSEPVNVIFVGFR	99.56	1.40E-09
	immulectin-2b	3	1254.5955	1254.5734	-0.022	30	39	YLDVIDGWMK	33.43	0.0061
			1307.6762	1307.9634	0.2873	97	108	GDFFSVEGIPLK	37.87	0.0015
			1471.732	1472.1292	0.3972	40	51	LHEIPANWHEAR	42.97	0.00051
	dVA-AP7	2	1083.5349	1083.4414	-0.0934	129	137	VQGLYYADR	39.59	0.0011
			1427.6245	1428.1754	0.551	111	121	GIYYEQYDYSK	66.29	2.80E-06
58	immulectin-3	3	790.4589	790.5534	0.0946	221	227	YPTGLIK	36.45	0.0028
			1360.6558	1361.5074	0.8517	299	310	HPNNIMPVPNNV	45.76	0.00024
			1735.8834	1736.9032	1.0197	181	194	FHNYGLPWSLAYLR	56.86	2.60E-05
59	immulectin III	4	1130.5469	1130.5834	0.0366	233	241	DLNQSNVWR	39.92	0.0014
			1419.7511	1419.9034	0.1524	220	232	GSEPVNVIFVGFR	79.89	9.70E-08
			1427.6245	1428.5314	0.907	112	122	GIYYEQYDYSK	57.9	2.30E-05
			1547.846	1548.6172	0.7711	219	232	KGSEPVNVIFVGFR	32.73	0.0089
	immulectin-2a	3	1240.5798	1240.6434	0.0636	30	39	YLDVVDGWMK	55.46	3.40E-05
			1307.6762	1307.7514	0.0753	97	108	GDFFSVEGIPLK	45.9	0.00026
			1471.732	1472.1622	0.4302	40	51	LHEIPANWHEAR	39.5	0.0012
	immulectin-2b	3	1254.5955	1254.6314	0.036	30	39	YLDVIDGWMK	45.39	0.00039
			1307.6762	1307.7514	0.0753	97	108	GDFFSVEGIPLK	45.9	0.00026
			1471.732	1472.1622	0.4302	40	51	LHEIPANWHEAR	39.5	0.0012
60	immulectin-2b	4	1189.5545	1189.4614	-0.0931	71	80	FAMASMMILK	50.74	9.40E-05
			1254.5955	1254.6534	0.058	30	39	YLDVIDGWMK	45.75	0.00036
			1449.7365	1449.9772	0.2407	84	96	QSVFTGIHATFSR	31.51	0.0063
			1471.732	1472.2492	0.5172	40	51	LHEIPANWHEAR	39.91	0.0011
61	PAP-1	2	935.4786	935.4234	-0.0552	289	296	LGMPIFDK	63.13	5.80E-06
			1433.7303	1434.4534	0.7231	263	276	LATGNDVFVAGWGK	119.18	1.50E-11
	immulectin-3	2	790.4589	790.5154	0.0566	221	227	YPTGLIK	26.82	0.027
			1360.6558	1361.4114	0.7557	299	310	HPNNIMPVPNNV	38.33	0.0013
66	attacin-1	3	1498.7528	1499.1802	0.4273	162	176	VGASASAAHTPLFDR	45.75	0.00028
			1677.8223	1678.0372	0.2149	118	131	LNVFHNDNHNLDVK	25.84	0.042

Spot	Protein name	Peptide count	Calc. mass	Obsrv. mass	Peptide delta	Start	End	Peptide sequence	Ion score*	E-value
66	attacin-1		1741.8747	1742.4502	0.5754	160	176	DKVGASASAAHTPLFDR	24.53	0.038
67	immulectin-2b	5	1254.5955	1254.6094	0.014	30	39	YLDVIDGWMK	44.78	0.00045
			1307.6762	1308.5534	0.8773	97	108	GDFFSVEGIPLK	55.59	3.60E-05
			1435.7711	1435.5674	-0.2037	97	109	GDFFSVEGIPLKK	39.69	0.0013
			1449.7365	1450.1302	0.3937	84	96	QSVFTGIHATFSR	23.21	0.039
			1989.9771	1990.8742	0.8971	217	233	EIFAQHLPASMVGNFWK	51.96	7.10E-05
	attacin-1	3	1273.5826	1273.5054	-0.0772	192	202	TTSLDFNADYK	50	0.00012
			1498.7528	1499.0872	0.3343	162	176	VGASASAAHTPLFDR	56.7	2.20E-05
			1677.8223	1678.1152	0.2929	118	131	LNVFHNDNHNLDVK	40.31	0.0014
68	attacin-1	8	1273.5826	1273.5054	-0.0772	192	202	TTSLDFNADYK	60.07	1.20E-05
			1347.7034	1347.6914	-0.012	65	77	NVFSAIGGLDLDK	86.47	2.50E-08
			1498.7528	1499.0302	0.2773	162	176	VGASASAAHTPLFDR	58.66	1.40E-05
			1516.7045	1517.1772	0.4726	190	202	DKTTSLDFNADYK	46.48	0.00023
			1644.7995	1645.1392	0.3397	190	203	DKTTSLDFNADYKK	31.48	0.0072
			1677.8223	1678.9552	1.1329	118	131	LNVFHNDNHNLDVK	27.35	0.024
			1741.8747	1742.3212	0.4464	160	176	DKVGASASAAHTPLFDR	50.83	9.00E-05
			1829.8756	1830.6532	0.7776	38	56	DTHGSVTVNSDGTS GAVVK	44.31	0.00038

*Ion scores > 22 indicate significant identity ($p < 0.05$).

Table B-3. MS/MS results for plasma proteins that bound to a control column of Protein-A Sepharose CL-4B beads without antibody and identified in Table 3-3.

Spot	Protein name	Peptide count	Calc. mass	Obsrv. mass	Peptide delta	Start	End	Peptide sequence	Ion score*	E-value
1c	immulectin-2b	7	1173.5596	1173.7154	0.1559	71	80	FAMASMMILK	66.99	2.50E-06
			1254.5955	1254.7454	0.15	30	39	YLDVIDGWMK	45.67	0.00035
			1307.6762	1307.8834	0.2073	97	108	GDFFSVEGIPLK	66.17	2.40E-06
			1435.7711	1435.9814	0.2103	97	109	GDFFSVEGIPLKK	41.53	0.00089
			1449.7365	1450.1314	0.395	84	96	QSVFTGIHATFSR	59.53	1.10E-05
			1471.732	1472.2642	0.5322	40	51	LHEIPANWHEAR	40.13	0.001
			1989.9771	1990.7542	0.7771	217	233	EIFAQHLPASMVGNFWK	56.98	2.10E-05
2c	immulectin-2b	5	1173.5596	1173.6574	0.0979	71	80	FAMASMMILK	55.29	3.70E-05
			1254.5955	1254.7214	0.126	30	39	YLDVIDGWMK	45.63	0.00036
			1435.7711	1435.8954	0.1243	97	109	GDFFSVEGIPLKK	63.84	5.00E-06
			1449.7365	1450.6194	0.883	84	96	QSVFTGIHATFSR	47.39	9.00E-05
3c	immulectin-2b	6	1173.5596	1173.7054	0.1459	71	80	FAMASMMILK	59.99	1.20E-05
			1254.5955	1254.6854	0.09	30	39	YLDVIDGWMK	59.8	1.40E-05
			1307.6762	1308.6554	0.9793	97	108	GDFFSVEGIPLK	37.47	0.0024
			1435.7711	1435.8934	0.1223	97	109	GDFFSVEGIPLKK	62.12	7.50E-06
			1471.732	1472.2402	0.5082	40	51	LHEIPANWHEAR	37.9	0.0017
			1989.9771	1990.5622	0.5851	217	233	EIFAQHLPASMVGNFWK	38.34	0.0016
4c	immulectin-2b	2	1189.5545	1189.5454	-0.0091	71	80	FAMASMMILK	50.37	0.0001
			1254.5955	1254.5834	-0.012	30	39	YLDVIDGWMK	36.46	0.0031
5c	immulectin-2b	4	1157.5647	1158.4934	0.9288	71	80	FAMASMMILK	56.32	3.30E-05
			1254.5955	1254.8514	0.256	30	39	YLDVIDGWMK	46.37	0.00026
			1471.732	1472.2372	0.5052	40	51	LHEIPANWHEAR	44.92	0.00034
			1989.9771	1990.2802	0.3031	217	233	EIFAQHLPASMVGNFWK	53.58	5.70E-05
6c	immulectin-2b	2	1189.5545	1189.7274	0.1729	71	80	FAMASMMILK	50.69	9.60E-05
			1471.732	1472.6002	0.8682	40	51	LHEIPANWHEAR	34.28	0.0039
7c	no match									
8c	no match									

Spot	Protein name	Peptide count	Calc. mass	Obsrv. mass	Peptide delta	Start	End	Peptide sequence	Ion score*	E-value
9c	serpin-1	1	1457.6998	1458.0494	0.3496	165	177	NLVDPDALDETTR	49.84	0.00012
10c	endochitinase	4	1119.6441	1120.5534	0.9094	263	272	LVVGIPFYGR	28.12	0.026
			1161.5917	1161.7374	0.1457	42	51	YGIEDIPVEK	51.41	7.50E-05
			1306.5942	1306.7534	0.1592	340	350	GTQWVGYEDPR	53.65	5.40E-05
			1328.6262	1329.3382	0.712	234	243	RPHDQWAYEK	31.53	0.0093
11c	proPO-p2	5	808.5171	808.6694	0.1524	183	189	TPIIIPR	39.02	0.0015
			1086.5305	1086.6234	0.0929	567	576	DLSIQGSDPR	62.19	9.30E-06
			1310.6619	1310.7834	0.1215	160	170	FLDSQVFTQAR	87.48	2.20E-08
			1451.7157	1452.8542	1.1384	469	481	GLDFSDRGPVYAR	45.45	0.0003
			1477.6321	1477.7454	0.1134	190	201	DYTATDLEEEHR	68.25	1.50E-06
12c	immulectin-2b	4	1157.5647	1157.8474	0.2828	71	80	FAMASMMILK	59.65	1.30E-05
			1449.7365	1450.3492	0.6127	84	96	QSVFTGIHATFSR	48.9	0.0001
			1471.732	1471.8954	0.1634	40	51	LHEIPANWHEAR	50.24	3.60E-05
			1763.8308	1763.0542	-0.7767	154	169	RIPDMVVTECGTVDSK	22.44	0.082
13c	immulectin-2b	2	1173.5596	1173.9654	0.4059	71	80	FAMASMMILK	35.08	0.004
			1471.732	1472.6932	0.9612	40	51	LHEIPANWHEAR	48.6	0.00014
	immulectin III	2	1130.5469	1130.6354	0.0886	233	241	DLNQSNVWR	31.8	0.009
			1427.6245	1428.7474	1.123	112	122	GIYYEQYDYSK	33.83	0.0064
	immulectin-3	1	1360.6558	1360.9834	0.3277	299	310	HPNNIMPVPNNV	25.33	0.026
14c	immulectin-3	2	790.4589	790.5634	0.1046	221	227	YPTGLIK	24.17	0.046
			1360.6558	1360.7594	0.1037	299	310	HPNNIMPVPNNV	30.51	0.011
	immulectin-2b	1	1189.5545	1189.6754	0.1209	71	80	FAMASMMILK	42.04	0.00037
15c	immulectin-2b	5	1173.5596	1173.7614	0.2019	71	80	FAMASMMILK	64.39	4.50E-06
			1254.5955	1254.7394	0.144	30	39	YLDVIDGWMK	44.71	0.00044
			1449.7365	1450.7152	0.9787	84	96	QSVFTGIHATFSR	41.56	0.00067
			1471.732	1472.3152	0.5832	40	51	LHEIPANWHEAR	46.03	0.00026
			1763.8308	1764.1882	0.3573	154	169	RIPDMVVTECGTVDSK	29.21	0.015
16c	immulectin-2b	2	1173.5596	1174.5834	1.0239	71	80	FAMASMMILK	44.32	0.00065
			1471.732	1472.2282	0.4962	40	51	LHEIPANWHEAR	41.73	0.00071
17c	immulectin-2b	4	1189.5545	1189.6314	0.0769	71	80	FAMASMMILK	20.84	0.093

Spot	Protein name	Peptide count	Calc. mass	Obsrv. mass	Peptide delta	Start	End	Peptide sequence	Ion score*	E-value
17c	immulectin-2b		1254.5955	1254.7774	0.182	30	39	YLDVIDGWMK	50.43	0.00011
			1449.7365	1450.1572	0.4207	84	96	QSVFTGIHATFSR	43.86	0.00032
			1471.732	1472.4022	0.6702	40	51	LHEIPANWHEAR	33.34	0.0048
	scolexin A	1	976.509	976.6294	0.1204	257	265	NGNLAVFSR	47.3	0.00032
18c	immulectin-3	1	790.4589	790.5894	0.1306	221	227	YPTGLIK	23.91	0.047
19c	proPO-p2	1	808.5171	807.6154	-0.9016	183	189	TPIIIPR	40.23	0.00033
	immulectin-3	1	790.4589	790.5834	0.1246	221	227	YPTGLIK	30.78	0.0097
20c	immulectin-3	1	790.4589	790.6174	0.1586	221	227	YPTGLIK	36.24	0.0026
21c	immulectin-3	1	790.4589	790.5874	0.1286	221	227	YPTGLIK	26.8	0.024
22c	SPH-2	3	813.4708	813.5674	0.0966	235	241	NDIALLR	30.78	0.0095
			946.5488	946.6574	0.1087	227	234	DFKPLSLK	28.11	0.0064
			1105.4716	1105.6254	0.1538	389	398	WGYGSSTYSV	26.15	0.024
23c	immulectin-2b	4	1173.5596	1173.8154	0.2559	71	80	FAMASMMILK	57.71	2.10E-05
			1254.5955	1254.6334	0.038	30	39	YLDVIDGWMK	56.85	1.10E-05
			1449.7365	1450.4182	0.6817	84	96	QSVFTGIHATFSR	38.05	0.0013
			1471.732	1472.2342	0.5022	40	51	LHEIPANWHEAR	37.63	0.0018
	immulectin-3	1	1360.6558	1360.9054	0.2497	299	310	HPNNIMPVPNNV	32.25	0.0056
24c	immulectin-3	1	790.4589	790.6294	0.1706	221	227	YPTGLIK	27.28	0.02
25c	immulectin-2b	2	1173.5596	1173.8014	0.2419	71	80	FAMASMMILK	53.1	6.10E-05
			1254.5955	1254.6614	0.066	30	39	YLDVIDGWMK	45.32	0.00015
	immulectin-3	2	790.4589	790.5874	0.1286	221	227	YPTGLIK	32.01	0.0072
			1360.6558	1361.6894	1.0337	299	310	HPNNIMPVPNNV	42.6	0.00052
26c	immulectin-2b	4	1157.5647	1157.7834	0.2188	71	80	FAMASMMILK	60.97	9.80E-06
			1254.5955	1255.4734	0.878	30	39	YLDVIDGWMK	45.54	0.00012
			1449.7365	1450.7302	0.9937	84	96	QSVFTGIHATFSR	31.48	0.0069
			1471.732	1472.3092	0.5772	40	51	LHEIPANWHEAR	34.4	0.0038
	immulectin III	2	1130.5469	1130.8494	0.3026	233	241	DLNQSNVWR	36.65	0.0023
			1427.6245	1427.8994	0.275	112	122	GIYYEQYDYSK	56.96	2.50E-05
	immulectin-3	2	790.4589	790.6314	0.1726	221	227	YPTGLIK	24.34	0.04

Spot	Protein name	Peptide count	Calc. mass	Obsrv. mass	Peptide delta	Start	End	Peptide sequence	Ion score*	E-value
26c	immulectin-3		1360.6558	1361.1074	0.4517	299	310	HPNNIMPVPNNV	39.97	0.00079
27c	immulectin-2b	7	1141.5697	1141.8834	0.3137	71	80	FAMASMMILK	73.07	5.90E-07
			1254.5955	1254.7374	0.142	30	39	YLDVIDGWMK	57.41	2.40E-05
			1307.6762	1307.8734	0.1973	97	108	GDFFSVEGIPLK	62.45	5.70E-06
			1435.7711	1436.5414	0.7703	97	109	GDFFSVEGIPLKK	60.58	1.20E-05
			1449.7365	1450.4002	0.6637	84	96	QSVFTGIHATFSR	49.9	8.20E-05
			1471.732	1472.6154	0.8834	40	51	LHEIPANWHEAR	54.47	4.00E-05
			1989.9771	1990.9882	1.0111	217	233	EIFAQHLPASMVGNFWK	47.75	0.00019
28c	immulectin-2b	5	1157.5647	1157.8374	0.2728	71	80	FAMASMMILK	66.82	2.50E-06
			1254.5955	1254.6874	0.092	30	39	YLDVIDGWMK	54.02	5.30E-05
			1307.6762	1307.8594	0.1833	97	108	GDFFSVEGIPLK	56.18	2.40E-05
			1449.7365	1450.6672	0.9307	84	96	QSVFTGIHATFSR	40.81	0.0008
			1471.732	1472.2792	0.5472	40	51	LHEIPANWHEAR	32.34	0.0061
	SPH-1b	3	925.5233	925.6154	0.0922	310	317	IEVPVVDR	28.06	0.014
			1467.6841	1467.7474	0.0633	172	184	IEPVNENEPDGQK	39.95	0.0011
			2647.2051	2647.4902	0.285	217	238	AGEWDTQHAKEPYPY QDRDVSR	31	0.0098
29c	immulectin III	4	1130.5469	1130.7254	0.1786	233	241	DLNQSNVWR	51.3	9.20E-05
			1419.7511	1419.9334	0.1824	220	232	GSEPVNVIFVGFR	73.93	3.90E-07
			1427.6245	1427.8494	0.225	112	122	GIYYEQYDYSK	59.45	1.40E-05
			1547.846	1548.8932	1.0471	219	232	KGSEPVNVIFVGFR	34	0.0068
	immulectin-4	4	1130.5469	1130.7254	0.1786	244	252	DLNQSNVWR	51.3	9.20E-05
			1364.7201	1364.9494	0.2294	38	49	LHLVPATWSDAR	41.66	0.00062
			1419.7511	1419.9334	0.1824	231	243	GSEPVNVIFVGFR	73.93	3.90E-07
			1547.846	1548.8932	1.0471	230	243	KGSEPVNVIFVGFR	34	0.0068
	immulectin-3	1	1360.6558	1361.6454	0.9897	299	310	HPNNIMPVPNNV	27.45	0.017
30c	immulectin-3	2	790.4589	790.6274	0.1686	221	227	YPTGLIK	29.5	0.012
			1360.6558	1361.6474	0.9917	299	310	HPNNIMPVPNNV	39.33	0.0011

*Ion scores > 22 indicate significant identity ($p < 0.05$).

Appendix C - Impact of Phospholipids on Prophenoloxidase Activation

Prophenoloxidase Activation by the Addition of Phospholipids

Bidla et al. (2009) found that the addition of inner membrane phospholipids (phosphatidylserine and phosphatidylinositol), but not outer membrane phospholipids (phosphatidylcholine and phosphatidylethanolamine) to hemolymph from *Drosophila melanogaster*, but not *Galleria mellonella* stimulated PO activity. These results suggest that the release of phospholipids from damaged cells may stimulate the activation of proPO after an insect has been injured. To investigate this idea, I used plasma from *Manduca sexta* to conduct prophenoloxidase assays in the presence or absence of phospholipids.

Materials and methods

Pooled aliquots of plasma from naïve day 2 fifth instar larvae were checked for low basal levels of PO activity that dramatically increased after incubation with *M. luteus* as described by Tong and Kanost (2005), with modification. Phospholipids used include L-α-phosphatidylserine (PS; Sigma P0474), L-α-phosphatidylinositol (PI; Sigma P0639), and L-α-phosphatidylcholine (PC; Sigma P3556) and were suspended in 50 mM Tris-HCl, 0.1 M NaCl, pH 7.5. Plasma (3µL) was mixed with buffer (50 mM Tris-HCl, 0.1 M NaCl, pH 7.5), *M. luteus* (2 µg), or different amounts of each phospholipid (0.1, 0.5, 1.0, 2.0, 10, or 50 µg). Samples were incubated for 10 min at room temperature, transferred to a 96-well plate, and PO activity was measured by adding 200 µL of 2 mM dopamine in 50 mM sodium phosphate buffer, pH 6.5. Absorbance at 470 nm was monitored for 30 min in a PowerWave XS plate reader (BioTek). One unit of PO activity was defined as a change in A_{470} of 0.001/min.

Results and conclusions

Plasma mixed with *M. luteus* (a positive control) had high levels of PO activity. However, regardless of the amount and type of phospholipid, PO activity did not significantly increase in comparison to mixture with buffer (Figure C-1, panels A and B). From these experiments, it can be concluded that the addition of phospholipids does not stimulate PO

activity in plasma from *M. sexta*. So the question remains, what stimulates PO activity in insects after wounding?

References

Bidla G, Hauling T, Dushay MS, & Theopold U (2009) Activation of insect phenoloxidase after injury: endogenous versus foreign elicitors. *J Innate Immun* **1**: 301-308

Tong Y & Kanost MR (2005) *Manduca sexta* serpin-4 and serpin-5 inhibit the prophenol oxidase activation pathway: cDNA cloning, protein expression, and characterization. *J Biol Chem* **280**: 14923-14931

Figures

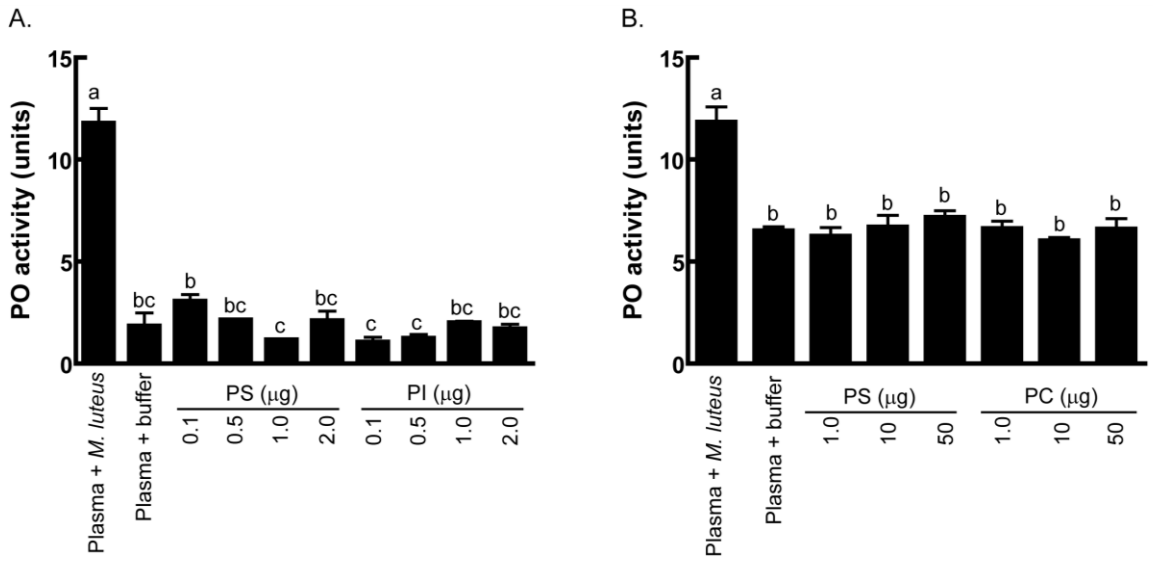

Figure C-1. Prophenoloxidase activation is not enhanced by the addition of phospholipids to plasma.

(A) Plasma (3µL) was mixed with buffer (50 mM Tris-HCl, 0.1 M NaCl, pH 7.5), *M. luteus* (2 µg), or phospholipid (0.1, 0.5, 1.0, 2.0 µg of PS or PI). (B) Plasma (3µL) was mixed with buffer (50 mM Tris-HCl, 0.1 M NaCl, pH 7.5), *M. luteus* (2 µg), or phospholipid (1.0, 10, or 50 µg of PS or PC). After incubation for 10 min at room temperature, PO activity was measured by adding 200 µL of 2 mM dopamine in 50 mM sodium phosphate buffer, pH 6.5. Absorbance at 470 nm was monitored for 30 min in a PowerWave XS plate reader (BioTek). One unit of PO activity was defined as a change in A_{470} of 0.001/min. The bars represent mean ± SD (n = 2). Bars labeled with different letters are significantly different (Analysis of Variance and Newman-Keuls test, $p < 0.05$). PS = phosphatidylserine, PI = phosphatidylinositol, PC = phosphatidylcholine